PAST AND PRESENT PROVENANCE OF THE AMAZON RIVER

Russell W. Mapes

A dissertation submitted to the faculty of the University of North Carolina at Chapel Hill in partial fulfillment of the requirements for the degree of Doctor of Philosophy in the Department of Geological Sciences.

Chapel Hill
2009

Approved by:

Drew Coleman

Allen Glazner

Lara Wagner

Stephen Meyers

Ronadh Cox

ABSTRACT

RUSSELL W. MAPES: Past and present provenance of the Amazon River
(Under the direction of Drew S. Coleman)

In its modern configuration, the Amazon River is well suited to test the assumptions upon which sediment provenance techniques rely. The scale of the system coupled with harsh weathering conditions and diverse geology allow for direct observation of sedimentary response to transport and environmental processes. Over 3,200 new U/Pb detrital zircon ages for fourteen Amazon River samples indicate that long-distance transport of zircon age populations is possible. In the western catchment, zircon ages are dominantly Phanerozoic, reflecting Andean sources. As sand progresses downstream, the presence of Proterozoic grains increases indicating Amazon Craton input, but even in the lowermost river reaches, 3000+ km from the Andes, ~30% of zircons are Phanerozoic. In spite of long transport distances, age spectra are heterogeneous suggesting that the technique is not a reliable quantitative assessment tool. Comparison of zircon provenance to other indicators shows that signals can vary widely for sediment derived in the same catchment. Specifically, techniques that rely upon chemically labile minerals are biased toward areas of physical weathering and high sediment output, whereas techniques that rely upon stable minerals areas are biased toward areas of chemical weathering and low sediment output. In the Amazon, the rate at which sediment is transported has a strong influence on the ultimate provenance signal; high transport rate yields source similar results while slowly transported sediment is sensitive toward weathering conditions. When exploring provenance of ancient deposits, multiple

indicators with different weathering responses should be used to create more complete sedimentary histories.

Previous drainage configurations have directed detritus to various locations across Amazonia. Comparison of zircon ages for modern sand to ages and sedimentologic data for Miocene and Cretaceous deposits details the occurrence of continent-scale drainage reorganization. As Gondwana split during the Late Cretaceous, drainage was directed west from a rift-shoulder near the Amazon mouth. During the Miocene, after rifting had ceased and as Andean uplift rates were at a maximum, drainage was split into two sub-basins separated by the Purus Arch. Once the Miocene Andean foreland basin was overfilled and the Purus Arch was overtopped, the modern Amazon River system was established during or after the latest Miocene.

ACKNOWLEDGEMENTS

I would like to thank my adviser, Dr. Drew Coleman for his guidance, friendship, and unique perspective on life. This project was entirely conceived and carried out during my time at UNC and it afforded me the unique opportunity to participate in all aspects of an international research project. Drew's willingness to let me take the reigns allowed me to gain experience that will be valuable for years to come. The guidance, regional knowledge, and companionship of Dr. Afonso Nogueira were invaluable to this project, without his help we would probably still be standing at the airport in Manaus. Additional thanks to Dr. Jonathan Lees, Dr. Mario Ruiz, and Angela Leguizamón Vega for sample collection in areas not visited by the author. Gratitude is also extended to the author's committee for their time and critical review of the investigation.

Funding for this project was provided by American Chemical Society- Petroleum Research Fund grant 41756-AC8, CNPq grant 554059/2006-1 to Afonso Nogueira, and FAPEAM grant 822/2003 to Adriana Horbe. Additional support was provided by the Department of Geological Sciences' Martin Trust Fund. Personal thanks go to Ryan Mills, Jesse Davis, Rebecca Lawrence, Taylor McCay, Greg Weiss, Todd Housh, Adriana Horbe, Humberto Abinader, and the University of North Carolina at Chapel Hill and Universidade Federal do Amazonas faculty and graduate students for their many insightful conversations and support.

Finally, I would like to thank my wife, Marissa, for her patience and understanding during this seemly unending process. I could not have done it without her.

TABLE OF CONTENTS

LIST OF TABLES

Table

LIST OF FIGURES

Figure

CHAPTER 1

INTRODUCTION

Formation of fluvial sediment is a complex process that is sensitive to geologic, climatic, and geographic factors. Sediment composition, although primarily a function of source rock composition, can be strongly altered by surface processes that occur during liberation and transport. In cold and dry environments where chemical weathering rates are low (Millot *et al.*, 2003), bulk sediment compositions are similar to the source rocks from which they were derived (Nesbit and Young, 1996; Potter *et al.*, 2001). In hot and wet environments where chemical weathering and secondary mineralization are common, source rocks are broken down and constituents are dispersed unevenly into the dissolved, suspended, and bedloads (Savage and Potter, 1991). As such, the environmental conditions that existed prior to deposition must be considered when attempting to connect sedimentary rocks with their detrital sources.

The foremost goal of provenance analysis is to understand the total range of sources that contributed sediment to a deposit and the relative importance of each. Many frequently used provenance techniques, like relative clast abundance and bulk sediment geochemistry (Potter, 1978; Dickinson and Suczek, 1979; Bhatia, 1983; Blatt, 1985), yield results that only qualitatively identify source rock tectonic setting but give valuable insights into predepositional weathering conditions. More direct source associations can be made

using bulk sediment isotopic methods (e.g. Goldstein *et al.*, 1984; McLennan *et al.*, 1993) and single grain geochronologic and isotopic techniques (e.g. Bernet *et al.*, 2004; Haines *et al.*, 2004) but these approaches do not give information on synsedimentation weathering conditions. Because degree of chemical weathering has such a strong influence on provenance interpretations, calibration of common techniques and comparison of results obtained via different methods is necessary to move the provenance methods toward the ultimate objective: quantitative analysis.

As a result of recent advances in fast microsampling techniques that have led to creation of large detrital datasets and sweeping conclusions about sediment sources, a push has been made toward understanding provenance results in a more quantitative sense (Weltje and von Eynatten, 2004). The most common calibration method has been direct application to modern sedimentary systems. To this end, many studies have been carried out in a variety of sedimentary, climatic, and geographic settings to evaluate the processes that create and alter provenance signals for specific techniques (e.g. Basu, 1976; Potter, 1986; Arribas *et al.*, 2000; Svendsen *et al.*, 2007). An area that has not received enough attention is comparison of results from a range of techniques on a single large sedimentary system.

The Amazon River is well suited for study of modern sediment provenance. The Amazon occupies the largest drainage basin on Earth at ~6 x 10^6 km^2 (Archer, 2005) and delivers over 6.3 x 10^{12} m^3/yr of dissolved, suspended, and bedload sediment to the Atlantic Ocean (Meade, 1996). The Amazon's >6,500 km length ranks second globally (Sioli, 1984). Weathering conditions in the Amazon drainage basin change from dominantly physical in the high Andes Mountains to dominantly chemical as the river travels ~5,000 km across lowland Amazonia. Geologically, the layout of the Amazon drainage is the best suited of any large

river system on Earth to test the reliability of sediment provenance techniques (Figure 1.1). The far western edge of the catchment exposes dominantly Phanerozoic igneous and metamorphic basement rocks, whereas the central and eastern reaches of the river expose basement rocks of Precambrian age leading to distinctive provenance signatures that are relatable to geography.

This dissertation includes three stand-alone chapters that deal with provenance of sediment from the Amazon River and its precursors. The first chapter (Chapter 2) addresses the apparent disparity between limited observations of zircon age population behavior in modern sedimentary systems, which suggest populations do not travel far from their sources, and studies focused on ancient deposits that interpret cross-continent transport of dominate age populations is possible. Because of the geologic layout of the Amazon drainage and orientation of the river itself, Andean zircons are used to estimate how far detrital age populations can travel. Furthermore, complete zircon age distributions for Amazon sands are used to address how age spectra compare to the total range of possible source ages to examine if detrital zircon provenance is a useful tool for quantitative provenance analysis.

The second chapter (Chapter 3) focuses on similarities and differences between new Nd-isotope and detrital zircon age spectra collected from the same sand samples and a large petrographic, geochemical, and isotopic dataset complied from numerous literature sources that focused on different aspects of Amazon River sediment provenance. When results are compared with one another, distinct differences in how each technique responds to source rock composition, weathering conditions, and transport style and distance become apparent. This analysis also suggests that in situations where a holistic understanding of sediment

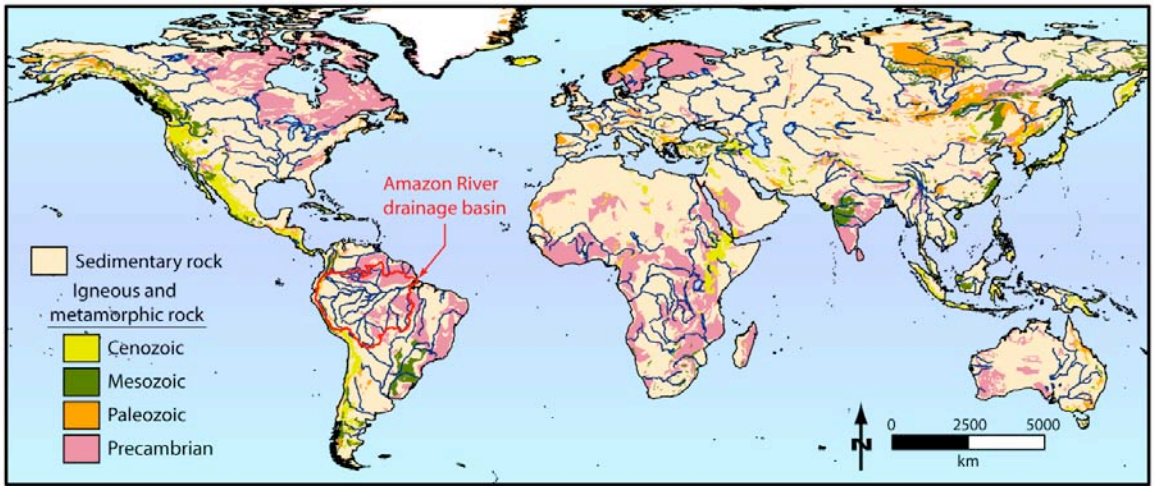

Figure 1.1- Global layout of igneous and metamorphic rocks and large fluvial systems (Bouysse, 2000).

provenance is desired, multiple provenance techniques that are sensitive to different source compositions and weathering phenomena should be employed.

The final chapter (Chapter 4) compares age spectra for detrital zircons from four Miocene-Cretaceous sandstones of lowland Amazonia to spectra for nearby modern Amazon sands. Dramatic differences in zircon age spectra coupled with sedimentologic data confirm the idea that a wholesale drainage inversion occurred in Amazonia since the late Cretaceous.

Examination of Amazon River sediment indicates that geology, climate, and geography are the primary factors that shape provenance signal, but also that other factors contribute to the signals revealed by each technique. Comparison of techniques highlights the observation that under the same environmental conditions, broadly similar methods can yield very different provenance signals. Results of Nd-isotopic and detrital zircon analysis of modern sand indicate that secondary factors like bedload sediment mixing and/or hydrodynamic fraction leave deposits inhomogeneous so that quantitative analysis of single sand samples is not possible. Finally, comparison of modern Amazon River detrital zircon age spectra to spectra from ancient deposits indicates that large fluvial systems can reorganize quickly and that provenance signals may be inherited from previous drainage configurations. These observations illustrate the complexity of sediment provenance analysis and underscore the need for a broad view of the system that existed when interpreting provenance data from rocks that have lost their sedimentary and tectonic context.

References

Archer, A.W., 2005, Review of Amazonian depositional systems: Special publication of the International Association of Sedimentologists, v. 35, p. 17-39.

Arribas J., Critelli S., Le Pera E., and Tortosa A., 2000, Composition of modern stream sand derived from a mixture of sedimentary and metamorphic source rocks (Henares River, Central Spain) Source: Sedimentary Geology, v. 133, p. 27-48.

Basu, A, 1976, Petrology of Holocene fluvial sand derived from plutonic source rocks-implications to paleoclimatic interpretation, Journal of Sedimentary Petrology, v. 46, p. 694-709.

Bernet, M., Brandon, M.T., Garver, J.I., and Molitor, B.R., 2004, Fundamentals of detrital zircon fission-track analysis for provenance and exhumation studies with examples from the European Alps, in Bernet, M., and Spiegel, C., eds., Detrital Thermochronology-Provenance analysis, exhumation, and landscape evolution of mountain belts, Geological Society of America Special Paper 378, p. 25-36.

Bhatia, M.R., 1983, Plate tectonics and geochemical composition of sands: Journal of Geology; v. 91, 611-227.

Blatt, H., 1985, Provenance studies in mudrocks: Journal of Sedimentary Petrology, v. 55, p. 69-75.

Bouysse, P., 2000, Geological Map Of The World; 1:25,000,000 scale, Commission for the Geological Map of the World- UNESCO, Paris.

Dickinson, W.R., and Suczek, C.A., 1979. Plate tectonics and sandstone compositions. American Association of Petroleum Geologists Bulletin, v. 63, p. 2164-2182

Goldstein, S.L., O'Nions, R.K., and Hamilton, P.J., 1984, A Sm-Nd isotopic study of atmospheric dusts and particulates from major river systems; Earth and Planetary Science Letters, v. 70 pp. 221-236.

Haines, P.W., Turner, S.P., Kelley, S.P., Wartho, J.-O. and Sherlock, S.C., 2004, 40Ar-39Ar dating of detrital muscovite in provenance investigations: a case study from the Adelaide Rift Complex, South Australia; Earth and Planetary Science Letters, v. 227, p. 297-311.

McLennan, S.M., Hemming, S., McDaniel, D.K., and Hanson, G.N., 1993, Geochemical approaches to sedimentation, provenance, and tectonics: Geological Society of America Special Paper, No. 284, p. 21-40.

Meade, R.H., 1996, River-sediment inputs to major rivers; in Milliman, J.D., and Haq, B.U., eds., Sea-level rise and costal subsidence, U.S. Government, pp. 63-85.

Millot, R., Gaillardet J., Dupré B., and Allégre C. J., 2003, Northern latitude chemical weathering rates: clues from the Mackenzie River Basin, Canada: Geochimica Cosmochimica Acta, v. 67, p. 1305-1329.

Nesbitt, H.W., and Young, G.M., 1982, Early Proterozoic climates and plate motions inferred from major element chemistry of lutites; Nature, v. 299, p. 715-717.

Potter, P.E., 1978, Significance and origin of big rivers; Journal of Geology, v. 86, p.13-33.

Potter, P.E., Huh, Y., Edmond, J.M., 2001, Deep-freeze petrology of Lena River sand, Siberia: Deep-freeze petrology of Lena River sand, Siberia, v. 29, p. 999-1002.

Savage, K.M., and Potter, P.E., 1991, Petrology of modern sands of the rios Guaviare and Inirida, southern Colombia; tropical climate and sand composition: Journal of Geology, v. 99, p.289-298.

Sioli, H, 1984, The Amazon and its main affluents: hydrography, morphology of the river courses, and river types, *in* Sioli, H. Ed., The Amazon: Limnology and landscape ecology of a mighty tropical river and its basin: Junk Publishers, p. 127-165.

Svendsen, J., Friis H., Stollhofen, H., Hartley, N., 2007, Facies discrimination in a mixed fluvio-eolian setting using elemental whole-rock geochemistry- applications for reservoir characterization: Journal of Sedimentary Petrology, v. 77, p. 22-33.

Weltje, G.J., and von Eynatten, H., 2004, Quantatative provenance analysis of sediments: review and outlook: Sedimentary Geology, v.171, p. 1-11.

CHAPTER 2

STRENGTHS AND LIMITATIONS OF ZIRCON AS A PROVENANCE INDICATOR: A BASIN-WIDE STUDY OF THE AMAZON RIVER

Abstract

New U/Pb detrital zircon ages for samples collected along the length of the Amazon River indicate that long distance transport of zircon age populations is possible in the fluvial setting. Tributary and mainstem detrital zircon ages are dominantly Phanerozoic in the western part of the catchment, reflecting Andean sources. Increases in the proportion of Neo- and Mesoproterozoic zircon age populations occur as the river travels east over the similarly aged Amazon craton; however, even in the lowermost reaches the fluvial Amazon, ~30% of zircons analyzed yielded Phanerozoic ages that are 3000+ km displaced from their original sources. Qualitatively, Amazon River detrital zircon ages reflect the range of zircon sources present in the drainage basin. Surprisingly though, in spite of long transport distances, the zircon provenance signal is non-homogeneous, even for samples collected in close proximity. These results indicate that zircons are poorly mixed within the bedload and suggest that single detrital zircon samples do not provide a basin-integrated provenance signal and thus, should not be used to estimate relative source region zircon contribution.

Introduction

The advent of high precision, short analytical time geochonologic techniques has led to a dramatic increase in the number of studies that employ U-Pb detrital

zircon geochronology. Acquisition of large datasets has revolutionized provenance and stratigraphic analysis and has led to technique broadening and maturation. A surprising outcome of several studies focused on deposits of various ages from northern and western North America is that significant proportions of zircon age distributions (~50%) appear to have been transported thousands of kilometers in fluvial systems from what is now eastern North America (Rainbird *et al.*, 1992; Riggs *et al.*, 1996; Dickinson and Gehrels, 2003; Rahl *et al.*, 2003; Wright and Wyld, 2003). Interpretations of long distance fluvial transport are not restricted to North America; Prokoplev *et al.* (2008) described evidence of a continent-scale fluvial system that persisted on the Siberian craton from Pennsylvanian-Jurassic time. However, since such long distance transport of zircon age populations has never been observed in any modern system restraint has been urged when making far-reaching source interpretations (Bassett, 2000).

In response to the rapid proliferation of large detrital zircon data sets, significant work has been done to ensure results of zircon provenance studies are unbiased and reproducible. Sircombe and Stern (2002) suggested changes to commonly used magnetic separation techniques to limit the possibility of biasing populations. Dodson *et al.* (1988), Vermeesch (2004), and Andersen (2005) presented statistical strategies for selecting appropriate number of grains to analyze per sample. Nemchin and Cawood (2005) discussed U-Pb specific issues that commonly affect data quality like $^{206}Pb/^{238}U$-$^{207}Pb/^{206}Pb$ age cutoffs and acceptable discordance levels. Single and multi-dimensional data visualization techniques were discussed (Sircombe, 2000; 2004; 2006; Vermeesch, 2005), statistical methods were developed to separate age spectra into individual components (Sambridge and Compston, 1994), and approaches were proposed for statistical comparison of multiple age distributions

(Berry *et al.*, 1998; Sircombe, 1999; Sircombe and Hazelton, 2004).

In addition to analytical and theoretical appraisals, the assumption of outcrop/local/regional age spectrum homogeneity has been evaluated for ancient deposits. DeGraaff-Surpless *et al.* (2003) analyzed zircons from the Cretaceous Methow Basin of the southern Canadian Cordillera. They found that age spectrum homogeneity was dependent on depositional environment; changes in age spectra for turbiditic deposits occurred in a systematic and predictable way, whereas fluvial age spectra were heterogeneous and changed unpredictably. Similarly, Sircombe *et al.* (2001) evaluated field-sampling strategies and found that the likelihood of missing important age populations was high if only a single sample was analyzed.

In contrast, few systematic studies have examined detrital zircon transport in modern sedimentary environments. Pell *et al.* (1997) compared expected age distributions for basement terranes to age spectra for Quaternary sands of the Australian Continental Dunefield. They found most windblown sands had multiple source areas, up to 850 km distant, but speculated that recent eolian transport distances were minor and concluded that most transport occurred in ancient fluvial and/or shallow marine environments. Sircombe (1999) evaluated age spectra for modern beach sands along the east coast of Australia and found that age were similar to local basement ages. However, Sircombe (1999) did suggest that in certain cases a 'favorable sedimentary pathway' could have greater control over provenance than source proximity.

In the fluvial environment, studies that have applied detrital zircon U-Pb techniques to modern sediment typically analyze only a single sample from a given system (Goldstein *et al.*, 1997; Eriksson *et al.* 2003; Admidon *et al.*, 2005; Campbell *et al.*, 2005; Iizuka *et al.*,

2005; Fletcher *et al.*, 2007). Studies that have analyzed multiple samples from the same river have found that significant differences exist between samples (Bodet and Schärer, 2000; Rino *et al.*, 2004; Stewart *et al.*, 2008). Only two systematic studies have evaluated behavior of detrital zircon age populations along modern rivers with known geologic and geomorphic characteristics. Link *et al.* (2005) found zircon point sources are most useful for establishing sediment sources for the Snake River in the northwestern USA and that provenance can be difficult to establish when multiple age populations of similar magnitude are present. They concluded that Middle Snake River age spectra effectively identified each of significant geologic age domains present in the drainage but because of sampling strategy and catchment geometry, they were not able to evaluate how spectra are modified during long distance transport. Detrital zircon U-Pb age spectra for five samples spaced along the length of the Frankland River in Australia show the proportion of Archean grains derived from the upper catchment decreases markedly from 100% where the river flows across Archean basement rocks to only 25% near the river mouth, suggesting detrital zircons are concentrated close to their sources Cawood *et al.* (1999).

The discrepancy between limited existing data for modern systems, which suggest detrital zircon is concentrated near its source and interpretations of ancient systems, which require long-distance transport of dominant age populations, highlights the need for further study of zircon transport dynamics. To adequately test the possibility of long-distance zircon transport in a modern system, catchment geometry must be organized such that a young tracer-population exists only in the headwaters so that zircon reworking does not disturb the primary zircon age signal. In this contribution, we address two distinct but interrelated

questions: how far and in what proportion can zircons be moved during fluvial transport; and how well do individual samples represent regional provenance?

Setting

The Amazon River provides the ideal study site. It is more than 6,500 km long (Sioli, 1984) and provides up to 5000 km of transcontinental transport (Domínguez, 2004) in flow that is both uniform and steady on long time and length scales. River gradient east of the Andes is very low, ranging from 1.5-4 cm/km for the ~2500 km stretch between Iquitos, Peru and the start of the Amazon estuary (Figure 2.1; Birkett *et al.*, 2002; LeFavour and Alsdorf, 2005). In general, the upper Amazon, known as the Solimões River in Brazil, receives sediment from tributaries that drain the high relief Andes and Andean foreland. The lower Amazon, below the Negro River confluence, receives Andean derived sediment from the upper Amazon and Madeira Rivers as well as material from tributaries that drain low relief, highly-weathered rocks of the Amazon Craton (Figure 2.1). The lower 800 km of the Amazon, east of Óbidos, Brazil, is tidally influenced with spring tidal range up to 6 m near the river mouth (Vital *et al.*, 1998; Archer, 2005).

The Andean headwaters provide Phanerozoic-aged zircons that are scarcely present elsewhere in the basin (Jenks, 1954; Sébrier and Soler, 1991; Atherton and Petford, 1996; Schenk *et al.*, 1997; Cobbing, 1999; Schobbenhaus, and Bellizza, 2001). Exposed granitoids, which are as young as ~3 Ma, and similarly aged volcanic cover rocks (Sébrier, and Soler, 1991; Petford *et al.*, 1996; Cobbing, 1999; Campbell *et al.*, 2001), provide young zircons to the Amazon system that can be tracked. East of the Andean highlands, the Amazon flows across the Amazon Craton, which consists of Archean to Mesoproterozoic igneous and metamorphic terranes that generally increase in age downstream (Figure 2.1; de Oliveira,

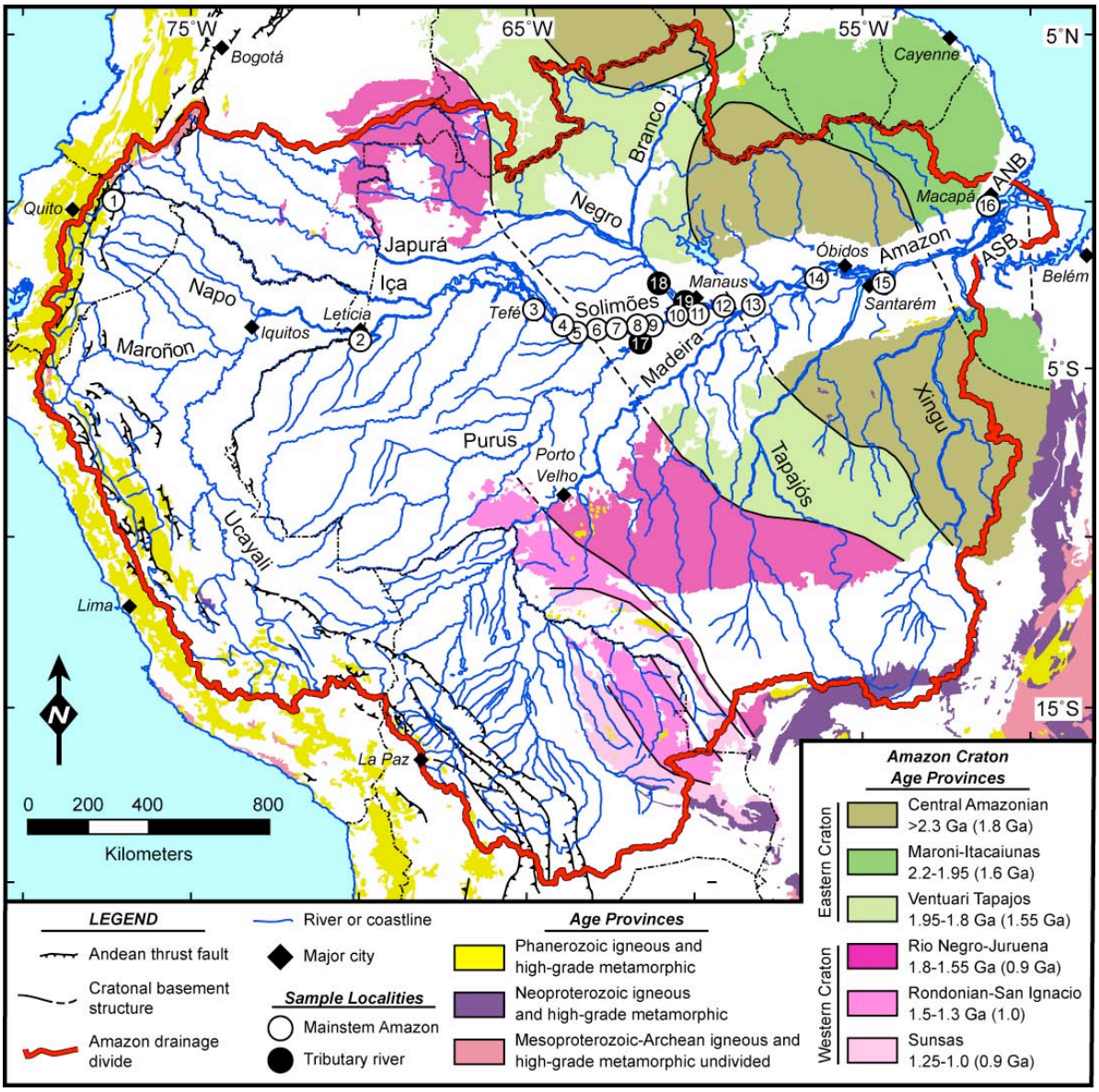

Figure 2.1- The Amazon River and its major tributaries. Map includes sample localities and geochronologic age provinces of northern South America (Cordani *et al.*, 2000; Costa *et al.*, 2000; Hearn *et al.*, 2000; Schobbenhaus, and Bellizza, 2001). Ages provided for basement provinces indicate dominate isotopic domain ages; parenthetical appendants indicate youngest rock ages within domain (Tassinari *et al.*, 2000). Unshaded areas are covered by sedimentary rocks primarily of Mesozoic or Cenozoic age (Hearn *et al.*, 2000).

1956; Trendall *et al.*, 1998; Tassinari *et al.*, 2000; Costa *et al.*, 2001; Santos *et al.*, 2002). Deep late Proterozoic-recent sedimentary basins (Mosmann et al., 1987; Cunha *et al.*, 1994; Feijó *et al.*, 1994) overlie the basement and represent potential reworked zircon sources where exposed (Tassinari *et al.*, 2000). The Amazon can thus be represented (crudely but effectively) as a two-component provenance system, with young source rocks restricted to the headwaters and a mainstem dominated by Precambrian basement exposures.

Methods

Samples of active sand were collected along the Amazon/Solimões River system from the eastern Andes in Ecuador to the onset of tidewater near Santarém, Brazil (Figure 2.1). Sampling occurred at low flow when fluvial bars were emergent. Care was taken to avoid localities where modern fluvial deposits could be confused with ancient deposits or areas of human activity. From each locality, approximately 10 kg of bulk sediment was collected.

All sand samples were unconsolidated. Visual inspection showed that the overwhelming majority of sand grains were monomineralic quartz with no appreciable weathering rind or coating. Bulk-sediment grain-size analysis was carried out on a representative aliquot using the procedures of Folk (1965). Approximately 500 g of bulk sand was split and dried for geochronology. Heavy minerals were separated using heavy liquids (MEI, $\rho = 3.3$ g/cm^3); no hydrodynamic separation was conducted. Separation using a Frantz magnetic barrier separator was carried out at very low current ($\leq$0.75 A, 10° front and side tilt) to remove the most magnetically susceptible heavy minerals without separating zircons into groups (Sircombe and Stern, 2002). Zircons were then concentrated in non-magnetic heavy mineral separates by removal of non-zircon grains. Zircon concentrates were then

moved en masse and placed in rows on adhesive strips, which were later incorporated into epoxy discs. Disc surfaces were polished in several steps, first by hand using fine wet/dry sandpaper (800, 1000, 2000 grit), then by machine-assisted diamond polishing (6, 1 μm particles) to expose fresh zircon cross-sections. Prior to analysis, the length and width of each grain was measured using software included with the mass-spectrometer.

Zircon U-Pb geochronology was conducted by laser ablation multicollector inductively coupled plasma mass spectrometry (LA-MC-ICPMS) at the University of Texas at Austin. Analytical methods are described in Appendix A. Age spectra for preferred ages are plotted using the algorithms of Sircombe (2000). Analyses with 2σ error ellipses that do not cross concordia or are >30% discordant (DeCelles *et al.*, 2007) are reported but not included in figures or probability density curves used for interpretation. For ages younger than 0.9 Ga, $^{206}Pb/^{238}U$ ages are used; otherwise $^{207}Pb/^{206}Pb$ (Sircombe and Hazelton, 2004) are used. To compare distributions, the Kolmogorov-Smirnov non-parametric test of statistical equivalence is employed (Berry *et al.*, 2001). The test procedure is modified slightly from the common technique (Press *et al.*, 1986) so that cumulative probability functions used to calculate the test value included analytical uncertainties similar to the procedure of Fletcher *et al.* (2007).

Basin wide geology and geography for display and area calculations utilize Geographic Information Systems shapefiles of Schobbenhaus and Bellizza (2001). Drainage basin boundaries for area calculations were created using the Seamless Shuttle Radar Topography Mission (SRTM) "Finished" 3 Arc Second (~90 meter) digital elevation models available from U.S. Geological Survey, EROS Data Center, Sioux Falls, SD.

Results

We measured 3274 new U-Pb zircon grain ages and sizes (Appendix A) for fourteen Amazon mainstem and tributary sand samples (Figure 2.1; Appendix B). Tributary samples were collected from: (1) an Andean tributary, the Aguarico River in Ecuador, (2) a large Andean foreland tributary, the Purus River, and (3) a large lowland cratonal tributary, the Rio Negro (Figure 2.1). All mainstem samples (samples #3-15; Figure 2.1) are very fine to medium grained, moderately to well sorted sands (Table 2.1). Between 52 and 193 individual analyses are presented per sample (Figure 2.2). Predictable changes are visible in major age population as the river moves from the Andes to the Atlantic, however age distributions are highly variable even within short distances where sediment sources have not appreciably changed. To simplify source comparisons, probability density curves have been divided into bins that correspond to large-scale northern South American geochronologic provinces and plotted against longitude, which is a proxy for river transport distance (Figure 2.3). Bin proportion precision, evaluated by bootstrapping subdistributions from a large dataset composed of all concordant mainstem zircon age analyses (Appendix C), indicates that major changes in age bin proportions are related to actual changes in sample age spectra (Figure 2.3).

Andean Aguarico River zircons yielded a single Phanerozoic age mode with only minor Precambrian zircon present (Figure 2.2). Age spectra for upper Amazon sand (samples #2-10) are dominated by a mid-late Phanerozoic and a Mesoproterozoic mode. Multiple subordinate populations exist in several samples including a late Cretaceous/Cenozoic population, a late-Cambrian/Neoproterozoic population, and very minor late Mesoproterozoic and Paleoproterozoic populations. Compared to upstream samples, lower

Table 2.1- Locations and summary statistics for individual zircon size measurements and bulk-sample grain size analysis for Amazon River sands. Data collected with assistance of Lawrence (2007).

Locality/ Sample	Latitude	Longitude	Median zircon length (μm)	Median zircon width (μm)	Median sand size (μm)	Sorting†	Skewness†	Kurtosis†	Description†
1	0.04857	-77.3057	167	115	341	1.553	-0.044	1.043	Medium grained, moderately well sorted, symmetrical, mesokurtic sand
2	-4.1518	-69.9490	147	88	309	1.418	-0.559	1.315	Medium grained, moderately well sorted, very fine skewed, leptokurtic sand
3	-3.2207	-64.7815	205	120	332	1.399	-0.068	1.090	Medium grained, well sorted, symmetrical, mesokurtic sand
4	-3.8764	-63.6491	180	100		-	-	-	-
5	-3.8559	-63.6041	215	128		-	-	-	-
6	-3.9255	-62.8996	115	65	113	1.853	-0.467	2.655	Very fine grained, moderately sorted, very fine skewed, very leptokurtic sand
7	-3.7890	-62.2238	205	105	193	1.224	-0.219	1.514	Fine grained, very well sorted, fine skewed, very leptokurtic sand
8	-3.6424	-61.4510	180	107	172	1.503	-0.445	1.674	Fine grained, moderately well sorted, very fine skewed, very leptokurtic sand
9	-3.6136	-61.2546	115	65	113	1.678	-0.446	2.180	Very fine grained, moderately sorted, very fine skewed, very leptokurtic sand
10	-3.2979	-60.3075	135	70	126	1.632	-0.555	2.654	Very fine grained, moderately sorted, very fine skewed, very leptokurtic sand
11	-3.0708	-59.7116	170	110		-	-	-	-
12	-3.2161	-59.2255	125	80		-	-	-	-
13	-3.3742	-58.7233	116	69		-	-	-	-
14	-2.2835	-56.3744	124	76	215	1.276	-0.539	1.388	Fine grained, well sorted, very fine skewed, leptokurtic sand
15	-2.4326	-54.3714	117	65	173	1.454	-0.326	0.738	Fine grained, moderately well sorted, very fine skewed, platykurtic sand
16‡	0.0866	-51.1986							
17	-4.0260	-61.5140	120	72	418	1.810	-0.407	1.770	Medium grained, moderately sorted, very fine skewed, very leptokurtic sand
18	-2.4352	-61.0622	115	68	282	1.541	-0.112	1.262	Medium grained, moderately well sorted, fine skewed mesokurtic sand
19	-3.1807	-60.0054	181	94	219	1.481	0.356	1.309	Fine grained, moderately well sorted, very coarse skewed, leptokurtic sand

† Sample grain size statistics calculated using GRADISTAT (Blott and Pye, 2001), values reported as in Folk (1968).
‡ Location estimated from Rino *et al.* (2003).

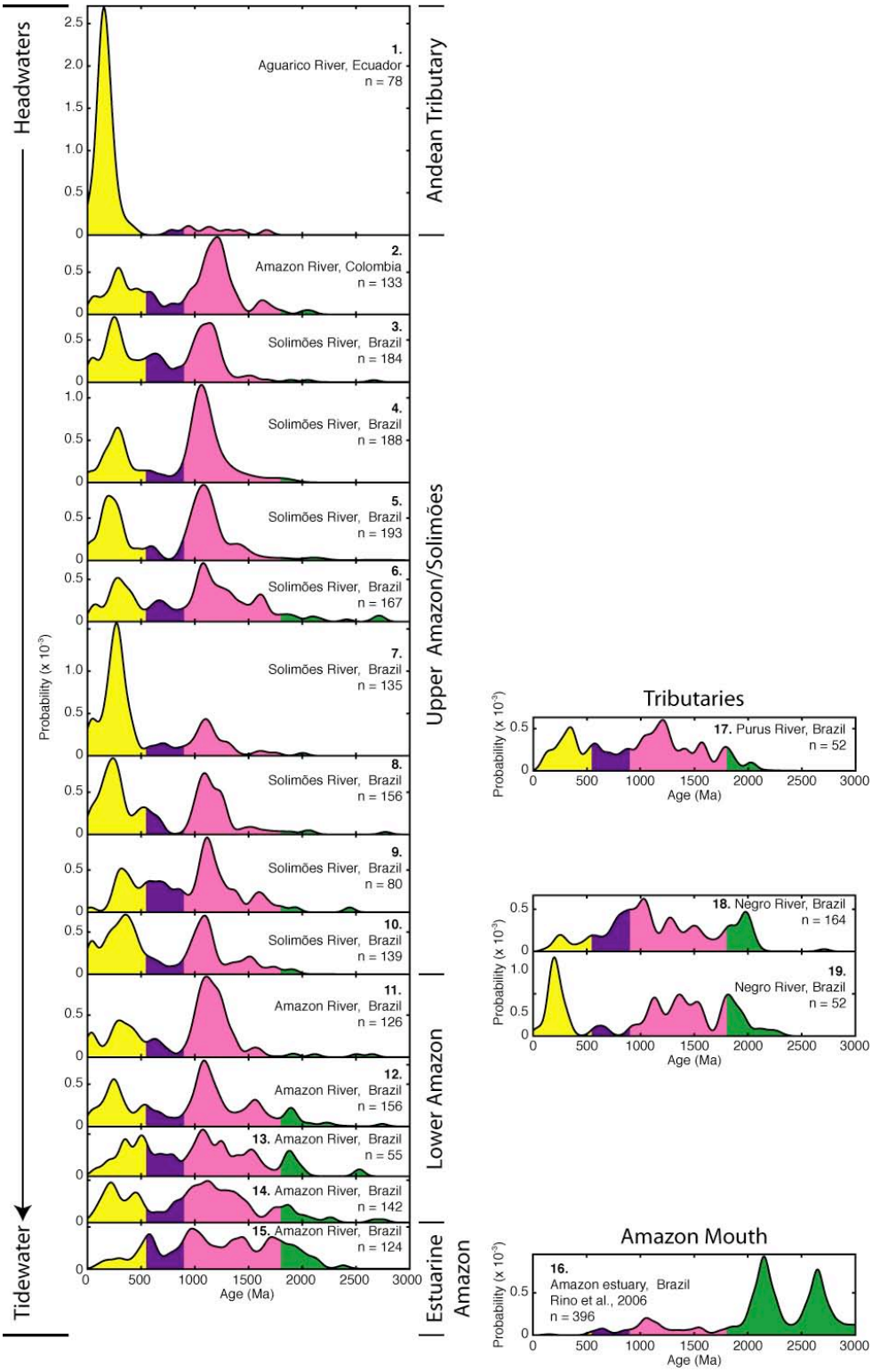

Figure 2.2- Probability density diagrams showing U-Pb zircon age distributions for modern Amazon River sands. Locality numbers on individual plots correspond to numbered samples on Figures 2.1 and 2.3. Ages for locality #16 of Rino *et al.* (2004) are estimated from the published histogram.

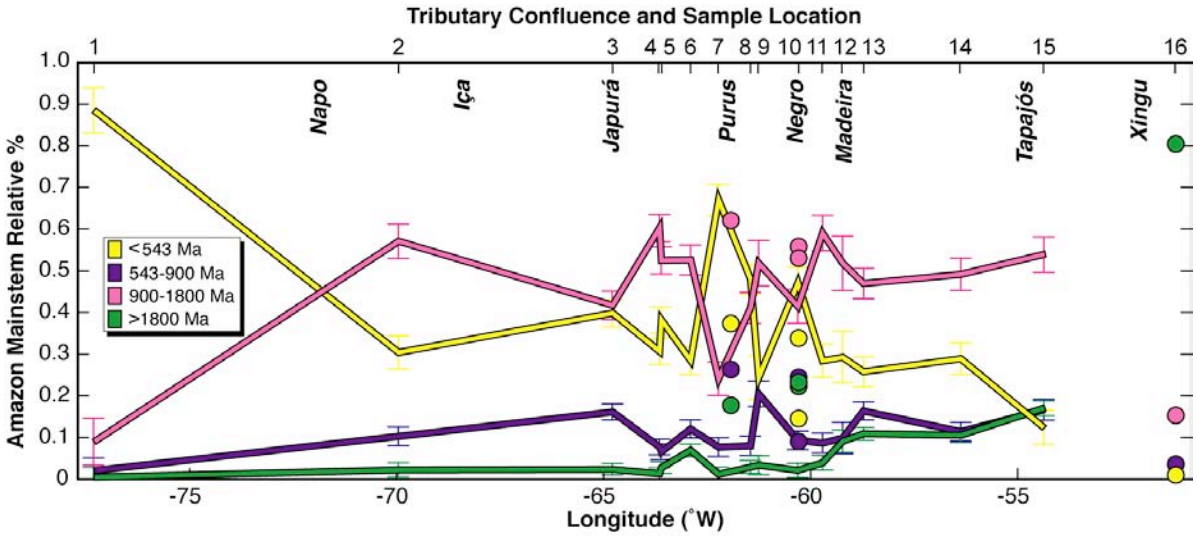

Figure 2.3- Downstream change in zircon age distribution along the Amazon River. Samples are sequenced west to east. Sample numbers along the top of the plot and age subdivisions are keyed to figure 2.1. Labels within the plot indicate location of major confluences. Proportions were calculated using probability density curves, error bars show uncertainties estimated using bootsrap methods (Appendix C). Filled points on plot show age distributions for tributary sands (Purus and Negro Rivers) and Amazon mouth sample (Rino *et al.*, 2004). The overall pattern shows an increase in old zircons (>1.8 Ga) at the expense of the young population (<543 Ma). Between sample localities #2 and #14, changes occur abruptly in a non-predictable manner. Major tributaries do not appear to disrupt age spectra to a significant extent.

Amazon age spectra (samples #11-14) are more dispersed and minor populations are more frequently present. Although the mid-late Phanerozoic and Mesoproterozoic modes are still dominant, modal magnitudes are generally less and variances are larger (Figure 2.2). As such, Paleoproterozoic and older zircon grains constitute a more significant proportion of lower Amazon age spectra than upstream.

The age distribution for Purus River sand (sample #17), like upper Amazon sand, is dominated by mid-Phanerozoic and Mesoproterozoic age modes. In contrast to upper Amazon samples, more Neo- and Paleoproterozoic zircons are present. Negro River sand, collected 150 river km from the Amazon confluence (locality #18), includes minor Phanerozoic and Neoproterozoic zircon but is dominated by Mesoproterozoic and Paleoproterozoic zircon populations. A second Negro River sand, collected only 10 km from the Amazon confluence (locality #19), includes a large Phanerozoic age mode as well as several significant Meso- and Paleoproterozoic populations. Because of proximity to the confluence and similarity to nearby Amazon River age spectra, it is likely that ages in this sand show the influence of meander-plain sediment mixing and do not reflect the primary, Negro River, age signature.

Estuarine Amazon River sand (locality #15) collected near the onset of tidal influence is devoid of any dominant age population (Figure 2.2). The sand lacks the significant middle-late Phanerozoic age mode present in all other fluvial samples and includes a significant Neoproterozoic population that is present only a minor population in other samples. Near the Amazon mouth, Rino *et al.* (2004) analyzed 369 zircon grains and found only a single Phanerozoic grain. Their distribution included minor Neo- and Mesoproterozoic age modes

and was dominated by Paleoproterozoic and Archean zircon grains, ages scarcely present upstream.

Discussion

Zircon age spectra are a catchment-wide product of several factors. The principal control on detrital age spectra is areal extent of a particular zircon age population within a drainage. Rock composition is also an important factor, Moecher and Samson (2006) contend that in extreme cases, Zr enriched terranes can contribute such an abundance of zircon that they effectively overwhelm age other age signals. Finally, source area denudation rate strongly influences regional zircon contribution. Since zircon is highly refractory under a range of surface weathering conditions (Fedo *et al.*, 2003), the majority of zircon present in the source remains intact during and after sedimentation (Speer, 1982). Taken together, zircon presence and regional denudation rate can be used to calculate idealized detrital zircon source yield (kg Myr^{-1} km^{-2}) with the relationship,

$$Yield = [Zr]_{WR} * \frac{mm_{zircon}}{mm_{Zr}} * ER * \rho_{WR} \quad (1)$$

where $[Zr]_{WR}$ is the whole rock Zr concentration in ppm, mm_{zircon} is the molar mass of zircon in g/mol, mm_{Zr} is the molar mass of Zr in g/mol, ER is the erosion rate in km/Myr, and ρ_{WR} is the bulk rock density in kg/m^3 (Figure 2.4). This relationship assumes all source rock Zr is partitioned into zircon and is transferred into the clastic load.

Utilizing this approach as well as measured data from northern South America (Stallard, 1985; Roddaz *et al.*, 2005; Georoc Expert Databases, http://georoc.mpch-mainz.gwdg.de/ [accessed July 2008]), Andean sources are predicted to contribute ~10x more zircon than either lowland exposed craton areas or lowland sedimentary deposits

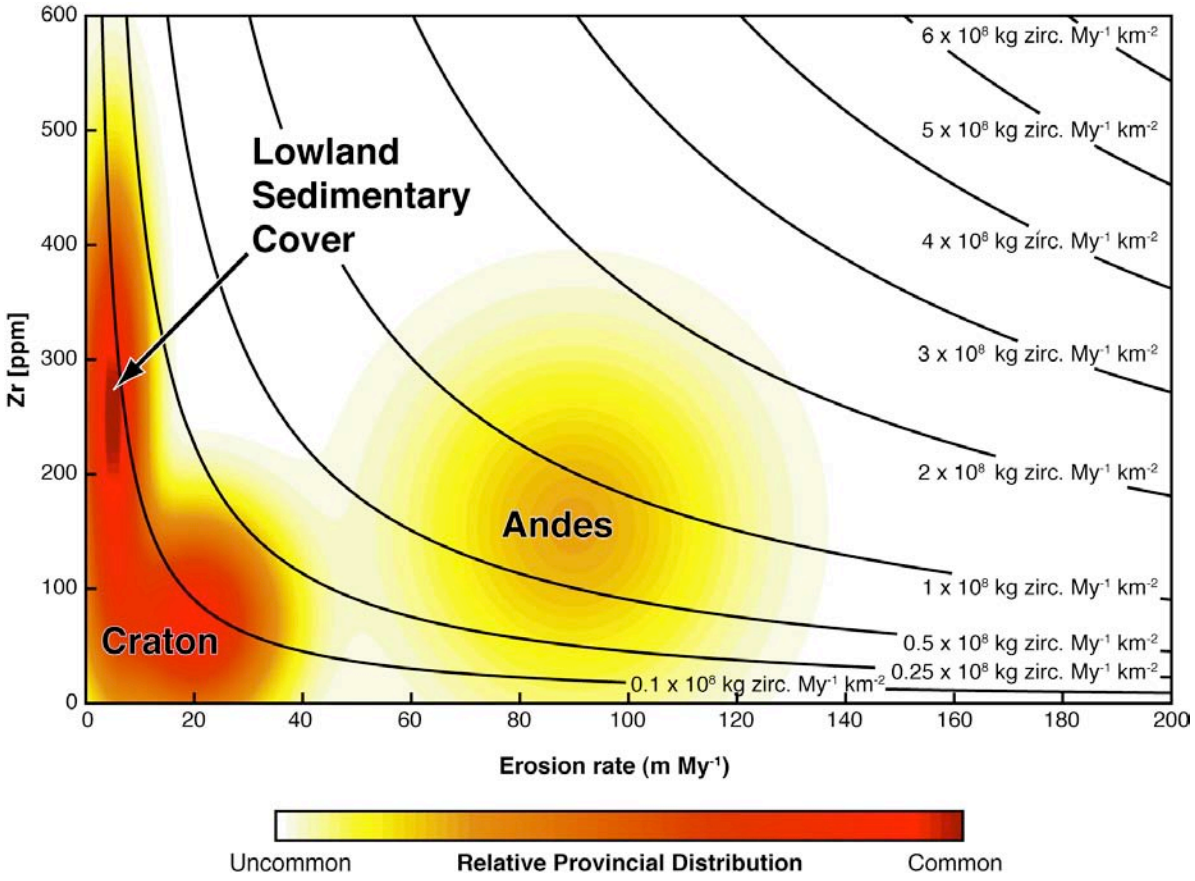

Figure 2.4- Idealized zircon yield for the most common rock types of the Amazon drainage basin. Andean areas contribute ~10x more zircon per unit area than rocks of lowland Amazonia. Yield curves were calculated assuming all Zr is partitioned into zircon and constant rock density (2.75 g/cm^3). Means and standard deviations used to calculate kernels for Zr content and weathering rates were taken from Stallard (1985), and calculated from data presented in Roddaz *et al.*, (2005), and large data compilations available as Georoc Expert Databases (http://georoc.mpch-mainz.gwdg.de/ [accessed July 2008]).

(Figure 2.4). Extrapolating these relationships across the entire area of the Amazon drainage, approximately 80% of zircon collected at the Amazon mouth are predicted to have been transported from the Andes, shield areas should contribute ~5% and lowland sedimentary rocks should contribute the ~15%.

Zircon provenance fidelity

In the simplest case, all age populations present in a drainage would be represented in detrital age spectra in similar abundance. For the Aguarico River comparison is straightforward because of its limited size and well known geology. Upstream of the sample locality, the 3,500 km^2 drainage exposes approximately 2% Precambrian basement, 40% Mesozoic and 12% Cenozoic igneous rock, 3% Paleozoic and Mesozoic metamorphic rock, and 40% Mesozoic and 3% Cenozoic sedimentary rock (Schobbenhaus and Bellizza, 2001). Cenozoic and Mesozoic zircons dominate detrital zircon ages, consistent with basin geology. Precambrian zircons grains make up 10% of the age distribution, which slightly over represents the presence primary sources of that age within the catchment, however, Precambrian grains are probably greatly underrepresented if metamorphic and sedimentary rocks, which likely contain abundant recycled Precambrian zircons (Chew *et al.*, 2007; Martin-Gombojav and Winkler, 2008), are considered. This indicates that age spectra are not simple area integrated mixtures and that factors other than presence contribute to formation of detrital zircon age spectra.

As Andean tributaries flow east and gradient decreases, direct comparison of age spectra to basement geology becomes difficult because primary zircon age populations are mixed with floodplain deposits that have complex and uncertain age distributions. At Leticia, Colombia (locality #2), the drainage area sampled reaches 9×10^5 km^2, 60% of which is

covered by Cenozoic sedimentary deposits (Schobbenhaus and Bellizza, 2001). Interestingly, although Phanerozoic igneous rocks make up just ~10% of the drainage area at Leticia and only ~4% near the Negro confluence (locality #10); grains of that age constitute 24-67% of the total age probability in the stretch. In contrast, early Mesoproterozoic zircons (~1.1 Ga) constitute a dominate population in upper Amazon samples while exposure of Mesoproterozoic basement rocks is rare (Miscovic and Schaltegger, 2008). Mesoproterozoic grains could potentially have been derived from Andean Paleozoic metamorphic rocks; however, if that were the case, a significant Neoproterozoic age population would also be expected (Chew *et al.*, 2007). Although ages found in upper Amazon samples are consistent with basement ages found upstream, population proportions cannot be explained by source exposure. Also, despite gross similarities between upper Amazon samples, changes between samples do not occur in a predictable manner (Figure 2.3). Minor modes present in several samples are not present in others and significant and unexplained changes in modal proportions of major age populations occur.

Age spectra for sand colleted on the lower Amazon River are characterized by an increase in the proportion of Precambrian grains, mostly older than 1.5 Ga. This change is consistent with addition of sand from cratonal tributaries like the Negro River (Figure 2.2).

At the onset of tidal influence, the proportion of Phanerozoic age probability, which is ≥24% for all fluvial samples, falls to 12% (locality #15), and the proportion Neoproterozoic and early Mesoproterozoic and older detrital grains increases compared to strictly fluvial samples. Similarly, Rino *et al.* (2004) found sand that contained <1% Phanerozoic zircon near the Amazon mouth (locality #16) although their sample was collected near the mouth of the Vila Nova ou Anauerapucu River and could represent ages of

locally derived sand (Figure 2.1; Tassinari *et al.*, 2000). At the present time, Amazon Estuary detrital zircon data are inadequate to understand why Andean zircon ages disappear from estuarine age spectra.

Similarity of age spectra

Differences between mainstem samples are not an artifact of sampling during data collection but reflect real population differences among sand samples. Samples collected in close proximity are expected to give similar results if sediment is well mixed. The Kolmogorov-Smirnov test (Press *et al.*, 1986; Fletcher *et al.*, 2007) successfully rejects the hypothesis of age spectrum equivalency at a 95% level of confidence for all but two consecutive upper Amazon samples, indicating that mixing is poor for age spectra in that river reach or spectra are changed via addition of externally derived zircon (Table 2.2). For the lower Amazon, equivalency could not be rejected for four consecutive samples, suggesting that better mixing occurs or that addition new zircon with unique ages is minimal in that stretch. Comparison of mainstem samples with similar grain size does not indicate that poor spectral mixing is related to grain size sorting.

Basin-wide trends

Although estimating zircon source yield based on presence has merit in drainages with well-known geology like those studied by Cawood *et al.* (2003) and Link *et al.* (2005), observation of age spectra from Amazon sub-catchments shows that for large drainages, a basin-wide zircon budget is difficult to construct. Adding complexity to the task is the fact that sedimentation across the majority of Amazonia is a transport-limited process, and substantial deposition and recycling occurs on the floodplain (Mertes *et al.*, 1996; Dunne *et*

Table 2.2- Table of Kolmogorov-Smirnov probabilities for comparison of Amazon River detrital zircon age spectra. Tests were run at a confidence level of 95%. For probabilities less than 0.05, the null hypothesis (distribution equivalency) is rejected. Values where the null hypothesis has failed to be rejected are highlighted in bold. Values that compare samples collected from similar sand grain sizes are italicized.

	Andes	Upper Amazon/Solimões									Lower Amazon				Amazon Estuary		Lowland Tributaries			Mainstem Compilation
Samp.	1	2	3	4	5	6	7	8	9	10	11	12	13	14	15	16	17	18	19	(#2-15)
1	-	*1 E-19*	*1 E-16*	5 E-20	1 E-14	1 E-21	1 E-09	9 E-12	1 E-19	8 E-16	3 E-20	6 E-19	3 E-16	5 E-20	2 E-27	6 E-44	2 E-14	3 E-30	5 E-10	7 E-29
2		-	*0.0048*	0.0379	**0.0559**	**0.2308**	1 E-09	0.014	**0.8799**	0.01	**0.9998**	**0.1308**	**0.3383**	**0.1538**	1 E-05	2 E-53	**0.4833**	1 E-04	0.0016	0.043
3			-	0.0052	**0.1704**	5 E-04	1 E-06	**0.5783**	**0.0514**	**0.763**	0.0044	0.0029	0.0199	3 E-04	4 E-10	9 E-70	0.0256	2 E-09	3 E-06	0.0207
4				-	**0.3548**	0.0056	4 E-10	0.0013	**0.4188**	0.0072	**0.2147**	0.0155	0.0031	0.0031	1 E-08	3 E-69	**0.0747**	1 E-07	2 E-05	0.0147
5					-	0.0127	4 E-07	**0.0911**	0.0142	**0.1823**	**0.0717**	0.0419	0.0409	0.0073	7 E-08	1 E-68	**0.1094**	5 E-07	7 E-05	0.0420
6						-	1 E-10	0.0016	***0.7724***	*0.0069*	**0.1518**	**0.9994**	**0.9652**	**0.9909**	0.0166	5 E-55	**1**	0.0045	**0.1015**	0.0458
7							-	0.0018	1 E-09	1 E-04	6 E-10	1 E-10	5 E-08	*1 E-10*	*5 E-19*	1 E-58	1 E-06	3 E-22	1 E-06	1 E-14
8								-	0.0012	**0.4626**	0.0046	0.0038	0.0052	*0.0013*	*3 E-08*	4 E-59	0.0365	4 E-59	3 E-05	3 E-03
9									-	*0.0082*	**0.9045**	**0.5014**	**0.8464**	**0.5838**	0.002	1 E-34	**0.8836**	0.0132	0.0137	0.0232
10										-	0.0076	0.0119	0.0265	0.0069	1 E-07	3 E-56	**0.0598**	0.0069	0.0001	0.0138
11												**0.097**	**0.2653**	**0.0922**	6 E-06	2 E-50	**0.3895**	1 E-04	0.0008	**0.0895**
12												-	**0.6943**	**0.9997**	0.0118	4 E-53	**0.9891**	0.0033	**0.0657**	**0.0501**
13													-	**0.9532**	**0.2585**	3 E-23	**1**	**0.1071**	**0.3667**	0.0397
14														-	*0.0403*	*9 E-47*	**1**	0.0087	**0.1938**	0.0179
15															-	*6 E-39*	**0.1893**	0.0403	**0.0515**	7 E-10
16																-	1 E-23	9 E-47	2 E-20	9 E-167
17																	-	**0.1138**	**0.2879**	**0.2324**
18																		-	0.0425	3 E-10
19																			-	0.0001

al., 1998). Because few detrital zircon age analyses exist for Amazonian sedimentary and metasedimentary rocks, and active floodplain aggradation occurring, there is little reason to expect Amazon River detrital zircon age spectra to proportionally reflect the ages and erosion rates found throughout the drainage. In spite of the complexity of zircon transport in the Amazon, it is possible to observe obvious trends that exist between sample localities and to comment on the importance of several processes that are expected to alter age spectra along the course of the river.

Assuming individual age spectra are regionally representative, which is likely a poor assumption, the most abrupt changes occur near the Andean Front and within the estuary (Figure 2.3). The decrease in the proportion of Phanerozoic grains proximal to the Andes can be explained by the dramatic increase in drainage area and diversity of basement rock types between localities #1 and #2. Although Aguarico ages generally confirm the geology of its catchment, they characterize only a small region of the Amazonian Andes. The age spectrum for the Leticia, Colombia sand, is consistent with derivation from a mixture of Phanerozoic Andean igneous rocks and high-grade metamorphic rocks of Peru and Ecuador (Chew *et al.*, 2007; Miscovic and Schaltegger, 2008). The change that appears to occur in the Amazon Estuary is yet to be explained.

Between the Andes and the Amazon estuary (localities #2-14), age spectra change surprisingly little. The proportion of Phanerozoic grains ranges from 24-67% and shows a weak decline with longitude, the proportion of 900-1800 Ga grains ranges from 24-59%, and the proportion of 543-900 Ma and >1800 Ma grains are below 20%. Although dramatic swings in relative proportions occur, such as the 39% increase in the proportion of Phanerozoic grains in the 80 km between localities #6 and #7, they do not define trends. In

fact, for sand collected near Óbidos (locality #14), 3000 km+ distant from Andean source rocks, the proportion of uniquely Andean age probability remains at ~30%. If the presence of Precambrian grains in Andean rocks are taken into account, the proportion of Andean derived grains could be as high as ~90% if the Leticia sand is taken as the 'total' Andean age signature. When these results are compared to those for the smaller Frankland River (Cawood *et al.*, 2003), commonalities appear. Amazon and Frankland River age spectra are dominated by grain ages of the highest relief areas within their drainages. In the Amazon Basin, the greatest relief exists in the Andes, whereas in the Frankland catchment the dominant age population present at the river mouth outcrops mid-system where a significant increase in river gradient occurs.

Why do age spectra change away from source?

Destruction

Zircon is one of the most stable minerals in sedimentary systems (Kalsbeek, 1967), especially at sizes typically utilized for geochronology (Poldervaart, 1955). Its hardness (7.5) and imperfect or poor cleavage (Deer *et al.*, 1992) make it more resistant to abrasion than most other minerals although destruction of less resistant metamict grains has been suggested as a mechanism to preferentially destroy zircons from high-U sources and concentrate low- to moderate-U zircons (Fedo *et al.*, 2003). Undoubtedly, some abrasion does occur during transport, as evidenced by broken and rounded zircon grains in Amazon sediments. Therefore as transport distance increases, an overall decrease in zircon grain size should occur.

Assessing metamict/high-U grain loss is difficult using the techniques employed in this study as no U concentration measurements were made. However, assessing grain size as a function of transport distance is possible. Phanerozoic zircons in upper Amazon sands are

generally larger and than lower Amazon zircons (Figure 2.5) although median zircon size correlates positively with median sand size (Table 2.2) so comparisons of zircon size from different host-sand sizes is tenuous. Comparison of four fine-grained sands (samples #7,8,14,15) that span 1,000 river km show a constant decrease in median Phanerozoic zircon size. In spite of notable differences in zircon size between sand samples, a general zircon size decrease with transport distance is noted. Therefore, it seems possible that long distance transport could preferentially remove far-traveled age populations and preferentially enriches age spectra with more proximal source signatures but this process appears to have a minor affect an Amazon age spectra.

Dilution

Lowland areas with no Andean fluvial links contribute ~70% of the water discharged at the Amazon mouth (Gibbs, 1967; Meade, 1994) indicating that a considerable amount of the total Amazon sediment output may be cratonally derived. However, only 5-20% of Amazon suspended sediment is believed to come from the Amazonian lowlands (Gibbs 1967; Meade, 1994). For lower Amazon bedload sediment, composition and detrital quartz morphology suggest an increased proportion of cratonal detritus (Franzinelli and Potter, 1985; McDainel, 1998), which is corroborated by the increase in the proportion of Mesoproterozoic and older zircon grains as the system progresses eastward (Figure 2.3). In the simplest case, large tributaries with distinctive age signatures should act as point sources and notable changes should occur in mainstem age spectra; however, no major changes appear to occur below large confluences (Figure 2.3). Although age spectra change between headwaters and tidewater, the Andean age signature in not significantly diluted as the river crosses lowland Amazonia.

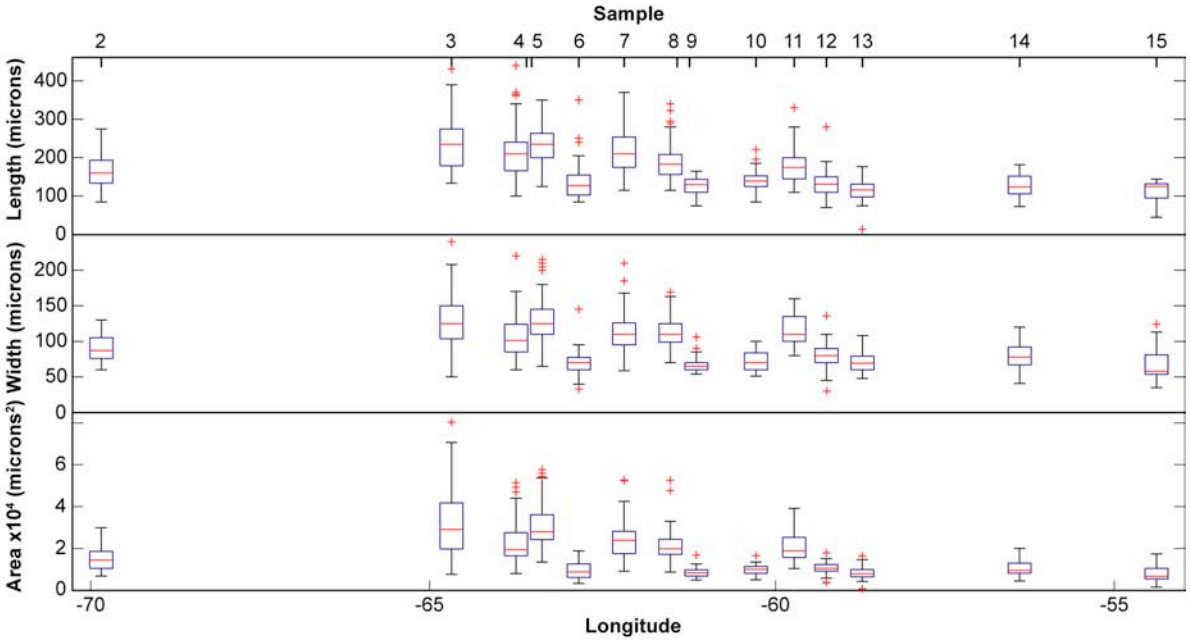

Figure 2.5- Box and whisker plot of grain dimensions for Phanerozoic Amazon mainstem zircons. Red lines in box indicate sample median, lower and upper box edges show the 25 and 75 percentiles, respectively, and whiskers include all data points that are not considered sample outiers (denoted by red crosses; see Martinez and Martinez, 2002). Grain area is the calculated product of width and length. Upper Amazon zircon grains are generally larger and have wider size ranges than lower Amazon grains; however, changes in zircon size do not occur predictably.

Aggradation/sequestration/placer formation

Both temporary storage and basin subsidence can act to sequester zircon grains at intermediate locations for long periods of time. Both storage and sequestration occur on a large scale in the Amazon basin. In fact, most of the material eroded from the Andes is deposited in the sub-Andean sedimentary basin and reworked in rapidly changing foreland and lowland river systems (Irion *et al.*, 1995). Johnsson and Meade (1990) documented sediment recycling by meandering at Macuapanim Island, Brazil, that reentrained floodplain sediment ranging in age between 6 and 125 ka. Räsänen *et al.* (1987) estimated that in local areas of subsidence within the Andean foreland, Quaternary deposit thickness exceeds 1,500 m.

When sediment is lost to aggradation, it is reasonable to assume that the coarsest and/or densest material is preferentially sequestered in proximal locations. Placer formation is common in stable cratonic-settings where depositional energies are high enough for sediment reworking (Robb, 2005) and zircon is one of the most common placer minerals (Force, 1991). Hypothetically, temporary sequestration coupled with foreland subsidence could cause Andean derived zircon grains to be preferentially deposited in western Amazonia and downstream Amazon age spectra to be biased toward cratonal ages. It is difficult to assess how large a role placer formation and riverbed aggradation play in changing zircon age spectra for the Amazon. Andean derived zircon grains are likely lost to the process at a higher rate that grains derived directly from the craton; however, enough uniquely Andean grains are present along the fluvial Amazon to identify the Andes as a significant zircon contributor.

Temporary storage/Cannibalism?

Since 66%+ of the Earth's surface is covered by sedimentary deposits (Blatt, 1992) and large rivers tend to traverse wide alluvial plains prior to reaching base level, sediment recycling is inevitable and can occur on a very large scale. The Amazon Basin is no exception; Cenozoic sedimentary deposits underly >50% of the catchment and a large proportion of active sediment is recycled. Dunne *et al.* (1998) estimated that annual input into the Brazilian Amazon is >100% output at the onset of the Amazon estuary and that net accumulation occurs on the floodplain. This means that a great deal of Andean derived sediment spends time in storage on the floodplain and that detrital zircon age spectra could deviate from those expected from solely primary zircon sources. Quantifying the ratio of first-cycle zircon to reworked grains in a sample is difficult and more sophisticated techniques, such as geo/thermochronologic double dating (e.g. Campbell *et al.*, 2005) may be better suited to answer this question; however, preliminary conclusions may be drawn from our data.

Detrital zircon data for three poor-moderately consolidated formations with unique age spectra that crop out along the banks of the lower Amazon allow for observation of the affects of floodplain recycling. Age spectra for the areally restricted Miocene Iranduba and Novo Remanso formations and the extensive Late Cretaceous Alter do Chão Formation (Mapes , this text) are uniformly Early Proterozoic detrital and dissimilar to any observed age spectra for the mainstem Amazon (Mapes, this text). Even after ~1000 km of flow that is sometimes in direct contact and always in close proximity to these deposits, the Early Proterozoic zircon age population remains minor in Amazon age spectra. Although Miocene and Cretaceous deposits are not a perfect analogue for recent floodplain sediments because of

their slightly higher degree of consolidation, addition of these deposits to active river sediment seems to have little affect on Amazon age spectra.

How thorough is mixing?

Local age spectrum similarity has never been directly evaluated for modern sediment but DeGraaff-Surpless *et al.* (2003) suggested that thorough mixing is not a safe assumption in fluvial deposits. If bedload homogenization is a normal phenomenon, Amazon River sediment should be well mixed because of long transport distance and duration and because flow is relatively constant year-round. Significant differences exist between samples collected in close proximity to one another (Table 2.3) suggesting poor sediment mixing (Figure 2.2). Comparison of individual sample spectra to a composite mainstem age distribution (samples #2-15; Table 2.3) reveals that thirteen mainstem samples are statistically different from the composite dataset, indicating that they do not represent a homogeneous background population. Although age modes do correlate with the source rock ages, modal magnitudes do not reflect catchment outcrop proportion or relative sediment contribution. Until local controls on detrital zircon population transport are better understood in a range of sedimentary environments (e.g. Lawrence, 2008), we suggest that age spectra modal magnitudes continue to be used as a qualitative measure of source contribution.

Conclusions

Age spectra for Amazon River sand record the range of sources that exist within the drainage basin in a qualitative sense and prove that long-distance fluvial transport of detrital zircon populations is possible. Zircons with uniquely Andean ages make up ~30% of the total age spectrum in sand collected at the onset of the Amazon estuary, 3000+ km displaced from

their igneous/high-grade metamorphic sources after transport in what is close to the worst-case scenario in terms of harshness of chemical weathering, sediment trapping on highly-vegetated banks, and aggradation in an active foreland basin. The actual proportion of Andean derived grains is likely larger, possibly as high as 90%, if Precambrian grains recycled from Andean sedimentary and metasedimentary rocks are considered. Furthermore, it does not appear that destruction, aggradation, dilution, or recycling have a significant effect on altering the primary, Andean age signature. These results indicate that the major control on zircon age spectra is relative stream gradient: areas with higher relief contribute the most zircon. Significant differences between age spectra, even for samples collected in close proximity, indicate that sediment mixing in the fluvial environment is not thorough enough to yield a characteristic and uniform age signal and therefore, age population proportions should not be used to quantitatively assess catchment geology or geography.

References

Admidon, W.H., Burbank, D.W., and Gehrels, 2005, U-Pb zircon ages as a sediment mixing tracer in the Nepal Himalaya; Earth and Planetary Science Letters, v. 235, p. 244-260.

Andersen, T., 2005, Detrital zircons as tracers of sedimentary provenance; limiting conditions from statistics and numerical simulation; Chemical Geology, v. 216, p. 249-270.

Archer, A.W., 2005, Review of Amazonian depositional systems. Special Publication of the International Association of Sedimentologists, v. 35, 17-39.

Atherton, M.P., and Pedford, N., 1996, Plutonism and the growth of Andean Crust at 9˚S from 100 to 3 Ma: Journal of South American Earth Science, v. 9, p. 1-9.

Bassett, K.N., 2000, Isotopic provenance and terrane tectonics: A warning about sediment transport distances; Geological Society of Australia, Abstracts, n. 59, p. 24.

Berry, R.F., Jenner, G.A., Meffre, M.N., and Tubrett, M.N., 2001, A North American provenance for Neoproterozoic to Cambrian in Tasmania? Earth and Planetary Science Letters, v. 192, p. 207-222.

Birkett, C.M., Mertes, L.A.K., Dunne, T., Costa, M.H., and Jasinski, M.J., Surface water dynamics in the Amazon Basin: Application of satellite radar altimetry; Journal of Geophysical Research, v. 107, p. 8059-8080.

Black, L.P., Kamo, S.L., Allen, C.M., Davis, D.W., Aleinikoff, J.N., Valley, J.W., Mundil, R., Campbell, I.H., Korsch, R.J., Williams, I.S., Foudoulis, C., 2004, Improved 206Pb/238U microprobe geochronology by the monitoring of a trace-element-related matrix effect; SHRIMP, ID-TIMS, ELA-ICP-MS and oxygen isotope documentation for a series of zircon standards; Chemical Geology, v. 205, p. 115-140.

Blatt, H., 1992, Sedimentay Petrology, W.H. Freeman and Company, New York, 514 p.

Bodet, F., and Schärer, U., 2000, Evolution of the SE-Asian continent from U-Pb and Hf isotopes in a single grain of zircon and baddeleyite from large rivers; Geochimica et Cosmochimica Acta, v. 64, p. 2067-2091.

Brito Neves, B.B. de, Fuck, R.A., Cordani, U.G., and Thomaz Filho, A., 1984, Influence of major basement structures on the evolution of the major sedimentary basins of Brazil: a case of tectonic heritage; Journal of Geodynamics, v. 1, p. 495-510.

Brito Neves, B.B., 1991, Tectonic evolution of South America during the Late Proterozoic: Precambrian Research, v. 53, p. 23-40.

Burke, K., and Lytwyn, J., 1993, Origin of the rift under the Amazon Basin as a result of continental collision during pan-African time. Int. Geol. Review. v. 35, pp. 881-897

Campbell, K.E. Jr., Heizler, M., Romero-Pittman, L., and Prothero, D.R., 2001, Upper Cenozoic chronostatigraphy on the southwestern Amazon basin: Geology, v. 29, p. 595-598.

Campbell, I.H., Reiners, P.W., Allen, C.M., Nicolescu, S., and Upadhyay, R., 2005, He-Pb double dating of detrital zircons from the Ganges and Indus Rivers: implication for quantifying sediment recycling and provenance studies; Earth and Planetary Science Letters, v. 237, p. 402-432.

Caputo, M.V., 1984, Stratigraphy, tectonics, paleogeography of northern basins of Brazil: PhD dissertation, University of California, Santa Barbara, 583 p.

Cawood, P. A., Nemchin, A.A., Freeman, M., and Sircombe, K.N., 2003, Linking source and sedimentary basin: Detrital zircon record of sediment flux along a modern river system and implications for provenance studies; Earth and Planetary Science Letters, v. 210, p. 259-268.

Chang, Z., Vervoort, J.D., McClelland, W.C., Knaack, C., 2006, U-Pb dating of zircon by LA-ICP-MS: Geochemistry, Geophysics, Geosystems, v. 7, 14 p.

Chew, D.M., Schaltegger, Košler, J., Whitehouse, M.J., Gutjahr, M., Spikings, R.A., and Miškovic, A., 2007, U-Pb geochronologic evidence for the evolution of the Gondwanan margin of the north-central Andes: Geological Society of America Bulletin, v. 119, p. 697-711.

Clemens, K. E., and Komar, P. D., 1988, Oregon beach-sand compositions produced by the mixing of sediments under a transgressing sea: Journal of Sedimentary Petrology, v. 58, p. 519-529.

Cobbing, E. J., 1999, The Costal Batholith of Peru, in Castro, A., Fernández, C. and Vigneresse, J.L. eds., Understanding granites: integrating new and classical techniques: Geological Society Special Publication, n. 168, London, 278 p.

Condie, K.C., Beyer, E., Belousova, E., Griffin, W.L., and O'Reilly, S.Y., 2005, U-Pb isotopic ages and Hf isotopic composition of single zircons: the search for juvinile Precambrian continental crust; Precambrian Research, v. 139, p. 42-100.

Costa, J.B.S., Hasui, Y., Borges, M. S., and Bemerguy, R.L., 1995, Arcabouço tectônico Mesozóico-Cenozóico da região da calha do Rio Amazonas; Geociências, v. 14, p. 77-103.

Costa, J.B.S., Bemerguy, R.L., Hasui, Y., and Borges, M. S., 2001, Tectonics and paleogeography along the Amazon River; Journal of South American Earth Sciences; v. 14, p. 335-347.

Cunha, P.R.C., Gonzaga, F.G., Coutinho, L.F.C., Feijo, F.J., 1994, Bacia do Amazonas, Boletim de Geociências da Petrobras; v. 8, p. 47-55.

DeCelles, P.G., Kapp, P., Ding, L., and Gehrels, G.E., 2007, Late Cretaceous to middle Tertiary basin evolution in the central Tibetan Plateau: Changing environments in response to tectonic partitioning, aridification, and regional elevation gain: Geological Society of America Bulletin, v. 119, p. 654-680.

Deer, W.A., Howie, R.A., Zussman, J., 1992, An introduction to the rock-forming minerals, 2nd edition:Prentice Hall, London, 696 p.

DeGraaff-Surpless, K.A., Mahoney, J.B., Wooden, J.L., and McWilliams, M., 2003, Lithofacies control in detrital zircon provenance studies; insights from the Cretaceous Methow Basin, southern Canadian Cordillera: Geological Society of America Bulletin, v.115, p. 899-915.

de Oliveira, A.I., 1956, Brazil, in Jenks, W.F., Handbook of South American geology: an explanation of the geologic map of South America: Memoirs: Boulder, Geological Society of America, 309 p.

Dickinson, W.R., and Gehrels, G.E., 2003, U-Pb ages of detrital zircons from Permian and Jurassic eolian sandstones of the Colorado Plateau, USA: paleogeographic implications. Sedimentary Geology. v. 163, p. 29-66.

Dickinson, W.R., and Gehrels, G.E., 2009, U-Pb ages of detrital zircons in Jurassic eolian and associated sandstones of the Colorado Plateau: Evidence for transcontinental dispersal and intraregional recycling of sediment: Geological Society of America Bulletin, v. 121, p. 408-433.

Dodson, H., Compston, W., Williams, I.S., and Wilson, J.F., 1988, A search for detrital zircons in Zimbabwean sediments. Journal of the Geological Society of London, v. 145, p. 977-983.

Domínguez, C., 2004, Importance of rivers for the transportation system of the Amazon, *in* Aragón, L.E., and Clusener-Godt, M., Núcleo de Altos Estudios Amazónicos. Issues of local and global use of water from the Amazon. Montevideo, UNESCO, p.77-100.

Driscoll, N.W., and Karner, G.D., 1994, Flexural deformation due to Amazon Fan loading: A feedback mechanism affecting sediment delivery to margins: Geology, v. 22, p. 1015-1018.

Dunne, T., Mertes, L.A.K., Meade, R.H., Richey, J.E., and Forsberg, B.R., 1998, Exchanges of sediment between the floodplain and channel of the Amazon River in Brazil; Geological Society of America Bulletin, v. 110, pp. 450-467.

Eriksson, K.A., Campbell, I.H., Palin, J.M., and Allen, C.M., 2003, Predominance of Grenville magmatism recorded in detrital zircons from modern Appalachian rivers; Journal of Geology, v. 111. P. 707-717.

Fedo, C.M., Sircombe, K.N., Rainbird, R.H., 2003, Detrital zircon analysis of the sedimentary record: Reviews in Mineralogy and Geochemistry, v. 53, p. 277-303.

Feijó, F.J. and Souza, R.G., 1994, Bacia do Acre; Boletim de Geociências da Petrobras; v. 8, p. 9-16.

Fletcher, J.M., Grove, M., Kimbrough, D., Lovera, O., and Gehrels, G.E., 2007, Ridge-trench and the Neogene tectonic evolution of the Magdalena shelf and southern Gulf of California: insights from detrital zircon U-Pb ages from the Magdalena fan and adjacent areas: Geological Society of America Bulletin, v. 1119, p. 1313-1336.

Force, E.R., 1991, Placer deposits: in Force, E.R., Eidel, J.J., and Maynard, J.B., Sedimentary and diagenetic mineral deposits: a basin analysis approach to exploration, Reviews in economic geology, v. 5, p. 131-140.

Folk, R.L., 1965, Petrology of sedimentary rocks: Austin, TX, Hemphill's, 159 p.

Franzinelli, E., Igreja, H., 2002, Modern sedimentation in the Lower Negro River, Amazonas State, Brazil: Geomorphology, v. 44, p. 259-271.

Franzinelli, E., Potter, P.E., 1985, Areias recentes dos rios da Bacia Amazônica: comosições petrográfica, textural e química: Revista Brasileira de Geociéncias, v. 15, p. 213-220.

Frihy, O.E., Lotfy, M. F., and Komar, P.D., 1995, Spatial variations in heavy minerals and patterns of sediment sorting along the Nile Delta, Egypt: Sedimentary Geology, v. 97, p. 33-41.

Garzione, C.N., Hoke, G.D., Libarkin, J.C., Withers, S., MacFadden, B., Eiler, J., Ghosh, P., and Mulch, A., 2008, Rise of the Andes: Science, v. 320, p. 1304-1307.

Gehrels, G.E., Dickinson, W.R., Ross, G.M., Stewart, J.H., and Howell, D.G., 1995, Detrital zircon reference for Cambrian to Triassic miogeoclinal strata of western North America: Geology, v. 23, p. 831-834.

Gibbs, R.J., 1967, The geochemistry of the Amazon River system: Part 1. The factors that control the salinity and the composition and concentration of the suspended solids: Geological Society of America Bulletin, v. 78, p. 1,223-1,232.

Goldstein, S.L., Arndt, N.T, and Stallard, R.F., 1997, The history of a continent from U-Pb ages of zircons from Orinoco River sand and Sm-Nd isotopes in Orinoco basin river sediments: Chemical Geology, v. 139, p. 271-286.

Hanchar, J.M., and Watson, E.B., 2003, Zircon saturation thermometry: Reviews in Mineralogy and Geochemistry, v. 53, p. 89-112.

Hearn, P., Hare, T., Schruben, P., Sherrill, D., LaMar, C., and Tsushima, P., 2000, Global GIS database: Digital Atlas of Central and South America: United States Geological Survey, Digital Data Series DDS-62-A.

Hoskin, P.W.O., and Schaltegger, U., 2003, The composition of zircon and igneous and metamorphic petrogenisis: Reviews in Mineralogy and Geochemistry, v. 53, p. 27-62.

Iizuka, T., Hirata, T., Komiya, T., Rino, S., Katayama, I., Motoki, A., and Maruyama, S., 2005, U-Pb and Lu-Hf isotope systematics of zircons from the Mississippi River sand: Implications for reworking and growth of continental crust; Geology, v. 33, p. 485-488.

Irion, G., Müller, de Mello, J.N., and Junk, W.J., 1995, Quaternary geology of the Amazonian Lowland: Geo-Marine Letters, v. 15, p. 172-178.

Jenks, W.F., 1954, Handbook of South American geology; an explanation of the geologic map of South America, Geological Society of America, 378 pgs.

Johnsson, M.J., 1993, The system controlling the composition of clastic sediments, *in* Johnsson, M.J., and Basu, A. eds., Processes controlling the composition of clastic sediments: Geological Society of America Special Paper 284, p. 1-19.

Johnsson, M.J., and Meade, R.H., 1990, Chemical weathering of fluvial sediments during alluvial storage: the Macuapanim Island point bar, Solimões River, Brazil: Journal of Sedimentary Petrology, v. 60, p. 827-842.

Kalsbeek, F., 1967, Evolution of zircons in sedimentary system and metamorphic rocks: a discussion; Sedimentology, v. 8, p. 163-167.

Krook, L., 1992, Evidence of Amazon provenance of a part of the sandy sediment in the coastal and shelf areasof the Guianas; in Prost, M.T., ed., Evolution des littoraux de Guyane et de la Zone Caribe méridionale pendent le Quaternarie: IGCP Project 274, Paris, Collections Colleques et Seminaires Institut Français de Recherche Scientifique Pour Le Développement en Coopération (ORSTOM) Editions, p. 307-319.

Lawrence, R.L., 2007, Testing for hydrodynamic fractionation of zircon populations in a sedimentary microenvironment: Senior thesis, Williams College, Williamstown, MA, 84 p.

Lawrence, R.L., Cox, R., Mapes, R.W., and Coleman, D.S., 2008, Hydrodynamic fractionation of zircon age populations in fluvial transport: Eos Transactions AGU, 89 (53), Fall Meeting Supplement, Abstract H51J-07.

LeFavour, G., and Alsdorf, D., 2005, Water slope and discharge in the Amazon River estimated using the shuttle radar topography mission digital elevation model: Geophysical Research Letters, v. 32, 5 p.

Li, M. Z., and Komar, P. D., 1992, Longshore grain sorting and beach placer formation adjacent to the Columbia River: Journal of sedimentary Petrology, v. 62, p. 429-441.

Link, P.K., Fanning, C.M., Beranek, L.P., 2005, Reliability and longitudinal change of detrital zircon age spectra in the Snake River system, Idaho and Wyoming: an example of reproducing the bumpy barcode: Sedimentary Geology, v. 182, p. 101-142.

Mapes, R.W., this text, Late Cretaceous to modern fluvial evolution of Amazonia and significance of the Purus Arch: Ph.D. dissertation, University of North Carolina at Chapel Hill, 27 p.

Martin-Gombojav, N., and Winkler, W., 2008, Recycling of Proterozoic crust in the Andean foreland of Ecuador: implications for orogenic development of the Northern Andes: Terra Nova, v. 20, p. 22-31.

Martinez, W.L., and Martinez, A.R., 2002, Computational Statistics Handbook with MATLAB, Chapman & Hall/CRC Publishing, Boca Raton, Florida, 591 p.

McDaniel, D.K., 1998, Provenance and weathering history of Amazon sediment; Ph.D. Dissertation, SUNY-Stony Brook, 188 p.

Meade, R.H., 1994, Suspended sediment of the modern Amazon and Orinoco Rivers; Quaternary International, v. 21, p. 29-39.

Mertes, L.A., Dunne, T., and Martinelli, L.A., 1996, Channel-floodplain geomorphology along the Solimões-Amazon River, Brazil. Geological Society of America Bulletin, v. 108, p. 1089-1107.

Miller, C.F., McDowell, S.M., and Mapes, R.W., 2003, Hot and cold granites? Implications of zircon saturation temperatures and preservation of inheritance: Geology, v. 31, no. 6, p. 529-532.

Milliman J.D., Summerhayes, C.P., Barretto, H.T., 1975, Quaternary sedimentation on the Amazon continental margin: a model: Geological Society of America Bulletin, v. 86, 610-614.

Miscovic, A., Schaltegger, U., 2008, Crustal growth along a 1.1 Ga non-collisional cratonic margin: U-Pb and Lu-Hf evidence from the Peruvian Eastern Cordillera: Goldschmidt Conference Abstracts, Vancouver, British Columbia, Canada, p. A635.

Moecher, D.P., and Samson, S.D., 2006, Differential zircon fertility of source terranes and natural bias in the detrital zircon record: implications for sedimentary provenance analysis: Earth and Planetary Science Letters, v. 247, p. 252-266.

Morton, A. C., and Johnsson, M. J., 1993, Factors influencing the composition of detrital heavy mineral suites in Holocene sands of the Apure River drainage basin, Venezuela, in Johnsson, M. J., and Basu, A., eds., Processes Controlling the Composition of Clastic Sediments: Special Paper: Boulder, Geological Society of America, p. 171-185.

Mosmann, R., Falkenhein, F.U.H., Gonçalves, A., Nepomuceno Filho, F., 1987. Oil and gas potential of the Amazon Paleozoic Basin: in Halbouty, M.T., ed., Future petroleum provinces of the world, AAPG Memoir 40, p. 207-241.

Nemchin, A.A., and Cawood, P.A., 2005, Discordance of the U-Pb system in detrital zircons: Implication for provenance studies of sedimentary rocks: Sedimentary Geology, v. 182, p. 143-162.

Pell S.D., Williams, I.S., and Chivas, A.R., 1997, The use of zircon-age fingerprints in determining the protosource for some Australian dune sands: Sedimentary Geology, v. 109, p. 233-260.

Petford, N., Atherton, M.P., and Halliday, A.N., 1996, Rapid magma production rates, underplating and remelting in the Andes: isotopic from the north and central Peru Andes: Journal of South American Earth Science, v. 9, p. 69-78.

Poldervaart, A., 1955, Zircons in rocks; Part 1, Sedimentary rocks; Part 2, Igneous rocks: American Journal of Science, v. 253, p. 433-461.

Posada, L.G., and Nordin, C.F., 1992, Total and unmeasured sediment loads of some tropical rivers: Eos, Transactions, American Geophysical Union, vol.73, p.137.Potter, P.E., 1978, Significance and origin of big rivers; Journal of Geology, v. 86, p. 13-33.

Potter, P.E., 1978, Significance and origin of big rivers: Journal of Geology, v. 86, p. 13-33.

Press, W.H., Flannery, B.P., Teukolsky, S.A., and Vetterling, W.T., 1986, Numerical recipes: the art of scientific computing: Cambridhe university Press, 818 p.

Prokopiev, A.V., Toro, J., Miller, E.L., Gehrels, G.E., 2008, The paleo-Lena River- 200 m.y. of transcontinental zircon transport in Siberia: Geology, v. 36, p. 699-702.

Rahl, J.M., Reiners, P.W., Campbell, I.H., Nicolescu, S., and Allen, C.M., Combined single-grain (U-Th)/He and U/Pb dating of detrital zircons from the Navajo Sandstione, Utah: Geology, v. 31, p. 761-764.

Rainbird, R.H., Heaman. L.M., and Young, 1992, Sampling Laurentia: detrital zircon geochronology offers evidence for an extensive Neoproterozoic river system originating fron the Grenville orogen: Geology, v. 20, p. 351-354.

Rainbird, R.H., McNicoll, V.J., Thériault, R.J., Heaman. L.M., Abbott, J.G., Long, D.G.F., and Thorkelson, D.J., 1997, Pan-continental river system draining Grenville orogen recorded by U-Pb and Sm-Nd geochronology of Neoproterozoic quartzarenites and mudrocks, northwestern Canada: Journal of Geology, v. 105, p. 1-17.

Räsänen, M.E., Salo, J.S., Kalliola, R.J., 1987, Fluvial perturbance in the western Amazon Basin: regulation by long-term sub-Andean tectonics: Science, v. 238, p.1398-1401.

Restrepo-Pace, P.A., Ruiz, J., Gehrels, G., and Cosca, M., 1997, Geochronology and Nd isotopic data of Grenville-age rocks in the Colombian Andes: new constraints for Late Proterozoic-Early Paleozoic paleocontinental reconstructions of the Americas; Earth and Planetary Science Letters, v. 150, pp. 427-441.

Riggs, N. R., Lehman, T. M., Gehrels, G. E., Dickinson, W.R., 1996, Detrital zircon link between headwaters and terminus of the Upper Triassic Chinle-Dockum paleoriver system: Science, v. 273, p. 97-100.

Rino, S., Motoki, A., Hirata, T., and Maruyama, S., 2003, U-Pb spot dating by LA/ICP-MS of single detrital zircon grains collected at the mouth of the Amazon River: continental crustal growth history of the Amazon River basin. Short Papers – IV South American Symposium on Isotope Geology, p. 108-110.

Rino, S., Komiya, T., Windley, B.F., Katayama, I., Motoki, A., and Hirata, T., 2004, Major episodic increases of continental crustal growth determined from zircon ages of river sands; implications for mantle overturns in the Early Precambrian: Physics of the Earth and Planetary Interiors, v. 146, p. 369-394.

Robb, L., 2005, Introduction to Ore-forming Processes: Blackwell Publishing, Hoboken, 373 p.

Roddaz, M., Viers, J., Brusset, Baby, P., Hérail, G., 2005, Sediment provenances and drainage evolution of the Neogene Amazonian foreland basin: Earth and Planetary Science Letters, v. 239, p. 57-78.

Ross, G.M., 1991, Tectonic setting of the Windermere Supergroup revisited: Geology, v. 19, p. 1125-1128.

Rossetti, D.F., 2001, Late Cenozoic sedimentary evolution in northeastern Pará, Brazil, within the context of sea level changes: Journal of South American Earth Sciences, v. 14, p. 77-89.

Rossetti, D.F., and Netto, R.G., 2006, First evidence of marine influence in the Cretaceous of the Amazonas Basin, Brazil: Cretaceous Research, v. 27, p. 513-528.

Sambridge, M.S. and Compston, W., 1994, Mixture modeling of multi-component data sets with application to ion-probe zircon ages. Earth and Planetary Science Letters, v. 128, pgs. 373-390

Santos, J.O.S., Hartman, L.A., McNaughton, N.J., and Fletcher, I.R., 2002, Timing of mafic magmatism in the Tapajós Province (Brazil) and implications for the evolution of the Amazon Craton: evidence from baddeleyite and zircon U-Pb SHRIMP geochronology: Journal of South American Earth Science, v. 15, p. 409-429.

Schenk, C.J., Viger, R.J., and Anderson, C.P., 1997, Maps showing geology, oil and gas fields, and geologic provinces of the South America region, U.S. Geological Survey Open-File Report 97-470D.

Schobbenhaus, C., and Bellizza, A., 2001, Geological map of South America, 1:5,000,000 scale: Commission for the Geological Map of the World- Companhia de Pesquisa de Recursos Minerais- Departamento Nacional de Produção Mineral- UNESCO, Brasilia.

Sébrier, M., and Soler, P., 1991, Tectonics and magmatism in the Peruvian Andes from late Oligocene time to the Present, in Harmon R. S., and Rapela, C. W., eds., Andean magmatism and its tectonic setting, Special Paper: Boulder, Geological Society of America, 309 p.

Sempere, T., Butler, R.F., Richards, D.R., Marshall, L.G., Sharp, W., Swisher, C.C., III, 1997, Stratigraphy and chronology of Upper Cretaceous-lower Paleogene strata in Bolivia and northwest Argentina: Geological Society of America Bulletin, v. 109, p. 709-727.

Sioli, H, 1984, The Amazon and its main affluents: hydrography, morphology of the river courses, and river types, in Sioli, H. Ed., The Amazon: Limnology and landscape ecology of a mighty tropical river and its basin: Junk Publishers, p. 127-165.

Sircombe, K.N., 1999, Tracing provenance through the isotope ages of litoral and sedimentary detrital zircon, eastern Australia; Sedimentary Geology, v. 124, p. 47-67.

Sircombe, K.N., 2000, Quantitative comparison of large sets of geochronological data using multivariate analysis: a provenance study example from Australia; Geochimica et Cosmochimica Acta, v. 64, p. 1593-1616.

Sircombe, K.N., 2004, AgeDisplay: an Excel workbook to evaluate and display univariate geochronological data using binned frequence histograms and probability density distributions; Computers & Geoscience, v. 30, p. 21-31.

Sircombe, K.N., 2006, Mountains in the shadows of time: three-dimensional density distribution mapping of U-Pb isotopic data as a visualization aid for geochronological information in concordia diagrams; Geochem. Geophys. Geosyst., 7, Q07013, doi:10.1029/2005GC001052.

Sircombe, K.N., Bleeker, W., and Stern, R.A., 2001, Detrital zircon geochronology and grain size analysis of a ~2800 Ma Mesoarchean proto-cratonic cover succession, Slave Province, Canada; Earth and Planetary Science Letters, v. 189, p. 207-220.

Sircombe, K.N., and Stern, R.A., 2002, An investigation of artificial biasing in detrital zircon U-Pb geochronology due to magnetic separation in sample preparation: Geochimica et Cosmochimica Acta, v. 66, p. 2379-2397.

Sircombe, K.N., and Hazelton, M.L., 2004, Comparison of detrital zircon age distributions by kernal function estimation: Sedimentary Geology, v. 171, p. 91-111.

Speer, J.A., 1982, Zircon: *in* Ribbe, P.H., ed., Reviews Mineralogy and Geochemistry, v. 5, p. 67-112.

Stacey, J.S., and Kramers, J.D., 1975, Approximation of terrestrial lead isotope evolution by a two-stage model: Earth and Planetary Science Letters, v. 26, p. 207-221.

Stallard, R.F., 1985, River chemistry, geology, geomorphology, and soils in the Amazon and Orinoco basins; in Drever, J.D. ed. The Chemistry of Weathering, D. Reidel Publishing Company, p. 293-316.

Sternberg, H.O., 1987, Aggravation of floods in the Amazon River as a consequence of deforestation? Geografiska Annaler, v. 69A, p. 201-219.

Stewart, R.J., Hallet, B., Zeitler, P.K., Malloy, M.A., Allen, C.M., and Trippett, D., 2008, Brahmaputra sediment flux dominated by highly localized rapid erosion from the easternmost Himalaya: Geology, v. 36, p. 711-714.

Tassinari, C.C.G, Bettencourt, J.S., Geraldes, M.C., Macambria, M.J.B., and Lafon, J.M., 2000, The Amazonian Craton, in Cordani, U.G., Milani, E.J., Thomaz Filho, A., and Campos, D.A., Tectonic evolution of South America, 31st International Geological Congress: Rio de Janeiro, p.41-99.

Trask, P. D., 1952, Sources of beach sand at Santa Barbara, California, as indicated by mineral grain studies, U.S. Army Beach Erosion Board Technical Memo N. 28, p. 24.

Trendall, A. F., Basei, M. A. S., de Laeter, J. R., and Nelson D. R. 1998, SHRIMP zircon U–Pb constraints on the age of the Carajás formation, Grão Pará Group, Amazon Craton: Journal of South American Earth Science, v. 11, p. 265-277.

Vermeesch, P., 2004, How many grains are needed for a provenance study? Earth and Planetary Science Letters: v. 224, p. 441-451.

Vital, H., Stattegger, K., and Garbe-Schönberg, C.-D., 1999, Composition and trace-element geochemistry of detrital clay and heavy-mineral suites of the lowermost Amazon River: a provenance study: Journal of Sedimentary Research, v. 69, p. 563-575.

Vital, H., and Stattegger, K., 2000a, Major and trace elements of stream sediments from the lowermost Amazon River: Chemical Geology, v. 196, p. 151-168.

Vital, H., and Stattegger, K., 2000b, Sediment dynamics in the lowermost Amazon: Journal of Coastal Research, v. 16, p. 316-328.

Vital, H., Stattegger, K., Posewang, J., and Theilen, F., 1998, Lowermost Amazon River: morphology and shallow seismic characteristics: Marine Geology, v. 152, p. 277-294.

Weltje, G.J., and von Eynatten, H., 2004, Quantatative provenance analysis of sediments: review and outlook: Sedimentary Geology, v.171, p. 1-11.

Wesselingh, F.P., Räsänen, M.E., Irion, Vonhof, H.B., Kaandorp, R., Renema, Romero Pittman, L., Gingras, M., 2002, Lake Pebas: a palaeoecological reconstruction of a Miocene, long-lived lake complex in western Amazonia: Cainozoic Research, v. 1, p. 35-81.

Wright, J.E. and Wyld, S.J., 2003, Appalachian, Gondwanan, Cordilleran interactions: A new geodynamic model for the Paleozoic tectonic evolution of the North American Cordillera. Abstracts with Programs, Geological Society of America. v. 35, p. 557.

CHAPTER 3

PROVENANCE FIDELITY: AN EXAMPLE FROM THE MODERN AMAZON RIVER

Abstract

A major pitfall of sediment provenance analysis is that it is often difficult to distinguish primary source signatures from those created by chemical alteration. Comparison of results for several techniques suggests that for modern Amazon River sediment, transport and weathering occur at different rates for specific portions of the clastic load. Whereas chemically labile minerals such as feldspars, micas, and amphiboles are common in sediment derived from areas dominated by physical weathering and high sediment output, clay minerals, quartz, and zircon are concentrated in catchments with strong chemical weathering and low sediment output. Provenance indicators that focus on suspended sediment best describe weathering conditions and rocks from high-relief source regions. Proxies that utilize bedload material do a better job at describing weathering conditions and rocks from low-relief source areas. The difference appears to be related to the amount of time detritus spends in transport across the Amazonian lowlands; most suspended sediment is transported and deposited before it can be fully altered by chemical processes whereas bedload sediment travels more slowly and is strongly altered by chemical weathering. These results indicate that when possible, multiple provenance indicators with different responses to chemical weathering should be used to create a more complete source rock picture and weathering history when studying sedimentary rocks.

Introduction

Provenance studies address phenomena that occur over a wide range of spatial and temporal scales; studies of modern fluvial systems commonly focus on small, upland catchments where detritus can be linked directly to source rocks (e.g. Amidon *et al.*, 2005; Ruhl and Hodges, 2005; Lease *et al.*, 2007) whereas studies of ancient deposits commonly attempt to describe the history of sediment derived in large catchments that may have included multiple distinct source regions. In many cases, a primary goal of provenance investigation is identification of source connections that have been lost due to drainage reorganization, erosion, or tectonic displacement (e.g. Dickinson and Gerhels, 2003; Goodge *et al.*, 2004; Prokoplev *et al.*, 2008). A number of techniques are used to establish sediment provenance and each has inherent strengths and weaknesses.

When comparing interpretations from studies that have employed different techniques, it is important to understand which proxy was used and how it responds under a range of conditions. For instance, modal sand composition provenance uses relative mineral abundances and other petrographic criteria to infer sand source (Dickinson and Suczek, 1979). These techniques work well for first-cycle unaltered sediments but in ancient deposits where climate change, tectonic rearrangement, and post-depositional alteration have occurred; interpretations become less certain (Blatt *et al.*, 1972; Potter, 1978; Franzanelli and Potter, 1983; Basu, 1985). Bulk sediment geochemical and isotopic techniques provide provenance averages that are weighted over entire drainage basins; as a result, they may be poor for identifying minor sources. Single mineral or mineral suite analysis is conducted on minerals that contain precise source information but unless a large number of grains is analyzed, significant detrital populations can go undetected (Vermeesch, 2004; Andersen,

2005). Detrital quartz and zircon are resistant to weathering so they are able to give long-term provenance information that may have survived through multiple sedimentary cycles (Pettijohn *et al.*, 1972) and as a result, can be biased toward reworked sedimentary sources. In contrast, feldspar, mica, and other minerals, which are generally unstable under surface and diagenetic conditions, are commonly assumed to be first-cycle (Helmold, 1985; Haines *et al.*, 2004; Gutiérrez-Alonso *et al.*, 2005) and derived from localities of low chemical weathering rate or high gradient and transport rate (Dickinson, 1985). Thus, whereas some provenance indicators may be biased toward the area that provides the most detritus, others are weighted toward basin-wide geology or previous drainage configurations.

In addition to source composition and weathering, transport mechanism and rate play a major role in shaping sediment composition. Transport rates for suspended sediments are much higher than those for the bedload (Nordin, 1985). Similarly, empirical evidence shows that within the bedload, grain size and average grain density differences can lead to variable transport rates (Trask, 1952; Poldervaart, 1955; Clemens and Komar, 1988). Thus, potential technique shortcomings must be understood when selecting appropriate provenance indicators.

Because a sizable petrographic, geochemical, and isotopic dataset has been created for modern Amazon River sediment, it is well suited for comparing the results of different provenance techniques. This paper focuses on the similarities and differences between several common provenance proxies and discusses which techniques are most useful at describing source rock relationships and weathering conditions that exist across the Amazon Basin. Henceforth, it will be necessary to discuss active sediments, ancient sediments, and sedimentary rocks. In general, discussion focuses on processes that occur on clastic sediment

prior to lithification and/or diagenesis; therefore, material is referred to as sediment independent of current state.

The Amazon River

At over 6 x 10^6 km^2, the Amazon River system is the largest drainage basin in the world (Archer, 2005) with river discharge on the order of 6.3 x 10^{12} m^3/yr (Meade, 1996). Because the catchment straddles the equator, maximum discharge is only 2-4x minimum (Meade *et al.*, 1991). The Amazon delivers 1.1-1.3 x 10^9 tons/yr of suspended sediment to the Atlantic Ocean (Meade, 1994) with bedload sediment yield estimated to be 1-6% of suspended sediment output (Posada and Nordin, 1992; Dunne *et al.*, 1998). Gibbs (1967) estimated that 82% of suspended sediment discharged at the Amazon mouth is Andes derived but more recent estimates have increased the proportion to 90-95% (Meade, 1994).

Physiographically, the Amazon basin is extremely varied (Figure 3.1). The Andes, which are largely above 3,000 m elevation, make up approximately 12% of the basin area, the Andean foreland makes up approximately 25%, shield areas, predominantly below 600 m elevation, make up 25%, and lowland sedimentary deposits comprise the remaining drainage area. East of the Andes, the Amazon has low gradient; a series of structural arches breaks the river into gradient domains that range from 1-4 cm/km (Mertes *et al.*, 1996; LeFavour and Alsdorf, 2005).

The geology of the basin is also diverse (Figure 3.1). The Amazonian Andes are made up predominantly of Paleozoic and Mesozoic metasedimentary rocks that are intruded by Mesozoic and younger plutonic rocks and blanketed by Late Cretaceous and Cenozoic volcanic cover (Feninger, 1982; Cobbing, 1985; Benavides-Cáceres, 1999; Petford *et al.*, 1996; Chew *et al.*, 2007). The northern Andean foreland system is composed mainly of

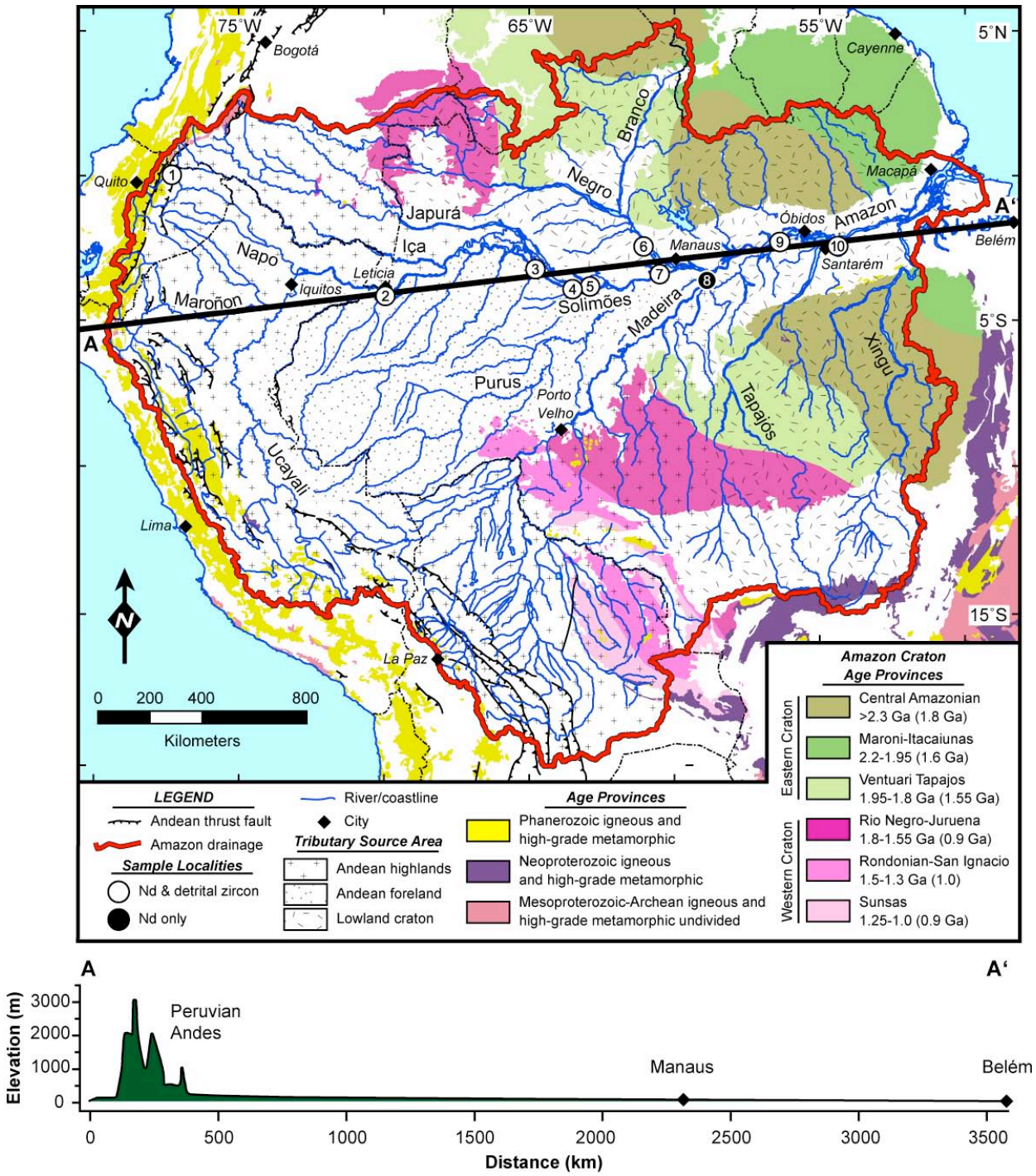

Figure 3.1- Generalized geology of the Amazon basin and surrounding areas. Note that young Andean rocks are only present at the headwaters of the drainage and that Precambrian basement rocks are present downstream. Sedimentary rocks of the lowlands and metamorphic and sedimentary rocks of the Andes have been stripped away. After Cordani *et al.* (2000), Costa *et al.* (2001), and Schobbenhaus and Bellizza (2001).

Miocene and younger clastic deposits derived largely from Andean erosion (Roddaz *et al.*, 2005; Räsänen *et al.*, 1995, Hovikoski *et al.*, 2005). East of the Andes, several southeast-northwest trending Archean-Mesoproterozoic basement provinces compose the Amazon Craton (Figure 3.1; Teixeira *et al.*, 1989; Tassinari *et al.*, 2000). The Amazon River mainstem runs along the axis of a late Precambrian aulacogen (Szatmarim, 1983; Burke and Lytwyn, 1993) filled by Neoproterozoic to recent sedimentary deposits and mafic volcanics (Figure 3.1; Milani and Tomaz Filho, 2000).

The Amazon Basin can be separated into three weathering/geologic domains: (1) The high Andes, dominated by physical weathering processes and high sediment output (~900 $t/km^2/yr$; Irion, 1991) and where the majority of Phanerozoic igneous and metamorphic rocks exist. Climate varies within the Amazonian Andes: local glacial and arid environments exist but conditions are generally warm and wet (Figure 3.2). (2) The Andean foreland region is composed mainly of early to mid-Cenozoic, poorly lithified Andean-derived sediments (Roddaz *et al.*, 2005) that have been subjected to intense chemical weathering and are currently undergoing fluvial reworking. (3) The Amazonian lowlands, which make up the largest area of the drainage are characterized by a tropical climate and wide expanses of highly chemically weathered Precambrian igneous and metamorphic rocks and Precambrian-Quaternary sedimentary deposits (Schobbenhaus and Bellizza, 2001) with low sediment output (~10 $t/km^2\ yr^{-1}$; Irion, 1991). The configuration of the Amazon Basin is ideal to test the soundness and usefulness of several provenance techniques because each geologic end-member case (young volcanic-arc rocks/ancient cratonal rocks) is also separated in terms of dominant weathering style.

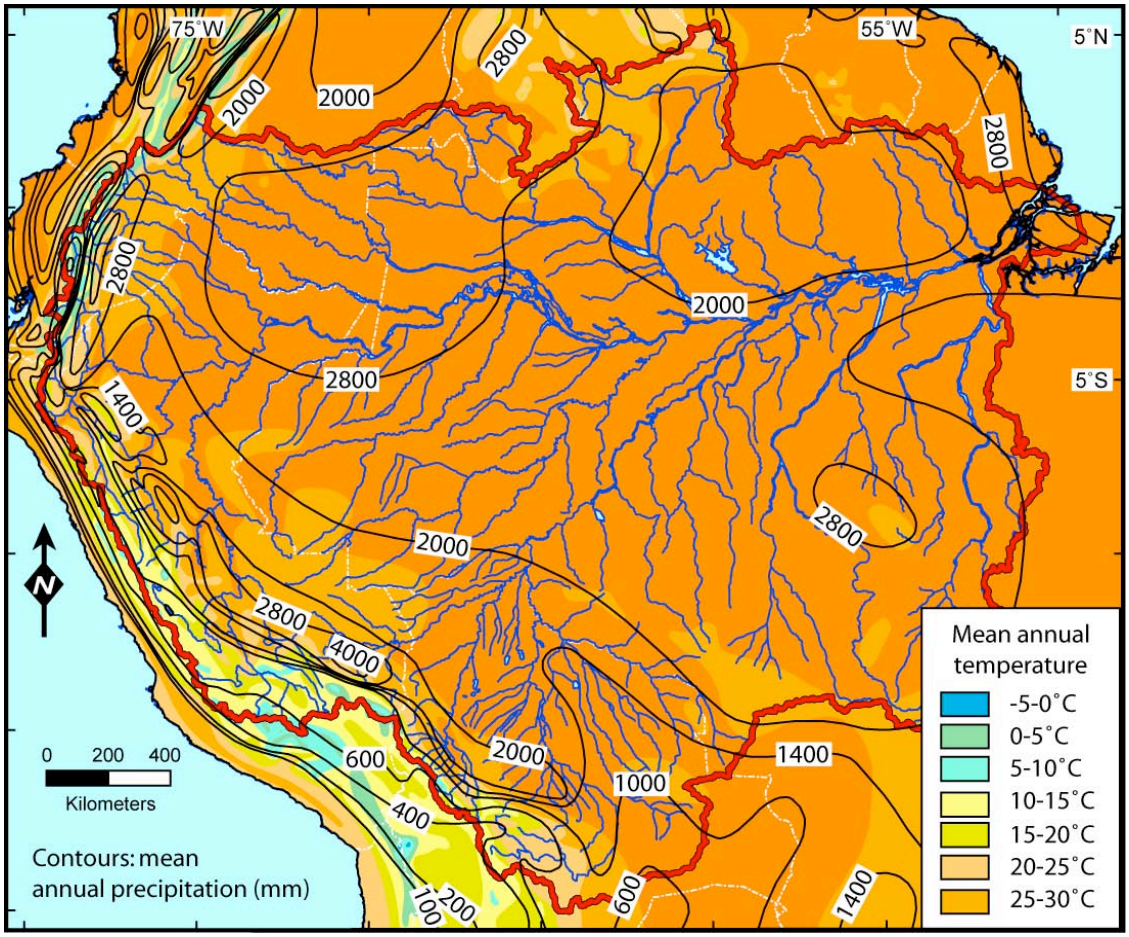

Figure 3.2- Average climatic conditions of northern South America. Color scale shows mean annual temperature. The Amazon basin (shown by red polygon) is characterized by hot and wet conditions. Contours show mean annual precipitation. Data from NOAA Observing Systems Architecture (NOSA).

Methods and Results

New Nd-isotope data were collected for seven widely spaced, active-channel sands from the mainstem Amazon River between the Andean foreland and the Amazon Estuary. In addition, data were collected for one sample from the Aquarico River, an Ecuadorian Andean tributary, a sample from the Madeira River, an Andean sourced river that traverses the Andean foreland and Amazon craton prior to joining the Amazon, and one sample from the Negro River, a large cratonal tributary (Figure 3.1). Bulk-sand samples were collected during low flow from emergent river bars between the Andes and the Amazon estuary. Sand samples were crushed to a powder using an alumina ceramic shatterbox. Powders were dissolved and samarium and neodymium were separated by cation exchange chromatographic column chemistry. Analysis was carried out by thermal ionization mass spectrometry at the University of North Carolina at Chapel Hill following the procedure of Kylander-Clark *et al.* (2005). Results are reported in table 3.1 and data are further described in Nagy (2008). For nine of the same samples, detrital zircon ages were also collected (Figure 3.1; Mapes, this text).

In addition to new data, a large geochemical, isotopic, and mineralogic database for Amazon River bedload and suspended sediment was created (Table 3.2). All data used were collected from bulk-sediment samples unless otherwise required by the particular provenance technique. Sampled material includes active sediment, recent floodplain deposits, and subaqueous delta and fan deposits. All samples presented are late Pleistocene in age or younger and although weathering zones may have locally reorganized since the late Pleistocene (Anhuf *et al.*, 2006), no noticeable temporal distinction is apparent in the data and information is regarded equally.

Table 3.1- Results of Nd-isotope analysis of Amazon River sand.

Sample-River	Longitude (°W)	Latitude (°S)	Sm (ppm)	Nd (ppm)	$^{143}Nd/^{144}Nd$	$^{147}Sm/^{144}Nd$	ε_{Nd}	T_{DM} (Ga)
1- Aguarico	77.3057	0.0486	5.483	28.988	0.512498 ± 0.000017	0.1143 ± 0.0009	-2.73	0.84
2- Amazon	69.9490	4.1519	5.029	25.156	0.512355 ± 0.000018	0.1209 ± 0.0012	-5.52	1.13
3- Solimões	64.7815	3.2208	2.847	14.861	0.512385 ± 0.000008	0.1158 ± 0.0008	-4.94	1.03
4- Solimões	62.8996	3.9256	5.192	25.940	0.512242 ± 0.000013	0.1210 ± 0.0007	-7.73	1.36
5- Solimões	62.2238	3.7891	5.283	27.239	0.512246 ± 0.000008	0.1172 ± 0.0010	-7.64	1.26
6- Negro	61.0622	2.4352	0.525	2.900	0.511694 ± 0.000010	0.1094 ± 0.0008	-18.42	1.97
7- Solimões	60.3076	3.2979	5.011	24.953	0.512245 ± 0.000007	0.1214 ± 0.0013	-7.67	1.36
8- Madeira	58.3740	3.1599	2.624	12.878	0.512229 ± 0.000009	01232 ± 0.0010	-7.97	1.38
9- Amazon	56.3744	2.2836	4.778	24.775	0.512122 ± 0.000023	0.1166 ± 0.0013	-10.07	1.47
10- Amazon	54.3715	2.4326	4.075	22.320	0.512190 ± 0.000035	0.1104 ± 0.0023	-8.73	1.26

Nd data normalized to $^{146}Nd/^{144}Nd = 0.7219$

Epsilon-Nd calculated assuming $^{143}Nd/^{144}Nd = 0.512638$.

Depleted mantle model ages (T_{DM}) calculated using the method of DePaolo (1981).

Table 3.2- Comparison of source interpretations results for several provenance indicator on modern and recent Amazon river sediment.

Technique	Location	Provenance Interpretation	References
Suspended Load			
Petrography	Entire basin	~82% of the suspended sediment discharged by the Amazon is Andean derived	Gibbs, 1967; Irion, 1983; Martinelli *et al.*, 1993; Meade, 1994; Michalopoulos and Aller, 1995; Vital *et al.*, 1999; Allard *et al.*, 1999; Guyot *et al.*, 2007
Major element geochemistry	Amazon floodplain, and river mouth	CIA indicates a dominantly cratonal source for river mouth sediment and Andean source for floodplain sediment; ICV indicates a highly weathered source	Martin and Maybeck, 1979; Sholkovitz and Price, 1980; Stallard, 1985; Martinelli *et al.*, 1993; McDaniel, 1998; Elbaz-Poulichet *et al.*, 1999; Vital and Stattegger, 2000
Trace element geochemistry	Mainstem from Iquitos, to the river mouth	Trace elements indicate a cratonal, highly weathered source; REE data are ambiguous	Martin and Maybeck, 1979; Gordeev *et al.*, 1985; Goldstein and Jacobsen, 1988; Nesbit *et al.*, 1990; Gaillardet *et al.*, 1997; McDaniel, 1998; Vital and Stattegger, 2000; Gerard *et al.*, 2003; Roddaz *et al.*, 2005
Bulk sediment isotope geochemistry	Lower Amazon	All isotope systems point to dominantly Andean provenance	McDaniel, 1998; Asmerom and Jacobsen, 1993; Gaillardet *et al.*, 1997; Allegre *et al.*, 1996
Bedload			
Petrography	Entire basin	Andean bulk sediments are characteristic of active continental source; foreland, lowland cratonal, and mouth bulk sediments indicate a dominantly highly weathered or recycled source; heavy minerals near the mouth indicate an Andean source	Stein (1979); Sedimentation Seminar, 1981; Franzinelli and Potter, 1983; Johnsson and Meade, 1990; Potter and Franzinelli, 1985; DeCelles and Hertel, 1989; Johnsson *et al.*, 1990; Konhauser *et al.*, 1994; McDaniel *et al.*, 1997; McDaniel, 1998; Vital *et al.*, 1999; Rimington *et al.*, 2000
Major element geochemistry	Entire basin	Major element data are mixed; SiO_2 content is high indicating a highly weathered or recycled source; K_2O/Na_2O, Al_2O_3/SiO_2, indicate a mixed igneous and recycled/chemically weathered source.	Franzinelli and Potter, 1985; Konhauser *et al.*, 1994; McDaniel, 1998; Vital and Stattegger, 2000
Trace element geochemistry	Madeira headwaters, middle-Amazon	Madeira foreland sediment is consistent with derivation from craton-like rocks, possibly reworked Andean metasediments; middle-Amazon sediments have a mafic igneous signature; REE yield ambiguous results	Basu *et al.*, 1990; Konhauser *et al.*, 1994; Vital and Stattegger, 2000; McDaniel, 1998; Gerard *et al.*, 2003
Bulk sediment isotope geochemistry	Entire basin	Bulk sediment Nd-model ages and ε_{Nd} become more craton-like downstream except for analyses taken from the Madeira headwaters which are similar to values at the Amazon mouth. Nd-isotope values for size splits suggest a range of cratonal sources. Sr- and Pb-isotopes yield ambiguous results.	Goldstein *et al.*, 1984; Basu *et al.*, 1990; McDaniel, 1998
Single mineral geochronology	Entire basin	Amazon River zircon samples suggest mixed Andean and far western cratonal sources with little input from the eastern craton. Mouth zircon samples indicate an eastern cratonal source. All K-bearing minerals indicate near total derivation from the Andes	McDaniel, 1998; Rino *et al.*, 2004; Mapes, this text

Suspended sediment- Petrographic techniques

Gibbs (1967) characterized Amazon basin suspended sediment concentration and composition. He found that Andean tributaries have high total suspended sediment concentrations with particle sizes ranging from <0.2 μm to >1000 μm composed of quartz, kaolinite, high-temperature mica, montmorillonite, feldspar, and chlorite, consistent with a dominantly physical weathering of igneous and metamorphic rocks. Cratonal river suspended sediment has a much narrower size range (0.2-6 μm) and lower total suspended sediment concentrations. Compositionally, intensely chemical weathered cratonal tributary sediment is dominated by kaolinite with only minor amounts of mica, quartz, and gibbsite. Gibbs (1967) found that the overall composition of the suspended sediment released into the Atlantic was slightly finer grained but has almost identical mineralogy to that of Andean tributaries and determined that 82% of the total suspended solids discharged by the Amazon are of Andean origin.

Suspended sediment- Bulk-sample geochemical techniques

Major element data for Amazon suspended sediment and recent mud deposits yield varied results. Geochemical indices sensitive to weathering conditions indicate that chemical weathering is strong. The chemical index of alteration

$$CIA = [Al_2O_3 / (Al_2O_3 + CaO + Na_2O + K_2O)] \times 100 \quad (1)$$

of Nesbitt and Young (1982) gives values of 79 ± 3 (1σ) for 17 samples of Amazon mouth mud, consistent with values published by Pettijohn (1975). These values are high when compared with unweathered granite values of ~50 or average shale (70-75) and are characteristic of fine-grained sediments that have undergone extreme chemical weathering (Nesbitt and Young, 1982). Amazon mouth CIA values are indistinguishable from lowland

tributary values (80 ± 4, n = 7) indicating a highly weathered, dominantly lowland source for Amazon suspended sediment. In contrast, recently deposited, fine-grained floodplain sediment collected from a 2,400 km stretch of the Amazon yield consistently lower values than mouth samples (Martinelli *et al.*, 1993). Values for CIA, in general increase from ~60 in the most upstream sample to 78 in the most downstream sample. Index of compositional variability,

$$ICV = [Fe_2O_3 + K_2O + Na_2O + CaO + MgO + MnO + TiO_2] / Al_2O_3 \quad (2)$$

values (Cox *et al.*, 1995) for Amazon suspended sediment change little as the river traverses the craton. Values of K_2O/Al_2O_3 for mainstem samples (0.15 ± 0.03, n = 39) and for cratonal tributaries (0.13 ± 0.02, n = 8) indicate that clay minerals dominate the suspended load and a moderate to high degree of chemical weathering is characteristic of the sediment source area (Figure 3.3).

Trace element ratios (Th/Sc, Th/U; McLennan *et al.*, 1993) for Amazon suspended sediments are most consistent with a cratonal (average continental crust) or recycled sedimentary detrital source. Rare earth element (REE) values for fine-grained Amazon sediment display chondrite-normalized light-REE enrichment and flat heavy-REE trends with ubiquitous negative Eu anomalies (Eu/Eu* = 0.7 ± 0.1, n = 25; Figure 3.4). Compared to the North American shale composite (NASC; Gromet *et al.*, 1984) values are generally enriched (1-10x). Cratonal tributary suspended sediment has similar chondrite normalized light-REE abundances and are slightly less enriched in heavy-REE (Figure 3.4). All trends are consistent with derivation from old upper continental crust or young volcanogenic crust (McLennan *et al.*, 1993).

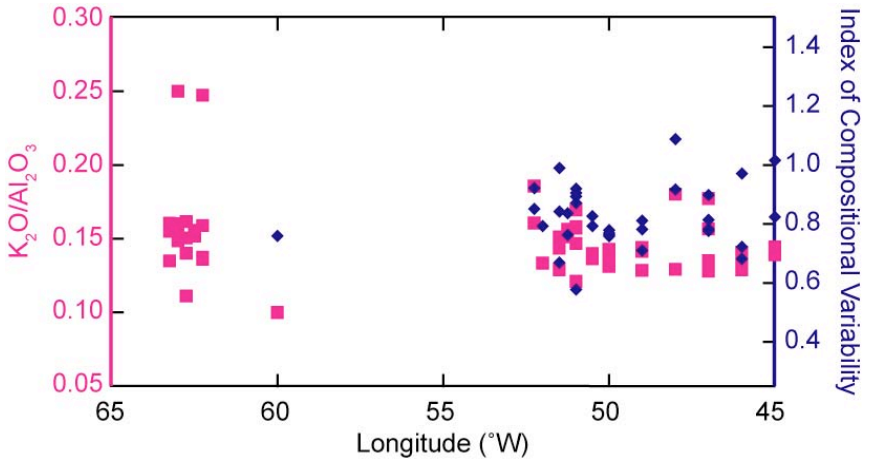

Figure 3.3- Major element ratios for Amazon River suspended sediment (Cox *et al.*, 1995). Compositions do not change noticeably along the lower reaches of the Amazon River and reflect presence of immature clay and non-clay silicate minerals, indicating dominantly Andean provenance.

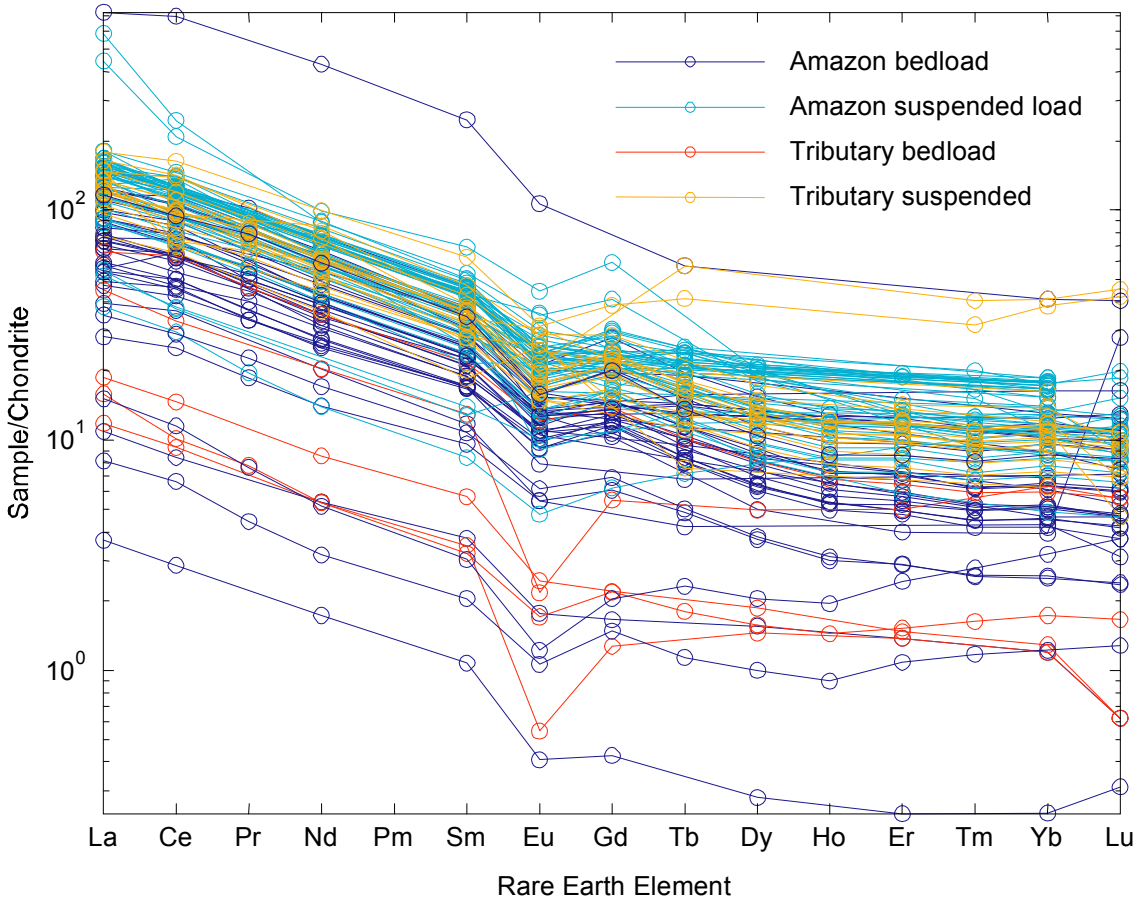

Figure 3.4- Chondrite normalized rare earth element diagram for Amazon River sediment. Rare earth element concentrations are higher for Amazon mainstem samples than for cratonal tributaries reflecting the higher abundance of Andean derived minerals.

Suspended sediment- Bulk-sample isotopic techniques

A compilation of suspended sediment values for the major isotope systems (Nd, Sr, Pb) gives three to six values along the entire length of the Amazon, which are concentrated in the between the Negro River confluence and the Amazon mouth. For all major systems, mainstem Amazon values vary little with location but appear to show a shift toward more cratonal values with distance from the Andes that correspond to introduction of detritus from cratonal tributaries. For example, in the Nd-system three Amazon suspended sediment analyses have ε_{Nd} values between -8.3 and -10.2 and Nd-model ages (DePaolo, 1981) ranging from 1.3-to 1.6 Ga, the furthest downstream yielding the lowest and oldest values respectively. Cratonal tributaries contribute sediment in much lower abundance (Meade, 1994) with ε_{Nd} values between -11.6 and -21.9 and Nd-model ages from 1.6-2.0 Ga, which likely accounts for the downstream decrease in ε_{Nd} and increase in model age (Figure 3.5). Fine-grained deposits of the Amazon delta and fan have Nd-model ages around 1.5 Ga. For the Sr-system, few data exist, but a slight increase in $^{87}Sr/^{86}Sr$ appears to occur between the Negro confluence and the river mouth, which is consistent with addition of cratonally derived suspended sediment. The isotopic signature of Amazon suspended sediment is dominantly Andean but ancient cratonal rocks, especially in the downstream reaches of the river, have a noticeable effect on isotopic composition.

Bedload sediment- Petrographic techniques

Franzinelli and Potter (1983) described active sediment for ninety-five samples from the mainstem Amazon and many of its tributaries. They found that Andean tributary sands were generally lithic arenites, similar to beach sands found on the South American Pacific coast (Potter, 1986). Sands of tributaries draining the Andean foreland and lowland craton

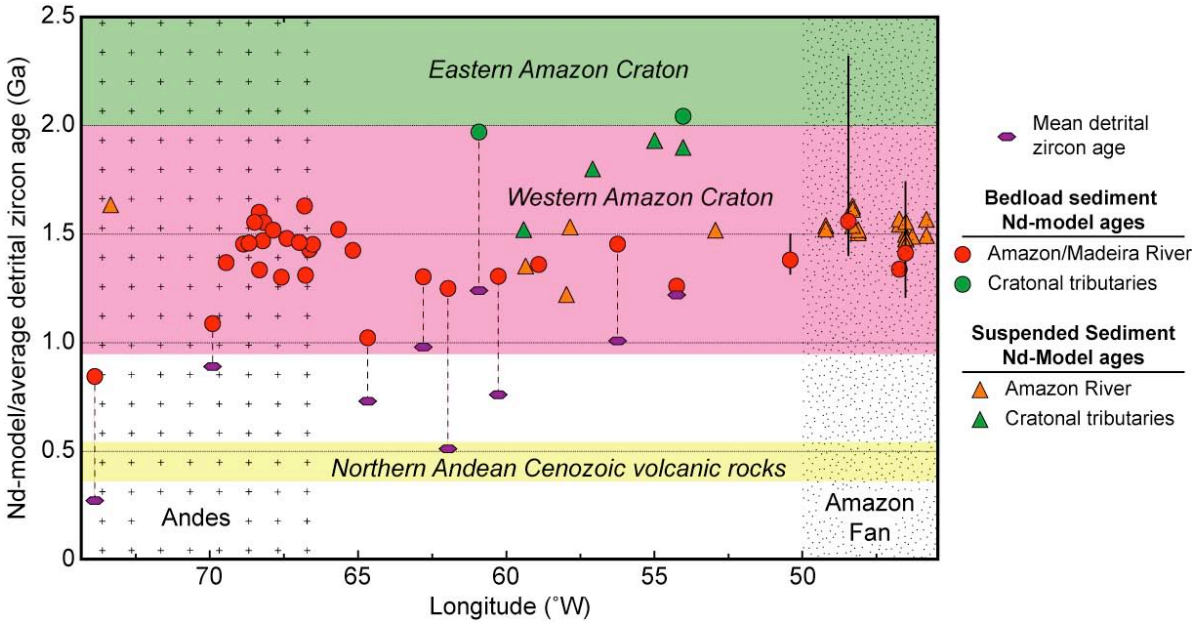

Figure 3.5- Neodymium depleted-mantle model ages and mean detrital zircon ages for bulk Amazon River sediment vs. sample longitude. Longitude roughly corresponds to river distance from the headwaters. Error bars on some bedload samples represent range of values gathered from grain size splits of bulk sands (Goldstein *et al.*, 1984; McDaniel, 1998). Dashed vertical tie lines connect mean detrital zircon grain ages (Mapes, this text) to Nd-model ages for bulk-sand analyzed from the same samples. Amazon Basin basement rock isotopic ratios and ages were taken from McCourt *et al.* (1984), Miller and Harris (1989), Soler and Rotach-Toulhoat. (1990), Petford *et al.* (1996), Restrepo-Pace *et al.* (1997), Kay *et al.* (1999), Macfarlane (1999), Ordonez Carmona and Pimental (2002), Egenhoff and Lucassen (2003), and Roddaz *et al.* (2005).

are generally sublithic or quartz arenites. They also found that quartz abundance increases downstream along the Amazon mainstem to the extent that sands become sublithic or quartz arenites near the river mouth indicating a mature, highly reworked or humid cratonic provenance for the entire basin. However, McDaniel (1998) points out that the abundance of both rounded and angular quartz attests to significant contribution of highly weathered material from both the craton and Andean foreland respectively. Franzinelli and Potter (1983) suggest that long-distance transport of sediment rich in labile minerals and rock fragments in a humid environment and short-term sedimentary storage can lead to formation of quartz arenites in first cycle sands. A case study conducted on recent Amazon deposits at Macuapanim Island, northwestern Brazil (Johnsson and Meade, 1990) agrees and further concludes that transformation of sands from lithic arenites or arkoses to quartz arenites can occur within floodplain sediments in less than 125 k.y. Franzanelli and Potter (1983) point out that mica content decreases rapidly once sand leaves the Andes and feldspar content remains relatively constant (~3%) along the entire length of the Amazon. They also note that sands of low relief, chemical weathering dominated, cratonal drainages are characterized by coarse quartz grains that are similar in size and shape to igneous and metamorphic quartz of cratonal source rocks.

Stein (1979) studied Amazon River heavy minerals and found that Andean rivers are dominated by hornblende and epidote ± hypersthene. Cratonal rivers contain negligible labile heavy minerals, indicating conditions of intense chemical weathering. Vital *et al.* (1999) state that zircon content does not increase downstream and that epidote and hornblende content are high near the Amazon mouth, consistent with derivation from Andean source rocks. Zircon-tourmaline-rutile indices (Hubert, 1962) are low for Amazon mouth sands (7-15) when

compared to cratonal tributaries (49-68) indicating that Andean sources dominate heavy mineral composition (Vital *et al.*, 1999).

Bedload sediment- Bulk-sample geochemical techniques

Bedload bulk-sediment chemical composition is useful for understanding both sediment source tectonic environment and synsedimentation weathering conditions. In general, Amazon bedload material is enriched in SiO_2 relative to potential source rocks, indicating a high degree of chemical weathering or sediment recycling. However, other indicators of chemical weathering and/or sediment recycling (e.g. K_2O/Na_2O and Al_2O_3/SiO_2) are highly variable and suggest a range of possible tectonic environments for sediment sources (Roser and Korsch, 1986).

Madeira River Th/U ratios (Bhatia and Crook, 1986) are consistent with a mixed primitive-arc/cratonal source whereas Amazon sands collected above the Madeira confluence suggest a dominantly primitive arc source. Madeira River headwaters sand have Th/Co (Cullers *et al.*, 1988) that are consistent with a dominantly granitic/cratonal source whereas Amazon sands suggest a more primitive, mafic-igneous source. Rare earth elements in Amazon River sand are slightly less enriched than in suspended sediments but display similar patterns and Eu anomalies ($Eu/Eu^* = 0.63 \pm 0.06$). Mainstem Amazon chondrite-normalized REE trends are similar to those for cratonal tributaries only more enriched (Figure 3.4).

Bedload sediment- Bulk-sample isotopic techniques

The Nd system is the best-represented isotopic system for Amazon River bedload sediment (Figure 3.5). For Andean tributary and mainstem sand of the upper Amazon drainage, ε_{Nd} and Nd-model ages change eastward, from -2.7 to -10.0 and 0.84 to 1.44 Ga

respectively, indicating that sand has dominantly Andean sources proximal to the Andes and an increased abundance of cratonal detritus downstream. In contrast, Nd-data for sand collected from Andean tributaries of the Madeira River (ε_{Nd} = -10.1 ± 1.5, T_{DM} = 1.46 ± 0.10 Ga, 1σ, n = 20; Basu *et al.*, 1990) are similar to values of the western Amazon Craton and lack any appreciable geographic trend. Bulk Amazon mouth and Pleistocene fan sands analyzed by McDaniel (1998; -8.7 and 1.54 Ga) and Goldstein *et al.* (1984; -9.2 and 1.36 Ga) are similar to Madeira headwaters sands but also appear to extend the trend toward increasing model age of Amazon mainstem sand. In addition to bulk-sediment Nd-isotope values, Goldstein *et al.* (1984) and McDaniel (1998) presented Nd-analyses for bedload sediment grain size fractions and found that individual fractions from single samples yielded highly varied results (Figure 3.5). For example, one sample for which eight size splits were analyzed gave model ages between 1.43 Ga and 2.03 Ga, a range almost equal to the entire range for bulk-sands across the drainage basin. The oldest model ages in that sample were restricted to the coarse-silt size fraction (62.5-31.25 μm), suggesting that heavy minerals concentrated that size split were recording a more cratonal provenance.

Only Basu *et al.* (1990) studied Sr-isotopes for bedload sediment in the Amazon Basin in the headwaters of the Madeira River. Their results for twenty analyses are very consistent ($^{87}Sr/^{86}Sr$ = 0.720 ± 0.003) suggesting derivation of detritus from the western Brazilian Shield with little to no indication of sediment input from juvenile Andean rocks (Harmon *et al.*, 1984; Beckinsdale *et al.*, 1985; Soler and Rotach-Toulhoat, 1990; Ordonez Carmona and Pimental, 2002). This result is somewhat surprising because the samples from eastward flowing rivers were collected in locations located west of the easternmost exposure

of Precambrian basement rocks possibly suggesting reworking of material from older deposits.

McDaniel (1998) presented whole rock Pb-isotope values for Amazon delta and fan sands. Bulk-sand Pb-ratios for three sands from two boreholes yielded similar results ($^{206}Pb/^{204}Pb$: 18.974-19.036, $^{207}Pb/^{204}Pb$: 15.673-15.707, and $^{208}Pb/^{204}Pb$: 38.91-39.01). Comparison to Pb-isotope ratios to ratios for Andean and cratonal rocks show that sands have unremarkable common-Pb ratios that lie in regions of significant overlap between potential sediment source regions (Harmon *et al.*, 1984; Todsal, 1996; Tyrrell *et al.*, 2006).

Bedload sediment- Single grain geochronologic techniques

McDaniel (1998) presented $^{40}Ar/^{39}Ar$ ages for 103 detrital feldspar, biotite, and hornblende grains from the modern Amazon delta and the Pleistocene fan (~25 ka). She found that 81% of the grains yielded ages younger than 250 Ma, consistent with derivation from Andean rocks. As for grains with cratonal ages, only five were found; three ~1.1 Ga aged feldspars and two feldspars with imprecise ages older than 1.5 Ga (Figure 3.6). In contrast, Rino *et al.* (2004) reported U-Pb and Pb-Pb ages for 369 single detrital zircons separated from a sample collected nearby at Santana Island, near Macapá, Brazil. Their two most significant age modes were centered at ~2.0 and ~2.6 Ga, a third, less significant mode was centered near 1.1 Ga. Unlike the feldspar, biotite and hornblende ages, 76% of the zircons analyzed were in the age range 2-3.5 Ga and only a single Phanerozoic-aged grain was identified. Detrital zircon data for fifteen samples collected on the Amazon mainstem between the Andean foreland and the Amazon Estuary (Mapes, this text) yielded very different results from the mouth zircon and the delta and fan feldspar, biotite, and hornblende. When results for all samples are combined (2003 grains), two major age peaks

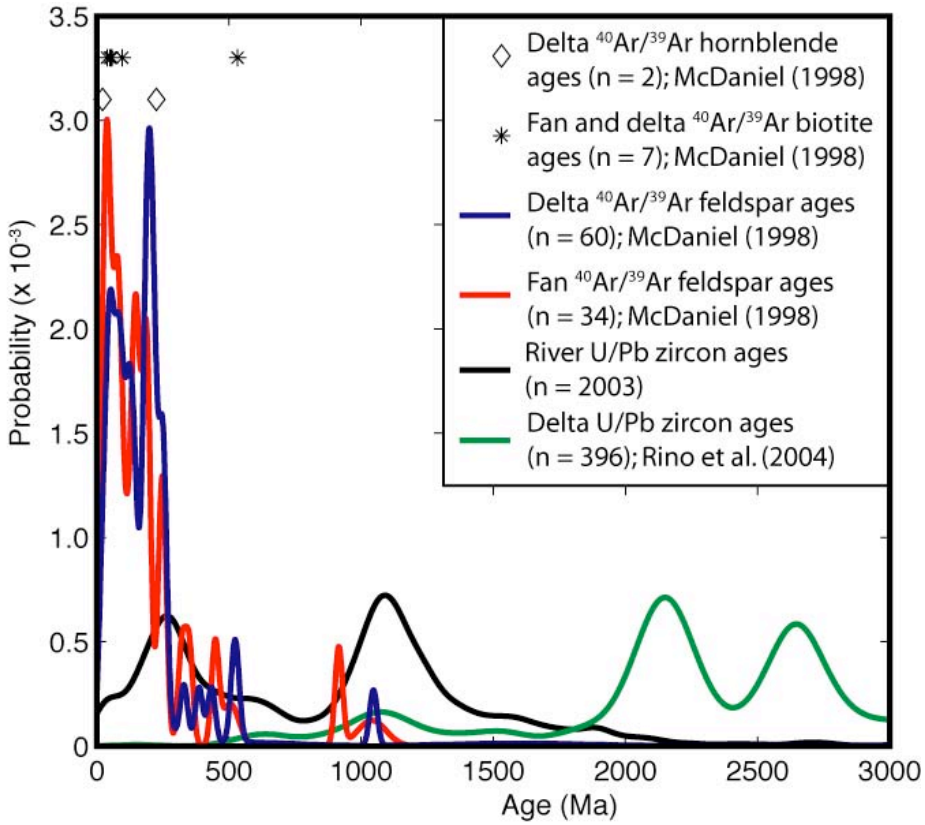

Figure 3.6- Age spectra for single-grain geochronology of various minerals from active and recently deposited sediment samples from the Amazon River. Ages used for probability density curve of Amazon delta zircons were estimated from histograms provided by Rino *et al.* (2004). Labile K-bearing minerals yield dominantly Andean ages while detrital zircon grains yield mixed Andean and cratonal ages.

exist at ~250 Ma and ~1.1 Ga. In all, 82 % of the zircon collected on the continent yielded ages younger than 1.3 Ga.

To allow direct comparison of detrital zircon ages (Mapes, this text) and Nd-model ages for the same samples, mean zircon age has been calculated (Figure 3.5). Mean zircon ages are consistently younger than Nd-model age and a positive relationship between the two exists (Figure 3.7) indicating that the techniques are recording similar sources. Both zircon mean age and Nd-model ages are oldest for the Negro River sample, consistent with its dominantly cratonal drainage area, and youngest for the Andean, Aguarico River sample, consistent with its catchment that lacks significant Precambrian source rocks (Schobbenhaus and Bellizza, 2001).

Discussion

Provenance fidelity- What is each technique recording?

Several factors work together to produce sediment. Source geology has a strong influence on clastic sediment composition; since in its simplest form, provenance is a mass balance problem, sediment mineralogy and geochemistry can only be as diverse as they were in the source rocks. Depending on situation specifics though, source rock diversity can either simplify or complicate provenance interpretations. In some cases, simple source rock types lead to specific provenance interpretations (e.g. mafic igneous source) while in others, simple sources lead to ambiguous results (e.g. mature sandstone source). Likewise, lithologically diverse sources can yield a range of sediment compositions that can lead to highly averaged and vague results.

Climate has a strong influence on sediment grain size and composition. Fluvio-glacial sediment ranges in size from coarse gravel to fine clay-sized detritus (Hoey, 2004) for most

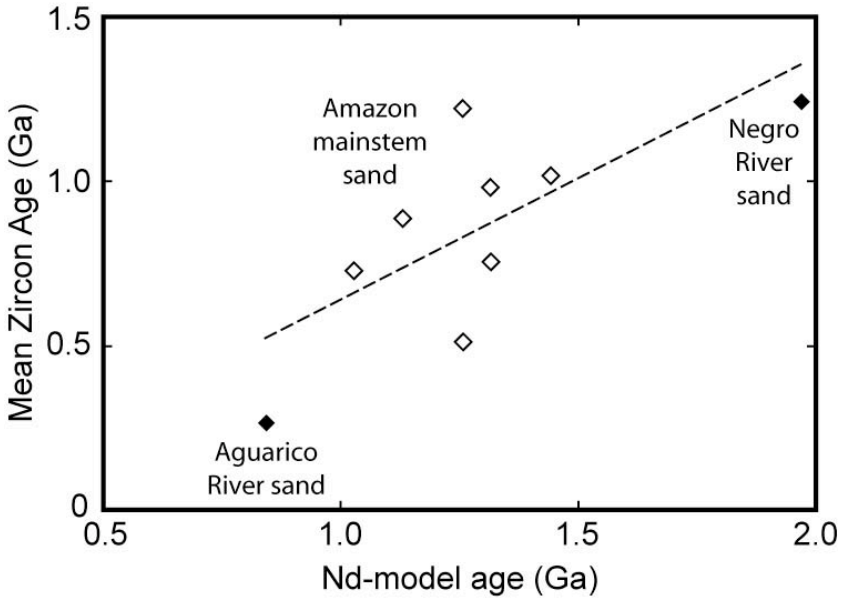

Figure 3.7- Mean detrital zircon grain ages (Mapes, this text) vs. Nd-model ages collected from the same active Amazon River sands show a positive relationship indicating that they reflect similar provenance.

source rock types. Grain sizes of sediment produced in low-relief humid environments are directly relatable to source rock mineralogy and composition; weathered granites produce abundant clay size material (from weathering of feldspars, micas, and amphiboles) and abundant quartz rich sand with grain sizes equivalent to the grain size of the primary grains in the source rock (Potter and Franzinelli, 1985). Sediments formed in cold and dry climates, reflect the mineralogy of the parent rocks (Potter *et al.*, 2001), whereas in humid climates, primary source minerals can undergo several phases of destruction and reconstitution.

Duration of weathering and transport strongly affect sediment composition. Prolonged physical weathering can destroy large grains and as a result, increase the amount of fine material delivered by a sedimentary system. Prolonged exposure to chemical weathering can redistribute the chemistry of all but the most stable minerals. Mineral transformation rates are governed by the kinetics of specific weathering reactions and take place over widely different timescales (Formoso, 2006; Yokoyama and Matsukura, 2006). Transport distance, rate, and time spent in temporary storage determines how thoroughly chemical processes transform sediments.

Finally, sediments are physically fractionated during sedimentation; particle size, specific gravity, and shape determine transport rates (Allen, 1985; Pye, 1994). Although sedimentary sorting primarily occurs as a result of transport strength, climate and source rock composition can play a large role in determining sediment particle size distribution and ultimately, post-transport homogeneity. Constituents of first cycle sediment in high latitude/elevation environments are separated predominantly based on physical characteristics. Since the bulk of detritus has similar physical properties (quartz, feldspar, lithic fragments), most sediment is chemically and mineralogically similar to its source rocks

regardless of grain size (Potter *et al.*, 2001; Millot *et al.*, 2003). In environments where chemical weathering dominates, sediments are first segregated chemically into dissolved material, fine-clays, and sand and then disbursed into the sedimentary system where it is segregated based on physical properties. The end result of chemical weathering followed by physical transport is well-sorted deposits with monotonous geochemistry.

The discrepancy between interpretations gathered from Amazon suspended sediment and bedload provenance proxies is likely related to sediment transport rate and weathering susceptibility. Dosseto *et al.* (2006), using Uranium-series disequilibria techniques, found that the average time it takes for suspended sediment to travel from Andean source areas to the Madeira-Amazon confluence (>2000 km) is <20 kyr. Clay composition indicates that fine-grained suspended sediment traverses the basin in less time than is required to chemically transformation unstable minerals and as a result, give an 'up to the moment' view of sediment provenance from the dominant sediment source. In contrast, bedload transport rates are lower and transport times are well within the timeframes necessary to allow chemical weathering processes to take their course. For sands, temporary floodplain storage is a major factor and in short periods of time (<125 kyr; Johnsson and Meade, 1990) sands with diverse primary compositions can become quartz arenites (Savage and Potter, 1991). Sand grains stay in punctuated transport long enough to be transformed by chemical weathering processes and as a result appear to be more sensitive to weathering conditions after initial entrainment.

For the modern Amazon basin three questions can now be discussed:

(1) What provenance techniques best describe the source of the bulk of river sediment?

Suspended sediment mineralogy gives strong evidence that the vast majority of sediment discharged by the Amazon River comes from the Andes; suspended load minerals described at the river mouth are nearly identical to those described at the base of the Andes and they exist in similar proportions (Gibbs, 1967; Irion, 1984). In the bedload, detrital feldspar, biotite, and hornblende $^{40}Ar/^{39}Ar$ ages (McDaniel, 1998) near the river mouth point to dominantly Andean sources for Amazon sand; grain ages are tightly grouped and are of an age that is uniquely Andean. Amazon mouth heavy mineral abundances and zircon-tourmaline-rutile indices (Vital *et al.*, 1999) show that sand was once far more immature. Bulk isotope ratios for coarse- and fine-sediment and mean detrital zircon grain ages for samples collected from the fluvial Amazon River are consistent with derivation from the Andes and/or the western portion of the Amazon craton.

(2) What provenance techniques best describe the geologic diversity of the Amazon Basin?

Detrital zircon U/Pb ages do a good job at describing the range of possible source ages within the Amazon catchment. Taken together, Amazon River samples (Mapes, this text) and the mouth sample of Rino *et al.* (2004) fully describe the range of source ages that exist throughout the Amazon Basin (Figure 3.6). However, no single detrital zircon sample age spectrum proportionally describes the areal distribution of basement ages across the basin.

(3) What provenance techniques best describe the dominant weathering conditions that exist in the Amazon Basin?

Even though physical weathering processes are important in delivering sediment to Andean tributaries, the Amazonian Andes are predominantly humid and heavily forested. The dominant weathering style throughout the basin is chemical. Major element geochemical indices (CIA; Nesbit and Young, 1982 and ICV; Cox *et al.*, 1995) do a good job of describing basin-wide weathering conditions. Mineralogical compositions and SiO_2 compositions for bedload sediments indicate a recycled sedimentary source or a high degree of chemically weathering on first-cycle sands.

Application to the geologic record

The large scale and harsh weathering conditions that characterize the Amazon Basin allow for physical and chemical processes to modify and segregate sediment to a degree possible few places on Earth. Currently existing provenance proxies do a good job at describing geologic diversity of the Amazon drainage but employing the entire range of techniques when studying ancient deposits would be time and cost prohibitive. Selection of particular provenance techniques must be made in the context of material available and desired results. For example, if information on dominant sediment contributing source areas is desired and sandstones are coupled with genetically related shales, bulk-sediment petrographic analysis of sandstone and shale could best describe the range of source rock-types and the pre-depositional weathering conditions that existed in a paleo-drainage basin. For situations where only sand sized material is sampled, comparison of major constituent mineralogy to heavy-mineral weathering indices could provide similar information. If

information about specific and possibly minor sources is desired, then single mineral isotopic and geochronologic analysis and specific trace element indicators are best suited.

How long will signatures survive?

Chemical processes do not cease once sediment is deposited. Diagenesis can alter sediment as strongly as chemical weathering (McLennan *et al.*, 1993; Cox *et al.*, 2002). This means that for particles susceptible to alteration and recrystallization during diagenesis (e.g. clay minerals, lithic fragments, feldspars, and labile heavy minerals) important provenance indicators may be completely lost even after they have survived sedimentation. Chemical and isotopic compositions of fine-grained sediments that have undergone diagenesis are generally still useful as provenance proxies as reactions are typically isochemical (Blatt, 1985; Cox and Lowe, 1995). Because of the porous nature of many sands, addition and subtraction of chemical species can be an issue during diagenesis although compositions are commonly interpreted to represent pre-diagenetic conditions (Cox and Lowe, 1995). Minerals like quartz and zircon are stable almost indefinitely in sedimentary systems (Pettijohn *et al.*, 1972) making their physical and chemical characteristics reliable for provenance interpretation even after sediment has undergone extreme weathering and diagenesis.

Conclusions

Commonly used sediment provenance indicators yield dramatically different results for modern Amazon River sediment (Figure 3.8). In general, Amazon sediment provenance is dominantly Andean, mineralogical maturity of sediment is related to intense chemical weathering in a tropical climate. As immature first-cycle sands are transported away from the Andes, they mature, ultimately becoming quartz arenites prior to deposition near the river

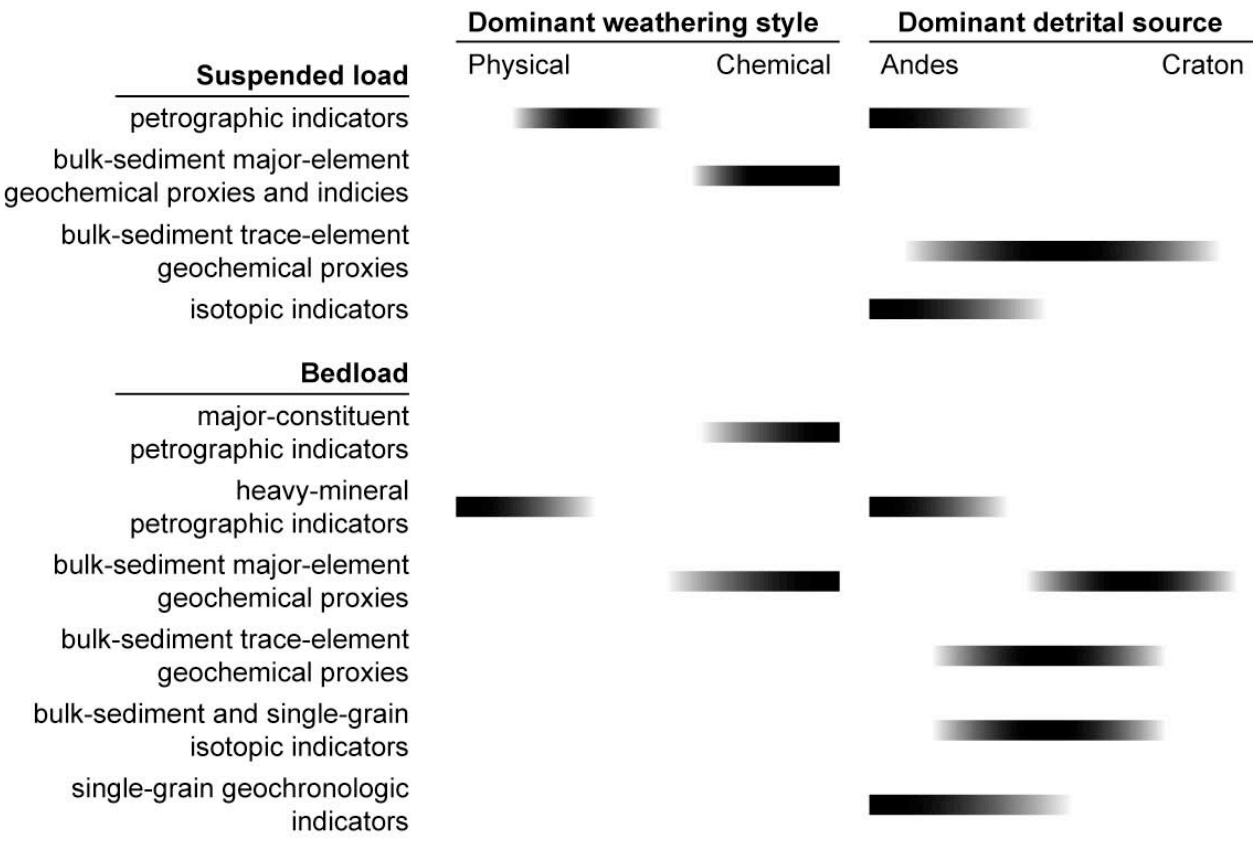

Figure 3.8- Comparison of provenance results for modern Amazon River clastic sediment.

mouth. In contrast, suspended sediment compositions stay constant from the Andes to the Atlantic. Isotopic compositions tend to become more craton-like downstream indicating increased input of lowland derived detritus.

All techniques do a poor job of characterizing the geology and areal relations of the entire drainage basin. Compositions are heavily biased towards areas that contribute the most sediment. Even though lowland areas constitute 7/8 of the basin area they contribute ~1/20 of the total sediment load. When interpreting results from ancient deposits it should be safe to assume that sedimentary signals from high relief areas of a drainage basin will overwhelm signals from areas of low relief regardless of areal extent.

Of most use to future studies is the observation that high transport rates (possibly 10^1 km/yr) make Amazon suspended sediments well suited to interpret Andean source rock compositions. Sand major constituent mineralogy and geochemistry appear to be better recorders of climate than source. They are transported at much lower rates (possibly $<10^{-2}$ km/yr) and as a result have mineralogies that are strongly affected by lowland chemical weathering. For the Amazon, provenance interpretations are strongest when coarse-grained sediments are linked to related fine-grained sediments.

References

Allen, J.R.L., 1985, Principles of sedimentology, George Allen and Unwin, London, 272 pgs.

Alexander, 1982, Leonardo da Vinci and fluvial geomorphology; American Journal of Science, v. 282, p. 735-755.

Allard, T., Ponthieu, M., Weber, T, Filizola, N., Guyot, J.-L., and Benedetti, M., 2002, Nature and properties of suspended solids in the Amazon Basin, Bulletin de la Société géologique de France, v. 173, p. 67-75.

Allégre, C.J., Dupré, B., Négrel, P., and Gaillardet, J., 1996, Sr-Nd-Pb isotope systematics in Amazon and Congo River systems: Constraints about erosion processes: Chemical Geology, v. 131, p. 93-112.

Amidon, W.H., Burbank, D.W., Gehrels, G.E, 2005, U-Pb zircon ages as a sediment mixing tracer in the Nepal Himalaya; Earth and Planetary Science Letters, v. 235, pp. 244-260.

Andersen, T., 2005, Detrital zircons as tracers of sedimentary provenance: limiting conditions from statistics and numerical simulation; Chemical Geology, v. 215, pp. 249-270.

Anhuf, D., Ledru, M.-P., Behling, H., Da Cruz, F.W., Jr., Cordeiro, R.C., Van der Hammen, T., Karmann, I., Marengo, J.A., De Oliveira P.E., Pessenda, L., Siffedine, A., Albuquerque, A.L., and Da Silva Dias, P.L., 2006, Paleo-environmental change in Amazonian and African rainforest during the LGM; Palaeogeography, Palaeoclimatology, Palaeoecology, v. 239, p. 510–527.

Archer, A.W., 2005, Review of Amazonian depositional systems: Special publication of the International Association of Sedimentologists, v. 35, p. 17-39.

Asmerom, Y., and Jacobsen, S.B., 1993, The Pb isotopic evolution of the Earth; inferences from river water suspended loads; Earth and Planetary Science Letters, v. 115, p. 245-256.

Basu, A.R., 1985, Influence of climate and relief on compositions of sands released at source areas; in Zuffa, G.G. ed., Provenance of Arenites, Reidel Publishing, p.1-18.

Basu, A.R., Sharma, M., and DeCelles, P.G., 1990, Nd, Sr-isotopic provenance and trace element geochemistry of Amazonian foreland basin fluvial sands, Bolivia and Peru; implications for ensialic Andean Orogeny: Earth and Planetary Science Letters, v. 100, p. 1-17.

Beckinsale, R., Sanchez-Fernández, A., Brook, M., Cobbing, E., Taylor, W., and Moore, N., 1985 - Rb-Sr whole-rock isochron and K-Ar age determinations for the Coastal Batholith of Peru, *in* Pitcher, W. S., Atherton, M. P., Cobbing, E. J., and Beckinsale, R. D.,

Magmatism at a plate edge. The Peruvian Andes: Glasgow, Blackie and Son Ltd., p. 177-202.

Benavides-Cáceres, V., 1999, Orogenic evolution of the Peruvian Andes: The Andean Cycle; in Skinner, B.J., ed., Geology and ore deposits of the Central Andes, Special Publication-Society of Economic Geologists, v. 7, pp. 61-107

Bhatia , M.R., and Crook, A.W., 1986, Trace element characteristics of graywackes and tectonic setting discrimination of sedimentary basins; Contributions to Mineralogy and Petrology, v. 92, p. 181-193.

Blatt, H., Middleton, G.V., and Murray, R., 1972, Origin of sedimentary rocks; Prentice Hall, Englewood Cliffs, New Jersey, 634 p.

Blatt, H., 1985, Provenance studies in mudrocks: Journal of Sedimentary Petrology, v. 55, p. 69-75.

Burke, K.C., and Lytwyn, J., 1993, Origin of the rift under the Amazon Basin as a result of continental collision during Pan-African time; International Geology Review, v.35, pp. 881-897.

Chew, D.M., Schaltegger, Ko□ler, J., Whitehouse, M.J., Gutjahr, M., Spikings, R.A., and Mi□kovic, A., 2007, U-Pb geochronologic evidence for the evolution of the Gondwanan margin of the north-central Andes: Geological Society of America Bulletin, v. 119, p. 697-711.

Clemens, K. E., and Komar, P. D., 1988, Oregon beach-sand compositions produced by the mixing of sediments under a transgressing sea: Journal of Sedimentary Petrology, v. 58, p. 519-529.

Cobbing, E.J., 1985, The tectonic setting of the Peruvian Andes; in Pitcher, W.S., Atherton, M.P., Cobbing, E.J., and Beckinsdale, R.D., eds., Magmatism at a plate edge: the Peruvian Andes, University of Liverpool, pp. 3-12.

Cordani, U.G., Sato, K., Teixeira, W., Tassinari, C.C.G., and Basei, M.A.S., 2000, Crustal evolution of the South American platform, in Cordani, U. G., Milani, E. J., Thomaz Filho, A., and Campos, D. A. eds., Tectonic Evolution of South America. Rio de Janeiro, p. 19-40.

Costa, J. B. S., Bemerguy, R. L., Hasui, Y., and Borges, M.S., 2001, Tectonics and paleogeography along the Amazon river. Journal of South American Earth Science, v. 14, p. 335-347.

Cox, R., Lowe, D.R., and Cullers, R.L., 1995, The influence of sediment recycling and basement composition on evolution of mudrock chemistry in the southwestern United States; Geochemica et Cosmochimica Acta, v. 59, p. 2919-2940.

Cox, R., Gutmann, E.D., and Hines, P.G., 2002, Diagenetic origin for quartz-pebble conglomerates: Geology, v. 30, p. 232-326.

Cullers, R.L., Basu, A., and Sutner, L.J., 1988, Geochemical signatures of provenance in sand-size material in soils and stream sediments near the Tobacco Root Batholith, Montana, U.S.A. Chemical Geology, v. 70, p. 335-348.

DeCelles, P.G., and Hertel, F., 1989, Petrology of fluvial sands from the Amazonian foreland basin, Peru and Bolivia, Geological Society of America Bulletin, v. 101, p. 1552-1562.

DePaolo, D.J., 1981, A neodymium and strontium isotopic study of the Mesozoic calc-alkaline granitic batholiths of the Sierra Nevada and Peninsular Ranges, California. Journal of Geophysical Research, v. 86, p. 10,470-10,488.

Dickinson, W.R., and Suczek, C.A., 1979. Plate tectonics and sandstone compositions. American Association of Petroleum Geologists Bulletin, v. 63, p. 2164-2182

Dickinson, W.R., 1985, Interpreting provenance relations from detrital modes of sandstones; *in* Zuffa, G.G. ed., Provenance of Arenites, Reidel Publishing, p. 333-361.

Dickinson, W.R., and Gehrels, G.E., 2003, U-Pb ages of detrital zircons from Permian and Jurassic sandstones of the Colorado Plateau, USA: paleogeographic implications; Sedimentary Geology, v. 163, pp. 29-66.

Dosseto, A., Bourdon, B., Gaillardet, J., Maurice-Bourgoin, L., and Allégre, C.J., 2006, Weathering and transport of sediments in the Bolivian Andes: time constraints from uranium-series isotopes; Earth and Planetary Science Letters, v. 248, p. 759-771.

Dunne, T., Mertes, L.A.K., Meade, R.H., Richey, J.E., and Forsberg, B.R., 1998, Exchanges of sediment between the floodplain and channel of the Amazon River in Brazil; Geological Society of America Bulletin, v. 110, pp. 450-467.

Egenhoff, S. and Lucassen, F., 2003, Chemical and isotopic composition of Lower to Upper Ordovician sedimentary rocks (Central Andes/South Bolivia) : Implications for their Source, Journal of Geology, v. 111, p. 487-497.

Elbaz-Poulichet, F., Seyler, P., Maurice-Bourgoin, L., Guyot, J.-L., and Dupuy, C., 1999, Trace element geochemistry in the upper Amazon drainage basin (Bolivia); Chemical Geology, v. 157, p. 319-334.

Faure, G., 1986, Principles of isotope geology: John Wiley and Sons, New York, 589 p.

Fedini, P.S., and Jardin, W.F., 2001, Is the Negro River Basin Amazon impacted by naturally occurring mercury? The Science of the Total Environment, v. 275, p. 71-82.

Feninger, T., 1982, The metamorphic “basement” of Ecuador; Geological Society of America Bulletin, v. 93, pp. 87-92.

Folk, R. L., 1968, Petrology of sedimentary rocks: Austin, University of Texas Press, 154 p.

Formoso, M.L.L, 2006, Some topics on geochemistry of weathering: a review: Anais da Acadademia Brasileira de Ciências, v. 78, p. 809-820.

Franzinelli, A. and Potter, P.E., 1983, Petrology, chemistry, and texture of modern river sands, Amazon River system; Journal of Geology, v. 91, pp. 23-39.

Gaillardet, J., Dupré, B., Allégre, C.J., and Negrél, P., 1997, Chemical and physical denudation in the Amazon River Basin: Chemical Geology, v. 142, p. 141-173.

Gibbs, R.J., 1967, The geochemistry of the Amazon River system: Part 1- The factors that control the salinity and the composition and concentration of the suspended solids; Geological Society of America Bulletin, v.78, p. 1203-1232.

Gerard, M., Seyler, P., Benedetti, M.F., Alves, V.P., Boaventura, G.R., and Sondag, F., 2003, Rare earth elements in the Amazon basin; Hydrological Processes, v. 17, p. 1379-1392.

Goldstein, S.L., O'Nions, R.K., and Hamilton, P.J., 1984, A Sm-Nd isotopic study of atmospheric dusts and particulates from major river systems; Earth and Planetary Science Letters, v. 70 pp. 221-236.

Goldstein, S.L., and Jacobsen, S.B., 1988, Rare earth element in river waters, Earth and Planetary Science Letters, v. 89, p. 35-47.

Goodge, J.W., Williams, I.S., and Myrow, P., 2004, Provenance of Neoproterozoic and lower Paleozoic siliciclastic rocks of the central Ross orogen, Antarctica: detrital record of rift-, passive-, and active-margin sedimentation; Geological Society of America Bulletin, v. 116, pp. 1253-1279.

Gordeev, V.V., Miklishansky, A.Z., Migdisov, A.A., and Artemyev, V.E., 1985, Rare element distribution in the surface suspended material of the Amazon River, some of its tributaries and estuary; in Degens, E.T., Kempe, S., Herrera, R., eds., Transport of carbon and minerals in major world rivers: Part 3, Mitteilungen aus dem Geologisch-Palaontologischen Institut der Universitat Hamburg, v. 58, p. 225-243.

Gromet, L.P., Dymek, R.F., Haskin, L.A., and Korotev, R.L., 1984, The "North American shale composite"; its compilation, major and trace element characteristics; Geochimica et Cosmochimica Acta, v.48, p. 2469-2482.

Gutiérrez-Alonso, G., Fernández,-Suárez, J, Collins, A.S., Abad, I., and Nieto, F., 2005, Amazonian Mesoproterozoic basement in the core of the Ibero-Armorican arc- ^{40}Ar-^{39}Ar detrital mica ages complement the zircons tale; Geology, v. 33, p. 637-640.

Guyot, J.L., Jouanneau, J.M., Soares, L., Boaventura, G.R., Maillet, N., Lagane, C., 2007, Clay mineral composition of river sediments in the Amazon Basin: Catena, v. 71, p. 340-356.`

Haines, P.W., Turner, S.P., Kelley, S.P., Wartho, J.-O. and Sherlock, S.C., 2004, ^{40}Ar-^{39}Ar dating of detrital muscovite in provenance investigations: a case study from the Adelaide Rift Complex, South Australia; Earth and Planetary Science Letters, v. 227, p. 297-311.

Harmon, R.S., Barreiro, B.A., Moorbath, S., Hoefs, J., Francis, P.W., Thorpe, R.S., Déruelle, B., McHugh, J., and Viglino, J.A., 1984, Regional O-, Sr-, and Pb-isotope relationships in late Cenozoic calc-alkaline lavas of the Andean Cordillera; Journal of the Geological Society of London, v. 141, p. 803-822.

Helmhold, K.P., 1985, Provenance of feldspathic sandstones- The effect of diagenesis on provenance interpretations: A review; in Zuffa, G.G. ed., Provenance of Arenites, Reidel Publishing, p. 139-163.

Hoey, T.B., 2004, The size of sedimentary particle; in Evans, D.J.A., and Benn, D.I., eds., A practicle guide to the study of glacial sediments: Arrnold Publishing, p. 52-77.

Hovikoski, J., Räsänen, M., Gingras, M., Roddaz, M., Brusset, S., Hermoza, W., Romero Pittman, L., and Lertola, K., 2005, Miocene semidiurnal tidal rhythmites in Madre de Dios, Peru; Geology, v. 33, p. 177-180.

Hubert, J.F., 1962, A zircon-tourmaline-rutile maturity index and the interdependence of the composition of heavy mineral assemblages with the gross composition and texture of sand stine; Journal of Sedimentary Petrology, v. 32, p. 440-450.

Irion, G., 1983, Clay mineralogy of the suspended load of the Amazon and of rivers in the Papua-New Guinea mainland; *in* Degens, E.T., Kempe, S., and Soliman, H., eds., Transport of carbon and minerals in major world rivers, SCOPE/UNEP Sonderband 55, p. 483-504.

Irion, G., 1991, Minerals in Rivers, *in* Degens, E.T., Kempe, S., and Richey, J.E., Biogeochemistry of major world rivers, SCOPE, John Wiley and Sons, p. 265-281.

Johnsson, M.J., and Meade, R.H., 1990, Chemical weathering of fluvial sediments during alluvial storage: the Macuapanim Island point bar, Solimões River, Brazil; Journal of Sedimentary Petrology, v. 60, p. 827-842.

Johnsson, M.J., Stallard, R.F., and Lundberg, N., 1990, Petrology of fluvial sands from the Amazonian foreland basin, Peru and Bolivia: Discussion and reply, Geological Society of America Bulletin, v. 102, p. 1727-1730.

Kay, S.M., Mpodozis, C., Coira, B., 1999, Neogene magmatism, tectonism, and mineral deposits of the Central Andes (22 degrees to 33 degrees S latitude); in Skinner, B.J. ed., Geology and ore deposits of the Central Andes, Society of Economic Geologists Special Publication, v. 7, p.27-59.

Konhauser, K.O., Fyfe, W.S., and Kronberg, B.I., 1994, Multi-element chemistry of some Amazonian waters and soils; Chemical Geology, v. 111, p.155-175.

Kylander-Clark, A. R. C., Coleman, D. S., Glazner, A. F. and Bartley, J. M., 2005, Evidence for 65 km of dextral slip across Owens Valley, California, since 83 Ma: Geological Society of America Bulletin, v. 117, p. 962-968.

Lease, R.O., Burbank, D.W., Gehrels, G.E., Wang, Z., Yuan, D., 2007, Signatures of mountain building: Detrital zircon U/Pb ages from northeastern Tibet; Geology, v. 35, p. 239-242.

LeFavour, G., and Alsdorf, D., 2005, Water slope and discharge in the Amazon River estimated using the shuttle radar topography mission digital elevation model; Geophysical Research Letters, v. 32, 5 p.

Macfarlane AW, 1999, Isotopic studies of northern Andean crustal evolution and ore metal sources. *in* Skinner, B., ed., Geology and ore deposits of the central Andes. Society of Economic Geologists Special Publication 7, p. 195–217.

Mapes, R.W., this text, Evaluating transcontinental detrital zircon transport in the modern Amazon River, in Past and present provenance of the Amazon River drainage basin: Ph.D. dissertation, University of North Carolina at Chapel Hill, 54 p.

Martin-Gombojav, N., and Winkler, W., 2008, Recycling of Proterozoic crust in the Andean foreland of Ecuador: implications for orogenic development of the Northern Andes: Terra Nova, v. 20, p. 22-31.

Martin, J.-M., and Maybeck, M., 1979, Elemental mass-balance of material carried by major world rivers; Marine Chemistry, v. 7, p. 173-206.

Martinelli, L.A., Victoria, R.L., Devol, A.H., Richey, J.E., and Forsberg, B.R., 1989, Suspended sediment load in the Amazon basin: an overview; GeoJournal, v. 19.4, p. 381-389.

McCourt, W.J., Aspden, J.A., and Brook, M., 1984, New geological and geochronological data from the Colombian Andes: continental growth by multiple accretion; Journal of the Geological Society of London, v. 141, p. 831-845.

McDaniel, D.K., 1998, Provenance and weathering history of Amazon sediment; Ph.D. dissertation, SUNY-Stony Brook, 188 p.

McDaniel, D.K., McLennan, S.M., and Hanson, G.N., 1997, 8. Provenance of Amazon Fan muds: Constraints from Nd and Pb isotopes; in Flood, R.D., Piper, D.J.W., Klaus, A., and Peterson, L.C. eds., Proceedings of the Ocean Drilling Program, v. 155, p. 169-176.

McLennan, S.M., 1989, Rare earth elements in sedimentary rocks: influence of provenance and sedimentary processes; in Lipin, B.R., and McKay, G.A., eds., Geochemistry and mineralogy or rare earth elements, Mineralogical Society of America Reviews in Mineralogy, v. 21, p. 168-200.

McLennan, S.M., Hemming, S., McDaniel, D.K., and Hanson, G.N., 1993, Geochemical approaches to sedimentation, provenance, and tectonics: Geological Society of America Special Paper, No. 284, p. 21-40.

Meade, R.H., 1994, Suspended sediment of the modern Amazon and Orinoco Rivers; Quaternary International, v. 21, p. 29-39.

Meade, R.H., 1996, River-sediment inputs to major rivers; in Milliman, J.D., and Haq, B.U., eds., Sea-level rise and costal subsidence, U.S. Government, pp. 63-85.

Meade, R.H., Rayo, J.M., Da Conceicão, S.C., and Natividade J.R.G., 1991, Backwater effects in the Amazon River basin of Brazil; Environmental Geology, v. 18, p. 105-114.

Mertes, L.A., Dunne, T., and Martinelli, L.A., 1996, Channel-floodplain geomorphology along the Solimões-Amazon River, Brazil. Geological Society of America Bulletin, v. 108, p. 1089-1107.

Michalopoulos, P., and Aller, R.C., 1995, Rapid clay mineral formation in Amazon delta sediments: reverse weathering and oceanic elemental cycles; Science, v. 270, p. 614-617.

Milani, E.J., and Thomaz Filho, A., 2000, Sedimentary basins of South America; *in* Cordani, U.G., Milani, E.J., Thomaz Filho, A., and Campos, D.A., Tectonic evolution of South America, 31st International Geological Congress, Rio de Janeiro, p. 389-449.

Miller, J.F., and Harris, N.B.W., 1989, Evolution of continental crust in the Central Andes; constraints from Nd isotope systematics; Geology, v. 17, pp. 615-617.

Millot, R., Gaillardet J., Dupré B., and Allégre C. J., 2003, Northern latitude chemical weathering rates: clues from the Mackenzie River Basin, Canada: Geochimica Cosmochimica Acta, v. 67, p. 1305-1329.

Nagy, L.A., 2008, Sm-Nd Bulk Sediment Analysis on Sands from the Amazon River Basin; Senior thesis, University of North Carolina at Chapel Hill, 20 p.

Nesbitt, H.W., and Young, G.M., 1982, Early Proterozoic climates and plate motions inferred from major element chemistry of lutites; Nature, v. 299, p. 715-717.

Nesbitt, H.W., MacRae, N.D., and Kronberg, B.I., 1990, Amazon deep-sea fan muds: light REE enriched products of extreme chemical weathering; Earth and Planetary Science Letters, v. 100, p. 118-123.

NOAA Observing Systems Architecture (NOSA), 15 March, 2009, < http://nosa.noaa.gov/>

Nobel, S.R., Aspden, J.A., and Jemielita, R., 1997, Northern Andean crustal evolution: New U-Pb geochronological constraints from Ecuador; Geological Society of America Bulletin, v. 109, pp. 789-798.

Nordin, C.F., 1985, The sediment loads of rivers, in Rodda, J.J., ed., Facets of Hydrology volume II, Wiley and Sons, p. 184-204.

Ordonez Carmona, O., and Pimental, M.M., 2002, Rb-Sr and Sm-Nd isotopic study of the Puqui Complex, Colombian Andes: Journal of South American Earth Sciences, v.15, p. 173-182.

Petford, N., Atherton, M.P., and Halliday, A.N., 1996, Rapid magma production rates, underplating and remelting in the Andes: isotopic from the north and central Peru Andes: Journal of South American Earth Science, v. 9, p. 69-78.

Pettijohn, F.J., Potter, P.E., and Siever, R., 1972, Sand and Sandstone, Springer-Verlag, New York, 618 p.

Poldevaart, A., 1955, Zircons in rocks: 1-Sedimentary rocks; American Journal of Science, v. 253, p. 433-461.

Posada, L.G., and Nordin, C.F., 1992, Total and unmeasured sediment loads of some tropical rivers: Eos, Transactions, American Geophysical Union, v. 73, p. 137.

Potter, P.E., 1978, Significance and origin of big rivers; Journal of Geology, v. 86, p.13-33.

Potter, P.E., and Franzinelli, E., 1985, Fraction analyses of modern river sand of Rios Negro and Solimões, Brazil, Implications for the origin of quartz-rich sandstones, Revista Brasileira de Geociências, v. 15, p. 31-35.

Potter, P.E., 1986, South America and a few grains of sand: Part 1- Beach Sands; Journal of Geology, v. 94, p. 301-319.

Potter, P.E., Huh, Y., Edmond, J.M., 2001, Deep-freeze petrology of Lena River sand, Siberia: Deep-freeze petrology of Lena River sand, Siberia, v. 29, p. 999-1002.

Prokopiev, A.V., Toro, J., Miller, E.L., Gehrels, G.E., 2008, The paleo-Lena River- 200 m.y. of transcontinental zircon transport in Siberia: Geology, v. 36, p. 699-702.

Pye, K., 1994, Sediment transport and depositional processes. Blackwell Scientific Publications, Oxford, 397 pgs.

Räsänen, M.E., Linna, A.M., Santos, J.C.R., and Negri, F.R., 1995, Late Miocene tidal deposits in the Amazonian foreland basin; Science, v. 269, pp. 386-390.

Restrepo-Pace, P.A., Ruiz, J., Gehrels, G., and Cosca, M., 1997, Geochronology and Nd isotopic data of Grenville-age rocks in the Colombian Andes: new constraints for Late Proterozoic-Early Paleozoic paleocontinental reconstructions of the Americas; Earth and Planetary Science Letters, v. 150, pp. 427-441.

Richey, J.E., Nobre, C., and Deser, C., 1989, Amazon River discharge and climate variability: Science, v. 246, p. 101-103.

Rimmington, N, Cramp, A., Morton, A., 2000, Amazon fan sands: implications for provenance; Marine and Petroleum Geology, v. 17, p. 267-284.

Rino, S., Komiya, T., Windley, B.F., Katayama, I., Motoki, A., and Hirata, T., 2004, Major episodic increases of continental crustal growth determined from zircon ages of river sands; implications for mantle overturns in the Early Precambrian: Physics of the Earth and Planetary Interiors, v. 146, p. 369-394.

Roddaz, M., Viers, J., Brusset, S., Baby, P., and Hérail, G., 2005, Sediment provenances and drainage evolution of the Neogene Amazonian foreland basin; Earth and Planetary Science Letters, v. 239, pp. 57-78.

Roser, B.P., and Korsch, R.J., 1986, Determination of tectonic setting of sandstone-mudstone suites using SiO_2 content and K_2O/Na_2O ratio; Journal of Geology, v. 94, p. 635-650.

Ruhl, K.W., and Hodges, K.V., 2005, The use of detrital mineral cooling ages to evaluate steady state assumptions in active orogens: an example from the central Nepalese Himalaya; Tectonics, v. 24, 14 pp.

Savage, K.M., and Potter, P.E., 1991, Petrology of modern sands of the Rios Guaviare and Inirida, southern Colombia; tropical climate and sand composition: Journal of Geology, v. 99, p.289-298.

Sedimentation Seminar, 1981, Comparison of methods of size analysis for sands of the Amazon-Solimões Rivers, Brazil and Peru; Sedimentology, v. 28, p. 123-128.

Schobbenhaus, C., and Bellizza, A., 2001, Geological map of South America, 1:5,000,000 scale: Commission for the Geological Map of the World- Companhia de Pesquisa de Recursos Minerais- Departamento Nacional de Produção Mineral- UNESCO, Brasilia.

Sholkovitz, E.R., and Price, N.B., 1980, The major-element chemistry of suspended matter in the Amazon Estuary; Geochimica et Cosmochimica Acta, v. 44, p. 163-171.

Soler. P., Rotach-Toulhoat, N., 1990, Sr-Nd isotope compositions of Cenozoic granitoids along a traverse of the central Peruvian Andes. Geological Journal, v. 25, p. 351–358.

Stallard, R.F., 1985, River chemistry, geology, geomorphology, and soils in the Amazon and Orinoco basins; *in* Drever, J.D. ed. The Chemistry of Weathering, D. Reidel Publishing Company, p. 293-316.

Stein, M.M., 1979, Schwermineralunterschungen an flussproben des Amazonas und seiner wichtigsten Nebenflüsse, hauptprüfung mineralogy: Institut für Sedimentforschung, Heidelberg, Germany, 74 p.

Szatmarim, P., 1983, Amazon rift and Pisco-Juruá fault: Their relation to the separation of North America from Gondwana; Geology, v. 11, pp 300-304.

Tassinari, C.C.G, Bettencourt, J.S., Geraldes, M.C., Macambria, M.J.B., and Lafon, J.M., 2000, The Amazonian Craton; *in* Cordani, U.G., Milani, E.J., Thomaz Filho, A., and Campos, D.A., Tectonic evolution of South America, 31st International Geological Congress, Rio de Janeiro, pp.41-99.

Teixeira, W., Tassinari, C.C.G., Cordani, U.G., and Kawashita, K., 1989, A review of the geochronology of the Amazonian Craton: tectonic implications; Precambrian Research, v. 42, pp. 213-227.

Todsal, R.M., 1996, The Amazon Laurentian connection as viewed from the central Andes, western Bolivia and northern Chile; Tectonics, v. 15, p. 827-842.

Trask, P. D., 1952, Sources of beach sand at Santa Barbara, California, as indicated by mineral grain studies, U.S. Army Beach Erosion Board Technical Memo N. 28, p. 24.

Tyrrell, S., Haughton, P.D.W., Daly, J.S., Kokfelt, T.F., and Gagnevin, D., 2006, The use of the common Pb isotope composition of detrital K-feldspar grains as a provenance tool and its application to the upper Carboniferous paleodrainage, northern England; Journal of Sedimentary Research, v. 76, p. 324-345.

Vermeesh, P., 2004, How many grains are needed for a provenance study? Earth and Planetary Science Letters; v. 224, pp. 441-451.

Vital, H., and Stattegger, K., 2000, Major and trace elements of stream sediments form the lowermost Amazon River; Chemical Geology, v. 168, p. 151-168.

Vital, H., Stattegger, K., and Garbe-Schönberg, C.-D., 1999, Composition and trace-element geochemistry of detrital clay and heavy mineral suites of the lowermost Amazon River: a provenance study; Journal of Sedimentary Research, v. 69, p. 563-575.

Yokoyama, T., and Matsukura, Y., 2006, Field and laboratory experiments on weathering rates of granodiorite: separation of chemical and physical processes: Geology, v. 34, p. 809-812.

CHAPTER 4

LATE CRETACEOUS TO MODERN FLUVIAL EVOLUTION OF AMAZONIA AND SIGNIFICANCE OF THE PURUS ARCH

Abstract

Detrital zircon ages and sedimentologic data for siliciclastic deposits along the Amazon River suggest that since the Cretaceous, a continent-scale drainage inversion occurred. During the Late Cretaceous, drainage was directed west from an uplifted rift-shoulder near the modern Amazon mouth. By the Miocene, northeastern South America had subsided and the Andes had uplifted enough to form two drainage sub-basins separated by the Purus Arch: an east-draining eastern fluvial basin and a restricted continental basin in western Amazonia. The drainage history of the western basin was complex but it appears that by late Miocene it was isolated. Once the continental basin was overfilled and the Purus Arch breached, the modern Amazon River system was established during or after the late Miocene.

Introduction

Few rivers on Earth rival the scale of the Amazon system. The Amazon drainage, the largest on earth at over 6 x 10^6 km^2 (Sioli, 1984), covers over one third of the South America. At over 6,500 km in length (Hoorn, 2006a), the river ranks in the top two globally. Annual river discharge surpasses that the next largest river by ~5x (Meade, 1996) and constitutes about 20% of the global fresh water total (Callede *et al.*, 2004). Annual sediment discharge ranks among the top three rivers at 1.1-1.3 x 10^9 tons (Meade, 1994). Biologically, Amazonia

contain approximately half of the total tropical rain forest area on the planet (Whitmore, 1998) and the region is home to some of the most diverse flora and fauna on Earth (Webb, 1995; Patton *et al.* 2000; Bates, 2001).

The scale and diversity of the modern Amazon River system owe themselves to a series of events that occurred across northern South America during and after the breakup of the Gondwana supercontinent. Rift related tectonism and Andean orogeny have had a profound effect on drainage patterns in the low-lying continental interior. Work by Hoorn (1995), Räsänen (1995), Roddaz *et al.* (2005), Hovikoski *et al.*, (2006) and many others have led to an understanding of how the western portion of the Amazon River system evolved from mid-Miocene time (16-10 Ma) until the present. Their work details the existence of an expansive continental water body that formed in response to uplift of the Andes and that at times during its history likely had marine connections to the Caribbean, Pacific, and/or Southern Atlantic. Across the basin, study of Amazon Fan and proximal deep-sea deposits indicate that the first appearance of Andean derived sediments into the Atlantic occurred between 11 and 10 Ma (Dobson *et al.*, 2001; Figueiredo *et al.*, 2008).

Acceptance of a single model for establishment modern Amazon system within the continental interior has been confounded by the remoteness and poor accessibility of the region. For example, Hoorn *et al.* (1995), and Wesselingh (2006) called for late Miocene establishment of the modern Amazon system after studying deposits in northwestern Amazonia. Roddaz *et al.* (2005) and Espurt *et al.* (2007) suggested that establishment of the modern Amazon system occurred no earlier than the Pliocene after studying deposits and structures in the Peruvian and Bolivian Andean foreland. Campbell *et al.* (2006) proposed formation of the modern Amazon system in the late Pliocene based on work in southwest

Amazonia, and Rossetti *et al.* (2005) suggested that east-directed fluvial transport through the Amazon trough did not commence until the late Pleistocene after studying deposits along the Brazilian Amazon trunk. General agreement exists that the Purus Arch (Figure 4.1), a low-lying topographic barrier, separated drainage between western and eastern Amazonia prior to establishment of the modern Amazon (Costa, 1991; Potter, 1997), but no direct evidence has been found to support its existence. We collected sedimentologic and detrital zircon U-Pb grain ages for Cretaceous, Miocene, and recent sands on either side of the Purus Arch to evaluate fluvial connections that existed in the region and to evaluate the importance of the arch as a topographic barrier over the last ~100 Ma.

Tectonic Setting

Detrital zircon ages are useful sediment source indicators in Amazonia because of the predictable layout of geochronologic provinces across South America and because the river crosses those provinces at a high angle (Figure 4.1). Major zircon forming events occurred in the Amazon Craton during a series of Archean to Mesoproterozoic accretionary and orogenic episodes (Almeidia *et al.*, 2000; Tassinari *et al.*, 2000). At approximately 1.1 Ga, craton formation climaxed in the Sunsas Orogeny during final amalgamation of the supercontinent Rodinia (Cordani *et al.*, 2000). Post-Sunsas time saw formation of passive margins on what are now the southern and eastern edges of the craton (Brito Neves and Cordani, 1991), which subsequently closed between 700 and 500 Ma during the Gondwana forming, Pan-African-Braziliano Orogeny (Ramos, 1988; Alvarenga *et al.*, 2000).

Deposition of continental sediments into the Amazon rift basin commenced in the late Proterozoic during the late stages of the Pan-African-Braziliano Orogeny (Caputo, 1984; Brito Neves and Cordani, 1991). Three major cycles of Phanerozoic sedimentation occurred

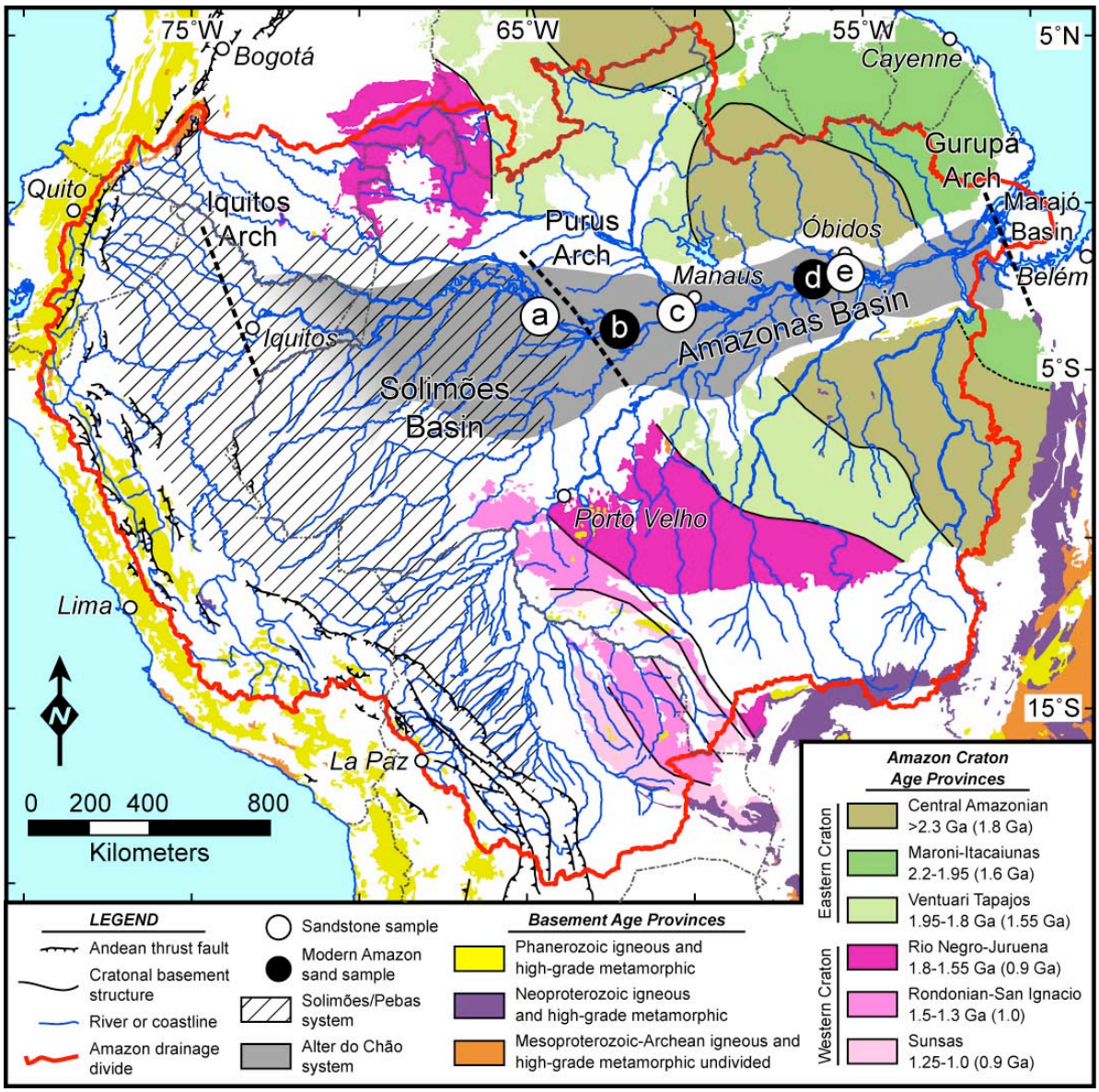

Figure 4.1- Igneous and high-grade metamorphic rock age provinces of the Amazon fluvial basin and surrounding areas and distribution of widespread Cretaceous Amazonas and Solimões basin sedimentary rocks (Tassinari *et al.*, 2000; Mosmann *et al.*, 1987; Hoorn; 1994; Schobbenhaus and Bellizza, 2001). Samples: a- Solimões Formation near Tefé, b- modern river sand near Codajás, c- Novo Remanso and Iranduba formations near Manacapuru, d- modern river sand near Juruti, e- Alter do Chão Formation at Serra de Óbidos.

depositing up to 6000 m of sediment into the Amazon aulocogen (Cunha *et al.*, 1994; Eiras *et al.*, 1994; Mosmann *et al.*, 1987). Several sedimentary basins separated by basement arches, each with a somewhat independent tectonic and sedimentary history, form the greater Amazon sedimentary basin (Figure 4.1; Brito Neves *et al.*, 1984).

After the Neoproterozoic, tectonic events that influenced zircon formation in western South American occurred independently of those to the east. Rifting of Rodina led to establishment of a passive margin along the western edge of the craton during the early Paleozoic (Ramos and Aleman, 2000). By late Ordovician, convergent tectonics were established along the entire length of the northern and central Andean margin (Chew *et al.*, 2007). From the Devonian to the early Triassic, a series of collisional events occurred in the northern Andes that juxtaposed Gondwana with Laurentia (Aleman and Ramos, 2000), while along the central Andean margin, subduction continued uninterrupted (Jaillard *et al.*, 2000). Jurassic rifting and subsidence created the passive Caribbean margin and modified the northern Andes, reinitiating subduction along the entire chain (Ramos and Aleman, 2000). Accretion of oceanic terranes occurred in the Colombian and Ecuadorian Andes from the late Cretaceous to early Cenozoic (Aleman and Ramos, 2000).

Events related to and following the breakup of Gondwana had the strongest influence on formation of the Amazon River system. Formation of the South American continent started in the Jurassic with opening of the South Atlantic (Macdonald *et al.*, 2003) that accompanied renewed tectonism within the Amazon trough (Caputo, 1991, 1984; Costa *et al.*, 2001, 2002). Opening of the central Atlantic occurred during the latest stages of rifting but by the late Aptian (~115 Ma), the Atlantic margin in the vicinity of the Amazon mouth had opened (Maisey, 2000). During the Cretaceous, the active Pacific margin was separated

from the Amazonian craton by a series of retroarc basins (Ramos and Aleman, 2000). Andean relief was minimal and localized; for example, the area that now makes up the Altiplano was at sea level until the early Paleocene (Gregory-Wodzicki, 2000). Foreland basin deposits in the central Andes (Horton *et al.*, 2001) indicate that significant uplift had begun by the Eocene. Exhumation of the Colombian (Gómez *et al.*, 2005) and Ecuadorian (Álava and Jaillard, 2005) Andes began in the late Cretaceous and continued into the Eocene but elevations throughout the northern and central Andes were probably less than 50% modern values into the mid-Miocene (Gregory-Wodzicki, 2000). A second, and more significant phase of Andean mountain building started at ~25 Ma and climaxed at ~10 Ma (Gregory-Wodzicki, 2000; Garizone *et al.*, 2008).

Surficial stratigraphy of the Amazon Trough

Exposed sediments in the eastern Amazon trough are dominated by the fluvial late Cretaceous to Neogene Alter do Chão Formation (Figure 4.2; Cunha *et al.*, 1994). Deposits are red to white, coarse- to medium-grained sands with interbedded quartz pebble conglomerate, claystone, siltstone, and shale intercalations. Thickness reaches 1,200 m in the far eastern Amazonas basin on the western flank of the Garupá Arch (Figure 4.2; Caputo, 1984) and thins to a maximum 400-600 m thick in the central and western Amazonas basin and the Solimões basin (Mosmann *et al.*, 1987). West of the Purus Arch, the Alter do Chão Formation disappears below the Solimões Formation.

In the far-western Amazonas basin, two Miocene sandy deposits have recently been described along the eastern flank of the Purus Arch (Rozo *et al.*, 2005; Abinader *et al.*, 2007). Both units overlie the Alter do Chão Formation and are covered by Quaternary sediments. The lower unit, termed the Iranduba Formation by Abinader *et al.*, (2007) is

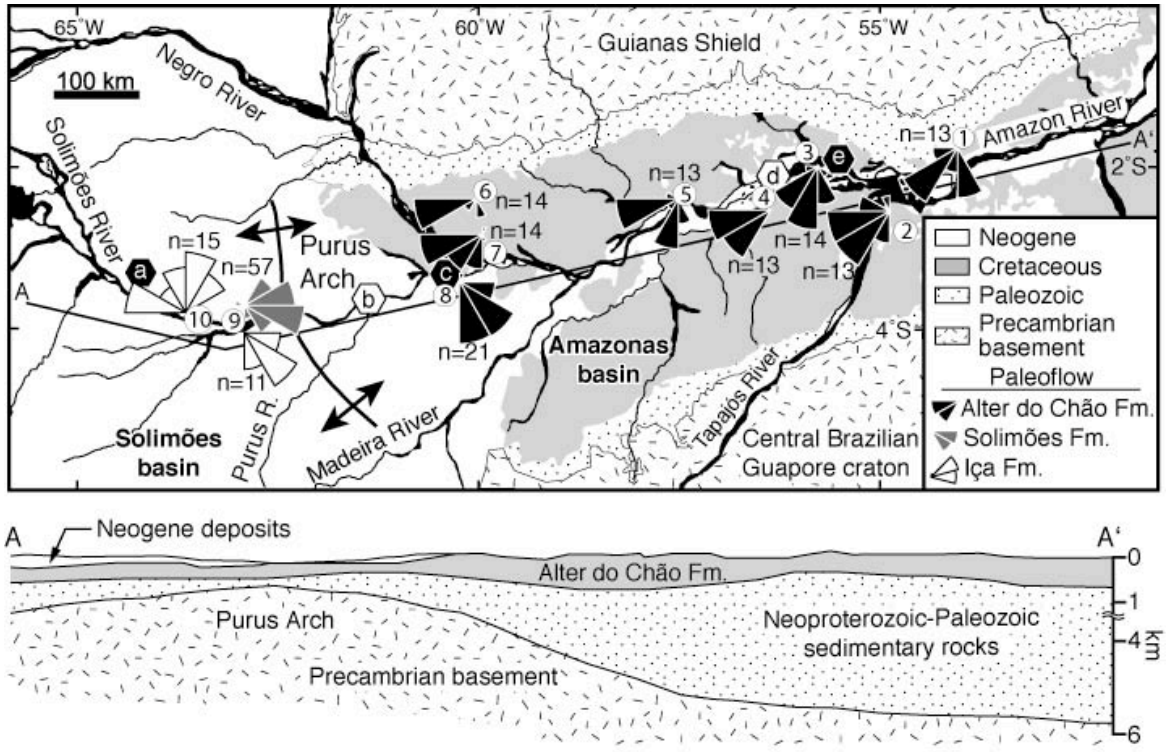

Figure 4.2- Generalized geology (Schobbenhaus and Bellizza, 2001) and paleoflow orientations for deposits along the central and eastern Amazon River. Measurements were taken on fluvial deposits (trough and tabular cross-beds) of the Iça and Alter do Chão formations and on distributary and deltaic deposits (longitudinal stratification and sigmoidal lobes) for the Solimões Formation. Lettered localities are detrital zircon samples; letters correspond to localities in figures 4.1 and 4.4. Numbered Localities: 1-Monte Alegre, 2-Alter do Chão, 3-Serra do Óbidos, 4-Serra de Parintins, 5-Serra do Pio, 6-Highway BR-174, 7-Manaus 8-Manacapuru-Iranduba, 9-Coari, 10-Barro Alto. Detrital zircon sample localities labeled with letters as in figures 4.1 and 4.2. Number beside rose indicates measured bedform quantity. Cross-section modified from (Caputo, 1985).

composed of reddish, coarse-medium grained, poorly-sorted sand, with trough and planar cross-stratification and intercalations of clay and mud. The upper unit is characterized by white, coarse-grained, ferruginous, massive sandstone and fine-medium grained sandstone with subordinate mudstone bodies and has been correlated with the Miocene Novo Remanso Formation (Rozo *et al.* 2005). Locally, the unit shows heterolytic inclined cross stratification with layers of gray clay rich in organic detritus and middle to late Miocene palynomorphs (Dino *et al.*, 2006). Abinader *et al.* (2007) interpreted both units as floodplain and/or fluvial-channel deposits laid down in a meandering or anastomosing fluvial environment.

Determining depositional timing on course-grained continental deposits is often problematic as biostratigraphic markers are often difficult to locate. However, weathering profiles developed across wide areas of eastern Amazonia allow for relative dating of deposits that otherwise lack age control. Bauxite deposits, which develop during prolonged periods of exposure, represent conspicuous horizons in rocks of eastern Amazonia and are generally restricted to pre-Eocene rocks (Truckenbrodt *et al.* 1991, Costa 1991). One such mature lateritic-bauxite profile is developed on the Alter do Chão Formation in the eastern Amazon trough (Figure 4.3; S1); particularly in the region surrounding Óbidos (Dennen & Norton 1977, Boulangé & Carvalho 1997 and Lucas 1997) indicating that the Alter do Chão Formation throughout the study area has a pre-Eocene depositional age, consistent with previous age estimates. Lateritic profiles developed on the Iranduba and Novo Remanso Formations lack bauxite (Figure 4.3; S3); such immature lateritic ferruginous crusts imply late Neogene formation (Costa, 1997) and indicate a middle to late Miocene depositional age for both units.

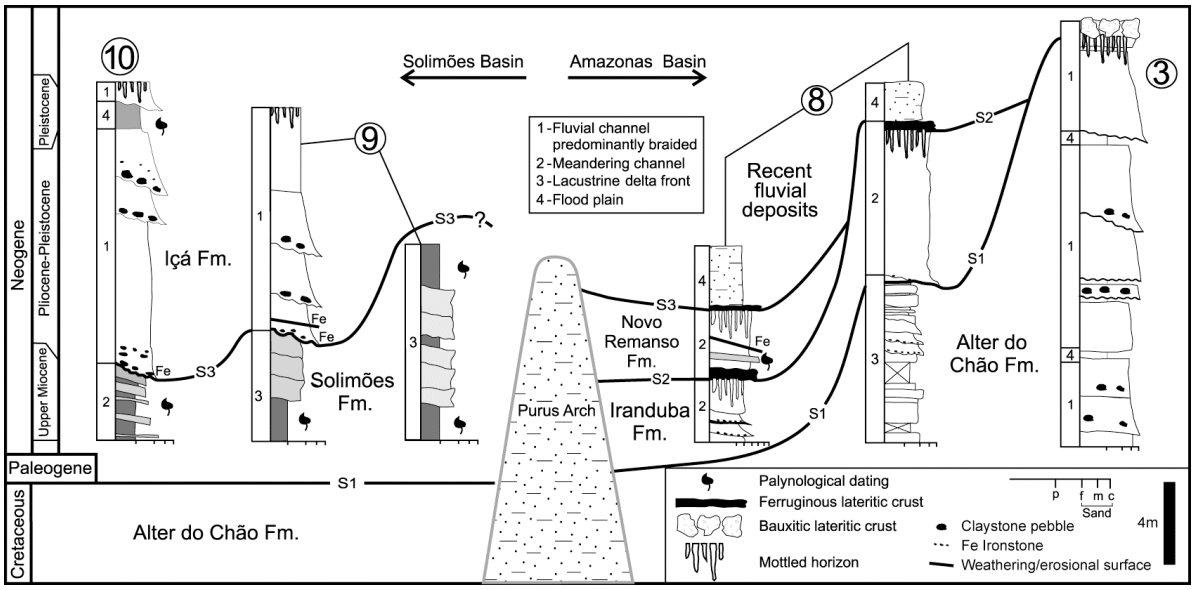

Figure 4.3- Stratigraphic columns and lateritic weathering profile correlation of exposed Cretaceous and Neogene deposits along the central and eastern Amazon River. Circled numbers next to columns correspond to localities in figures 4.2.

The Solimões Formation unconformably overlies the Alter do Chão Formation over a wide area in the Solimões Basin (Wesselingh *et al.*, 2006). The Solimões Formation is represented by grey to green, massive to laminated clays with lignite interbeds and fine-coarse grained white sands (Caputo, 1984). Leguizamón Vega (2006) described four different facies of the unit in the eastern Solimões basin proximal to the Purus Arch; lacustrine prodelta, lacustrine delta front, delta plain, and meandering fluvial channel deposits. She suggests the deposits formed in a prograding fluvial/marginal lacustrine system that originated to the west and butted against the Purus Arch in the east. A late Miocene age is indicated for fine-grained facies of the Solimões Formation in the Coari region, adjacent to the Purus Arch, by presence of fossil pollen spore *Echitricolorites spinosus* (Superzone X *sensu* Muller *et al.*, 1987) and confirmed by the presence of *Echiperiporites akanthos,* which does not reach the Pliocene epoch. Reworked mid-Miocene palynomorphs *Crassoretitriletes vanraadshoovenii* and *Grimsdalea magnaclavata* are also consistent with a late Miocene depositional age.

Also in the Solimões Basin, the Plio/Pliestocene Içá Formation lies unconformably above the Solimões Formation (Figure 4.3). The Içá Formation is a fine-coarse grained, white to light reddish, poorly cross-bedded, feldpathic sandstone with secondarily argillite interpreted to be of fluvial origin (Rossetti *et al*., 2005).

Unlike Neogene deposits of the Amazonas Basin, no lateritic profiles were developed in the Solimões or Içá Formations. The difference is likely explained by the separate subsidence histories of the Solimões and Amazonas basins. During the Neogene, the Solimões Basin subsided at a higher rate than the Amazonas Basin and as a result, deposits were not exposed long enough for laterite profiles to form.

Methods

Samples were obtained from three localities that span over 650 km total distance (Figure 4.1). One Cretaceous, Alter do Chão Formation sample was obtained from riverbank deposits at Óbidos similar to those described above. One sand sample of the Miocene Novo Remanso Formation and a sample of Iranduba Formation sand were collected from the same locality at Manacapuru on the eastern flank of the Purus Arch. Finally, a single sample of the Miocene Solimões Formation was collected west of the Purus Arch, near Tefé, from fluvial point bar deposits.

From each sample, zircons were separated from bulk sand using heavy methylene iodide (ρ = 3.2 g/cm^3), minor magnetic separation, and hand picking. Care was taken to insure that selected zircons were representative of the entire zircon suite in terms of sizes, shapes, and colors. Analysis was conducted by laser-ablation inductively-coupled-plasma multi-collector mass-spectrometry at the University of Texas at Austin following the procedure of Mapes (this text). Ages used for provenance interpretation and presentation are concordant at the 2σ confidence level or have $^{206}Pb/^{238}U$ ages within 30% of their $^{207}Pb/^{235}U$ ages. Individual age modes and modal proportions for each distribution were explored using the deconvolution method of Sambridge and Compston (1994).

Results

Four hundred ninety four individual detrital zircon U-Pb ages for four different samples were collected (Appendix D; Figure 4.4). These results are compared to age spectra for active Amazon River sand samples collected close to sandstone sample localities (Mapes, this text) to evaluate temporal source relations.

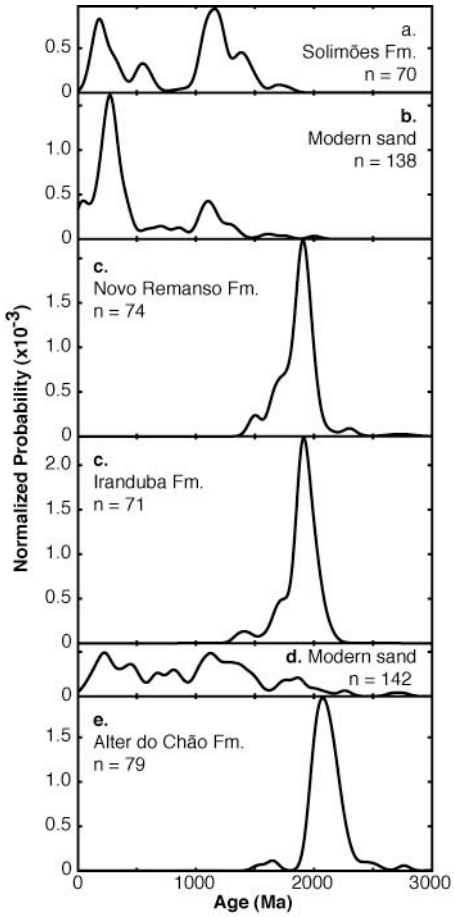

Figure 4.4- Probability density diagrams of detrital zircon ages for modern fluvial sand and Cretaceous and Miocene sandstones from the Amazon basin. Samples are arranged from upstream to downstream. Sample designation as in figure 4.1. Samples (b) and (d) are from Mapes, (this text), localities # 7 and #14 respectively.

Over 70% of the detrital zircon ages for the Alter do Chão sample from Óbidos yielded ages between 2.0 and 2.3 Ga, ages that are typical of basement rocks to the north and east in the Maroni-Itacaiunas and Central Amazonian provinces of northeastern Brazil and the eastern Guyanas (Figures 4.1 and 4.4; Delor *et al.*, 2003). Minor occurrence of older grains could be from Paleoproterozoic and Archean rocks in the central Amazon province and the three youngest analyses could have been derived from sparse post-orogenic igneous rocks described in the Maroni-Itacaiúnas province of Brazil (Tassinari *et al.*, 2000). Therefore zircon grains from Alter do Chão deposits require no sedimentary connection with the western Amazonian Craton or the Andes during sedimentation.

Detrital zircon grain ages for the Novo Remanso and Iranduba Formations are similar and appear to reflect the same sediment sources (Figure 4.4). Both age spectra display a single prominent age mode centered near 1.9 Ga suggesting that the dominant source area was nearby in the Ventuari-Tapajós province. Subordinate populations in both samples near 1.7 Ga and grain ages as young as 1.4 Ga suggest that some detritus may have come from as far west as the adjacent Rio Negro-Juruena province that includes minor anorogenic intrusions as young as ~1.4 Ga (Tassinari *et al.*, 2000). Like the Alter do Chão samples, Miocene sands collected at Manacapuru appear to require no far-traveled sediment source and could have been derived completely from local basement rocks.

In contrast, the Solimões Formation age spectrum is composed of several age populations younger than 1.5 Ga (Figure 4.4). The youngest significant age mode is centered near 210 Ma, an age consistent with Andean derivation. Older age peaks that are well represented in the data are centered around 550 Ma, probably Braziliano related, 1110 Ma, typical ages for Sunsas rocks, and 1400 Ma, likely Rondonian-San Ignacio derived. In

addition to these populations a minor age peak exists around 1720 Ma. The Andean and cratonal ages in the Solimões Formation sample suggest the dominant sediment source was to the west of their present location and requires little contribution of sediment from lowland cratonal areas.

Age spectra for modern sands indicate dominantly Andean provenance (Figure 4.4). The upstream sample yielded two dominant age modes near 250 and 1130 Ma. Zircon ages for the downstream sand are more uniformly distributed with several modes of similar magnitude between 0 and 2.0 Ga. Although diluted by cratonal zircon ages, Andean sourced zircon is still present as a significant age population. The similarity of the Solimões Formation age spectrum to modern sands suggests that they share related Andean source areas.

Implications for basin development

Alter do Chão deposition

The final breakup of Gondwana and opening of the central Atlantic is recorded in sediments in a series of rift-related basins along the northeastern Brazil continental margin. Late Aptian (~115 Ma) deltaic, lacustrine, and eolian deposits to the east of the Gurupá Arch were deposited during early stages of rifting (Paz *et al.*, 2005). By the early Albian (~110 Ma), rifting was complete and deposits in coastal basins indicate a thoroughgoing marine connection had been established (Rossetti, 1996). In the continental Amazonas and Solimões basins, evidence for a period of erosion is shown by a significant unconformity that exists between Late Paleozoic deposits and the Albian-Cenomanian Alter do Chão Formation (Caputo, 1984; Cunha *et al.*, 1994; Eiras *et al.*, 1994). Cretaceous Marajó Basin rift-related sediments are separated from Amazonas Basin continental sediments by a narrow gap

centered on the Gurupá Arch (Caputo, 1984; Wanderley Filho *et al.*, 2006; Paz *et al.*, 2005), indicating that the area around the Amazon mouth was uplifted during the mid-Cretaceous. Furthermore, Costa *et al.* (2003) interpreted that Albian sicliciclastic sediments of the Marajó Basin were shed to eastward off of a rift-related Gurupá Arch horst. Inevitably, this uplift would have blocked fluvial transport across the arch and likely would have shed material off of its opposite flank, toward the west.

Stratigraphic interpretations of uplift existence are corroborated by apatite fission track data from the eastern Central Brazilian Shield that indicate that 3-7 km of denudation took place after the mid-Paleozoic with the dominant phase occurring from ~130-60 Ma (Harman *et al.*, 1998). A rift-related uplift that trended from the southeastern most Amazon Craton past the current Amazon mouth to the Guyana Highlands during the Cretaceous (Zonneveld, 1985; Potter, 1997), would have subjected rocks of the Central Amazonian and Maroni-Itacaiúnas geochronologic provinces to weathering and would have created drainage networks that fed the evolving rift basins to the east and filled shallow continental depressions to the west of the rift shoulder. Detrital zircon ages collected for the Alter do Chão Formation at Óbidos are consistent with a wholly eastern cratonal detrital source and require no sedimentary connection with the western Amazon Craton or the Andes. These results are also consistent with Caputo (1984) who interpreted the main sediment source for Alter do Chão sands to be basement rocks exposed near the modern Rio Xingu mouth. Paleo-flow indicators (Figure 4.2), large conglomerate clasts, and stratigraphic data (Caputo, 1984; Mosmann *et al.*, 1987; Cunha *et al.*, 1994; Erias *et al.*, 1994) suggest that Alter do Chão sediments were deposited in a high-energy, west-southwest directed fluvial system. Marginal-marine or lacustrine Alter do Chão facies near Manaus indicate that the system

energy had decreased and neared base level (Rossetti and Netto, 2006) (Figure 4.1) prior to reaching the western continental margin. Distal deposits now located high in the Andes suggest that the system may have emptied into a low-energy, underfilled retroarc foreland basin (Sempere 1995; Sempere *et al.*, 1997).

Cenozoic Amazonas Basin deposition

In the Amazonas Basin, the period between the late Cretaceous and the mid-Cenozoic is poorly represented in the sedimentary record (Caputo, 1984; Cunha, 1994) suggesting continued subareal exposure (Rossetti, 2001). By the late Paleogene, the eastern margin of South America near the Amazon mouth had denuded and/or subsided to a level where the dominant control on sedimentation was eustatic. Three significant inundations and subsequent regressions occurred between the late Oligocene and the early Pleistocene that deposited sediments in marginal marine and shelf environments (Rossetti, 2001). Palynomorphs within the Novo Remanso Formation and weathering profiles throughout the mid-Cenozoic section around Manaus led Abinader *et al.* (2007) to correlate the Iranduba Formation with the Pirabas-Lower Barreiras Formations and the Novo Remanso Formation with the upper and middle portions of the Barreiras Formation that outcrop in the area of the Amazon estuary (Rossetti, 2001). The recognition of Cenozoic fluvial deposits in the Amazonas basin whose zircon sources appear to have been in the vicinity of the Purus Arch and the existence of correlative marginal marine and shelf sediments suggest that the eastern Amazon basin acted independent of the western Amazon basin during the Miocene. Furthermore, the detrital zircon age signature of mixed Rondonian-San Ignacio/Ventuari-Tapajós ages instead of Ventuari-Tapajós/Central Amazonian ages for both the Iranduba and the Novo Remanso formations, southeast directed paleoflow indicators in the Novo Remanso

formation (Rozo *et al.*, 2005), and the shared sedimentary/weathering history with deposits on the Atlantic margin suggest east directed fluvial transport on the eastern side of the Purus arch and sedimentary connection with the Atlantic coast during the Miocene. Therefore, we disagree with the model of Rossetti *et al.* (2005) that concludes the Purus Arch had ceased to be a significant topographic barrier prior to the Cretaceous and that fluvial transport across the western Amazonas basin was west directed into the Solimões basin until the late Pleistocene. Our data also indicate that establishment of the modern Amazon system could not have occurred prior to the Late Miocene.

Cenozoic Solimões Basin deposition

The Cenozoic evolution of the northern and central Andean foreland which led to development of the modern Amazon drainage is the result of complex interaction between Andean uplift (Garzione *et al.*, 2008), overthrusting and isostatic and elastic readjustment of large areas of lowland Amazonia (McQuarrie *et al.*, 2005; Roddaz *et al.*, 2006a), discrete pulses of sedimentation (Roddaz *et al.*, 2005a), and periods of erosion (Campbell *et al.*, 2006). The resulting sedimentary history, west of the Purus Arch, has apparently been variable between situations where the foreland acted as both a filled and overfilled basin (Catuneanu, 2004; Hoorn, 1994b, 2006; Roddaz *et al.*, 2005), a relationship that led to drastically different sediment sources for different foreland regions throughout its Cenozoic history.

Agreement exists that the Solimões Formation, called the Pebas Formation in Peru and Colombia (Hoorn, 2006b), is composed of marginal and shallow lacustrine deposits that represent eastward progradation of Andean derived sediment into a shallow, dominantly continental basin (Lutrubesse *et al.*, 1987). Fossil diversity (Wesselingh *et al.*, 2002; Vonhof

et al., 2003) and apparent tidal facies (Räsänen *et al.*, 1995; Hovikoski *et al.*, 2005) suggest at least temporary connections with marine environs. The Solimões/Pebas system occupied a large lowland area adjacent to the Andean foreland (Figure 4.1; Hoorn, 1994b) and through its late Oligocene to late Miocene history (Wesselingh *et al.*, 2002) may have had one or more outlets including the paleo-Caribbean near modern Lake Maracaibo (Hoorn *et al.*, 1995; Roddaz *et al.*, 2006b), the Pacific through a gap in the developing Andes near Guayaquil (Potter, 1997; Campbell *et al.*, 2006), or possibly even into the Paranan Seaway through Bolivia to the south (Hovikoski *et al.*, 2005; Roddaz *et al.*, 2006b).

During the late Miocene in the eastern Solimões basin, the Andean derived Solimões Formation was deposited unconformably on Alter do Chão Formation (Eiras *et al.*, 1994) against the western flank of the Purus Arch in an embayment between the Guyana and Guapore Shields. Solimões Formation zircon ages (Figure 4.4), facies interpretations (Leguizamón Vega, 2006), and east directed paleoflow measurements (Figure 4.2) indicate that during the late Miocene, even in the most distant and restricted sections of the Solimões/Pebas system, sand-sized Andean sediment was being transported uninterrupted more than 1,000 km across lowland Amazonia.

Palynomorphs in the uppermost Solimões Formation deposits near the Purus Arch suggest they are younger than the upper Solimões Formation near Leticia, Colombia (Hoorn, 1993). The occurrence of older deposits in the Pebas/Solimões system that record cratonal provenance like the Mariñame and Apaporis sands (Hoorn, 1994b; 2006) and the development of an Andean forebuldge, the Iquitos Arch (Figure 4.1) as early late-Miocene (Roddaz *et al.*, 2005a; 2005b) suggest a complex history of basin subsidence/base-level change and deposition. However, the detrital zircon age spectra indicate that by the end of

the Miocene Andean sediment had reached even the most distal portions of the Solimões/Pebas basin and that widespread lacustrine areas had been replaced by dominantly fluvial environments.

Sedimentation in western Amazonia was followed the basin-wide Ucayali peneplanation event that ended at ca. 9.0-9.5 Ma (Campbell *et al.*, 2006). Denudation was more thorough proximal to the Andes and as a result the age of the exposed Solimões Formation generally youngs in an easterly direction. As in the Amazonas basin, our detrital zircon age data do not place any lower age limit on the time of fluvial overtopping of the Purus Arch however they do suggest that at the time of the onset of Ucayali peneplanation western Amazonia had become an isolated continental basin and that the nature of the Andean foreland was overfilled.

Conclusions

Detrital zircon grain ages and paleoflow measurements indicate the primary source of mid-Cretaceous, Alter do Chão Formation sediments was to the east in rocks of the Maroni-Itacaiúnas and Central Amazonian geochronologic provinces uplifted as a result of Gondwana rifting. West directed transport carried sediment from northeastern South America through the Amazon trough possibly into an incipient retroarc foreland basin (Figure 4.5). By mid-Miocene time, the rift-shoulder had apparently subsided enough to initiate east directed flow off of the Purus Arch in the central portion of the modern Amazon drainage basin. Concurrently, in the western portion of the modern Amazon drainage basin, the Solimões Formation fluvial/marginal lacustrine system prograded eastward from the Andes, toward the Purus Arch. Sometime during or after the late Miocene the shallow foreland basin was

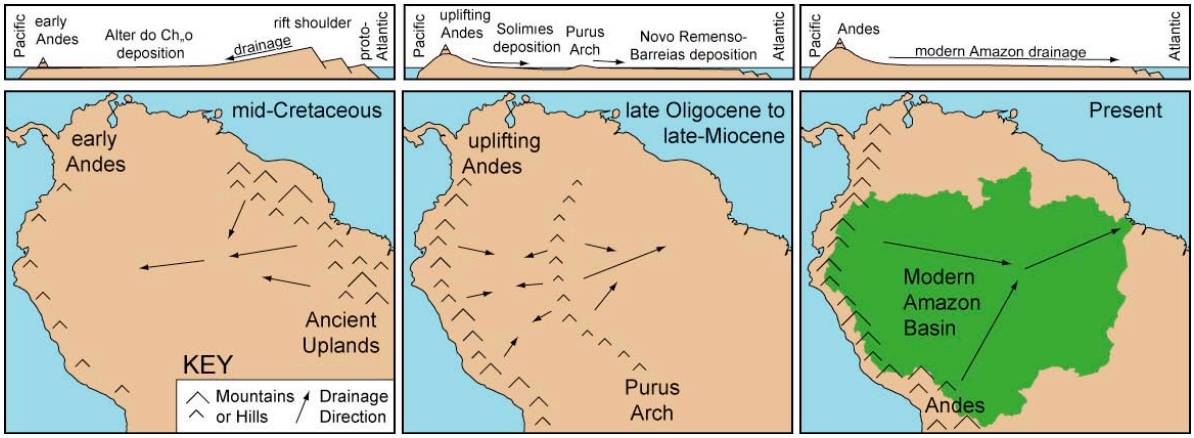

Figure 4.5- Proposed Cretaceous-modern drainage evolution of Amazonia. Cretaceous drainage of northern South America was west-directed off of an uplift created by rifting of Gondwana. Subsidence of the eastern continental margin and uplift of the Andean margin during the Cenozoic created two separate drainage sub-basins that were separated by the Purus Arch. Eventual overtopping of the arch created the modern Amazon drainage system during or after the late Miocene.

overfilled, the Purus Arch was breached either by headward erosion from the east or fluvial downcutting from the west and the modern Amazon drainage was established.

References

Abinader, H.D., Nogueira, A.C.R., Mapes, R.W., and Coleman, D.S., 2007, Estratigrafia do Cenozóico da porção centro-oeste da Bacia do Amazonas: in XI Congresso da Abequa, Belém, Brazil, resumos in CD-ROM.Aleman, A., and Ramos, V.A., 2000, Northern Andes; in Cordani, U.G., Milani, E.J., Thomaz Filho, A., and Campos, D.A., Tectonic evolution of South America, 31st International Geological Congress, Rio de Janeiro, pp.453-480.

Almeida, F.F.M. de, Brito Neves, B.B. de, Carneiro, C.D.R., 2000, The origin and evolution of the South American platform; Earth-Science Reviews, v. 50, p. 77-111.

Alvarenga, C.J.S. de, Moura, C.A.V., Gorayeb, P.S. de S., and Abreu, F. de A.M. de, 2000, Paraguay and Araguaia belts; *in* Cordani, U.G., Milani, E.J., Thomaz Filho, A., and Campos, D.A., Tectonic evolution of South America, 31st International Geological Congress, Rio de Janeiro, pp.183-193.

Bates, J., 2001. Avian diversification in Amazonia: evidence for historical complexity and a vicariance model for a basin diversification pattern. *in* Vieira, I.C., Silva, J.M.C., Oren, D.C., D'Incao, M.A. (Eds.), Diversidade Biológica e Cultural da Amazônia. Museu Paraense Emilio Goeldi, Belém, p. 119 – 139.

Black, L.P., Kamo, S.L., Allen, C.M., Davis, D.W., Aleinikoff, J.N., Valley, J.W., Mundil, R., Campbell, I.H., Korsch, R.J., Williams, I.S., and Foudoulis, C., 2004, Improved $^{206}Pb/^{238}U$ microprobe geochronology by the monitoring of a trace element related matrix effect: SHRIMP, ID-TIMS, ELA-ICP-MS and oxygen isotope documentation for a series of zircon standards; Chemical Geology, v. 205, p. 115-140.

Brito Neves, B.B. de, and Cordani, U.G., 1991, Tectonic evolution of South America during the Late Proterozoic; Precambrian Research, v. 53, p. 23-40.

Brito Neves, B.B. de, Fuck, R.A., Cordani, U.G., and Thomaz Filho, A., 1984, Influence of major basement structures on the evolution of the major sedimentary basins of Brazil: a case of tectonic heritage; Journal of Geodynamics, v. 1, p. 495-510.

Buck, W.R., 1986, Small-scale convection induced by passive rifting: the cause for uplift of rift shoulders; Earth and Planetary Science Letters, v. 77, p. 362-372.

Burke, K., and Lytwyn, J., 1993, Origin of the rift under the Amazon Basin as a result of continental collision during pan-African time. Int. Geol. Review. v. 35, pp. 881-897

Callede, J., Guyot, J.L., Ronchail, J., L'Hôte, Y., Niel, H., 2004, Evolution of the River Amazon's discharge at Óbidos from 1903 to 1999: Hydrological Sciences, v. 49, p. 85-97.

Caputo, M.V., 1984, Stratigraphy, tectonics, paleoclimatology, and paleogeography of northern basins of Brazil [Ph.D. thesis]: Santa Barbara, University of California, 583 p.

Chew, D.M., Schaltegger, U., Kosler, J., Whitehouse, M.J., Gutjahr, M., Spikings, R.A., and Miskovic, A., 2007, U-Pb geochronologic evidence for the evolution of the Gondwanan margin of the north-central Andes; Geological Society of America Bulletin, v. 119, p. 687-711.

Coltorti, M., and Ollier, C.D., 2000, Geomorphic and tectonic evolution of the Ecuadorian Andes: Geomorphology, v. 32, p. 1-19.

Cordani, U.G., Sato, K., Teixeira, W., Tassinari, C.C.G., and Basei, M.A.S., 2000, Crustal evolution of the south American platform; *in* Cordani, U.G., Milani, E.J., Thomaz Filho, A., and Campos, D.A., Tectonic evolution of South America, 31st International Geological Congress, Rio de Janeiro, pp.19-40.

Costa, J.B.S., Bemerguy, R.L., Hasui, Y., and Borges, M. S., 2001, Tectonics and paleogeography along the Amazon River; Journal of South American Earth Sciences; v. 14, p. 335-347.

Costa, J.B.S., Hasui, Y., Bemerguy, R.L., Soares-Júnior A.V., and Villegas, J.M.C., 2002, Tectonics and paleogeography of the Marajó Basin, northern Brazil; Anais da Academia Brasileira de Ciências, v. 74, p. 519-531.

Costa, J.B.S., Hasui, Y., Borges, M. S., and Bemerguy, R.L., 1995, Arcabouço tectônico Mesozóico-Cenozóico da região da calha do Rio Amazonas; Geociências, v. 14, p. 77-103.

Cunha, P.R.C., Gonzaga, F.G., Coutinho, L.F.C., Feijo, F.J., 1994, Bacia do Amazonas, Boletim de Geociências da Petrobras; v. 8, p. 47-55.

Costa, J.B.S., Hasui, Y., and Bemerguy, R.L., Soares-Júnior, A.V., and Villegas, J.M.C., 2003, Tectonics and paleogeography of the Marajó Basin, northern Brazil: Anais da Academia Brasileira de Ciências, v. 74, p. 519-531.

Delor, C., Lahondére, D., Egal, E., Lafon, J.-E., Cocherie, A., Guerrot, C., Rossi, P., Truffert, C., Théveniaut, H., Phillips, D., and Avelar, V.G. de, 2003, Transamazonian crustal growth and reworking as revealed by the 1:500,000-scale geological map of French Guiana (2nd edition), Géologie de la France, no. 2-3-4, p. 5-57.

Dino, R., da Silva, O.B., Abrahão, D., 1999, Caracterização palinológica e estratigráfica de estrasos Cretáceous da Formação Alter do Chão, Bacia do Amazonas; Boletim do 5˚ Simpósio sobre o Cretáceo do Brasil, p. 557-565.

Eiras, J.F., Becker, C.R., Souza, E.M., Gonzago, F.G., da Silva, J.G.F., Daniel, L.M.F., Matsuda, N.S., and Feijó, F.J., 1994, Bacia do Solimões; Boletim de Geociências da Petrobras; v. 8, p. 17-45.

Espurt, N., Baby, P., Brusset, S., Roddaz, M., Hermoza, W., Regard, V., Antoine, P.-O., and Salas-Gismondi, R., How does the Nazca Ridge subduction influence the modern Amazonian foreland basin? Geology, v. 35, p. 515-518.

Feijó, F.J. and Souza, R.G., 1994, Bacia do Acre; Boletim de Geociências da Petrobras; v. 8, p. 9-16.

Figueiredo, J., Hoorn, C., van der Ven, P., Soares, E., 2008, Birth of the Amazon River and stages of development: New evidence from the Amazon Fan (Foz do Amazonas, Late Miocene to Present): Geophysical Research Abstracts, EGU General Assembly, v. 10.

Garizone, C.N., Hoke, G.D., Libarkin, J.C., Withers, S., MacFadden, Eiler, J., Ghosh, P., Mulch, A., 2008, Rise of the Andes: Science v. 320, p. 1304-1307.

Gregory-Wodzicki, K.M., 2000, Uplift history of the central and northern Andes: A review: Geological Society of America Bulletin, v. 112, p. 1091-1105.

Harman, R., Gallagher, K., Brown, R., Raza, A., and Bizzi, L., 1998, Accelerated denudation and tectonic/geomorphic reactivation of the cratons of northeastern Brazil during the late Cretaceous; Journal of Geophysical Research, v. 103, p. 27,091-27,105.

Hoorn, C., Guerrero, J., Sarmiento, G.A., and Lorente, M.A., 1995, Andean tectonics as a cause for changing drainage patterns in Miocene northern South America: Geology, v. 23, p. 237-240.

Hoorn, C., 2006, Birth of the mighty Amazon. Scientific American, May, p. 52-59.

Hoorn, C., 2006, Mangrove forests and marine incursions in Neogene Amazonia (lower Apaporis River, Colombia): Palaios, v. 21, p.197-209

Horton, B.K., Hampton, B.A., and Waanders, G.L., 2001, Paleogene synorogenic sedimentation in the Altiplano plateau and implications for initial mountain building in the central Andes: Geological Society of America Bulletin; v. 113, p. 1387-1400.

Hovikoski, J., Räsänen, M., Gingras, M., Roddaz, M., Brusset, S., Hermoza, W., Romero Pittman, L., and Lertola, K., 2005, Miocene semidiurnal tidal rythmites in Madre de Dios, Peru: Geology, v. 33, p. 177-180.

Jaillard, E., Hérail, G., Monfret, T., Díaz-Martínez E., Baby, P., Lavenu, A., and Dumont, J.F., 2000, Tectonic evolution of the Andes of Ecuador, Peru, Bolivia, and Northernmost Chile; *in* Cordani, U.G., Milani, E.J., Thomaz Filho, A., and Campos, D.A., Tectonic evolution of South America, 31st International Geological Congress, Rio de Janeiro, pp.481-559.

Lamb, S., 2004, Devil in the Mountain: Princeton University Press, 352 p.

Lamb, S., and Davis, P., 2003, Cenozoic climate change as a possible cause for the rise of the Andes: Nature, v. 425, p. 792-797.

Leguizamón Vega, A.M., 2006, Reconstituição paleoambiental dos depósitos Miocenos na região centro oriental da Bacia Do Solimões; unpublished Master's thesis, Universidade Federal do Amazonas, Manaus, 92 p.

Leguizamón Vega, A.M., Nogueira, A.C.R., Mapes, R.W., and Coleman, D.S., 2006, A Late-Miocene delta-lacustrine system in the eastern Solimões Basin: prelude to the modern Amazon River: Geological Society of America Abstracts with Programs, v. 38, no. 7, pg. 144.

Loewy, S.L., Connelly, J.N., and Dalziel, I.W.D., 2004, An orphaned basement block: the Arequipa-Antofalla basement of the central Andean margin of South America; Geological Society of America Bulletin, v. 116, p. 171-187.

Lutrubesse, E.M., Bocquentin, J., Santos, J.C.R., and Ramonell, C.G., 1997, Paleoenvironmental model for the Late Cenozoic of southwestern Amazonia: paleontology and geology: Acta Amazonica, v. 27, p. 103-118.

Macdonald, D., Gomez-Perez, I., Franzese, J., Spalletti, L., Lawver, L., Gahagan, L., Dalziel, I., Thomas, C., Trewin, N., Hole, M., and Paton, D., 2003, Mesozoic break-up of SW Gondwana: implications for regional hydrocarbon potential of the southern South Atlantic: Marine and Petroleum Geology, v. 20, p. 287–308.

Maisey, J.G., 2000, Continental breakup and the distribution of fishes of Western Gondwana during the Early Cretaceous; Cretaceous Research, v. 21, p. 381-314.

Mosmann, R., Falkenhein, F.U.H., Gonçalves, A., Nepomuceno Filho, F., 1987. Oil and gas potential of the Amazon Paleozoic Basin: *in* Halbouty, M.T., ed., Future petroleum provinces of the world, AAPG Memoir 40, p. 207-241.

Paces, J.B., and Miller, J.D., 1993, Precise U-Pb ages of Duluth Complex and related mafic intrusions, northeastern Minnesota: Geochronological insights to physical, petrogenetic, paleomagnetic, and tectonomagmatic processes associated with the 1.1 Ga Midcontinent Rift System; Journal of Geophysical Research, v. 98, p. 13997-14013.

Patton, J.L., Silva, M.N., Malcolm, J.R., 2000. Mammals of the Rio Juruá and the evolutionary and ecological diversification of Amazonia. Bulletin of the American Museum of Natural History v. 244, p. 1 – 306.

Paz, J.D.S., Rossetti, D.S., AND Macambira, M.J.B., 2005, An Upper Aptian saline pan/lake from the Brazilian equatorial margin: integration of facies and isotopes; Sedimentology, v. 52, p. 1303-1321.

Potter, P.E., 1997, The Mesozoic and Cenozoic paleodrainage of South America: a natural history: Journal of South American Earth Sciences: v. 10, p. 331-344.

Press, W.H., Flannery, B.P., Teukolsky, S.A., and Vetterling, W.T., 1986, Numerical recipes: the art of scientific computing: Cambridge University Press, 818 p.

Ramos, V.A., 1988, Late Proterozoic- Early Paleozoic of South America – a collisional history; Episodes, v. 11, p. 168-174.

Ramos , V.A., and Aleman, A., 2000, Tectonic evolution of the Andes; *in* Cordani, U.G., Milani, E.J., Thomaz Filho, A., and Campos, D.A., Tectonic evolution of South America, 31st International Geological Congress, Rio de Janeiro, p. 635-685.

Räsänen, M.E., Linna, A.M., Santos, J.C.R., and Negri, F.R., 1995, Late Miocene tidal deposits in the Amazonian foreland basin: Science, v. 269, p. 386-390.

Roddaz, M., Viers, J., Brussett, S., Baby, P., Boucayrand, C., and Hérail, G., 2006a, Controls on weathering and provenance in the Amazonian foreland basin: insights from major and trace element geochemistry of Neogene Amazonian sediments; Chemical Geology, v. 226, p. 31-65.

Roddaz, M., Brussett, S., Baby, P., and Hérail, G., 2006b, Miocene tidal influenced sedimentation to continental Pliocene sedimentation in the forebuldge-backbuldge depozones of the Beni-Mamore foreland Basin (northern Bolivia); Journal of South American Earth Sciences, v. 20, p. 351-368.

Rossetti, D.F., 2001, Late Cenozoic sedimentary evolution in northeastern Pará, Brazil, within the context of sea level changes; Journal of South American Earth Sciences, v. 14, p. 77-89.

Rossetti, D.F., de Toledo, P.M., and Góes, A.M., 2005, New geological framework for western Amazonia (Brazil) and implications for biogeography and evolution: Quaternary Research, v. 63, p. 78-89.

Rossetti, D.F., and Netto, R.G., 2006, First evidence of marine influence in the Cretaceous of the Amazonas Basin, Brazil: Cretaceous Research, v. 27, p. 513-528.

Rozo, J.M.G., Nogueira, A.C.R., Horbe, A.M.C., and Carvalho, A.S., 2005, Depósitos Neógenos da Bacia do Amazonas; Contribuições a Geologia da Amazônia, v. 4, p. 201-207.

Sadowski, G.R., 2000, The São Luís craton and the Gurupi fold belt; *in* Cordani, U.G., Milani, E.J., Thomaz Filho, A., and Campos, D.A., Tectonic evolution of South America, 31st International Geological Congress, Rio de Janeiro, pp.97-99.

Sambridge, M.S. and Compston, W., 1994, Mixture modeling of multi-component data sets with application to ion-probe zircon ages; Earth and Planetary Science Letters, v. 128, p. 373-390.

Schobbenhaus, C., and Bellizza, A., 2001, Geological map of South America, 1:5,000,000 scale: Commission for the Geological Map of the World- Companhia de Pesquisa de Recursos Minerais- Departamento Nacional de Produção Mineral- UNESCO, Brasilia.

Sempere, T., 1995, Phanerozoic evolution of Bolivia and adjacent regions; *in* Tankard, A.J., Suárez S., R., and Welsink, H.J., Petroleum basins of South America, AAPG Memoir 62, p. 207-230.

Sempere, T., Butler, R.F., Richards, D.R., Marshall, L.G., Sharp, W., Swisher, C.C., III, 1997, Stratigraphy and chronology of Upper Cretaceous-lower Paleogene strata in Bolivia and northwest Argentina; Geological Society of America Bulletin, v. 109, p. 709-726.

Sioli, H., 1984. The Amazon and its main affluents: Hydrography, morphology of the river courses, and river types. In: Sioli (ed), The Amazon: Limnology and Landscape Ecology. Monographiae biologicae, v. 56. Dr. W. Junk Publishers. Boston.

Tassinari, C.C.G, Bettencourt, J.S., Geraldes, M.C., Macambria, M.J.B., and Lafon, J.M., 2000, The Amazonian Craton; *in* Cordani, U.G., Milani, E.J., Thomaz Filho, A., and Campos, D.A., Tectonic evolution of South America, 31st International Geological Congress, Rio de Janeiro, pp.41-99.

Teixeira, W., Tassinari, C.C.G., Cordani, U.G., and Kawashita, K., 1989, A review of the Amazonian craton: tectonic implications; Precambrian Research, v. 42, p. 213-227.

Vital, H., Stattegger, K., and Garbe-Schönberg, C.-D., 1999, Composition and trace-element geochemistry of detrital clay and heavy mineral suites of the lowermost Amazon River: a provenance study; Journal of Sedimentary Research, v. 69, p. 563-575.

Vonhof, H.B., Wesselingh, F.P., Kaandorp, R.J.G., Davies, G.R., van Hinte, J.E., Gurrero, J., Räsänen, M., Romero-Pittman, L., and Ranzi, A., 2003, Paleogeography of Miocene western Amazonia: isotopic composition of molluscan shells constrains the influence of marine incursions: Geological Society of America Bulletin, v. 115, p. 983-993.

Wanderley Filho, J.R., Travassos, W.A.S., and Alves, D.B., 2006, The diabase in the Amazonian Paleozoic basins - hero or villain? Boletim de Geociências da Petrobras; v. 14, p. 177-184.

Webb, S.D., 1995, Biological implications of the Middle Miocene Amazon Seaway: Science v. 269, p. 361-362.

Zonneveld J.I.S., 1985, Geomorphological notes on the continental border in the Guyanas (N. South America); Zeitschrift Fur Geomorphologie, Supplementband. V. 54, p. 71-83.

APPENDIX A

ANALYTICAL METHODS FOR U/PB GEOCHRONOLOGY

Microsampling was accomplished using a LUV213 Nd-YAG laser with an operating wavelength of 213 nm; other laser parameters include a lasing frequency of 10 Hz, a beam diameter of 30 μm, and laser fluence around 50 J/cm^2. Helium was used as the carrier gas with argon added before the torch as a make-up gas. Isotope measurements were made using a GVI IsoProbe multicollector, magnetic-sector ICP-MS. ^{238}U, ^{207}Pb, and ^{206}Pb were measured simultaneously on Faraday cups using 10^{11}, 10^{12} and 10^{11} ohm amplifiers, respectively, while ^{204}(Pb+Hg), and ^{202}Hg were also simultaneously measured on channeltrons in ion-counting mode. Twenty one-second measurements were collected for each analysis. Individual analyses lasted approximately 2 minutes. Three on-peak background measurements were averaged for blocks of five zircons run in quick succession or after analytical stoppages. Uranium background integrations were run with the laser off while Pb background integrations were run while ablating a young, in-house zircon standard, UT-1, that contains no measurable Pb. Ablation pits were typically ~15 microns in depth.

Progressive Pb/U fractionation during the course of an analysis was ubiquitous; this phenomenon is thought to increase with laser pit depth (Chang *et al.*, 2006). As a result, interelement fractionation was assumed to occur in a linear manner and the initial ^{206}Pb/^{238}U was calculated by regression of ^{206}Pb/^{238}U versus time (Figure A.1). Uncertainties reported for Pb/U values are based on confidence limits for linear regression. Because

changes in isotope fractionation were minimal during short runs, $^{207}Pb/^{206}Pb$ is assumed to be normally distributed and the reported values are means of all cycles where ratios did not depart significantly from trends. Problematic data associated with mid-run sample loss, analysis of mounting medium, transition to mineral zones of different ages, or other unforeseen problems were not included in sample means. A common-Pb correction was not applied when $^{206}Pb/^{204}Pb$ >5000, ratios were corrected using the Stacey and Kramers (1975) Pb-model. Instrumental drift and drift in systematic fractionation were corrected using an in-house zircon standard S97-19 (1086 Ma). Five to ten zircon standards were analyzed prior to and after analysis of unknown grains and corrections were made assuming linear drift during each analytical session. Correction quality was assessed by analyzing the zircon standard Temora 2 (417 Ma; Black *et al.*, 2004). In all cases, calculated ages compared well to the published age (Appendix B).

Stated uncertainties for all $^{207}Pb/^{206}Pb$ analyses displayed in probability density curves (Figure 1.2) and used to calculate relative input from northern South American basement provinces (Figure 1.3) are analytical. Measured error estimates for $^{206}Pb/^{238}U$ are replaced when internal analytical precision exceeds external precision. External precision is taken as the standard deviation of the $^{206}Pb/^{238}U$ age for over 160 individual analyses of standard Temora 2 (35 Ma). Probability density curve are normalized to the number of analyses per sample to allow direct comparison of modal magnitudes.

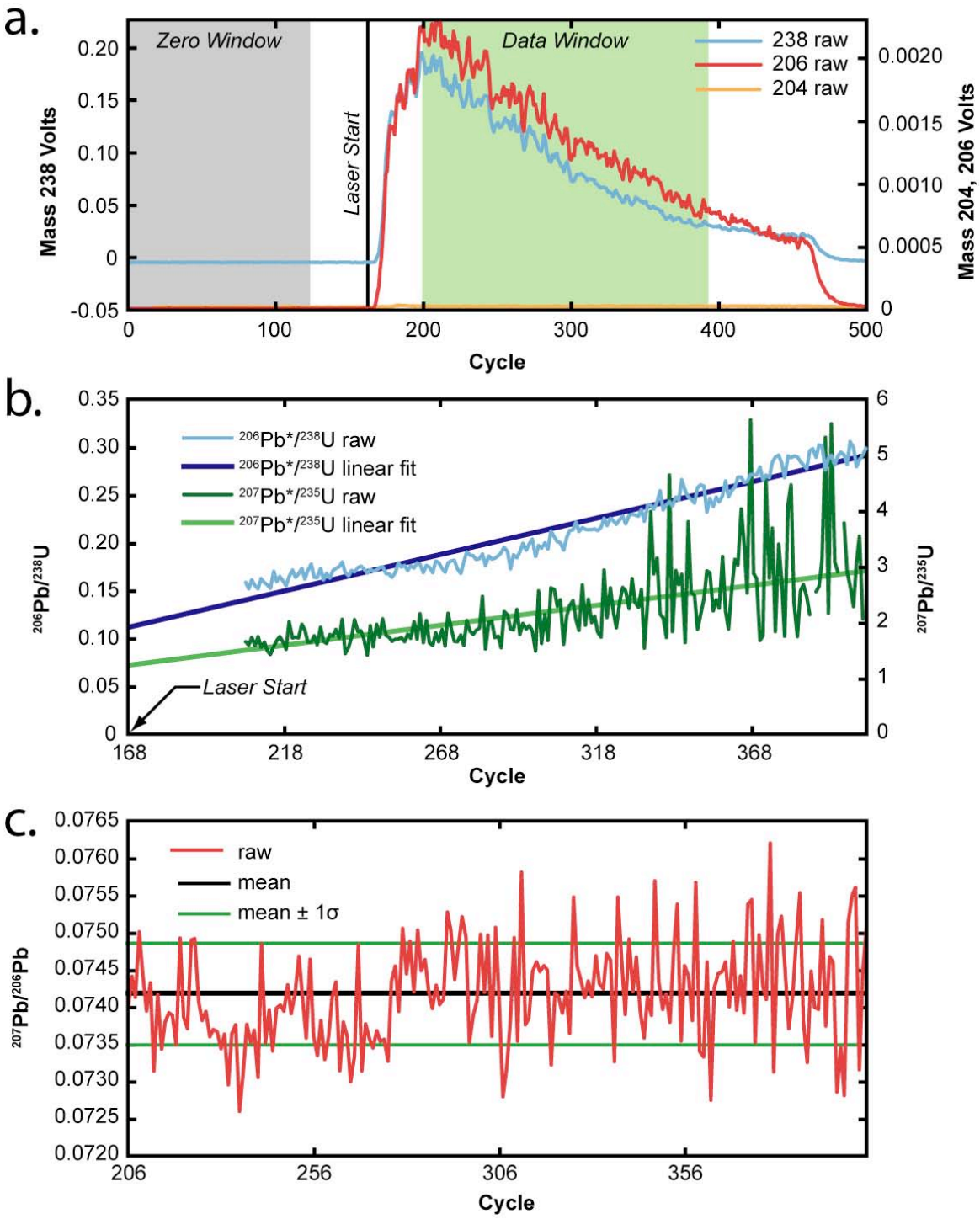

Figure A.1- Example of a single LA-ICP-MS zircon analysis. a) Sample signal, note the lag time between turning the laser on and the maximim signal strength and the signal decay with time. b) U/Pb ratio measurments. Negativly sloping trends are a result of U-Pb fractionation during sampling, U/Pb ratio calculated as intercept at laser start time. c) $^{207}Pb/^{206}Pb$ ratios are calculated assuming Pb-Pb fractionation is negligible.

APPENDIX B

LA-ICP-MS U-PB AND PB-PB AGES AND SIZE MEASUREMENTS FOR ZIRCONS FROM SANDS OF THE AMAZON RIVER DRAINAGE BASIN.

$^{206}Pb^*/^{238}U$	± 2σ (abs)	$^{207}Pb^*/^{235}U$	± 2σ (abs)	$^{207}Pb^*/^{206}Pb^*$	± 2σ (abs)	corr. coef.	$^{206}Pb^*/^{238}U$ age (Ma)	± 2σ (Ma)	$^{207}Pb^*/^{235}U$ age (Ma)	± 2σ (Ma)	$^{207}Pb^*/^{206}Pb^*$ age (Ma)	± 2σ (Ma)	Length (μm)	Width (μm)	Accept/ Reject
1. Aguarico River, Ecuador (0.0486°N, 77.3057°W)															
0.02331	0.00063	0.044	0.020	0.014	0.013	0.365	43	20	149	4			151	115	r
0.02092	0.00069	0.056	0.014	0.0195	0.0072	0.559	56	14	133	4			272	127	r
0.03617	0.00090	0.122	0.046	0.024	0.019	0.663	117	41	229	6			172	85	r
0.02240	0.00052	0.0764	0.0085	0.0247	0.0052	0.472	75	8	143	3			209	129	r
0.01921	0.00061	0.068	0.014	0.0257	0.0075	0.529	67	13	123	4			218	140	r
0.01827	0.00040	0.0648	0.0095	0.0257	0.0073	0.305	64	9	117	3			241	115	r
0.02434	0.00065	0.089	0.029	0.027	0.016	0.514	87	27	155	4			178	125	r
0.02221	0.00048	0.0835	0.0082	0.0273	0.0055	0.415	81	8	142	3			145	101	r
0.02052	0.00050	0.080	0.010	0.0284	0.0069	0.410	78	10	131	3			185	122	r
0.01861	0.00057	0.075	0.023	0.029	0.013	0.511	73	22	119	4			293	161	r
0.02342	0.00060	0.095	0.013	0.0293	0.0082	0.462	92	12	149	4			234	98	r
0.02364	0.00065	0.100	0.018	0.031	0.012	0.429	96	17	151	4			146	126	r
0.01931	0.00045	0.085	0.016	0.032	0.012	0.364	83	15	123	3			180	108	r
0.02272	0.00073	0.101	0.015	0.0324	0.0069	0.622	98	14	145	5			300	127	r
0.02397	0.00072	0.108	0.021	0.033	0.013	0.460	104	19	153	5			147	112	r
0.02009	0.00051	0.0911	0.0081	0.0329	0.0056	0.400	89	8	128	3			138	98	r
0.00315	0.00011	0.0143	0.0048	0.033	0.017	*	14	5	20	1			217	203	a
0.02130	0.00053	0.104	0.015	0.036	0.010	0.445	101	14	136	3			212	130	a
0.02551	0.00063	0.128	0.013	0.0363	0.0069	0.558	122	12	162	4			150	83	a
0.02056	0.00067	0.107	0.018	0.0377	0.0094	0.577	103	17	131	4			168	150	a
0.02193	0.00086	0.115	0.040	0.038	0.025	0.460	110	36	140	5			125	110	a
0.01850	0.00054	0.102	0.017	0.0402	0.0098	0.521	99	16	118	3			257	154	a
0.03226	0.00071	0.180	0.017	0.0405	0.0068	0.686	168	15	205	4			154	127	a
0.003447	0.000078	0.0194	0.0023	0.0409	0.0093	*	20	2	22	1			213	77	a
0.01965	0.00078	0.112	0.013	0.0413	0.0070	0.575	108	12	125	5			303	132	a
0.03727	0.00081	0.213	0.011	0.0415	0.0040	0.703	196	9	236	5			123	97	a
0.01920	0.00067	0.111	0.028	0.042	0.016	0.539	107	26	123	4			265	187	a
0.02398	0.00054	0.1434	0.0074	0.0434	0.0039	0.565	136	7	153	3			188	65	a
0.02429	0.00052	0.1455	0.0035	0.0434	0.0010	0.769	138	3	155	3			289	162	a
0.0085	0.0027	0.05	0.13	0.04	0.22	*	51	126	55	17			300	156	a
0.03200	0.00099	0.194	0.015	0.0440	0.0044	0.760	180	13	203	6			162	121	a
0.01783	0.00062	0.110	0.038	0.045	0.023	0.496	106	35	114	4			270	224	a
0.01821	0.00057	0.112	0.016	0.0446	0.0092	0.520	108	14	116	4			300	170	a
0.0454	0.0017	0.280	0.015	0.0448	0.0026	0.856	251	12	286	10			124	103	a
0.02436	0.00058	0.151	0.013	0.0450	0.0084	0.478	143	12	155	4			144	96	a
0.0425	0.0016	0.264	0.020	0.0450	0.0056	0.780	238	16	268	10			199	112	a
0.02963	0.00060	0.1850	0.0057	0.0453	0.0022	0.697	172	5	188	4			246	84	a
0.03110	0.00064	0.1954	0.0088	0.0456	0.0039	0.647	181	7	197	4			130	71	a
0.03030	0.00077	0.196	0.031	0.047	0.011	0.713	182	26	192	5	42	567	259	100	a
0.02446	0.00067	0.160	0.013	0.0473	0.0071	0.551	150	11	156	4	67	355	133	115	a
0.01980	0.00046	0.129	0.011	0.0474	0.0074	0.418	124	10	126	3	69	370	158	122	a
0.02417	0.00099	0.159	0.047	0.048	0.027	0.516	150	41	154	6	80	1371	217	213	a
0.01956	0.00057	0.1298	0.0060	0.0481	0.0026	0.657	124	5	125	4	107	127	204	156	a
0.03437	0.00072	0.230	0.012	0.0486	0.0048	0.681	210	10	218	4	128	233	103	70	a
0.03239	0.00098	0.2179	0.0087	0.0488	0.0018	0.832	200	7	206	6	137	88	180	119	a
0.02535	0.00072	0.1718	0.0062	0.0492	0.0016	0.795	161	5	161	5	155	76	226	130	a
0.01924	0.00043	0.1328	0.0070	0.0500	0.0047	0.430	127	6	123	3	197	218	152	95	a
0.02035	0.00066	0.141	0.015	0.0503	0.0077	0.589	134	14	130	4	210	354	250	145	a
0.0298	0.0012	0.209	0.011	0.0509	0.0024	0.824	193	9	189	8	235	108	165	123	a
0.02698	0.00082	0.1916	0.0075	0.0515	0.0019	0.801	178	6	172	5	263	84	183	136	a

$^{206}Pb^*/^{238}U$	± 2σ (abs)	$^{207}Pb^*/^{235}U$	± 2σ (abs)	$^{207}Pb^*/^{206}Pb^*$	± 2σ (abs)	corr. coef.	$^{206}Pb^*/^{238}U$ age (Ma)	± 2σ (Ma)	$^{207}Pb^*/^{235}U$ age (Ma)	± 2σ (Ma)	$^{207}Pb^*/^{206}Pb^*$ age (Ma)	± 2σ (Ma)	Length (μm)	Width (μm)	Accept/ Reject
0.00364	0.00010	0.0260	0.0012	0.0517	0.0037	*	26	1	23	1	272	164	133	99	a
0.0297	0.0011	0.212	0.016	0.0517	0.0051	0.750	195	13	189	7	274	224	205	145	a
0.02391	0.00070	0.171	0.014	0.0519	0.0079	0.543	161	12	152	4	283	346	165	115	a
0.02025	0.00045	0.1459	0.0077	0.0523	0.0049	0.460	138	7	129	3	297	215	150	90	a
0.02257	0.00050	0.1635	0.0065	0.0525	0.0034	0.578	154	6	144	3	309	146	156	121	a
0.02082	0.00047	0.1551	0.0084	0.0540	0.0052	0.482	146	7	133	3	372	217	140	90	a
0.02606	0.00065	0.1967	0.0055	0.0547	0.0014	0.792	182	5	166	4	401	59	150	79	a
0.00327	0.00011	0.0247	0.0046	0.055	0.020	*	25	5	21	1	406	837	230	109	a
0.01837	0.00058	0.139	0.023	0.055	0.013	0.523	132	21	117	4	411	542	297	130	a
0.02770	0.00060	0.2107	0.0047	0.05517	0.00065	0.889	194	4	176	4	419	26	186	133	a
0.02060	0.00045	0.1587	0.0049	0.0559	0.0025	0.591	150	4	131	3	447	98	135	110	a
0.02122	0.00073	0.165	0.020	0.056	0.013	0.461	155	18	135	5	464	512	290	88	a
0.01929	0.00042	0.1507	0.0071	0.0567	0.0046	0.449	143	6	123	3	479	180	130	96	a
0.02844	0.00099	0.2228	0.0090	0.0568	0.0024	0.786	204	7	181	6	484	94	140	72	a
0.03424	0.00088	0.271	0.011	0.0573	0.0034	0.750	243	9	217	5	504	129	180	138	a
0.01975	0.00044	0.1569	0.0090	0.0576	0.0060	0.440	148	8	126	3	515	229	250	107	a
0.02096	0.00053	0.167	0.018	0.058	0.012	0.444	157	15	134	3	523	439	144	102	a
0.02905	0.00067	0.235	0.026	0.059	0.013	0.582	214	21	185	4	553	498	243	97	a
0.02052	0.00087	0.167	0.025	0.059	0.016	0.448	157	21	131	5	564	598	155	99	a
0.03677	0.00089	0.299	0.019	0.0589	0.0064	0.726	265	15	233	6	565	238	160	117	a
0.02024	0.00053	0.1646	0.0097	0.0590	0.0061	0.474	155	8	129	3	566	225	171	136	a
0.02007	0.00046	0.163	0.015	0.0591	0.0099	0.424	154	13	128	3	569	365	168	138	a
0.0445	0.0010	0.365	0.016	0.0596	0.0043	0.790	316	12	280	6	589	157	103	100	a
0.00302	0.00038	0.0248	0.0051	0.060	0.022	*	25	5	19	2	593	801	154	69	a
0.0600	0.0019	0.496	0.016	0.05990	0.00051	0.881	409	11	376	11	600	18	130	115	a
0.03055	0.00071	0.258	0.017	0.0612	0.0070	0.665	233	13	194	4	647	245	146	58	a
0.0333	0.0014	0.282	0.014	0.0614	0.0021	0.879	252	11	211	9	652	74	164	108	a
0.02137	0.00049	0.181	0.012	0.0614	0.0075	0.478	169	10	136	3	652	262	210	60	a
0.02054	0.00052	0.174	0.021	0.061	0.014	0.427	163	19	131	3	653	506	150	115	a
0.0539	0.0020	0.464	0.020	0.0624	0.0023	0.904	387	14	338	12	688	80	197	81	a
0.0696	0.0016	0.603	0.015	0.0628	0.0012	0.651	479	10	434	10	702	41	130	80	a
0.03255	0.00068	0.283	0.029	0.063	0.013	0.628	253	23	206	4	710	451	167	85	a
0.0285	0.0014	0.250	0.050	0.064	0.024	0.610	227	41	181	9	731	812	162	140	a
0.02110	0.00064	0.189	0.029	0.065	0.019	0.445	176	25	135	4	773	620	139	135	r
0.1291	0.0033	1.157	0.040	0.0650	0.0024	0.664	780	19	782	19	775	77	154	118	a
0.01835	0.00074	0.165	0.011	0.0651	0.0070	0.471	155	10	117	5	779	226	135	68	r
0.02575	0.00060	0.2318	0.0087	0.0653	0.0038	0.648	212	7	164	4	783	124	125	117	a
0.0419	0.0025	0.378	0.055	0.065	0.017	0.757	326	40	265	16	787	540	229	226	a
0.0256	0.0015	0.235	0.030	0.066	0.015	0.584	214	25	163	9	819	486	120	61	r
0.02701	0.00081	0.2482	0.0089	0.0666	0.0025	0.774	225	7	172	5	827	79	127	62	r
0.02538	0.00060	0.235	0.019	0.067	0.010	0.565	214	16	162	4	843	323	130	127	r
0.02407	0.00090	0.226	0.041	0.068	0.024	0.525	207	34	153	6	872	725	158	120	r
0.02592	0.00064	0.245	0.030	0.068	0.017	0.530	222	25	165	4	882	522	157	90	r
0.03300	0.00097	0.311	0.024	0.0684	0.0091	0.693	275	18	209	6	882	275	245	58	r
0.0237	0.0010	0.225	0.041	0.069	0.024	0.528	206	34	151	6	896	708	190	52	r
0.0673	0.0025	0.647	0.027	0.0698	0.0026	0.924	507	17	420	15	921	77	133	93	a
0.02674	0.00059	0.2581	0.0079	0.0700	0.0030	0.698	233	6	170	4	929	88	185	90	r
0.1058	0.0031	1.035	0.031	0.07098	0.00092	0.871	722	15	648	18	957	27	157	121	a
0.02020	0.00050	0.200	0.019	0.072	0.013	0.425	185	16	129	3	982	374	160	142	r
0.02087	0.00049	0.208	0.014	0.0722	0.0089	0.470	192	12	133	3	993	250	130	114	r
0.00669	0.00035	0.069	0.016	0.074	0.025	*	67	15	43	2	1052	673	147	106	r

$^{206}Pb^*/^{238}U$	± 2σ (abs)	$^{207}Pb^*/^{235}U$	± 2σ (abs)	$^{207}Pb^*/^{206}Pb^*$	± 2σ (abs)	corr. coef.	$^{206}Pb^*/^{238}U$ age (Ma)	± 2σ (Ma)	$^{207}Pb^*/^{235}U$ age (Ma)	± 2σ (Ma)	$^{207}Pb^*/^{206}Pb^*$ age (Ma)	± 2σ (Ma)	Length (μm)	Width (μm)	Accept/ Reject
0.0192	0.0010	0.199	0.032	0.075	0.023	0.405	184	27	123	6	1063	607	176	115	r
0.02701	0.00062	0.281	0.011	0.0755	0.0049	0.650	251	9	172	4	1081	130	155	100	r
0.02221	0.00049	0.231	0.018	0.075	0.011	0.496	211	15	142	3	1081	299	158	111	r
0.0310	0.0014	0.323	0.022	0.0755	0.0077	0.721	284	17	197	9	1083	205	138	90	r
0.1436	0.0040	1.510	0.043	0.07629	0.00094	0.900	935	18	865	23	1103	25	477	169	a
0.01897	0.00048	0.200	0.021	0.077	0.015	0.377	185	18	121	3	1109	394	163	109	r
0.1045	0.0035	1.134	0.038	0.0787	0.0012	0.850	770	18	641	20	1164	30	154	88	a
0.0199	0.0022	0.216	0.057	0.079	0.032	0.538	199	48	127	14	1165	814	84	84	r
0.0362	0.0013	0.404	0.045	0.081	0.016	0.714	345	33	229	8	1218	396	200	150	r
0.02044	0.00051	0.229	0.013	0.0813	0.0080	0.475	209	11	130	3	1228	194	130	100	r
0.02642	0.00061	0.297	0.021	0.081	0.011	0.593	264	17	168	4	1233	261	131	128	r
0.02150	0.00074	0.244	0.033	0.082	0.021	0.460	222	27	137	5	1252	505	195	130	r
0.0399	0.0014	0.461	0.034	0.0837	0.0077	0.821	385	24	252	9	1287	179	162	147	r
0.0234	0.0010	0.272	0.029	0.084	0.012	0.670	244	23	149	7	1295	276	256	122	r
0.1444	0.0042	1.679	0.054	0.0843	0.0019	0.808	1001	21	870	24	1300	44	248	140	a
0.00366	0.00010	0.0429	0.0037	0.085	0.014	*	43	4	24	1	1317	321	245	110	r
0.0881	0.0024	1.034	0.032	0.0852	0.0023	0.509	721	16	544	14	1319	53	160	115	r
0.01714	0.00062	0.202	0.029	0.086	0.023	0.276	187	24	110	4	1330	528	200	121	r
0.0432	0.0020	0.518	0.031	0.0869	0.0065	0.837	424	21	273	12	1358	143	120	97	r
0.0448	0.0024	0.54	0.15	0.087	0.040	0.788	437	99	283	15	1362	893	160	118	r
0.1930	0.0073	2.399	0.092	0.09014	0.00090	0.948	1242	27	1138	40	1429	19	213	76	a
0.02398	0.00060	0.304	0.028	0.092	0.016	0.538	269	22	153	4	1463	328	160	70	r
0.02022	0.00069	0.262	0.027	0.094	0.018	0.430	237	22	129	4	1510	368	240	162	r
0.0243	0.0014	0.323	0.023	0.0964	0.0077	0.730	284	17	155	9	1555	150	146	84	r
0.0199	0.0018	0.269	0.036	0.098	0.020	0.549	242	29	127	11	1588	386	220	65	r
0.1868	0.0061	2.637	0.087	0.10240	0.00084	0.942	1311	24	1104	33	1668	15	277	159	a
0.02369	0.00090	0.337	0.031	0.103	0.013	0.673	295	23	151	6	1680	226	245	164	r
0.0490	0.0063	0.78	0.52	0.11	0.14	0.785	583	296	308	39	1880	2205	92	91	a
0.0357	0.0020	0.575	0.045	0.117	0.013	0.773	461	29	226	12	1909	198	113	74	r
0.0260	0.0015	0.419	0.054	0.117	0.026	0.617	355	39	165	9	1909	400	245	104	r
0.0303	0.0010	0.494	0.033	0.118	0.013	0.693	408	22	192	7	1929	191	210	90	r
0.0323	0.0017	0.551	0.058	0.124	0.022	0.694	446	38	205	11	2009	323	158	80	r
0.0308	0.0014	0.559	0.051	0.132	0.020	0.694	451	33	196	9	2119	264	146	90	r
0.0312	0.0017	0.580	0.058	0.135	0.022	0.699	465	37	198	11	2164	286	148	138	r
0.02451	0.00058	0.458	0.021	0.135	0.010	0.606	383	15	156	4	2170	134	148	95	r
0.03159	0.00075	0.605	0.017	0.1388	0.0042	0.808	480	11	200	5	2213	52	143	133	r
0.0203	0.0015	0.451	0.070	0.161	0.043	0.486	378	49	130	9	2469	453	200	150	r
0.0244	0.0014	0.577	0.097	0.171	0.053	0.558	463	63	155	9	2572	517	199	103	r
0.0421	0.0018	1.065	0.069	0.183	0.017	0.803	737	34	266	11	2684	155	131	104	r
0.0516	0.0069	1.36	0.46	0.191	0.064	0.888	872	197	324	42	2752	552	143	105	r
0.02509	0.00068	0.685	0.030	0.198	0.014	0.643	530	18	160	4	2811	113	153	136	r
0.0250	0.0026	0.78	0.12	0.225	0.038	0.752	584	69	159	17	3017	272	304	180	r
0.0058	0.0011	0.200	0.041	0.251	0.050	*	185	34	37	7	3193	314	156	62	r
0.077	0.010	2.74	0.77	0.259	0.028	0.971	1340	209	477	62	3239	170	163	93	r
0.0691	0.0041	2.66	0.33	0.280	0.023	0.944	1318	91	431	24	3360	127	182	82	r
0.02406	0.00088	0.929	0.051	0.280	0.022	0.651	667	27	153	6	3364	124	232	99	r
0.0796	0.0065	3.36	0.30	0.306	0.022	0.939	1495	69	494	39	3502	113	146	118	r
0.0278	0.0036	1.21	0.18	0.315	0.051	0.776	804	82	177	22	3546	248	170	80	r
0.0383	0.0020	1.71	0.11	0.323	0.023	0.835	1011	41	243	12	3584	107	133	130	r
0.00099	0.00090	0.049	0.046	0.36	0.23	*	48	44	6	6	3739	999	185	54	r
0.0500	0.0040	2.55	0.39	0.370	0.029	0.939	1286	110	315	25	3789	120	171	140	r

$^{206}Pb^*/^{238}U$	± 2σ (abs)	$^{207}Pb^*/^{235}U$	± 2σ (abs)	$^{207}Pb^*/^{206}Pb^*$	± 2σ (abs)	corr. coef.	$^{206}Pb^*/^{238}U$ age (Ma)	± 2σ (Ma)	$^{207}Pb^*/^{235}U$ age (Ma)	± 2σ (Ma)	$^{207}Pb^*/^{206}Pb^*$ age (Ma)	± 2σ (Ma)	Length (μm)	Width (μm)	Accept/ Reject
2. Amazon RIver, Colombia (4.1519˚S, 69.9490˚W)															
0.01339	0.00050	0.0008	0.0075	0.0004	0.0079	*	1	8	86	3			166	85	r
0.02235	0.00051	0.007	0.013	0.0024	0.0081	*	8	13	142	3			245	121	r
0.1172	0.0033	0.079	0.067	0.0049	0.0065	0.861	77	63	714	19			140	130	r
0.03942	0.00097	0.044	0.012	0.0081	0.0042	0.635	44	12	249	6			241	133	r
0.0454	0.0011	0.070	0.011	0.0111	0.0031	0.725	68	10	286	7			146	113	r
0.01987	0.00090	0.0663	0.0094	0.0242	0.0064	0.404	65	9	127	6			185	106	r
0.02240	0.00052	0.0764	0.0085	0.0247	0.0052	0.472	75	8	143	3			167	116	r
0.0545	0.0016	0.2226	0.0088	0.0296	0.0015	0.462	204	7	342	10			150	75	r
0.01268	0.00082	0.050	0.032	0.029	0.036	*	50	30	81	5			130	110	r
0.0867	0.0029	0.421	0.025	0.0352	0.0030	0.902	357	18	536	17			157	115	r
0.1496	0.0043	0.805	0.037	0.0390	0.0021	0.784	600	21	899	24			141	91	r
0.0637	0.0030	0.316	0.019	0.0359	0.0028	0.483	278	15	398	18			248	87	r
0.04003	0.00091	0.1906	0.0056	0.0345	0.0013	0.817	177	5	253	6			230	110	a
0.0490	0.0015	0.237	0.010	0.0351	0.0021	0.838	216	8	309	9			130	103	a
0.0504	0.0016	0.252	0.022	0.0362	0.0056	0.801	228	18	317	10			253	97	a
0.0522	0.0015	0.304	0.016	0.0422	0.0035	0.826	270	13	328	9			137	106	a
0.1551	0.0055	1.137	0.049	0.0532	0.0019	0.848	771	23	929	31	335	81	143	112	a
0.1320	0.0036	0.989	0.046	0.0543	0.0031	0.588	698	23	799	21	384	128	111	107	a
0.0432	0.0011	0.2647	0.0072	0.0445	0.0011	0.876	238	6	272	6			148	130	a
0.02429	0.00052	0.1455	0.0035	0.0434	0.0010	0.769	138	3	155	3			187	99	a
0.1396	0.0075	1.13	0.22	0.059	0.017	0.938	768	106	842	43	559	630	145	78	a
0.0959	0.0027	0.707	0.020	0.05350	0.00053	0.912	543	12	590	16	350	23	171	99	a
0.0418	0.0010	0.2706	0.0066	0.04694	0.00054	0.748	243	5	264	6	46	28	104	87	a
0.1602	0.0050	1.411	0.047	0.0639	0.0012	0.894	894	20	958	28	737	40	210	81	a
0.0085	0.0027	0.05	0.13	0.04	0.22	*	51	126	55	17			185	102	a
0.1618	0.0061	1.470	0.058	0.0659	0.0012	0.914	918	24	967	34	803	39	140	90	a
0.00672	0.00027	0.0424	0.0090	0.046	0.019	*	42	9	43	2	-15	1003	180	80	a
0.0503	0.0011	0.3574	0.0090	0.0516	0.0011	0.492	310	7	316	7	266	49	275	105	a
0.1592	0.0069	1.577	0.070	0.0718	0.0014	0.911	961	28	952	38	981	40	240	100	a
0.1076	0.0045	0.925	0.039	0.06235	0.00056	0.946	665	21	659	26	686	19	110	85	a
0.186	0.019	1.99	0.22	0.0776	0.0045	0.898	1112	74	1099	102	1137	115	127	120	a
0.0739	0.0018	0.583	0.014	0.05723	0.00040	0.901	466	9	459	11	500	16	111	94	a
0.1710	0.0057	1.771	0.060	0.07514	0.00050	0.962	1035	22	1018	32	1072	13	124	109	a
0.1502	0.0053	1.502	0.060	0.0725	0.0021	0.830	931	24	902	29	1000	58	120	108	a
0.1255	0.0051	1.175	0.052	0.0679	0.0020	0.826	789	24	762	29	866	62	201	86	a
0.1818	0.0066	2.004	0.074	0.07996	0.00069	0.955	1117	25	1077	36	1196	17	167	110	a
0.0570	0.0015	0.441	0.011	0.05614	0.00024	0.928	371	8	357	9	458	9	185	70	a
0.126	0.013	1.19	0.13	0.0685	0.0061	0.787	795	61	764	72	882	184	203	86	a
0.00544	0.00014	0.0366	0.0032	0.0488	0.0083	*	36	3	35	1	138	399	199	70	a
0.0396	0.0011	0.295	0.012	0.0539	0.0033	0.783	262	9	251	7	369	138	135	80	a
0.1614	0.0057	1.704	0.060	0.07657	0.00036	0.972	1010	22	965	31	1110	10	152	105	a
0.1562	0.0061	1.628	0.063	0.07558	0.00041	0.971	981	25	935	34	1084	11	250	64	a
0.0977	0.0026	0.863	0.023	0.06403	0.00091	0.846	632	13	601	15	743	30	150	75	a
0.1608	0.0049	1.710	0.052	0.07714	0.00032	0.972	1012	19	961	27	1125	8	224	89	a
0.0470	0.0011	0.3603	0.0088	0.05562	0.00093	0.568	312	7	296	7	437	37	131	75	a
0.0775	0.0021	0.650	0.020	0.0608	0.0017	0.607	508	12	481	12	633	59	110	72	a
0.0668	0.0016	0.543	0.014	0.0590	0.0010	0.691	441	9	417	9	566	38	106	92	a
0.0717	0.0019	0.594	0.016	0.06006	0.00054	0.875	473	10	446	11	606	19	171	93	a
0.1684	0.0073	1.853	0.080	0.07978	0.00056	0.967	1064	28	1004	40	1191	14	180	55	a
0.0810	0.0021	0.692	0.019	0.0620	0.0012	0.740	534	12	502	13	674	42	130	104	a

$^{206}Pb^*/^{238}U$	± 2σ (abs)	$^{207}Pb^*/^{235}U$	± 2σ (abs)	$^{207}Pb^*/^{206}Pb^*$	± 2σ (abs)	corr. coef.	$^{206}Pb^*/^{238}U$ age (Ma)	± 2σ (Ma)	$^{207}Pb^*/^{235}U$ age (Ma)	± 2σ (Ma)	$^{207}Pb^*/^{206}Pb^*$ age (Ma)	± 2σ (Ma)	Length (μm)	Width (μm)	Accept/ Reject
0.0927	0.0028	0.821	0.025	0.06422	0.00080	0.873	608	14	571	16	749	26	140	90	a
0.1585	0.0065	1.708	0.072	0.0782	0.0014	0.911	1012	27	948	36	1151	34	90	75	a
0.03779	0.00087	0.2863	0.0069	0.05495	0.00082	0.510	256	5	239	5	410	33	206	123	a
0.04092	0.00096	0.3146	0.0098	0.0558	0.0022	0.824	278	8	259	6	443	87	170	80	a
0.1436	0.0040	1.510	0.043	0.07629	0.00094	0.900	935	18	865	23	1103	25	172	140	a
0.0674	0.0033	0.566	0.029	0.0609	0.0013	0.823	456	19	420	20	637	47	140	65	a
0.0935	0.0027	0.851	0.054	0.0660	0.0065	0.904	625	30	576	16	807	205	126	44	a
0.1441	0.0043	1.533	0.046	0.07715	0.00038	0.961	944	18	868	24	1125	10	178	100	a
0.1045	0.0029	0.990	0.027	0.06871	0.00028	0.958	699	14	641	17	890	8	153	83	a
0.02249	0.00050	0.1667	0.0049	0.0538	0.0020	0.667	157	4	143	3	361	86	142	80	a
0.1186	0.0032	1.176	0.032	0.07190	0.00071	0.904	789	15	723	18	983	20	80	76	a
0.0855	0.0021	0.769	0.020	0.0653	0.0011	0.771	579	12	529	13	783	35	112	76	a
0.165	0.011	1.89	0.13	0.08320	0.00097	0.963	1078	45	983	61	1274	23	100	55	a
0.1639	0.0052	1.881	0.063	0.0833	0.0012	0.905	1075	22	978	29	1275	28	110	80	a
0.1029	0.0071	0.980	0.078	0.0691	0.0047	0.698	694	40	631	41	902	140	105	99	a
0.1403	0.0058	1.500	0.062	0.07754	0.00063	0.953	931	25	847	33	1135	16	217	76	a
0.0421	0.0010	0.3338	0.0089	0.0575	0.0014	0.872	292	7	266	6	509	55	230	130	a
0.1313	0.0036	1.367	0.039	0.0755	0.0010	0.882	875	17	795	21	1082	26	120	82	a
0.1428	0.0044	1.543	0.049	0.07834	0.00097	0.906	948	19	861	25	1156	24	190	75	a
0.1259	0.0055	1.291	0.056	0.07439	0.00094	0.926	842	25	764	31	1052	25	161	99	a
0.1477	0.0060	1.623	0.071	0.0797	0.0023	0.833	979	27	888	33	1189	58	140	87	a
0.1354	0.0037	1.434	0.040	0.07683	0.00065	0.926	903	17	819	21	1117	17	122	50	a
0.1439	0.0056	1.566	0.065	0.0789	0.0022	0.828	957	26	867	31	1171	56	190	121	a
0.02798	0.00065	0.2136	0.0068	0.0554	0.0024	0.724	197	6	178	4	427	95	160	85	a
0.0992	0.0029	0.943	0.030	0.0690	0.0015	0.767	675	16	610	17	898	46	120	65	a
0.1466	0.0079	1.617	0.087	0.07999	0.00037	0.980	977	34	882	44	1197	9	118	105	a
0.1584	0.0047	1.814	0.055	0.08302	0.00048	0.957	1050	20	948	26	1270	11	155	115	a
0.1381	0.0041	1.485	0.045	0.07799	0.00087	0.909	924	18	834	23	1147	22	156	113	a
0.1274	0.0038	1.326	0.042	0.0755	0.0013	0.858	857	18	773	22	1081	34	150	85	a
0.1365	0.0064	1.461	0.069	0.07766	0.00050	0.966	915	28	825	36	1138	13	120	58	a
0.0949	0.0025	0.894	0.025	0.0684	0.0010	0.819	649	13	584	15	880	32	155	65	a
0.00943	0.00041	0.068	0.010	0.053	0.015	*	67	10	61	3	314	661	207	68	a
0.0513	0.0013	0.424	0.011	0.05990	0.00052	0.818	359	8	323	8	600	19	144	115	a
0.1514	0.0045	1.711	0.051	0.08193	0.00032	0.969	1013	19	909	25	1244	8	110	105	a
0.1219	0.0033	1.257	0.044	0.0748	0.0027	0.604	827	20	742	19	1063	73	74	43	a
0.0787	0.0021	0.710	0.022	0.0655	0.0018	0.584	545	13	488	13	789	59	85	80	a
0.1406	0.0064	1.540	0.071	0.0794	0.0014	0.906	947	28	848	36	1183	35	130	75	a
0.0450	0.0022	0.366	0.020	0.0591	0.0028	0.884	317	15	284	14	570	105	236	63	a
0.0769	0.0024	0.693	0.026	0.0654	0.0026	0.921	535	16	477	14	787	82	166	60	a
0.1487	0.0047	1.683	0.062	0.0821	0.0024	0.778	1002	23	894	26	1247	57	180	72	a
0.1420	0.0041	1.587	0.046	0.08106	0.00054	0.944	965	18	856	23	1223	13	148	79	a
0.1382	0.0041	1.536	0.046	0.08062	0.00022	0.977	945	18	834	23	1212	5	130	72	a
0.1363	0.0038	1.507	0.044	0.0802	0.0012	0.864	933	18	824	22	1201	30	150	125	a
0.1269	0.0034	1.362	0.041	0.0778	0.0017	0.784	873	18	770	20	1142	44	170	85	a
0.1387	0.0038	1.547	0.043	0.08090	0.00037	0.958	949	17	837	22	1219	9	121	66	a
0.1417	0.0045	1.600	0.051	0.08187	0.00065	0.938	970	20	854	25	1242	16	133	120	a
0.1663	0.0096	2.04	0.12	0.0889	0.0013	0.942	1129	40	992	53	1403	28	100	67	a
0.1354	0.0042	1.505	0.047	0.08063	0.00029	0.971	933	19	819	24	1213	7	106	99	a
0.1469	0.0042	1.696	0.060	0.0837	0.0027	0.718	1007	23	884	24	1287	62	203	58	a
0.1175	0.0037	1.237	0.069	0.0763	0.0057	0.933	817	31	716	22	1104	150	140	105	a
0.1347	0.0050	1.499	0.060	0.0807	0.0019	0.836	930	25	815	29	1215	47	144	128	a

$^{206}Pb^*/^{238}U$	± 2σ (abs)	$^{207}Pb^*/^{235}U$	± 2σ (abs)	$^{207}Pb^*/^{206}Pb^*$	± 2σ (abs)	corr. coef.	$^{206}Pb^*/^{238}U$ age (Ma)	± 2σ (Ma)	$^{207}Pb^*/^{235}U$ age (Ma)	± 2σ (Ma)	$^{207}Pb^*/^{206}Pb^*$ age (Ma)	± 2σ (Ma)	Length (μm)	Width (μm)	Accept/ Reject
0.0916	0.0024	0.889	0.025	0.0703	0.0014	0.746	646	13	565	14	938	40	210	100	a
0.1201	0.0042	1.277	0.047	0.0771	0.0017	0.827	836	21	731	24	1124	44	98	98	a
0.02681	0.00061	0.2117	0.0060	0.0573	0.0019	0.745	195	5	171	4	501	74	127	83	a
0.1278	0.0036	1.396	0.043	0.0792	0.0016	0.809	887	18	775	21	1178	40	217	126	a
0.1405	0.0041	1.599	0.047	0.08258	0.00050	0.948	970	18	847	23	1259	12	130	70	a
0.265	0.011	4.52	0.18	0.12377	0.00088	0.966	1734	34	1514	54	2011	13	130	65	a
0.1406	0.0041	1.609	0.047	0.08295	0.00036	0.962	974	18	848	23	1268	9	140	100	a
0.1392	0.0039	1.588	0.050	0.0827	0.0018	0.799	966	20	840	22	1263	44	160	100	a
0.1356	0.0053	1.534	0.068	0.0820	0.0027	0.775	944	27	820	30	1246	65	140	93	a
0.1510	0.0044	1.801	0.053	0.08650	0.00062	0.941	1046	19	906	25	1349	14	112	89	a
0.1496	0.0050	1.781	0.059	0.08634	0.00066	0.943	1039	22	899	28	1346	15	153	89	a
0.1489	0.0045	1.779	0.054	0.08663	0.00031	0.970	1038	20	895	25	1352	7	125	122	a
0.1325	0.0036	1.503	0.045	0.0823	0.0016	0.812	932	18	802	21	1253	38	170	120	a
0.1457	0.0043	1.729	0.052	0.08605	0.00087	0.914	1019	19	877	24	1339	20	150	90	a
0.1090	0.0047	1.145	0.051	0.0762	0.0014	0.871	775	24	667	27	1101	38	152	70	a
0.1285	0.0037	1.440	0.043	0.0813	0.0010	0.886	906	18	779	21	1229	24	115	94	a
0.1295	0.0036	1.461	0.041	0.08186	0.00053	0.938	915	17	785	21	1242	13	132	85	a
0.1533	0.0058	1.881	0.074	0.0890	0.0018	0.869	1074	26	920	32	1404	38	165	85	a
0.1499	0.0045	1.833	0.059	0.0886	0.0016	0.850	1057	21	901	25	1396	35	130	98	a
0.0865	0.0023	0.863	0.037	0.0724	0.0043	0.905	632	20	535	14	997	122	175	105	a
0.0508	0.0013	0.451	0.017	0.0644	0.0032	0.846	378	12	320	8	755	106	170	91	a
0.1868	0.0061	2.637	0.087	0.10240	0.00084	0.942	1311	24	1104	33	1668	15	217	192	a
0.0695	0.0037	0.660	0.037	0.0689	0.0029	0.618	515	23	433	22	897	88	135	65	a
0.1946	0.0064	2.851	0.097	0.1062	0.0013	0.915	1369	25	1146	34	1736	23	105	85	a
0.0639	0.0023	0.600	0.035	0.0681	0.0055	0.873	477	22	399	14	872	167	142	108	a
0.1230	0.0036	1.413	0.057	0.0833	0.0038	0.946	895	24	748	21	1277	89	175	100	a
0.0911	0.0029	0.942	0.030	0.07501	0.00080	0.882	674	16	562	17	1069	22	88	82	a
0.1713	0.0072	2.361	0.100	0.09997	0.00091	0.947	1231	30	1019	40	1623	17	98	92	a
0.02805	0.00065	0.2393	0.0092	0.0619	0.0038	0.674	218	8	178	4	670	130	155	110	a
0.0494	0.0031	0.455	0.035	0.0667	0.0062	0.860	381	24	311	19	828	192	263	73	a
0.1572	0.0054	2.122	0.078	0.0979	0.0019	0.855	1156	25	941	30	1584	36	115	43	a
0.1730	0.0069	2.47	0.10	0.1036	0.0010	0.939	1263	29	1029	38	1689	18	77	72	a
0.0419	0.0025	0.378	0.055	0.065	0.017	0.757	326	40	265	16	787	540	192	115	a
0.1144	0.0067	1.343	0.081	0.0852	0.0023	0.854	864	35	698	39	1319	52	185	83	a
0.1540	0.0068	2.115	0.096	0.0996	0.0016	0.899	1154	31	924	38	1617	31	109	61	a
0.1203	0.0042	1.46	0.12	0.088	0.011	0.930	916	51	732	24	1388	233	160	80	a
0.0951	0.0030	1.057	0.048	0.0806	0.0047	0.921	732	24	586	18	1212	115	210	70	a
0.0558	0.0015	0.541	0.025	0.0703	0.0049	0.846	439	17	350	9	938	143	157	64	a
0.0455	0.0016	0.427	0.019	0.0680	0.0037	0.848	361	14	287	10	869	112	182	84	a
0.00840	0.00030	0.0706	0.0087	0.061	0.014	*	69	8	54	2	636	509	142	110	a
0.1401	0.0044	1.914	0.070	0.0991	0.0027	0.729	1086	24	845	25	1608	51	125	102	a
0.1682	0.0066	2.57	0.11	0.1110	0.0023	0.855	1293	31	1002	37	1816	38	160	141	a
0.2070	0.0069	3.69	0.12	0.12917	0.00062	0.963	1568	27	1213	37	2087	8	155	125	a
0.1305	0.0042	1.785	0.072	0.0993	0.0038	0.567	1040	26	790	24	1610	71	143	66	r
0.0642	0.0021	0.681	0.038	0.0770	0.0063	0.869	528	23	401	13	1122	162	118	91	r
0.1969	0.0077	3.50	0.14	0.1288	0.0014	0.923	1526	31	1159	41	2081	20	99	74	r
0.203	0.012	3.75	0.23	0.1337	0.0011	0.963	1582	48	1193	65	2147	14	71	68	r
0.1791	0.0081	3.07	0.14	0.1243	0.0016	0.919	1425	36	1062	44	2019	23	155	105	r
0.2811	0.0099	7.26	0.26	0.18736	0.00097	0.960	2144	32	1597	50	2719	9	125	85	r
0.1478	0.0050	2.260	0.093	0.1109	0.0037	0.660	1200	29	889	28	1814	61	110	83	r
0.2737	0.0096	7.20	0.25	0.19083	0.00078	0.967	2137	31	1560	49	2749	7	168	80	r

$^{206}Pb^*/^{238}U$	± 2σ (abs)	$^{207}Pb^*/^{235}U$	± 2σ (abs)	$^{207}Pb^*/^{206}Pb^*$	± 2σ (abs)	corr. coef.	$^{206}Pb^*/^{238}U$ age (Ma)	± 2σ (Ma)	$^{207}Pb^*/^{235}U$ age (Ma)	± 2σ (Ma)	$^{207}Pb^*/^{206}Pb^*$ age (Ma)	± 2σ (Ma)	Length (μm)	Width (μm)	Accept/ Reject
0.0530	0.0017	0.567	0.037	0.0776	0.0081	0.826	456	24	333	10	1138	208	170	65	r
0.0582	0.0014	0.650	0.037	0.0810	0.0076	0.837	508	23	365	8	1220	185	114	89	r
0.2104	0.0074	4.46	0.16	0.1536	0.0016	0.912	1723	30	1231	39	2386	18	116	106	r
0.0860	0.0045	1.104	0.058	0.09312	0.00046	0.957	755	28	532	27	1490	9	76	72	r
0.1337	0.0039	2.107	0.072	0.1143	0.0031	0.642	1151	24	809	22	1869	49	114	88	r
0.0937	0.0035	1.248	0.046	0.09657	0.00026	0.968	822	21	577	20	1559	5	145	74	r
0.0942	0.0036	1.290	0.049	0.09934	0.00060	0.931	841	22	580	21	1612	11	130	66	r
0.180	0.012	3.64	0.25	0.14674	0.00095	0.969	1559	55	1067	68	2308	11	127	97	r
0.02913	0.00075	0.307	0.014	0.0764	0.0054	0.690	272	11	185	5	1106	142	285	65	r
0.2030	0.0080	4.61	0.19	0.1648	0.0027	0.865	1752	34	1192	43	2506	27	145	97	r
0.034	0.022	0.37	0.45	0.08	0.16	0.718	321	336	218	135	1161	4071	124	95	a
0.00490	0.00031	0.0475	0.0066	0.070	0.018	*	47	6	32	2	936	536	121	88	r
0.02139	0.00087	0.226	0.013	0.0766	0.0061	0.622	207	11	136	6	1111	160	120	63	r
0.0548	0.0019	0.675	0.048	0.089	0.010	0.830	524	29	344	12	1412	219	189	104	r
0.03051	0.00095	0.342	0.023	0.0812	0.0095	0.676	298	18	194	6	1226	229	130	65	r
0.0609	0.0016	0.926	0.080	0.110	0.016	0.839	665	42	381	10	1803	269	143	89	r
0.1134	0.0063	2.40	0.17	0.154	0.012	0.944	1244	52	693	36	2387	136	96	74	r
0.0826	0.0027	1.642	0.066	0.1442	0.0058	0.930	987	26	512	16	2278	69	93	82	r
0.00884	0.00047	0.118	0.012	0.097	0.018	*	114	11	57	3	1569	338	183	111	r
0.0314	0.0055	0.495	0.090	0.114	0.015	0.865	409	61	199	34	1870	242	129	124	r
0.0476	0.0033	0.847	0.078	0.129	0.015	0.853	623	43	300	20	2085	198	133	99	r
0.0632	0.0015	1.252	0.036	0.1438	0.0044	0.903	824	16	395	9	2273	52	150	105	r
0.0608	0.0041	1.376	0.100	0.1643	0.0084	0.932	879	43	380	25	2500	86	170	106	r
0.01215	0.00036	0.206	0.011	0.123	0.011	0.013	190	9	78	2	2002	164	105	75	r
0.0521	0.0058	1.45	0.20	0.202	0.031	0.873	911	82	327	35	2846	253	99	53	r
3. Solimões River, Brazil (3.2208˚S, 64.7815˚W)															
0.00090	0.00017	0.002	0.024	0.02	0.19	*	2	24	6	1			295	125	a
0.0229	0.0011	0.072	0.040	0.023	0.015	0.732	71	38	146	7			275	145	r
0.00663	0.00033	0.022	0.026	0.025	0.039		23	26	43	2			150	124	r
0.00774	0.00039	0.027	0.026	0.026	0.034		27	26	50	2			347	87	r
0.0237	0.0011	0.102	0.046	0.031	0.016	0.749	99	42	151	7			400	220	r
0.00628	0.00086	0.029	0.041	0.034	0.053	0.067	29	40	40	6			250	145	a
0.00740	0.00037	0.035	0.021	0.034	0.029		35	20	48	2			173	99	a
0.0435	0.0018	0.227	0.077	0.038	0.014	0.867	208	63	274	11			225	160	a
0.00249	0.00018	0.0121	0.0069	0.035	0.037	*	12	7	16	1			240	190	a
0.0237	0.0013	0.125	0.071	0.038	0.025	0.752	120	64	151	8			340	140	a
0.00695	0.00032	0.036	0.012	0.038	0.015	0.123	36	12	45	2			245	190	a
0.0311	0.0012	0.169	0.024	0.0395	0.0062	0.817	159	21	197	8			390	165	a
0.0760	0.0038	0.484	0.061	0.0462	0.0071		401	42	472	23	8	369	182	87	a
0.1103	0.0055	0.77	0.14	0.051	0.012		582	82	674	32	237	529	221	103	a
0.1710	0.0084	2.12	0.12	0.0898	0.0024	0.893	1154	40	1017	46	1422	51	175	75	a
0.0330	0.0015	0.197	0.023	0.0433	0.0086	0.701	183	20	209	10			207	150	a
0.1399	0.0077	1.075	0.074	0.0557	0.0035	0.799	741	36	844	43	441	139	225	230	a
0.253	0.014	4.42	0.29	0.1269	0.0034	0.911	1716	54.4767	1452	72	2055	47	205	140	a
0.0328	0.0016	0.200	0.074	0.044	0.019	0.822	185	62.8042	208	10			240	160	a
0.0502	0.0025	0.321	0.055	0.0464	0.0100		283	42.4052	316	15	18	517	257	125	a
0.0229	0.0011	0.138	0.014	0.0437	0.0054		131	12.0734	146	7			358	172	a
0.216	0.020	3.07	0.33	0.1029	0.0041	0.922	1425	82.3031	1262	104	1677	75	225	90	a
0.1021	0.0050	0.76	0.14	0.054	0.010	0.950	575	82.8232	627	29	377	419	240	125	a
0.0670	0.0033	0.462	0.030	0.0500	0.0036	0.903	386	20.9719	418	20	196	169	145	120	a
0.1778	0.0090	2.09	0.13	0.0851	0.0027	0.887	1144	43.6121	1055	49	1317	61	300	145	a

$^{206}Pb^*/^{238}U$	± 2σ (abs)	$^{207}Pb^*/^{235}U$	± 2σ (abs)	$^{207}Pb^*/^{206}Pb^*$	± 2σ (abs)	corr. coef.	$^{206}Pb^*/^{238}U$ age (Ma)	± 2σ (Ma)	$^{207}Pb^*/^{235}U$ age (Ma)	± 2σ (Ma)	$^{207}Pb^*/^{206}Pb^*$ age (Ma)	± 2σ (Ma)	Length (μm)	Width (μm)	Accept/ Reject
0.259	0.014	4.13	0.27	0.1158	0.0031	0.922	1660	53.9617	1483	74	1892	48	125	100	a
0.0474	0.0018	0.313	0.021	0.0480	0.0028	0.904	277	15.9585	298	11	98	138	320	130	a
0.1681	0.0081	1.89	0.11	0.0815	0.0022	0.899	1077	38.0165	1002	45	1233	53	290	75	a
0.0893	0.0045	0.673	0.040	0.0547	0.0032		522	24.0303	551	26	398	131	323	154	a
0.393	0.030	9.82	0.86	0.1814	0.0047	0.944	2418	80.3550	2135	141	2665	43	170	135	a
0.0400	0.0018	0.266	0.020	0.0483	0.0033	0.885	240	16.3803	253	11	116	162	250	130	a
0.1739	0.0090	1.92	0.10	0.0802	0.0021	0.900	1089	36.1858	1033	49	1201	52	215	155	a
0.0636	0.0026	0.456	0.030	0.0520	0.0029	0.579	382	21.0510	397	16	287	126	270	135	a
0.0356	0.0016	0.238	0.012	0.0484	0.0020	0.870	216	10	225	10	121	97	295	208	a
0.0945	0.0039	0.735	0.055	0.0564	0.0037	0.639	560	32	582	23	469	145	155	125	a
0.1703	0.0087	1.827	0.099	0.0778	0.0021	0.899	1055	35	1014	48	1142	53	225	190	a
0.188	0.010	2.13	0.13	0.0823	0.0030	0.874	1159	42	1109	56	1253	72	260	110	a
0.1761	0.0091	1.91	0.10	0.0787	0.0021	0.904	1085	36	1046	50	1165	52	146	143	a
0.0359	0.0016	0.243	0.014	0.0491	0.0028	0.835	221	11	228	10	153	134	235	125	a
0.1789	0.0095	1.94	0.11	0.0786	0.0021	0.906	1094	37	1061	52	1161	53	230	100	a
0.1781	0.0091	1.92	0.12	0.0783	0.0022	0.907	1089	41	1057	50	1155	57	205	145	a
0.201	0.011	2.32	0.13	0.0840	0.0022	0.913	1219	40	1178	58	1292	52	180	150	a
0.0405	0.0020	0.279	0.023	0.0499	0.0050		250	18	256	13	190	234	232	124	a
0.1605	0.0080	1.51	0.11	0.0684	0.0058		936	46	959	45	881	176	213	111	a
0.0847	0.0042	0.657	0.035	0.0562	0.0031		513	21	524	25	461	120	134	161	a
0.191	0.011	2.12	0.14	0.0805	0.0022	0.921	1155	46	1126	58	1210	55	270	125	a
0.0401	0.0018	0.277	0.020	0.0501	0.0051	0.796	248	16	253	11	200	235	275	165	a
0.1691	0.0087	1.753	0.095	0.0751	0.0020	0.902	1028	35	1007	48	1072	53	240	125	a
0.185	0.010	2.00	0.15	0.0785	0.0028	0.900	1116	49	1093	57	1160	70	95	100	a
0.1159	0.0057	0.983	0.057	0.0615	0.0018	0.876	695	29	707	33	657	64	120	110	a
0.0950	0.0045	0.763	0.040	0.0582	0.0022	0.784	576	23	585	27	538	82	135	100	a
0.0984	0.0040	0.800	0.040	0.0590	0.0018	0.824	597	23	605	23	565	67	125	120	a
0.1729	0.0089	1.789	0.098	0.0750	0.0020	0.903	1042	36	1028	49	1070	54	160	110	a
0.0439	0.0018	0.310	0.015	0.0512	0.0016	0.650	274	12	277	11	249	70	230	75	a
0.1701	0.0087	1.741	0.094	0.0742	0.0019	0.905	1024	35	1013	48	1047	53	295	100	a
0.1398	0.0069	1.279	0.067	0.0664	0.0018	0.887	836	30	843	39	819	57	150	100	a
0.01937	0.00088	0.129	0.017	0.048	0.011	0.459	123	15	124	6	106	524	230	130	a
0.0400	0.0018	0.281	0.017	0.0509	0.0033	0.842	251	13	253	11	235	148	190	195	a
0.0533	0.0024	0.388	0.019	0.0527	0.0018	0.642	333	14	335	15	318	78	240	90	a
0.0326	0.0012	0.225	0.015	0.0499	0.0032	0.852	206	13	207	8	191	149	335	240	a
0.1203	0.0060	1.048	0.097	0.0632	0.0069		728	48	732	35	716	232	117	94	a
0.195	0.011	2.12	0.14	0.0789	0.0021	0.930	1155	47	1148	62	1169	53	200	80	a
0.1551	0.0078	1.487	0.054	0.0696	0.0013		925	22	929	43	915	37	178	135	a
0.02677	0.00096	0.1817	0.0091	0.0492	0.0019	0.850	170	8	170	6	159	92	170	130	a
0.1811	0.0096	1.88	0.12	0.0755	0.0020	0.919	1076	41	1073	52	1081	54	126	115	a
0.1046	0.0050	0.881	0.045	0.0610	0.0017	0.853	641	24	641	29	641	60	245	115	a
0.0485	0.0022	0.351	0.018	0.0524	0.0018	0.584	305	13	305	14	305	80	190	115	a
0.1559	0.0079	1.51	0.12	0.0702	0.0073	0.552	934	50	934	44	935	212	185	140	a
0.0981	0.0049	0.812	0.028	0.0601	0.0012		604	16	603	29	606	45	228	120	a
0.1104	0.0053	0.947	0.049	0.0622	0.0018	0.849	676	26	675	31	680	63	115	90	a
0.0555	0.0021	0.410	0.021	0.0536	0.0020	0.633	349	15	348	13	354	84	205	115	a
0.0232	0.0010	0.1570	0.0083	0.0491	0.0025	0.760	148	7	148	6	153	118	175	125	a
0.1199	0.0052	1.056	0.055	0.0639	0.0018	0.866	732	27	730	30	737	60	165	135	a
0.1953	0.0098	2.114	0.074	0.0785	0.0013		1153	24	1150	53	1159	34	104	109	a
0.0437	0.0020	0.313	0.015	0.0520	0.0014	0.658	277	12	276	12	286	62	185	80	a
0.1987	0.0099	2.175	0.078	0.0794	0.0016		1173	25	1168	54	1182	39	184	134	a

$^{206}Pb^*/^{238}U$	± 2σ (abs)	$^{207}Pb^*/^{235}U$	± 2σ (abs)	$^{207}Pb^*/^{206}Pb^*$	± 2σ (abs)	corr. coef.	$^{206}Pb^*/^{238}U$ age (Ma)	± 2σ (Ma)	$^{207}Pb^*/^{235}U$ age (Ma)	± 2σ (Ma)	$^{207}Pb^*/^{206}Pb^*$ age (Ma)	± 2σ (Ma)	Length (μm)	Width (μm)	Accept/ Reject
0.0511	0.0026	0.374	0.020	0.0531	0.0031		323	15	321	16	334	132	364	100	a
0.1403	0.0074	1.31	0.10	0.0679	0.0035	0.823	852	45	846	42	865	106	105	50	a
0.00647	0.00036	0.042	0.020	0.047	0.025	0.094	42	19	42	2	58	1264	240	70	a
0.0402	0.0020	0.287	0.017	0.0518	0.0035		256	13	254	12	275	153	431	164	a
0.0652	0.0041	0.500	0.053	0.0555	0.0048	0.556	411	36	407	25	434	192	210	95	a
0.1401	0.0070	1.319	0.047	0.0683	0.0014		854	20	845	40	877	41	237	78	a
0.1170	0.0050	1.035	0.055	0.0642	0.0020	0.843	721	27	713	29	747	67	205	85	a
0.1804	0.0098	1.82	0.11	0.0733	0.0024	0.894	1053	39	1069	54	1021	67	180	120	a
0.249	0.012	3.18	0.11	0.0926	0.0019		1452	27	1433	65	1480	40	191	92	a
0.1082	0.0051	0.937	0.049	0.0628	0.0021	0.820	671	26	662	30	703	72	225	125	a
0.0415	0.0015	0.299	0.014	0.0523	0.0018	0.541	266	11	262	9	300	78	275	175	a
0.1778	0.0089	1.87	0.10	0.0764	0.0040		1072	36	1055	49	1105	104	193	121	a
0.1722	0.0086	1.786	0.057	0.07523	0.00053		1040	21	1024	48	1075	14	188	106	a
0.0446	0.0022	0.326	0.019	0.0529	0.0034		286	14	281	14	326	144	144	80	a
0.1522	0.0076	1.502	0.057	0.0716	0.0019		931	23	913	43	974	55	172	96	a
0.1690	0.0084	1.748	0.056	0.07502	0.00034		1026	21	1006	47	1069	9	192	123	a
0.1751	0.0091	1.722	0.094	0.0713	0.0019	0.909	1017	35	1040	50	966	55	260	120	a
0.0409	0.0015	0.296	0.013	0.0526	0.0015	0.604	264	10	258	9	310	65	245	140	a
0.0874	0.0041	0.721	0.036	0.0599	0.0017	0.812	551	21	540	24	598	63	235	150	a
0.1057	0.0045	0.918	0.050	0.0630	0.0022	0.810	661	26	648	26	708	75	150	105	a
0.1589	0.0075	1.601	0.089	0.0731	0.0019	0.902	971	35	951	42	1017	54	265	115	a
0.1686	0.0084	1.747	0.057	0.07515	0.00085		1026	21	1005	47	1073	23	147	96	a
0.0863	0.0034	0.711	0.035	0.0598	0.0017	0.804	545	20	533	20	595	63	350	140	a
0.1106	0.0055	0.977	0.032	0.06406	0.00061		692	16	676	32	743	20	168	100	a
0.254	0.013	3.37	0.11	0.09611	0.00033		1497	25	1461	66	1550	6	175	143	a
0.1607	0.0080	1.640	0.059	0.0740	0.0015		986	23	961	45	1042	42	252	150	a
0.1608	0.0080	1.642	0.054	0.07406	0.00071		987	21	961	45	1043	19	315	197	a
0.1650	0.0084	1.705	0.092	0.0750	0.0020	0.900	1011	34	985	47	1067	53	200	130	a
0.1969	0.0098	2.231	0.078	0.0822	0.0015		1191	25	1158	53	1250	35	273	110	a
0.1784	0.0089	1.920	0.064	0.07804	0.00093		1088	22	1058	49	1148	24	101	99	a
0.1575	0.0079	1.597	0.052	0.07359	0.00063		969	20	943	44	1030	17	298	126	a
0.0883	0.0036	0.738	0.040	0.0606	0.0022	0.758	561	23	545	21	626	80	260	160	a
0.195	0.011	1.97	0.12	0.0730	0.0026	0.898	1104	42	1150	60	1015	73	161	85	a
0.0297	0.0011	0.212	0.019	0.0516	0.0047	0.822	195	16	189	7	267	210	305	155	a
0.0288	0.0014	0.2044	0.0097	0.0515	0.0025		189	8	183	9	261	113	149	133	a
0.1579	0.0079	1.613	0.054	0.0741	0.0010		975	21	945	44	1044	28	208	88	a
0.0827	0.0041	0.684	0.040	0.0600	0.0035		529	24	512	25	603	126	191	103	a
0.0427	0.0016	0.316	0.020	0.0537	0.0030	0.892	279	15	270	10	359	127	260	205	a
0.0372	0.0017	0.271	0.019	0.0529	0.0048	0.798	244	15	235	11	326	204	325	137	a
0.0284	0.0013	0.202	0.011	0.0517	0.0024	0.822	187	9	181	8	271	105	235	104	a
0.141	0.013	1.39	0.16	0.0712	0.0042	0.877	883	67	851	73	964	119	320	205	a
0.1425	0.0064	1.406	0.078	0.0715	0.0021	0.875	891	33	859	36	973	60	205	145	a
0.1448	0.0071	1.438	0.076	0.0720	0.0021	0.874	905	32	872	40	987	60	210	205	a
0.1816	0.0091	2.012	0.087	0.0804	0.0030		1120	29	1076	50	1206	73	214	121	a
0.1690	0.0085	1.810	0.061	0.0777	0.0011		1049	22	1007	47	1139	28	173	128	a
0.1398	0.0062	1.383	0.073	0.0717	0.0019	0.882	882	31	844	35	978	55	230	145	a
0.1863	0.0093	2.11	0.10	0.0820	0.0039		1151	34	1101	51	1246	92	148	102	a
0.0490	0.0023	0.374	0.022	0.0553	0.0031	0.885	322	16	308	14	425	127	256	172	a
0.0733	0.0032	0.600	0.040	0.0593	0.0031	0.625	477	25	456	19	578	115	255	135	a
0.1386	0.0061	1.368	0.072	0.0716	0.0020	0.878	875	31	837	35	975	56	220	190	a
0.1852	0.0093	2.10	0.13	0.0824	0.0057		1150	44	1095	51	1255	135	218	187	a

$^{206}Pb^*/^{238}U$	± 2σ (abs)	$^{207}Pb^*/^{235}U$	± 2σ (abs)	$^{207}Pb^*/^{206}Pb^*$	± 2σ (abs)	corr. coef.	$^{206}Pb^*/^{238}U$ age (Ma)	± 2σ (Ma)	$^{207}Pb^*/^{235}U$ age (Ma)	± 2σ (Ma)	$^{207}Pb^*/^{206}Pb^*$ age (Ma)	± 2σ (Ma)	Length (μm)	Width (μm)	Accept/ Reject
0.1584	0.0074	1.668	0.092	0.0764	0.0020	0.898	996	35	948	41	1105	52	190	120	a
0.0398	0.0015	0.298	0.013	0.0543	0.0014	0.615	265	10	251	9	384	59	320	185	a
0.1494	0.0097	1.54	0.12	0.0749	0.0028	0.889	948	48	898	54	1065	76	200	115	a
0.1512	0.0070	1.571	0.091	0.0754	0.0024	0.873	959	36	908	39	1078	63	250	150	a
0.0374	0.0019	0.280	0.015	0.0543	0.0031		251	12	237	12	383	126	186	123	a
0.0379	0.0017	0.285	0.016	0.0544	0.0034	0.837	254	13	240	11	390	138	295	160	a
0.0527	0.0026	0.416	0.022	0.0572	0.0033		353	16	331	16	500	125	178	78	a
0.1619	0.0083	1.763	0.095	0.0789	0.0022	0.890	1032	35	968	46	1171	54	185	170	a
0.1575	0.0076	1.69	0.11	0.0780	0.0028	0.861	1006	40	943	43	1146	72	220	100	a
0.1507	0.0069	1.590	0.086	0.0765	0.0020	0.888	966	34	905	39	1109	53	145	125	a
0.1586	0.0074	1.718	0.097	0.0785	0.0022	0.886	1015	36	949	41	1160	56	265	175	a
0.1260	0.0063	1.241	0.044	0.0714	0.0014		819	20	765	36	970	41	167	91	a
0.1638	0.0083	1.805	0.100	0.0800	0.0025	0.872	1047	36	978	46	1196	62	260	170	a
0.1595	0.0074	1.756	0.097	0.0799	0.0021	0.892	1029	36	954	41	1194	52	235	160	a
0.0454	0.0021	0.356	0.022	0.0568	0.0039	0.858	309	16	286	13	486	152	200	120	a
0.0983	0.0042	0.903	0.073	0.0666	0.0046	0.592	653	39	605	25	824	145	140	95	a
0.1445	0.0066	1.538	0.091	0.0772	0.0027	0.842	946	37	870	37	1127	71	305	116	a
0.1381	0.0069	1.451	0.080	0.0762	0.0044		910	33	834	39	1101	116	223	137	a
0.0409	0.0019	0.323	0.018	0.0573	0.0029	0.873	284	14	258	12	502	112	310	135	a
0.0600	0.0028	0.506	0.030	0.0611	0.0037	0.903	416	21	376	17	642	129	240	115	a
0.00315	0.00031	0.022	0.028	0.052	0.070	*	22	28	20	2	264	3113	335	130	a
0.0679	0.0031	0.599	0.030	0.0640	0.0022	0.674	476	19	423	19	741	72	180	125	a
0.0295	0.0015	0.236	0.037	0.058	0.012		215	30	187	9	531	441	168	125	a
0.0393	0.0018	0.326	0.019	0.0601	0.0034	0.856	286	14	248	11	609	121	305	110	a
0.0711	0.0033	0.662	0.037	0.0675	0.0033	0.487	516	23	443	20	854	102	165	135	a
0.0305	0.0015	0.250	0.066	0.059	0.021		226	53	194	10	582	764	222	98	a
0.01096	0.00055	0.085	0.016	0.056	0.015		83	15	70	3	457	578	251	118	a
0.1017	0.0053	1.069	0.062	0.0763	0.0022	0.818	738	30	624	31	1103	58	155	80	a
0.0478	0.0033	0.42	0.12	0.064	0.019	0.885	357	82	301	20	741	623	195	115	a
0.1380	0.0076	1.72	0.21	0.0904	0.0090	0.568	1016	78	833	43	1434	189	215	180	a
0.00912	0.00046	0.074	0.025	0.059	0.027		72	24	59	3	556	1014	184	106	a
0.1561	0.0078	2.18	0.48	0.101	0.028		1174	153	935	44	1645	509	341	112	a
0.00799	0.00045	0.066	0.035	0.060	0.036	0.285	65	33	51	3	590	1295	160	110	a
0.0485	0.0022	0.475	0.032	0.0709	0.0059	0.854	394	22	305	14	956	171	190	115	a
0.0449	0.0024	0.448	0.030	0.0724	0.0039	0.895	376	21	283	15	998	110	180	85	r
0.0226	0.0014	0.213	0.023	0.0683	0.0066	0.797	196	19	144	9	878	199	135	60	r
0.00742	0.00043	0.087	0.033	0.085	0.037	0.211	85	31	48	3	1324	839	245	130	a
0.00503	0.00032	0.067	0.024	0.097	0.058	*	66	22	32	2	1558	1124	165	122	r
0.00097	0.00014	0.015	0.011	0.111	0.084	*	15	11	6	1	1814	1373	140	115	r
0.00586	0.00050	0.116	0.021	0.144	0.035	*	112	19	38	3	2270	426	240	160	r
0.00068	0.00011	0.0268	0.0070	0.285	0.085	*	27	7	4	1	3391	462	200	80	r
0.000112	0.000035	0.0062	0.0048	0.40	0.30		6	5	1	0	3909	1131	480	140	r
0.00124	0.00095	0.082	0.084	0.48	0.26	*	80	79	8	6	4180	811	200	160	r
0.207	0.010	1.95	0.13	0.0683	0.0017		1098	46	1213	56	877	55	130	82	a
0.1390	0.0069	1.142	0.072	0.0596	0.0015		774	34	839	39	590	59	122	66	a
0.1744	0.0087	1.57	0.11	0.0653	0.0017		959	42	1036	48	784	57	128	91	a
0.1540	0.0077	1.376	0.088	0.0648	0.0016		879	38	923	43	1710	330	141	97	a
0.1190	0.0059	0.978	0.072	0.0596	0.0015		693	37	725	34	590	72	144	50	a
0.0766	0.0038	0.566	0.034	0.0536	0.0016		455	22	476	23	353	70	151	70	a
0.1031	0.0052	0.817	0.053	0.0575	0.0018		606	29	633	30	509	72	153	42	a
0.293	0.015	3.84	0.30	0.0950	0.0024		1601	63	1656	73	1528	49	153	70	a

$^{206}Pb^*/^{238}U$	± 2σ (abs)	$^{207}Pb^*/^{235}U$	± 2σ (abs)	$^{207}Pb^*/^{206}Pb^*$	± 2σ (abs)	corr. coef.	$^{206}Pb^*/^{238}U$ age (Ma)	± 2σ (Ma)	$^{207}Pb^*/^{235}U$ age (Ma)	± 2σ (Ma)	$^{207}Pb^*/^{206}Pb^*$ age (Ma)	± 2σ (Ma)	Length (μm)	Width (μm)	Accept/ Reject
0.219	0.011	2.43	0.17	0.0805	0.0020		1253	50	1279	58	1208	52	156	90	a
0.1074	0.0054	0.899	0.057	0.0607	0.0018		651	31	658	31	627	68	161	81	a
0.206	0.010	2.24	0.15	0.0790	0.0020		1195	48	1207	55	1172	52	187	86	a
0.204	0.010	2.21	0.15	0.0787	0.0020		1184	48	1194	55	1164	52	134	91	a
0.0697	0.0035	0.528	0.032	0.0550	0.0016		431	21	434	21	412	70	154	50	a
0.0946	0.0047	0.779	0.045	0.0597	0.0015		585	26	582	28	594	58	211	102	a
0.1970	0.0099	2.15	0.15	0.0792	0.0020		1165	48	1159	53	1176	53	182	101	a
0.0579	0.0029	0.432	0.024	0.0541	0.0014		365	17	363	18	377	61	166	74	a
0.1705	0.0085	1.75	0.11	0.0744	0.0019		1026	42	1015	47	1052	52	181	114	a
0.1278	0.0064	1.165	0.071	0.0662	0.0017		785	33	775	37	811	56	143	119	a
0.1804	0.0090	1.91	0.13	0.0769	0.0020		1085	45	1069	49	1118	53	188	79	a
0.0785	0.0039	0.638	0.037	0.0589	0.0016		501	23	487	24	563	61	169	107	a
0.1585	0.0079	1.65	0.11	0.0754	0.0019		989	41	948	44	1080	52	163	114	a
0.0336	0.0017	0.248	0.017	0.0536	0.0021		225	14	213	10	356	94	155	126	a
0.0393	0.0020	0.296	0.023	0.0547	0.0025		264	18	248	12	402	112	263	90	a
0.0485	0.0024	0.400	0.024	0.0597	0.0019		342	18	306	15	594	71	169	77	a
0.0366	0.0018	0.332	0.023	0.0657	0.0027		291	18	232	11	797	90	166	81	a
0.0549	0.0027	0.550	0.033	0.0727	0.0019		445	22	344	17	1005	60	175	74	a
0.0209	0.0010	0.279	0.048	0.097	0.012		250	38	133	7	1710	338	153	122	r
0.1610	0.0081	5.53	4.77	0.249	0.098		1906	742	962	45	3180	864	149	53	r
4. Solimões River, Brazil (3.8765°S, 63.6491°W)															
0.1717	0.0086	1.733	0.017	0.0732	0.0043		1021	47	1021	6	1020	59	235	165	a
0.0789	0.0039	0.6281	0.0024	0.0577	0.0027		490	24	495	1	519	52	300	145	a
0.1820	0.0091	1.841	0.020	0.0734	0.0043		1078	50	1060	7	1024	59	230	170	a
0.1900	0.0095	1.982	0.023	0.0757	0.0046		1121	52	1109	8	1086	61	235	120	a
0.00791	0.00040	0.09	0.00	0.079	0.010		51	3	84	0	1171	128	330	110	r
0.1910	0.0096	2.106	0.026	0.0800	0.0052		1127	52	1151	9	1196	64	180	105	a
0.1708	0.0085	1.718	0.017	0.0730	0.0042		1016	47	1015	6	1013	59	245	105	a
0.1620	0.0081	1.612	0.015	0.0722	0.0041		968	45	975	6	991	58	185	135	a
0.00720	0.00036	0.054	0.000	0.0545	0.0071		46	2	53	0	391	147	200	80	a
0.1818	0.0091	1.908	0.021	0.0761	0.0046		1077	50	1084	7	1099	61	265	115	a
0.00241	0.00012	0.02	0.00	0.052	0.031		15	1	17	0	281	683	280	100	a
0.00247	0.00012	0.02	0.00	0.058	0.056		16	1	20	0	515	1068	265	130	a
0.00216	0.00011	0.01	0.00	0.041	0.011		14	1	12	0	-277	335	210	100	a
0.1755	0.0088	1.837	0.020	0.0759	0.0046		1042	48	1059	7	1093	61	460	120	a
0.0312	0.0016	0.22412	0.00029	0.0521	0.0022		198	10	205	0	291	48	234	220	a
0.0404	0.0020	0.28515	0.00066	0.0513	0.0030		255	13	255	1	252	66	225	115	a
0.0279	0.0014	0.22499	0.00082	0.0585	0.0077		177	9	206	1	550	143	365	135	a
0.0412	0.0021	0.29903	0.00066	0.0526	0.0028		261	13	266	1	311	61	240	110	a
0.0207	0.0010	0.17975	0.00043	0.0629	0.0073		132	7	168	0	706	123	155	135	a
0.0272	0.0014	0.19701	0.00034	0.0526	0.0034		173	9	183	0	312	73	210	110	a
0.1733	0.0087	1.998	0.025	0.0836	0.0060		1030	48	1115	8	1283	70	210	115	a
0.0860	0.0043	0.6750	0.0028	0.0569	0.0028		532	26	524	2	488	54	240	115	a
0.1713	0.0086	2.035	0.024	0.0862	0.0059		1019	47	1127	8	1342	67	300	90	a
0.250	0.012	3.245	0.061	0.0943	0.0071		1436	65	1468	15	1514	71	290	135	a
0.00219	0.00011	0.01	0.00	0.043	0.021		14	1	13	0	-163	610	340	120	a
0.01147	0.00057	0.19694	0.00044	0.125	0.024		74	4	183	0	2022	172	220	85	r
0.1364	0.0068	1.379	0.011	0.0733	0.0044		824	39	880	5	1022	61	205	100	a
0.0442	0.0022	0.34415	0.00085	0.0565	0.0032		279	14	300	1	471	62	220	160	a
0.1136	0.0057	1.0017	0.0061	0.0639	0.0034		694	33	705	3	739	56	120	115	a
0.1671	0.0084	1.653	0.016	0.0717	0.0041		996	46	991	6	978	58	130	100	a

$^{206}Pb^*/^{238}U$	± 2σ (abs)	$^{207}Pb^*/^{235}U$	± 2σ (abs)	$^{207}Pb^*/^{206}Pb^*$	± 2σ (abs)	corr. coef.	$^{206}Pb^*/^{238}U$ age (Ma)	± 2σ (Ma)	$^{207}Pb^*/^{235}U$ age (Ma)	± 2σ (Ma)	$^{207}Pb^*/^{206}Pb^*$ age (Ma)	± 2σ (Ma)	Length (μm)	Width (μm)	Accept/ Reject
0.0257	0.0013	0.21244	0.00054	0.0599	0.0060		164	8	196	0	600	108	215	165	a
0.1540	0.0077	1.559	0.015	0.0734	0.0044		923	43	954	6	1025	61	160	125	a
0.1847	0.0092	2.013	0.025	0.0791	0.0053		1092	50	1120	8	1174	66	300	100	a
0.1653	0.0083	1.645	0.016	0.0722	0.0042		986	46	988	6	991	58	180	130	a
0.1795	0.0090	1.889	0.021	0.0763	0.0047		1064	49	1077	7	1103	61	160	155	a
0.1692	0.0085	1.729	0.017	0.0741	0.0044		1008	47	1019	6	1044	59	155	130	a
0.1805	0.0090	1.848	0.020	0.0743	0.0044		1069	49	1063	7	1049	60	185	115	a
0.205	0.010	2.131	0.026	0.0753	0.0045		1204	55	1159	9	1076	61	300	70	a
0.1460	0.0073	1.488	0.013	0.0739	0.0044		878	41	925	5	1039	59	195	110	a
0.0941	0.0047	1.0112	0.0061	0.0779	0.0050		580	28	709	3	1145	63	205	85	a
0.0451	0.0023	0.35282	0.00079	0.0567	0.0028		284	14	307	1	482	55	295	80	a
0.0429	0.0021	0.32912	0.00073	0.0557	0.0029		271	13	289	1	439	58	220	100	a
0.1841	0.0092	1.923	0.022	0.0757	0.0046		1090	50	1089	8	1088	61	165	125	a
0.00633	0.00032	0.06517	0.00018	0.075	0.032		41	2	64	0	1060	437	295	90	r
0.1763	0.0088	1.808	0.019	0.0744	0.0044		1047	48	1048	7	1052	60	185	105	a
0.1791	0.0090	1.876	0.020	0.0759	0.0046		1062	49	1073	7	1094	61	270	100	a
0.216	0.011	2.430	0.038	0.0816	0.0059		1260	57	1252	11	1237	71	315	85	a
0.1748	0.0087	1.779	0.018	0.0738	0.0044		1039	48	1038	7	1036	60	250	100	a
0.1895	0.0095	2.023	0.024	0.0774	0.0049		1118	52	1123	8	1133	63	240	100	a
0.1841	0.0092	1.913	0.021	0.0754	0.0045		1089	50	1085	7	1078	60	230	125	a
0.1937	0.0097	2.142	0.027	0.0802	0.0053		1141	53	1162	9	1202	65	265	125	a
0.1952	0.0098	2.017	0.024	0.0749	0.0045		1149	53	1121	8	1067	60	245	90	a
0.1779	0.0089	1.851	0.020	0.0755	0.0046		1055	49	1064	7	1081	61	150	105	a
0.1678	0.0084	1.703	0.017	0.0736	0.0043		1000	46	1010	6	1030	60	219	95	a
0.0411	0.0021	0.29763	0.00082	0.0525	0.0035		260	13	265	1	309	76	335	140	a
0.0561	0.0028	0.4996	0.0034	0.0646	0.0078		352	17	411	2	761	128	255	170	a
0.0257	0.0013	0.17718	0.00021	0.0499	0.0023		164	8	166	0	192	54	195	100	a
0.1809	0.0090	1.919	0.021	0.0769	0.0047		1072	50	1088	7	1120	61	243	129	a
0.1641	0.0082	1.824	0.020	0.0806	0.0053		980	46	1054	7	1212	64	226	108	a
0.1799	0.0090	1.836	0.020	0.0740	0.0045		1067	49	1059	7	1042	61	207	78	a
0.1721	0.0086	1.732	0.017	0.0730	0.0042		1024	48	1020	6	1013	59	203	140	a
0.1813	0.0091	2.073	0.031	0.0829	0.0068		1074	50	1140	10	1268	80	202	92	a
0.1718	0.0086	1.787	0.019	0.0755	0.0046		1022	47	1041	7	1081	61	129	108	a
0.1010	0.0051	0.9218	0.0052	0.0662	0.0037		620	30	663	3	812	59	192	89	a
0.1892	0.0095	2.070	0.027	0.0793	0.0054		1117	51	1139	9	1180	67	189	107	a
0.1761	0.0088	1.802	0.019	0.0742	0.0044		1046	48	1046	7	1047	60	196	106	a
0.1832	0.0092	1.968	0.022	0.0779	0.0048		1084	50	1105	8	1145	62	122	103	a
0.283	0.014	4.21	0.10	0.1079	0.0093		1606	71	1676	20	1764	78	199	82	a
0.0404	0.0020	0.36222	0.00094	0.0650	0.0042		255	13	314	1	775	67	172	124	a
0.1765	0.0088	1.854	0.020	0.0762	0.0046		1048	49	1065	7	1100	61	134	114	a
0.0365	0.0018	0.31069	0.00076	0.0618	0.0041		231	11	275	1	668	72	226	74	a
0.0441	0.0022	0.5180	0.0016	0.0851	0.0060		278	14	424	1	1318	68	195	82	r
0.1839	0.0092	1.915	0.021	0.0755	0.0045		1088	50	1086	7	1083	60	188	80	a
0.1953	0.0098	2.066	0.025	0.0768	0.0047		1150	53	1138	8	1115	61	120	85	a
0.0569	0.0028	0.4250	0.0013	0.0542	0.0028		357	17	360	1	377	59	203	85	a
0.202	0.010	2.231	0.029	0.0803	0.0051		1184	54	1191	9	1203	63	172	104	a
0.0785	0.0039	0.6137	0.0022	0.0567	0.0026		487	23	486	1	481	50	133	128	a
0.0647	0.0032	0.7069	0.0036	0.0792	0.0063		404	20	543	2	1177	78	156	87	r
0.0812	0.0041	0.6471	0.0025	0.0578	0.0027		504	24	507	2	521	51	171	73	a
0.203	0.010	2.148	0.027	0.0768	0.0047		1190	55	1164	9	1117	61	136	116	a
0.1998	0.0100	2.257	0.032	0.0819	0.0058		1174	54	1199	10	1244	70	172	71	a

$^{206}Pb^*/^{238}U$	± 2σ (abs)	$^{207}Pb^*/^{235}U$	± 2σ (abs)	$^{207}Pb^*/^{206}Pb^*$	± 2σ (abs)	corr. coef.	$^{206}Pb^*/^{238}U$ age (Ma)	± 2σ (Ma)	$^{207}Pb^*/^{235}U$ age (Ma)	± 2σ (Ma)	$^{207}Pb^*/^{206}Pb^*$ age (Ma)	± 2σ (Ma)	Length (μm)	Width (μm)	Accept/ Reject
0.1955	0.0098	2.072	0.025	0.0769	0.0047		1151	53	1139	8	1117	61	145	90	a
0.1917	0.0096	1.964	0.022	0.0743	0.0044		1131	52	1103	8	1049	60	131	47	a
0.1738	0.0087	1.821	0.020	0.0760	0.0048		1033	48	1053	7	1094	63	162	136	a
0.219	0.011	2.511	0.049	0.0832	0.0074		1276	58	1275	14	1273	87	187	110	a
0.0930	0.0046	0.7896	0.0038	0.0616	0.0032		573	27	591	2	660	56	175	128	a
0.234	0.012	2.935	0.050	0.0909	0.0066		1356	61	1391	13	1445	69	169	119	a
0.1765	0.0088	1.821	0.019	0.0748	0.0045		1048	49	1053	7	1064	60	169	112	a
0.1750	0.0087	1.799	0.019	0.0746	0.0045		1039	48	1045	7	1057	60	177	137	a
0.0459	0.0023	0.6829	0.0049	0.108	0.017		290	14	529	3	1763	143	292	73	r
0.1778	0.0089	1.847	0.020	0.0753	0.0045		1055	49	1062	7	1077	61	256	122	a
0.1533	0.0077	1.810	0.019	0.0856	0.0058		919	43	1049	7	1330	66	146	112	a
0.1823	0.0091	1.898	0.021	0.0755	0.0045		1079	50	1080	7	1082	60	133	112	a
0.0454	0.0023	0.35345	0.00088	0.0565	0.0031		286	14	307	1	472	60	240	76	a
0.0527	0.0026	0.4697	0.0017	0.0647	0.0044		331	16	391	1	763	71	170	104	a
0.0245	0.0012	0.18449	0.00051	0.0545	0.0062		156	8	172	0	394	127	153	112	a
0.1109	0.0055	1.0635	0.0078	0.0696	0.0046		678	32	736	4	916	68	129	96	a
0.0410	0.0021	0.32271	0.00079	0.0570	0.0034		259	13	284	1	493	66	232	83	a
0.0943	0.0047	0.7584	0.0035	0.0583	0.0028		581	28	573	2	542	53	217	78	a
0.207	0.010	2.141	0.028	0.0752	0.0048		1211	55	1162	9	1073	64	83	40	a
0.0515	0.0026	0.4392	0.0024	0.0619	0.0066		324	16	370	2	670	114	154	107	a
0.0439	0.0022	0.32640	0.00061	0.0540	0.0023		277	14	287	0	370	48	131	110	a
0.1823	0.0091	1.999	0.019	0.0795	0.0040		1080	50	1115	6	1185	50	189	96	a
0.345	0.017	5.37	0.13	0.1129	0.0081		1910	83	1880	21	1847	65	154	115	a
0.1913	0.0096	1.995	0.018	0.0756	0.0036		1129	52	1114	6	1086	48	168	99	a
0.1023	0.0051	0.8389	0.0033	0.0595	0.0023		628	30	619	2	585	41	142	135	a
0.0667	0.0033	0.6058	0.0032	0.0659	0.0053		416	20	481	2	803	84	197	134	a
0.0516	0.0026	0.38770	0.00091	0.0545	0.0025		324	16	333	1	391	51	154	126	a
0.0651	0.0033	0.5450	0.0017	0.0607	0.0029		407	20	442	1	628	51	180	105	a
0.0244	0.0012	0.23913	0.00085	0.071	0.010		156	8	218	1	957	149	128	98	r
0.1652	0.0083	2.369	0.027	0.1040	0.0073		986	46	1233	8	1697	64	141	69	a
0.1905	0.0095	1.997	0.019	0.0760	0.0037		1124	52	1114	6	1096	49	240	77	a
0.0248	0.0012	0.17647	0.00021	0.0517	0.0025		158	8	165	0	271	56	440	100	a
0.0533	0.0027	0.4298	0.0014	0.0585	0.0037		335	16	363	1	548	69	141	101	a
0.0951	0.0048	0.7368	0.0025	0.0562	0.0020		586	28	561	1	460	40	149	72	a
0.1617	0.0081	1.799	0.016	0.0807	0.0043		966	45	1045	6	1214	53	185	70	a
0.0410	0.0020	0.33166	0.00081	0.0587	0.0035		259	13	291	1	556	65	220	102	a
0.0440	0.0022	0.34785	0.00079	0.0574	0.0030		277	14	303	1	507	57	142	64	a
0.204	0.010	2.376	0.027	0.0844	0.0047		1198	55	1235	8	1302	54	148	116	a
0.0426	0.0021	0.37806	0.00069	0.0644	0.0028		269	13	326	1	756	45	190	140	a
0.0459	0.0023	0.33840	0.00056	0.0535	0.0019		289	14	296	0	350	41	175	80	a
0.0739	0.0037	0.5853	0.0016	0.0575	0.0022		459	22	468	1	509	42	109	92	a
0.1823	0.0091	1.836	0.017	0.0730	0.0036		1079	50	1058	6	1015	50	119	115	a
0.0407	0.0020	0.28255	0.00042	0.0503	0.0018		257	13	253	0	209	42	169	124	a
0.0309	0.0015	0.33326	0.00092	0.0783	0.0070		196	10	292	1	1155	89	338	106	r
0.0262	0.0013	0.19175	0.00034	0.0532	0.0036		166	8	178	0	336	77	361	98	a
0.1753	0.0088	1.793	0.015	0.0742	0.0035		1041	48	1043	5	1046	47	164	119	a
0.01753	0.00088	0.10895	0.00025	0.0451	0.0060		112	6	105	0	-52	162	156	106	a
0.1775	0.0089	1.845	0.016	0.0754	0.0036		1053	49	1062	6	1080	48	227	130	a
0.1839	0.0092	2.059	0.024	0.0812	0.0051		1088	50	1135	8	1227	61	120	63	a
0.1788	0.0089	1.824	0.015	0.0740	0.0035		1060	49	1054	6	1041	47	175	113	a
0.202	0.010	2.141	0.021	0.0769	0.0038		1185	54	1162	7	1119	49	151	111	a

$^{206}Pb^*/^{238}U$	± 2σ (abs)	$^{207}Pb^*/^{235}U$	± 2σ (abs)	$^{207}Pb^*/^{206}Pb^*$	± 2σ (abs)	corr. coef.	$^{206}Pb^*/^{238}U$ age (Ma)	± 2σ (Ma)	$^{207}Pb^*/^{235}U$ age (Ma)	± 2σ (Ma)	$^{207}Pb^*/^{206}Pb^*$ age (Ma)	± 2σ (Ma)	Length (μm)	Width (μm)	Accept/ Reject
0.1940	0.0097	1.994	0.019	0.0745	0.0036		1143	53	1113	6	1056	49	185	150	a
0.1999	0.0100	2.105	0.021	0.0764	0.0037		1175	54	1151	7	1106	49	220	95	a
0.1731	0.0087	1.685	0.013	0.0706	0.0032		1029	48	1003	5	945	46	110	80	a
0.1884	0.0094	2.146	0.028	0.0826	0.0056		1113	51	1164	9	1260	67	150	145	a
0.1879	0.0094	1.969	0.019	0.0760	0.0039		1110	51	1105	6	1094	51	120	80	a
0.0294	0.0015	0.24377	0.00040	0.0601	0.0033		187	9	222	0	608	60	140	90	a
0.0306	0.0015	0.22150	0.00025	0.0524	0.0019		195	10	203	0	304	42	125	85	a
0.1785	0.0089	1.766	0.014	0.0717	0.0033		1059	49	1033	5	978	47	165	95	a
0.1843	0.0092	1.867	0.016	0.0734	0.0035		1091	50	1069	6	1026	48	205	95	a
0.1672	0.0084	1.921	0.021	0.0833	0.0053		997	46	1088	7	1277	62	140	75	a
0.0498	0.0025	0.4209	0.0011	0.0613	0.0032		313	15	357	1	649	55	100	80	a
0.0366	0.0018	0.26960	0.00050	0.0534	0.0027		232	11	242	0	348	57	230	80	a
0.1705	0.0085	1.700	0.013	0.0723	0.0033		1015	47	1009	5	995	47	145	120	a
0.339	0.017	5.43	0.14	0.1163	0.0087		1881	82	1890	22	1900	67	155	95	a
0.239	0.012	2.823	0.037	0.0857	0.0047		1381	62	1362	10	1331	53	140	95	a
0.1919	0.0096	2.059	0.020	0.0778	0.0039		1132	52	1135	7	1142	49	140	120	a
0.1752	0.0088	1.778	0.015	0.0736	0.0034		1041	48	1037	5	1031	47	125	110	a
0.211	0.011	2.643	0.033	0.0909	0.0054		1233	56	1313	9	1445	57	150	80	a
0.242	0.012	2.551	0.032	0.0766	0.0040		1395	63	1287	9	1110	52	240	90	a
0.0627	0.0031	0.4503	0.0010	0.0521	0.0018		392	19	377	1	289	40	210	70	a
0.0461	0.0023	0.3790	0.0015	0.0597	0.0050		290	14	326	1	592	91	260	105	a
0.0427	0.0021	0.31651	0.00065	0.0537	0.0026		270	13	279	0	359	54	295	130	a
0.1334	0.0067	1.0911	0.0085	0.0593	0.0035		807	38	749	4	579	63	155	85	a
0.1845	0.0092	1.867	0.016	0.0734	0.0034		1091	50	1070	6	1026	47	205	115	a
0.1385	0.0069	1.2194	0.0080	0.0639	0.0030		836	39	809	4	737	50	175	60	a
0.1732	0.0087	1.709	0.014	0.0716	0.0034		1030	48	1012	5	974	49	280	115	a
0.1669	0.0083	1.668	0.013	0.0725	0.0033		995	46	996	5	1000	47	175	125	a
0.1425	0.0071	1.4152	0.0095	0.0720	0.0034		859	40	895	4	987	48	285	85	a
0.1413	0.0071	1.387	0.012	0.0712	0.0044		852	40	883	5	962	63	120	95	a
0.00678	0.00034	0.09	0.00	0.0922	0.0096		44	2	84	0	1471	99	235	95	r
0.0505	0.0025	0.5678	0.0022	0.0816	0.0062		317	16	457	1	1236	75	200	90	r
0.1157	0.0058	0.9700	0.0061	0.0608	0.0033		706	34	688	3	633	59	175	125	a
0.01941	0.00097	0.13555	0.00041	0.0507	0.0080		124	6	129	0	225	182	275	100	a
0.1999	0.0100	2.074	0.020	0.0752	0.0036		1175	54	1140	7	1075	48	275	95	a
0.273	0.014	3.730	0.064	0.0990	0.0062		1557	70	1578	14	1606	59	175	100	a
0.01527	0.00076	0.16073	0.00029	0.0763	0.0090		98	5	151	0	1104	117	165	75	r
0.255	0.013	3.180	0.047	0.0906	0.0052		1462	66	1452	11	1438	55	155	100	a
0.1622	0.0081	1.547	0.011	0.0692	0.0031		969	45	949	5	904	46	160	140	a
0.317	0.016	4.74	0.10	0.1087	0.0075		1773	78	1775	19	1778	63	180	90	a
0.1267	0.0063	1.2681	0.0090	0.0726	0.0041		769	36	832	4	1003	57	205	55	a
0.1945	0.0097	2.601	0.046	0.0970	0.0088		1146	53	1301	13	1567	85	165	65	a
0.1186	0.0059	1.0489	0.0057	0.0641	0.0029		723	34	728	3	746	48	170	100	a
0.254	0.013	3.309	0.051	0.0946	0.0057		1457	66	1483	12	1520	57	150	50	a
0.215	0.011	2.185	0.022	0.0738	0.0035		1254	57	1176	7	1036	47	155	85	a
0.203	0.010	2.113	0.021	0.0756	0.0036		1190	55	1153	7	1084	48	135	100	a
0.0535	0.0027	0.4702	0.0011	0.0638	0.0028		336	16	391	1	733	46	165	95	a
0.1464	0.0073	1.4120	0.0093	0.0700	0.0031		881	41	894	4	927	46	180	65	a
0.1949	0.0097	1.980	0.018	0.0737	0.0035		1148	53	1109	6	1033	48	135	100	a
0.210	0.011	2.188	0.026	0.0755	0.0043		1229	56	1177	8	1083	58	300	85	a
0.209	0.010	2.240	0.023	0.0778	0.0039		1222	56	1194	7	1142	50	120	70	a
0.0530	0.0027	0.4078	0.0011	0.0558	0.0027		333	16	347	1	444	54	160	65	a

$^{206}Pb^*/^{238}U$	± 2σ (abs)	$^{207}Pb^*/^{235}U$	± 2σ (abs)	$^{207}Pb^*/^{206}Pb^*$	± 2σ (abs)	corr. coef.	$^{206}Pb^*/^{238}U$ age (Ma)	± 2σ (Ma)	$^{207}Pb^*/^{235}U$ age (Ma)	± 2σ (Ma)	$^{207}Pb^*/^{206}Pb^*$ age (Ma)	± 2σ (Ma)	Length (μm)	Width (μm)	Accept/ Reject
0.1555	0.0078	1.554	0.011	0.0725	0.0033		932	44	952	4	1000	47	165	125	a
0.257	0.013	2.769	0.035	0.0782	0.0039		1474	66	1347	10	1152	49	165	90	a
0.1752	0.0088	1.777	0.017	0.0736	0.0040		1041	48	1037	6	1030	55	240	100	a
0.0480	0.0024	0.3718	0.0014	0.0562	0.0045		302	15	321	1	461	88	370	90	a
0.1793	0.0090	1.860	0.016	0.0753	0.0036		1063	49	1067	6	1076	49	135	95	a
0.0473	0.0024	0.7680	0.0029	0.1177	0.0093		298	15	579	2	1921	71	300	85	r
0.1988	0.0099	2.014	0.019	0.0735	0.0035		1169	54	1120	7	1026	49	160	95	a
0.0522	0.0026	0.4511	0.0018	0.0627	0.0049		328	16	378	1	699	83	240	75	a
0.0440	0.0022	0.33379	0.00069	0.0550	0.0026		278	14	292	1	414	52	195	95	a
0.206	0.010	2.166	0.022	0.0762	0.0037		1209	55	1170	7	1099	48	220	80	a
0.1863	0.0093	1.895	0.017	0.0738	0.0035		1101	51	1079	6	1035	47	125	75	a
0.1692	0.0085	1.710	0.014	0.0733	0.0035		1008	47	1012	5	1022	49	240	135	a
0.202	0.010	2.093	0.021	0.0752	0.0037		1186	54	1147	7	1073	49	148	95	a
0.0253	0.0013	0.20946	0.00064	0.0600	0.0072		161	8	193	1	602	131	180	95	a
0.216	0.011	2.535	0.053	0.0850	0.0083		1262	58	1282	15	1315	94	95	75	a
0.1897	0.0095	1.947	0.018	0.0744	0.0035		1120	52	1098	6	1054	48	125	65	a
0.0540	0.0027	0.4050	0.0013	0.0544	0.0031		339	17	345	1	388	64	190	60	a
5. Solimões River, Brazil (3.8560˚S, 63.6041˚W)															
0.0274	0.0014	0.18196	0.00058	0.0482	0.0056		174	9	170	1	109	138	235	165	a
0.224	0.011	2.557	0.039	0.0829	0.0057		1302	59	1288	11	1266	67	300	145	a
0.0506	0.0025	0.38511	0.00099	0.0552	0.0028		318	16	331	1	420	56	235	120	a
0.0274	0.0014	0.17775	0.00033	0.0471	0.0032		174	9	166	0	55	81	330	110	a
0.0236	0.0012	0.17879	0.00090	0.055	0.012		150	7	167	1	413	239	180	105	a
0.00338	0.00017	0.02	0.00	0.0477	0.0058		22	1	22	0	82	144	245	105	a
0.1737	0.0087	1.763	0.017	0.0736	0.0041		1032	48	1032	6	1032	57	185	135	a
0.1661	0.0083	1.704	0.017	0.0744	0.0045		991	46	1010	6	1052	61	200	80	a
0.0424	0.0021	0.3927	0.0011	0.0672	0.0043		267	13	336	1	845	67	265	115	a
0.0976	0.0049	0.8048	0.0053	0.0598	0.0040		600	29	600	3	597	73	262	120	a
0.0275	0.0014	0.20300	0.00055	0.0536	0.0053		175	9	188	0	355	112	280	100	a
0.1502	0.0075	1.494	0.012	0.0721	0.0040		902	42	928	5	990	56	265	130	a
0.1799	0.0090	1.850	0.019	0.0746	0.0042		1066	49	1063	7	1058	57	210	100	a
0.1596	0.0080	1.600	0.015	0.0727	0.0041		955	45	970	6	1006	57	460	120	a
0.1830	0.0092	1.910	0.020	0.0757	0.0044		1084	50	1085	7	1087	58	234	220	a
0.1762	0.0088	1.829	0.019	0.0753	0.0043		1046	48	1056	7	1076	58	225	115	a
0.1989	0.0099	2.191	0.027	0.0799	0.0050		1169	54	1178	9	1194	61	365	135	a
0.00289	0.00014	0.02	0.00	0.063	0.024		19	1	25	0	697	410	240	110	r
0.0976	0.0049	0.8045	0.0037	0.0598	0.0028		600	29	599	2	597	51	155	135	a
0.0492	0.0025	0.3871	0.0010	0.0570	0.0030		310	15	332	1	493	58	210	110	a
0.0720	0.0036	0.5442	0.0021	0.0548	0.0029		448	22	441	1	404	58	210	115	a
0.239	0.012	2.947	0.048	0.0895	0.0061		1381	62	1394	13	1414	66	240	115	a
0.306	0.015	7.81	0.37	0.185	0.028		1722	76	2210	43	2698	127	300	90	a
0.0415	0.0021	0.2039	0.0012	0.0357	0.0051		262	13	188	1	-656	197	285	160	a
0.00271	0.00014	0.05	0.00	0.138	0.034		17	1	51	0	2204	216	255	130	r
0.0732	0.0037	3.128	0.063	0.310	0.085		456	22	1440	16	3520	212	210	100	r
0.00346	0.00017	0.05	0.00	0.097	0.032		22	1	46	0	1564	312	156	150	r
0.0409	0.0020	0.32381	0.00075	0.0574	0.0033		258	13	285	1	508	62	310	115	a
0.00303	0.00015	0.02	0.00	0.059	0.019		20	1	25	0	568	353	175	130	a
0.1860	0.0093	1.941	0.021	0.0757	0.0044		1100	51	1095	7	1087	58	175	160	a
0.1617	0.0081	1.673	0.016	0.0750	0.0043		966	45	998	6	1070	58	205	100	a
0.0220	0.0011	0.16179	0.00023	0.0534	0.0034		140	7	152	0	345	72	175	100	a
0.1652	0.0083	1.633	0.015	0.0717	0.0039		986	46	983	6	978	56	190	145	a

$^{206}Pb^*/^{238}U$	± 2σ (abs)	$^{207}Pb^*/^{235}U$	± 2σ (abs)	$^{207}Pb^*/^{206}Pb^*$	± 2σ (abs)	corr. coef.	$^{206}Pb^*/^{238}U$ age (Ma)	± 2σ (Ma)	$^{207}Pb^*/^{235}U$ age (Ma)	± 2σ (Ma)	$^{207}Pb^*/^{206}Pb^*$ age (Ma)	± 2σ (Ma)	Length (μm)	Width (μm)	Accept/ Reject
0.1941	0.0097	2.064	0.024	0.0771	0.0046		1144	53	1137	8	1124	60	225	130	a
0.0379	0.0019	0.2703	0.0010	0.0517	0.0052		240	12	243	1	273	115	215	130	a
0.0194	0.00097	0.12724	0.00027	0.0475	0.0051		124	6	122	0	73	128	225	160	a
0.206	0.010	2.458	0.034	0.0866	0.0057		1207	55	1260	10	1351	64	250	165	a
0.0487	0.0024	0.35426	0.00071	0.0528	0.0022		306	15	308	1	319	47	135	120	a
0.252	0.013	3.324	0.064	0.0955	0.0072		1451	65	1487	15	1538	71	255	160	a
0.1632	0.0082	1.645	0.015	0.0731	0.0041		975	45	988	6	1016	57	145	70	a
0.0493	0.0025	0.35402	0.00077	0.0521	0.0023		310	15	308	1	289	50	220	130	a
0.1855	0.0093	2.055	0.024	0.0803	0.0051		1097	51	1134	8	1205	62	155	115	a
0.1331	0.0067	1.2812	0.0093	0.0698	0.0038		805	38	837	4	923	56	165	120	a
0.1288	0.0064	1.2620	0.0088	0.0710	0.0039		781	37	829	4	959	55	160	130	a
0.0394	0.0020	0.29813	0.00077	0.0549	0.0036		249	12	265	1	407	73	270	145	a
0.00602	0.00030	0.06	0.00	0.068	0.016		39	2	56	0	870	250	300	165	r
0.1562	0.0078	1.537	0.014	0.0714	0.0042		936	44	945	6	969	60	200	130	a
0.1668	0.0083	1.691	0.019	0.0735	0.0048		994	46	1005	7	1029	66	460	104	a
0.1706	0.0085	1.734	0.021	0.0737	0.0052		1015	47	1021	8	1033	71	460	104	a
0.0576	0.0029	0.6493	0.0026	0.0818	0.0056		361	18	508	2	1241	67	335	140	r
0.0414	0.0021	0.30884	0.00066	0.0541	0.0028		261	13	273	1	376	58	350	140	a
0.1857	0.0093	1.925	0.017	0.0752	0.0036		1098	51	1090	6	1074	48	160	140	a
0.0267	0.0013	0.20579	0.00031	0.0560	0.0031		170	8	190	0	451	62	160	140	a
0.1499	0.0075	1.4152	0.0099	0.0685	0.0032		901	42	895	4	883	48	260	180	a
0.0755	0.0038	0.5965	0.0017	0.0573	0.0022		469	23	475	1	504	43	255	170	a
0.0967	0.0048	0.7965	0.0030	0.0597	0.0023		595	28	595	2	594	42	195	100	a
0.1941	0.0097	2.052	0.020	0.0767	0.0038		1144	53	1133	7	1113	50	175	100	a
0.244	0.012	3.094	0.050	0.0918	0.0060		1410	64	1431	12	1463	62	370	110	a
0.0450	0.0022	0.3882	0.0012	0.0626	0.0042		284	14	333	1	695	71	225	115	a
0.0333	0.0017	0.26159	0.00038	0.0570	0.0025		211	10	236	0	492	48	160	120	a
0.0481	0.0024	0.34552	0.00062	0.0521	0.0020		303	15	301	0	292	43	250	85	a
0.1832	0.0092	1.904	0.018	0.0754	0.0038		1084	50	1082	6	1079	51	155	150	a
0.1655	0.0083	1.654	0.013	0.0725	0.0034		987	46	991	5	1000	47	215	175	a
0.1571	0.0079	1.941	0.019	0.0896	0.0055		940	44	1095	6	1417	59	130	125	a
0.1769	0.0088	1.835	0.016	0.0752	0.0038		1050	49	1058	6	1075	50	220	130	a
0.207	0.010	2.237	0.026	0.0783	0.0043		1214	56	1193	8	1154	55	140	120	a
0.0222	0.0011	0.19526	0.00063	0.0637	0.0092		142	7	181	1	731	154	350	160	a
0.0991	0.0050	0.7954	0.0031	0.0582	0.0023		609	29	594	2	538	43	195	165	a
0.0836	0.0042	0.7272	0.0043	0.0631	0.0045		518	25	555	3	710	76	232	115	a
0.0283	0.0014	0.21477	0.00041	0.0550	0.0037		180	9	198	0	414	75	270	150	a
0.1767	0.0088	1.801	0.015	0.0739	0.0035		1049	49	1046	5	1039	48	245	200	a
0.1905	0.0095	1.969	0.018	0.0750	0.0036		1124	52	1105	6	1068	48	285	110	a
0.0214	0.0011	0.17610	0.00032	0.0596	0.0050		137	7	165	0	591	91	253	215	a
0.0972	0.0049	0.7960	0.0037	0.0594	0.0028		598	29	595	2	581	51	205	175	a
0.1909	0.0095	2.054	0.020	0.0780	0.0039		1126	52	1133	7	1147	50	225	125	a
0.1688	0.0084	1.667	0.013	0.0716	0.0033		1006	47	996	5	975	47	235	95	a
0.0488	0.0024	0.3841	0.0010	0.0571	0.0031		307	15	330	1	496	59	345	125	a
0.214	0.011	2.312	0.025	0.0784	0.0039		1249	57	1216	8	1158	50	155	85	a
0.239	0.012	3.262	0.049	0.0991	0.0063		1380	62	1472	12	1608	59	110	100	a
0.1883	0.0094	2.037	0.019	0.0784	0.0040		1112	51	1128	7	1158	50	225	175	a
0.00852	0.00043	0.08	0.00	0.0709	0.0077		55	3	81	0	956	111	240	80	r
0.0395	0.0020	0.27659	0.00036	0.0508	0.0017		250	12	248	0	232	38	205	180	a
0.1660	0.0083	1.611	0.014	0.0704	0.0038		990	46	975	6	941	55	195	135	a
0.0301	0.0015	0.24568	0.00073	0.0591	0.0058		191	9	223	1	572	107	260	100	a

$^{206}Pb^*/^{238}U$	± 2σ (abs)	$^{207}Pb^*/^{235}U$	± 2σ (abs)	$^{207}Pb^*/^{206}Pb^*$	± 2σ (abs)	corr. coef.	$^{206}Pb^*/^{238}U$ age (Ma)	± 2σ (Ma)	$^{207}Pb^*/^{235}U$ age (Ma)	± 2σ (Ma)	$^{207}Pb^*/^{206}Pb^*$ age (Ma)	± 2σ (Ma)	Length (μm)	Width (μm)	Accept/ Reject
0.0297	0.0015	0.19491	0.00028	0.0476	0.0023		189	9	181	0	77	58	295	115	a
0.1040	0.0052	0.8738	0.0043	0.0609	0.0029		638	30	638	2	637	51	230	155	a
0.273	0.014	3.859	0.069	0.1024	0.0067		1558	70	1605	15	1668	61	245	125	a
0.1902	0.0095	2.056	0.020	0.0784	0.0040		1122	52	1134	7	1158	51	325	165	a
0.1641	0.0082	1.940	0.019	0.0858	0.0052		979	46	1095	7	1333	58	230	110	a
0.1951	0.0098	2.147	0.022	0.0798	0.0041		1149	53	1164	7	1193	51	215	155	a
0.1739	0.0087	1.769	0.015	0.0738	0.0035		1034	48	1034	5	1035	48	300	105	a
0.1720	0.0086	1.678	0.013	0.0707	0.0033		1023	47	1000	5	949	48	185	120	a
0.0217	0.0011	0.22068	0.00043	0.0739	0.0067		138	7	202	0	1037	91	455	120	r
0.1640	0.0082	1.666	0.013	0.0737	0.0035		979	46	995	5	1033	48	245	155	a
0.207	0.010	2.272	0.025	0.0797	0.0042		1212	55	1204	8	1189	52	200	105	a
0.224	0.011	2.381	0.026	0.0772	0.0038		1300	59	1237	8	1128	50	155	80	a
0.211	0.011	2.099	0.021	0.0721	0.0034		1235	56	1148	7	989	47	140	95	a
0.00306	0.00015	0.01	0.00	0.034	0.020		20	1	14	0	-827	853	310	140	a
0.00	0.00	0.010	0.000	0.057	0.014		8	0	10	0	480	278	200	120	a
0.0471	0.0024	0.35667	0.00068	0.0550	0.0022		296	15	310	1	411	46	260	130	a
0.1464	0.0073	1.3752	0.0088	0.0681	0.0030		881	41	878	4	872	45	200	155	a
0.00245	0.00012	0.01	0.00	0.044	0.034		16	1	15	0	-126	973	195	100	a
0.1892	0.0095	2.001	0.019	0.0767	0.0038		1117	51	1116	6	1114	49	140	140	a
0.0423	0.0021	0.3419	0.0012	0.0586	0.0049		267	13	299	1	553	92	240	110	a
0.0365	0.0018	0.26003	0.00051	0.0516	0.0028		231	11	235	0	268	61	305	110	a
0.0513	0.0026	0.3964	0.0011	0.0561	0.0032		322	16	339	1	455	63	150	90	a
0.0307	0.0015	0.20420	0.00056	0.0482	0.0043		195	10	189	0	110	106	230	130	a
0.0646	0.0032	0.5590	0.0022	0.0628	0.0038		403	20	451	1	702	65	220	150	a
0.1822	0.0091	2.262	0.035	0.0900	0.0076		1079	50	1200	11	1426	81	230	125	a
0.1989	0.0099	2.177	0.022	0.0794	0.0041		1169	54	1174	7	1181	51	185	140	a
0.0478	0.0024	0.4222	0.0011	0.0641	0.0034		301	15	358	1	745	56	335	65	a
0.1675	0.0084	1.700	0.013	0.0736	0.0035		998	46	1009	5	1031	48	200	150	a
0.265	0.013	3.265	0.050	0.0894	0.0051		1514	68	1473	12	1413	55	220	125	a
0.0529	0.0026	0.4256	0.0015	0.0583	0.0038		332	16	360	1	541	71	240	100	a
0.1641	0.0082	1.667	0.013	0.0737	0.0035		980	46	996	5	1033	48	180	160	a
0.1573	0.0079	1.683	0.015	0.0776	0.0043		942	44	1002	6	1138	55	240	140	a
0.0208	0.0010	0.12195	0.00074	0.043	0.012		133	7	117	1	-193	366	305	145	a
0.202	0.010	2.115	0.021	0.0761	0.0037		1184	54	1154	7	1098	49	210	95	a
0.1878	0.0094	1.970	0.018	0.0761	0.0037		1109	51	1105	6	1097	49	180	115	a
0.227	0.011	2.852	0.038	0.0911	0.0053		1319	60	1369	10	1449	55	195	140	a
0.1833	0.0092	1.959	0.018	0.0775	0.0038		1085	50	1101	6	1134	49	150	110	a
0.1933	0.0097	2.089	0.022	0.0784	0.0042		1139	52	1145	7	1157	53	130	100	a
0.1790	0.0090	1.831	0.016	0.0742	0.0036		1062	49	1057	6	1046	49	240	145	a
0.0430	0.0021	0.3377	0.0011	0.0570	0.0043		271	13	295	1	491	83	190	120	a
0.1657	0.0083	1.910	0.027	0.0836	0.0071		988	46	1084	9	1283	83	270	160	a
0.1815	0.0091	1.925	0.017	0.0769	0.0038		1075	50	1090	6	1119	49	175	110	a
0.0314	0.0016	0.2397	0.0012	0.0554	0.0089		199	10	218	1	430	180	275	210	a
0.1971	0.0099	2.136	0.022	0.0786	0.0040		1160	53	1161	7	1163	51	240	155	a
0.0232	0.0012	0.15625	0.00016	0.0489	0.0022		148	7	147	0	141	52	175	160	a
0.201	0.010	2.166	0.022	0.0783	0.0039		1178	54	1170	7	1155	50	150	130	a
0.1892	0.0095	1.950	0.018	0.0747	0.0037		1117	51	1098	6	1061	50	245	100	a
0.0401	0.0020	0.28950	0.00042	0.0523	0.0019		254	12	258	0	299	42	170	130	a
0.1546	0.0077	1.517	0.011	0.0712	0.0032		927	43	937	4	962	46	180	150	a
0.00628	0.00031	0.04	0.00	0.044	0.015		40	2	38	0	-89	414	180	140	a
0.204	0.010	2.166	0.023	0.0771	0.0040		1196	55	1170	7	1123	52	185	155	a

$^{206}Pb^*/^{238}U$	± 2σ (abs)	$^{207}Pb^*/^{235}U$	± 2σ (abs)	$^{207}Pb^*/^{206}Pb^*$	± 2σ (abs)	corr. coef.	$^{206}Pb^*/^{238}U$ age (Ma)	± 2σ (Ma)	$^{207}Pb^*/^{235}U$ age (Ma)	± 2σ (Ma)	$^{207}Pb^*/^{206}Pb^*$ age (Ma)	± 2σ (Ma)	Length (μm)	Width (μm)	Accept/ Reject
0.0920	0.0046	0.9492	0.0043	0.0749	0.0037		567	27	678	2	1065	49	140	120	a
0.00962	0.00048	0.05950	0.00037	0.045	0.029		62	3	59	0	-63	791	225	120	a
0.1762	0.0088	1.834	0.016	0.0755	0.0037		1046	48	1058	6	1082	50	190	130	a
0.0420	0.0021	0.4049	0.0016	0.0699	0.0068		265	13	345	1	924	99	235	125	r
0.0374	0.0019	0.2819	0.0011	0.0547	0.0059		237	12	252	1	399	122	245	180	a
0.1910	0.0095	2.076	0.021	0.0789	0.0041		1127	52	1141	7	1169	51	170	100	a
0.222	0.011	3.391	0.054	0.1106	0.0079		1295	59	1502	12	1809	65	145	125	a
0.1902	0.0095	2.017	0.019	0.0769	0.0038		1123	52	1121	6	1118	49	300	150	a
0.0282	0.0014	0.19014	0.00028	0.0489	0.0026		179	9	177	0	142	61	145	100	a
0.0376	0.0019	0.2663	0.0016	0.0514	0.0083		238	12	240	1	259	186	255	130	a
0.308	0.015	4.79	0.11	0.1126	0.0081		1733	76	1783	19	1842	65	280	130	a
0.380	0.019	6.83	0.22	0.131	0.011		2074	89	2090	28	2105	73	155	130	a
0.376	0.019	6.96	0.22	0.134	0.011		2060	89	2106	29	2151	75	240	220	a
0.1846	0.0092	2.088	0.020	0.0820	0.0043		1092	50	1145	7	1246	52	155	90	a
0.253	0.013	4.507	0.094	0.129	0.011		1455	65	1732	18	2086	73	170	120	a
0.0244	0.0012	0.1430	0.0010	0.042	0.012		156	8	136	1	-200	365	220	125	a
0.1912	0.0096	2.448	0.028	0.0929	0.0055		1128	52	1257	8	1485	56	200	105	a
0.1881	0.0094	1.988	0.019	0.0766	0.0038		1111	51	1111	6	1112	50	160	155	a
0.1801	0.0090	1.925	0.018	0.0775	0.0039		1068	49	1090	6	1134	50	205	140	a
0.0265	0.0013	0.19406	0.00020	0.0531	0.0020		169	8	180	0	331	43	125	110	a
0.0391	0.0020	0.29037	0.00093	0.0538	0.0044		247	12	259	1	363	93	262	205	a
0.1839	0.0092	1.946	0.018	0.0767	0.0038		1088	50	1097	6	1114	50	285	110	a
0.0473	0.0024	0.34248	0.00060	0.0525	0.0020		298	15	299	0	308	42	270	125	a
0.1180	0.0059	1.2390	0.0071	0.0762	0.0037		719	34	818	3	1099	49	200	154	a
0.1865	0.0093	1.956	0.018	0.0761	0.0038		1102	51	1101	6	1098	50	330	145	a
0.240	0.012	2.914	0.037	0.0879	0.0047		1389	63	1386	10	1381	51	195	155	a
0.207	0.010	2.282	0.023	0.0799	0.0039		1213	56	1207	7	1195	48	270	120	a
0.0819	0.0041	0.6471	0.0020	0.0573	0.0021		507	24	507	1	504	40	275	140	a
0.1794	0.0090	1.829	0.015	0.0739	0.0033		1064	49	1056	5	1040	45	180	130	a
0.220	0.011	2.581	0.029	0.0852	0.0044		1280	58	1295	8	1320	50	165	155	a
0.1843	0.0092	1.890	0.016	0.0744	0.0033		1090	50	1078	6	1052	45	140	115	a
0.0231	0.0012	0.14790	0.00014	0.0464	0.0018		147	7	140	0	16	48	235	200	a
0.0290	0.0014	0.23319	0.00035	0.0584	0.0030		184	9	213	0	543	56	230	110	a
0.1101	0.0055	0.9392	0.0040	0.0619	0.0024		673	32	672	2	670	41	167	150	a
0.0322	0.0016	0.21857	0.00027	0.0493	0.0019		204	10	201	0	161	45	200	105	a
0.1919	0.0096	2.087	0.021	0.0789	0.0041		1131	52	1145	7	1170	51	175	85	a
0.0223	0.0011	0.16089	0.00017	0.0523	0.0025		142	7	151	0	300	54	170	160	a
0.0605	0.0030	0.6365	0.0021	0.0764	0.0041		378	18	500	1	1105	53	250	100	r
0.256	0.013	3.198	0.045	0.0907	0.0050		1468	66	1457	11	1441	53	210	175	a
0.0725	0.0036	0.5599	0.0020	0.0560	0.0027		451	22	451	1	452	53	180	115	a
0.0280	0.0014	0.20264	0.00028	0.0525	0.0026		178	9	187	0	306	57	175	145	a
0.1731	0.0087	1.706	0.013	0.0715	0.0031		1029	48	1011	5	972	44	200	155	a
0.1722	0.0086	1.762	0.014	0.0742	0.0034		1024	48	1032	5	1048	47	185	125	a
0.1898	0.0095	2.006	0.018	0.0767	0.0036		1120	52	1118	6	1113	46	210	185	a
0.0422	0.0021	0.29799	0.00042	0.0513	0.0017		266	13	265	0	252	38	215	125	a
0.1776	0.0089	1.853	0.018	0.0757	0.0041		1054	49	1064	6	1086	54	265	135	a
0.0291	0.0015	0.21342	0.00031	0.0531	0.0027		185	9	196	0	334	57	235	110	a
0.00	0.00	0.01	0.00	0.0594	0.0057		7	0	9	0	582	104	200	115	a
0.225	0.011	2.729	0.033	0.0880	0.0047		1308	59	1336	9	1382	51	280	105	a
0.0263	0.0013	0.20061	0.00042	0.0553	0.0044		167	8	186	0	424	89	240	140	a
0.1786	0.0089	1.824	0.015	0.0741	0.0034		1059	49	1054	5	1043	46	220	105	a

$^{206}Pb^*/^{238}U$	± 2σ (abs)	$^{207}Pb^*/^{235}U$	± 2σ (abs)	$^{207}Pb^*/^{206}Pb^*$	± 2σ (abs)	corr. coef.	$^{206}Pb^*/^{238}U$ age (Ma)	± 2σ (Ma)	$^{207}Pb^*/^{235}U$ age (Ma)	± 2σ (Ma)	$^{207}Pb^*/^{206}Pb^*$ age (Ma)	± 2σ (Ma)	Length (μm)	Width (μm)	Accept/ Reject
0.0244	0.0012	0.17152	0.00019	0.0510	0.0024		155	8	161	0	242	54	180	135	a
0.242	0.012	2.949	0.038	0.0883	0.0047		1399	63	1394	10	1388	51	150	115	a
0.1999	0.0100	2.154	0.021	0.0782	0.0038		1175	54	1166	7	1151	48	160	155	a
0.1633	0.0082	1.594	0.012	0.0708	0.0032		975	45	968	5	951	46	235	120	a
0.0396	0.0020	0.30561	0.00051	0.0560	0.0024		250	12	271	0	452	47	200	130	a
0.0553	0.0028	0.4053	0.0013	0.0532	0.0031		347	17	345	1	337	67	215	115	a
0.1783	0.0089	1.800	0.014	0.0732	0.0033		1057	49	1045	5	1020	45	250	125	a
0.1442	0.0072	1.3909	0.0091	0.0699	0.0032		869	41	885	4	927	46	205	125	a
0.1629	0.0081	1.614	0.011	0.0719	0.0031		973	45	976	4	982	44	145	125	a
0.1558	0.0078	1.537	0.010	0.0716	0.0031		934	44	945	4	973	44	275	135	a
0.206	0.010	2.269	0.023	0.0800	0.0039		1206	55	1203	7	1197	48	195	130	a
0.0699	0.0035	0.5301	0.0022	0.0550	0.0033		436	21	432	1	411	67	350	140	a
0.0889	0.0044	0.7267	0.0028	0.0593	0.0025		549	26	555	2	578	47	255	120	a
0.0524	0.0026	0.39732	0.00091	0.0550	0.0024		329	16	340	1	414	49	210	150	a
0.00771	0.00039	0.04817	0.00010	0.045	0.012		50	2	48	0	-40	333	240	120	a
0.1518	0.0076	1.510	0.010	0.0721	0.0032		911	43	935	4	990	44	195	130	a
0.0245	0.0012	0.17500	0.00030	0.0518	0.0037		156	8	164	0	276	81	240	120	a
6. Solimões River, Brazil (3.9256˚S, 62.8996˚W)															
0.186	0.032	3.49	0.67	0.137	0.013	0.831	1525	152	1097	177	2183	170	90	40	r
0.246	0.014	5.63	0.53	0.166	0.018	0.972	1921	81	1416	74	2520	182	90	60	r
0.248	0.015	5.41	0.33	0.1581	0.0042	0.884	1886	53	1428	76	2436	45	90	65	r
0.1796	0.0097	2.54	0.15	0.1028	0.0030	0.873	1285	42	1065	53	1675	53	150	70	a
0.1829	0.0099	2.54	0.14	0.1009	0.0027	0.886	1285	42	1083	54	1641	50	160	60	a
0.250	0.015	4.68	0.29	0.1355	0.0037	0.896	1764	51	1441	75	2171	48	115	100	a
0.1684	0.0087	2.12	0.12	0.0912	0.0025	0.879	1155	38	1003	48	1452	53	95	75	a
0.229	0.013	3.79	0.23	0.1200	0.0034	0.894	1590	49	1330	69	1956	50	100	45	a
0.333	0.021	8.64	0.57	0.1878	0.0050	0.904	2300	60	1855	101	2723	44	135	90	a
0.199	0.011	2.65	0.16	0.0966	0.0030	0.891	1315	45	1170	61	1559	58	135	60	a
0.272	0.016	4.83	0.30	0.1289	0.0034	0.913	1790	52	1549	81	2083	46	100	70	a
0.1749	0.0091	2.08	0.11	0.0864	0.0023	0.893	1143	37	1039	50	1347	52	165	75	a
0.196	0.011	2.53	0.15	0.0936	0.0027	0.898	1282	43	1156	59	1501	54	90	75	a
0.0827	0.0044	0.586	0.037	0.0513	0.0033	0.632	468	24	512	26	257	148	100	33	a
0.246	0.014	3.85	0.23	0.1134	0.0030	0.912	1604	49	1419	74	1855	48	115	45	a
0.217	0.013	3.00	0.19	0.1004	0.0027	0.914	1408	48	1265	68	1632	49	105	65	a
0.224	0.013	3.18	0.28	0.1028	0.0099	0.660	1452	68	1305	69	1675	179	95	60	a
0.217	0.012	2.98	0.17	0.0993	0.0026	0.909	1401	44	1268	63	1611	49	125	100	a
0.1789	0.0093	2.11	0.12	0.0857	0.0024	0.894	1153	38	1061	51	1331	53	135	80	a
0.218	0.012	2.98	0.18	0.0994	0.0026	0.910	1403	45	1270	65	1613	49	100	40	a
0.180	0.010	2.13	0.13	0.0856	0.0024	0.903	1158	42	1068	57	1330	54	70	55	a
0.01294	0.00053	0.0787	0.0047	0.0441	0.0040	0.231	77	4	83	3	-106	224	100	55	a
0.222	0.012	3.06	0.18	0.0999	0.0029	0.904	1423	45	1294	65	1623	53	11	85	a
0.230	0.013	3.24	0.19	0.1024	0.0027	0.913	1467	45	1332	67	1668	48	95	60	a
0.247	0.014	3.70	0.23	0.1088	0.0029	0.917	1571	49	1421	74	1779	48	150	110	a
0.0414	0.0023	0.272	0.043	0.048	0.014	0.740	244	34	262	15	78	701	130	45	a
0.375	0.027	9.45	0.71	0.1827	0.0048	0.928	2383	69	2054	126	2677	44	160	60	a
0.1517	0.0075	1.309	0.068	0.0626	0.0017	0.900	850	30	910	42	695	58	75	55	a
0.190	0.011	2.27	0.14	0.0866	0.0025	0.903	1202	42	1121	58	1351	55	125	60	a
0.0476	0.0020	0.320	0.019	0.0488	0.0039	0.836	282	14	300	13	138	185	240	70	a
0.0642	0.0028	0.452	0.026	0.0511	0.0038	0.883	379	18	401	17	244	172	200	70	a
0.1731	0.0088	1.92	0.10	0.0806	0.0024	0.885	1089	36	1029	48	1212	58	150	90	a
0.207	0.011	2.56	0.15	0.0898	0.0025	0.908	1289	43	1212	61	1421	53	130	70	a

$^{206}Pb^*/^{238}U$	± 2σ (abs)	$^{207}Pb^*/^{235}U$	± 2σ (abs)	$^{207}Pb^*/^{206}Pb^*$	± 2σ (abs)	corr. coef.	$^{206}Pb^*/^{238}U$ age (Ma)	± 2σ (Ma)	$^{207}Pb^*/^{235}U$ age (Ma)	± 2σ (Ma)	$^{207}Pb^*/^{206}Pb^*$ age (Ma)	± 2σ (Ma)	Length (μm)	Width (μm)	Accept/ Reject
0.234	0.013	3.18	0.19	0.0983	0.0026	0.918	1451	46	1357	70	1593	50	110	70	a
0.1139	0.0052	0.922	0.045	0.0587	0.0017	0.854	663	24	695	30	557	65	140	50	a
0.228	0.013	3.01	0.18	0.0958	0.0025	0.919	1409	46	1322	68	1544	50	110	65	a
0.263	0.017	3.91	0.26	0.1080	0.0029	0.929	1616	54	1503	86	1766	48	90	70	a
0.1392	0.0068	1.214	0.062	0.0632	0.0018	0.885	807	29	840	38	716	60	145	70	a
0.1061	0.0048	0.855	0.046	0.0584	0.0030	0.714	627	25	650	28	545	113	165	70	a
0.1207	0.0058	1.013	0.052	0.0608	0.0018	0.867	710	26	735	33	634	63	80	70	a
0.1738	0.0089	1.87	0.10	0.0781	0.0021	0.898	1071	36	1033	49	1149	54	155	80	a
0.1680	0.0086	1.774	0.095	0.0766	0.0020	0.900	1036	35	1001	48	1110	53	90	55	a
0.0363	0.0015	0.246	0.011	0.0492	0.0017	0.879	223	9	230	9	156	79	250	70	a
0.1383	0.0068	1.226	0.065	0.0643	0.0023	0.855	812	30	835	38	751	74	110	80	a
0.389	0.026	8.37	0.59	0.1561	0.0041	0.937	2272	64	2118	122	2414	44	85	50	a
0.445	0.034	11.61	0.92	0.1894	0.0050	0.941	2573	74	2371	151	2737	43	105	40	a
0.191	0.011	2.13	0.15	0.0811	0.0041	0.848	1158	48	1124	62	1223	100	90	60	a
0.1032	0.0047	0.838	0.040	0.0589	0.0016	0.847	618	22	633	27	563	61	140	55	a
0.195	0.011	2.19	0.13	0.0817	0.0022	0.914	1179	40	1147	58	1238	52	65	55	a
0.1214	0.0060	1.037	0.058	0.0619	0.0026	0.807	722	29	739	35	672	91	70	65	a
0.1686	0.0085	1.749	0.094	0.0753	0.0021	0.893	1027	35	1004	47	1076	57	70	55	a
0.1183	0.0055	1.007	0.055	0.0617	0.0029	0.764	707	28	721	32	665	102	260	50	a
0.0610	0.0026	0.446	0.020	0.0531	0.0016	0.706	375	14	381	16	333	70	175	75	a
0.229	0.013	2.79	0.16	0.0884	0.0023	0.923	1352	44	1328	67	1392	51	105	80	a
0.273	0.016	3.78	0.24	0.1006	0.0028	0.926	1589	50	1554	81	1635	53	75	50	a
0.209	0.012	2.40	0.14	0.0833	0.0023	0.918	1244	43	1224	63	1277	54	101	65	a
0.214	0.012	2.48	0.15	0.0844	0.0022	0.921	1267	42	1248	63	1301	51	105	55	a
0.202	0.011	2.25	0.13	0.0811	0.0022	0.918	1198	42	1184	61	1223	53	105	50	a
0.367	0.023	6.54	0.45	0.1294	0.0039	0.932	2052	60	2014	111	2090	53	125	50	a
0.0655	0.0029	0.493	0.029	0.0545	0.0040	0.891	407	20	409	18	393	163	130	65	a
0.206	0.012	2.31	0.14	0.0814	0.0024	0.916	1215	43	1207	64	1230	57	90	65	a
0.202	0.011	2.24	0.13	0.0803	0.0021	0.919	1193	41	1186	60	1204	53	105	75	a
0.1796	0.0095	1.87	0.10	0.0754	0.0021	0.908	1070	37	1065	52	1080	55	160	60	a
0.241	0.014	2.97	0.18	0.0893	0.0025	0.926	1401	47	1394	74	1411	54	75	60	a
0.269	0.016	3.56	0.22	0.0961	0.0028	0.925	1542	49	1536	80	1549	55	180	65	a
0.251	0.014	3.16	0.19	0.0913	0.0025	0.927	1448	47	1444	75	1453	52	90	50	a
0.187	0.010	1.98	0.11	0.0766	0.0021	0.912	1109	39	1108	55	1111	55	115	60	a
0.1783	0.0093	1.83	0.10	0.0746	0.0021	0.905	1058	36	1058	51	1057	56	130	45	a
0.282	0.018	3.84	0.25	0.0987	0.0030	0.929	1602	53	1602	88	1600	57	80	70	a
0.288	0.017	3.97	0.25	0.1000	0.0027	0.935	1628	51	1630	86	1625	50	95	65	a
0.1582	0.0081	1.543	0.085	0.0707	0.0023	0.878	948	34	947	45	950	67	90	55	a
0.232	0.013	2.75	0.16	0.0860	0.0023	0.927	1341	45	1343	69	1338	52	130	85	a
0.1678	0.0086	1.671	0.090	0.0722	0.0019	0.905	998	34	1000	48	992	54	110	55	a
0.352	0.025	5.68	0.42	0.1171	0.0031	0.949	1928	64	1943	120	1913	47	70	50	a
0.0498	0.0021	0.363	0.017	0.0528	0.0016	0.645	314	12	313	13	321	68	155	70	a
0.199	0.011	2.15	0.13	0.0784	0.0024	0.906	1165	41	1170	59	1156	61	70	50	a
0.0422	0.0018	0.302	0.014	0.0518	0.0016	0.546	268	11	266	11	278	70	135	70	a
0.279	0.016	3.72	0.23	0.0964	0.0026	0.935	1575	49	1589	83	1556	50	100	80	a
0.228	0.013	2.64	0.16	0.0839	0.0023	0.925	1311	44	1324	68	1291	53	80	55	a
0.180	0.010	1.83	0.11	0.0739	0.0022	0.909	1057	40	1066	56	1040	60	145	75	a
0.1789	0.0097	1.82	0.10	0.0737	0.0020	0.913	1052	37	1061	53	1034	54	100	80	a
0.236	0.015	2.79	0.21	0.0855	0.0057	0.836	1352	57	1367	76	1328	128	95	70	a
0.241	0.014	2.87	0.17	0.0865	0.0023	0.931	1375	45	1393	71	1348	51	115	70	a
0.352	0.022	5.50	0.36	0.1135	0.0030	0.944	1901	57	1943	105	1856	48	80	65	a

$^{206}Pb^*/^{238}U$	± 2σ (abs)	$^{207}Pb^*/^{235}U$	± 2σ (abs)	$^{207}Pb^*/^{206}Pb^*$	± 2σ (abs)	corr. coef.	$^{206}Pb^*/^{238}U$ age (Ma)	± 2σ (Ma)	$^{207}Pb^*/^{235}U$ age (Ma)	± 2σ (Ma)	$^{207}Pb^*/^{206}Pb^*$ age (Ma)	± 2σ (Ma)	Length (μm)	Width (μm)	Accept/ Reject
0.1060	0.0050	0.907	0.046	0.0620	0.0020	0.824	655	25	650	29	675	69	130	75	a
0.0949	0.0046	0.787	0.040	0.0601	0.0017	0.840	589	23	584	27	609	60	115	70	a
0.1085	0.0050	0.934	0.046	0.0625	0.0020	0.825	670	24	664	29	690	68	135	65	a
0.0436	0.0018	0.315	0.014	0.0523	0.0017	0.532	278	11	275	11	299	73	115	85	a
0.227	0.013	2.59	0.17	0.0828	0.0038	0.875	1298	47	1318	67	1266	90	140	60	a
0.01078	0.00059	0.071	0.018	0.048	0.024	*	70	17	69	4	99	1182	125	75	a
0.1451	0.0071	1.391	0.076	0.0695	0.0029	0.824	885	32	874	40	913	85	190	60	a
0.197	0.011	2.06	0.12	0.0757	0.0020	0.923	1136	41	1161	60	1088	54	95	55	a
0.0346	0.0014	0.246	0.011	0.0515	0.0014	0.458	223	9	219	9	263	64	115	55	a
0.211	0.012	2.28	0.13	0.0782	0.0021	0.926	1206	41	1236	63	1153	52	90	75	a
0.0684	0.0030	0.533	0.025	0.0566	0.0016	0.763	434	16	426	18	474	61	90	50	a
0.1635	0.0082	1.662	0.087	0.0737	0.0020	0.896	994	33	976	45	1034	55	100	80	a
0.0716	0.0031	0.564	0.029	0.0571	0.0028	0.549	454	19	446	19	497	108	85	65	a
0.210	0.012	2.25	0.13	0.0777	0.0021	0.926	1197	42	1230	64	1139	53	110	70	a
0.283	0.017	3.54	0.22	0.0908	0.0024	0.940	1535	49	1604	84	1442	50	125	80	a
0.199	0.011	2.06	0.12	0.0749	0.0020	0.922	1135	39	1171	59	1067	53	105	65	a
0.131	0.011	1.22	0.14	0.0679	0.0091	0.607	811	64	792	63	864	278	60	40	a
0.0498	0.0021	0.372	0.017	0.0542	0.0015	0.653	321	12	313	13	378	63	85	55	a
0.1135	0.0052	1.013	0.049	0.0647	0.0017	0.856	711	25	693	30	766	57	90	55	a
0.1640	0.0084	1.689	0.091	0.0747	0.0020	0.898	1004	34	979	46	1060	54	120	80	a
0.253	0.015	2.91	0.19	0.0835	0.0028	0.920	1385	48	1454	77	1281	66	75	70	a
0.02046	0.00084	0.1415	0.0072	0.0501	0.0030	0.663	134	6	131	5	201	141	115	65	a
0.1245	0.0060	1.153	0.059	0.0672	0.0021	0.845	779	28	756	34	843	66	120	75	a
0.0479	0.0021	0.358	0.016	0.0542	0.0016	0.622	311	12	302	13	379	66	205	70	a
0.0942	0.0042	0.802	0.038	0.0617	0.0018	0.810	598	21	580	25	665	63	160	100	a
0.1581	0.0084	1.621	0.090	0.0743	0.0020	0.897	978	35	946	47	1050	55	155	75	a
0.253	0.015	2.83	0.17	0.0813	0.0021	0.939	1364	46	1452	76	1228	51	100	50	a
0.233	0.013	2.51	0.15	0.0782	0.0021	0.933	1274	43	1348	69	1152	53	105	65	a
0.0672	0.0029	0.533	0.029	0.0575	0.0036	0.901	434	19	420	18	512	138	95	65	a
0.1575	0.0081	1.616	0.087	0.0744	0.0020	0.897	977	34	943	45	1053	53	130	60	a
0.0384	0.0016	0.282	0.013	0.0532	0.0021	0.870	252	10	243	10	339	90	130	145	a
0.0820	0.0037	0.684	0.041	0.0605	0.0044	0.913	529	25	508	22	620	157	105	70	a
0.0380	0.0016	0.280	0.015	0.0534	0.0035	0.815	250	12	240	10	346	148	155	80	a
0.0753	0.0033	0.616	0.028	0.0594	0.0017	0.769	487	18	468	20	581	62	135	75	a
0.1014	0.0049	0.896	0.048	0.0641	0.0027	0.756	650	26	623	28	744	88	140	60	a
0.0575	0.0025	0.449	0.021	0.0566	0.0017	0.681	376	15	361	15	475	66	85	70	a
0.1525	0.0075	1.562	0.081	0.0743	0.0021	0.878	955	32	915	42	1049	58	115	65	a
0.0643	0.0028	0.512	0.024	0.0578	0.0016	0.739	420	16	402	17	521	61	95	65	a
0.1546	0.0076	1.597	0.083	0.0750	0.0021	0.882	969	33	926	43	1067	57	130	100	a
0.1094	0.0060	0.994	0.082	0.0659	0.0074	0.927	701	42	669	35	804	236	115	80	a
0.1505	0.0075	1.544	0.082	0.0744	0.0021	0.882	948	33	904	42	1053	56	120	60	a
0.245	0.014	2.56	0.15	0.0759	0.0021	0.936	1289	43	1411	72	1093	54	75	60	a
0.1559	0.0077	1.627	0.084	0.0757	0.0020	0.887	981	33	934	43	1087	54	165	80	a
0.1590	0.0087	1.677	0.096	0.0765	0.0021	0.895	1000	37	951	49	1108	56	115	70	a
0.0329	0.0014	0.241	0.011	0.0533	0.0017	0.876	220	9	208	9	340	72	130	90	a
0.0448	0.0019	0.343	0.020	0.0554	0.0042	0.830	299	15	283	12	429	170	115	75	a
0.220	0.015	2.14	0.17	0.0706	0.0040	0.888	1162	55	1282	80	946	116	90	55	a
0.1414	0.0068	1.443	0.074	0.0740	0.0021	0.869	907	31	852	38	1042	57	180	75	a
0.1675	0.0085	1.846	0.098	0.0800	0.0021	0.894	1062	35	998	47	1196	52	120	80	a
0.0632	0.0027	0.513	0.024	0.0589	0.0017	0.704	421	16	395	17	565	64	100	55	a
0.0508	0.0022	0.400	0.019	0.0571	0.0023	0.902	341	14	319	13	494	90	190	95	a

$^{206}Pb^*/^{238}U$	± 2σ (abs)	$^{207}Pb^*/^{235}U$	± 2σ (abs)	$^{207}Pb^*/^{206}Pb^*$	± 2σ (abs)	corr. coef.	$^{206}Pb^*/^{238}U$ age (Ma)	± 2σ (Ma)	$^{207}Pb^*/^{235}U$ age (Ma)	± 2σ (Ma)	$^{207}Pb^*/^{206}Pb^*$ age (Ma)	± 2σ (Ma)	Length (μm)	Width (μm)	Accept/ Reject
0.1514	0.0077	1.604	0.086	0.0768	0.0022	0.878	972	34	909	43	1117	57	80	50	a
0.1279	0.0061	1.267	0.064	0.0718	0.0019	0.866	831	29	776	35	982	54	105	60	a
0.0939	0.0043	0.843	0.043	0.0651	0.0025	0.741	621	24	579	26	777	81	145	60	a
0.0446	0.0020	0.351	0.018	0.0570	0.0025	0.888	305	13	281	12	490	95	90	50	a
0.1415	0.0069	1.498	0.077	0.0768	0.0021	0.873	929	31	853	39	1115	54	95	50	a
0.1610	0.0080	1.815	0.096	0.0817	0.0024	0.873	1051	35	963	44	1239	58	140	70	a
0.1337	0.0064	1.393	0.078	0.0756	0.0037	0.746	886	33	809	36	1084	98	135	70	a
0.0207	0.0026	0.154	0.020	0.0537	0.0026	0.462	145	18	132	17	360	110	195	90	a
0.1434	0.0069	1.573	0.080	0.0796	0.0022	0.864	960	31	864	39	1187	55	130	75	a
0.0355	0.0015	0.280	0.015	0.0571	0.0035	0.810	250	12	225	9	496	137	110	88	a
0.1234	0.0059	1.280	0.066	0.0753	0.0026	0.813	837	29	750	34	1076	68	110	95	a
0.1584	0.0079	1.84	0.10	0.0844	0.0030	0.840	1061	36	948	44	1301	69	75	60	a
0.0542	0.0023	0.456	0.027	0.0611	0.0048	0.858	381	19	340	14	641	168	115	75	a
0.0401	0.0018	0.324	0.023	0.0587	0.0063	0.779	285	17	253	11	555	234	170	70	a
0.00916	0.00041	0.068	0.011	0.053	0.018	*	66	11	59	3	349	751	105	85	a
0.01151	0.00047	0.0856	0.0087	0.054	0.010	*	83	8	74	3	368	433	150	90	a
0.0375	0.0016	0.303	0.014	0.0585	0.0020	0.885	268	11	237	10	549	75	155	75	a
0.0375	0.0016	0.303	0.023	0.0587	0.0076	0.744	269	18	237	10	557	281	115	60	a
0.0320	0.0013	0.255	0.015	0.0578	0.0050	0.739	231	12	203	8	521	192	160	80	a
0.0693	0.0031	0.626	0.041	0.0655	0.0060	0.883	493	26	432	19	790	192	110	55	a
0.0945	0.0044	0.930	0.055	0.0714	0.0047	0.931	668	29	582	26	968	134	115	100	a
0.00969	0.00044	0.073	0.012	0.054	0.018	*	71	11	62	3	390	727	85	72	a
0.1283	0.0064	1.412	0.095	0.0798	0.0061	0.518	894	40	778	36	1193	152	135	40	a
0.00788	0.00058	0.059	0.021	0.054	0.038	*	58	20	51	4	382	1592	140	70	a
0.0599	0.0026	0.530	0.026	0.0642	0.0027	0.916	432	17	375	16	748	89	85	75	a
0.0477	0.0023	0.409	0.021	0.0622	0.0022	0.492	348	15	300	14	681	77	130	60	a
0.0878	0.0040	0.888	0.043	0.0733	0.0023	0.747	645	23	543	23	1023	62	80	40	a
0.0783	0.0042	0.768	0.051	0.0711	0.0051	0.919	578	29	486	25	960	147	175	50	a
0.00399	0.00016	0.0308	0.0022	0.0560	0.0066	*	31	2	26	1	453	262	155	85	a
0.0470	0.0021	0.422	0.027	0.0650	0.0060	0.825	357	20	296	13	775	195	105	80	a
0.0552	0.0026	0.517	0.033	0.0679	0.0056	0.865	423	22	346	16	865	170	150	45	a
0.0543	0.0024	0.512	0.028	0.0684	0.0044	0.876	420	19	341	15	881	134	350	40	a
0.0793	0.0035	0.842	0.041	0.0770	0.0028	0.611	620	22	492	21	1121	74	95	60	a
0.0452	0.0020	0.431	0.022	0.0692	0.0035	0.874	364	16	285	12	903	104	145	55	a
0.1175	0.0056	1.490	0.077	0.0920	0.0032	0.752	926	31	716	32	1467	65	135	55	a
0.0492	0.0021	0.492	0.028	0.0726	0.0049	0.858	406	19	309	13	1001	138	110	70	r
0.1199	0.0056	1.586	0.079	0.0960	0.0028	0.784	965	31	730	32	1547	55	150	60	r
0.1232	0.0067	1.76	0.10	0.1039	0.0032	0.799	1033	37	749	38	1695	56	110	55	r
0.01536	0.00068	0.1475	0.0083	0.0696	0.0049	0.514	140	7	98	4	918	144	210	50	r
0.1565	0.0089	2.83	0.17	0.1312	0.0039	0.815	1364	45	938	49	2114	53	150	95	r
0.0975	0.0059	1.418	0.089	0.1055	0.0029	0.792	896	37	599	34	1723	50	95	55	r
0.1135	0.0054	1.845	0.094	0.1179	0.0036	0.702	1062	34	693	31	1924	55	140	70	r
0.00405	0.00024	0.0410	0.0099	0.073	0.035	*	41	10	26	2	1025	973	155	50	r
0.00796	0.00036	0.082	0.010	0.075	0.018	*	80	10	51	2	1068	481	180	80	r
0.00455	0.00019	0.0471	0.0033	0.0751	0.0086	*	47	3	29	1	1071	230	95	65	r
0.0570	0.0034	0.758	0.051	0.0965	0.0048	0.925	573	29	357	21	1557	93	170	60	r
0.0580	0.0026	0.784	0.061	0.098	0.012	0.844	587	35	363	16	1588	228	105	50	r
0.1463	0.0084	3.37	0.29	0.167	0.018	0.950	1497	68	880	47	2528	183	170	75	r
0.00431	0.00029	0.0561	0.0076	0.094	0.023	*	55	7	28	2	1517	454	110	85	r
0.01158	0.00053	0.242	0.018	0.152	0.018	0.087	220	15	74	3	2365	199	220	65	r
0.01195	0.00064	0.282	0.031	0.171	0.033	*	252	25	77	4	2569	323	75	60	r

$^{206}Pb^*/^{238}U$	± 2σ (abs)	$^{207}Pb^*/^{235}U$	± 2σ (abs)	$^{207}Pb^*/^{206}Pb^*$	± 2σ (abs)	corr. coef.	$^{206}Pb^*/^{238}U$ age (Ma)	± 2σ (Ma)	$^{207}Pb^*/^{235}U$ age (Ma)	± 2σ (Ma)	$^{207}Pb^*/^{206}Pb^*$ age (Ma)	± 2σ (Ma)	Length (μm)	Width (μm)	Accept/ Reject
7. Solimões River, Brazil (3.7891°S, 62.2238°W)															
0.00898	0.00047	0.015	0.028	0.012	0.026	0.234	15	28	58	3			165	150	r
0.00976	0.00056	0.018	0.029	0.013	0.024	0.327	18	29	63	4			335	100	r
0.0276	0.0014	0.053	0.022	0.0140	0.0055		53	21	176	9			169	91	r
0.01463	0.00073	0.030	0.017	0.0148	0.0082		30	16	94	5			330	62	r
0.001648	0.000082	0.004	0.015	0.018	0.066		4	15	11	1			320	105	r
0.00590	0.00048	0.018	0.020	0.022	0.029		18	20	38	3			300	100	r
0.01922	0.00096	0.078	0.017	0.0293	0.0064		76	16	123	6			168	127	r
0.0505	0.0025	0.317	0.027	0.0455	0.0037		279	21	318	16			272	99	a
0.248	0.015	4.22	0.30	0.1232	0.0033	0.922	1678	59	1430	80	2004	47	130	100	a
0.0292	0.0012	0.176	0.024	0.0438	0.0064	0.810	165	21	186	8			150	75	a
0.0274	0.0014	0.169	0.013	0.0446	0.0035		158	12	174	9			260	63	a
0.1720	0.0087	2.00	0.15	0.0844	0.0038	0.836	1116	50	1023	48	1302	88	140	150	a
0.210	0.012	2.83	0.18	0.0977	0.0026	0.918	1364	49	1231	62	1580	49	165	110	a
0.1462	0.0072	1.211	0.096	0.0601	0.0034	0.820	806	44	879	40	607	123	265	85	a
0.00351	0.00016	0.0208	0.0067	0.043	0.016		21	7	23	1			154	135	a
0.0945	0.0047	0.702	0.072	0.0539	0.0047		540	43	582	28	365	198	160	112	a
0.0616	0.0031	0.423	0.042	0.0498	0.0046		358	30	385	19	185	216	252	103	a
0.0427	0.0017	0.280	0.033	0.0475	0.0060	0.872	250	26	269	10	76	299	135	115	a
0.0342	0.0014	0.223	0.029	0.0472	0.0066	0.838	204	24	217	9	57	334	130	130	a
0.240	0.013	3.34	0.22	0.1011	0.0028	0.923	1492	52	1386	70	1644	51	195	95	a
0.0482	0.0024	0.333	0.015	0.0501	0.0020		292	11	304	15	197	93	253	168	a
0.0292	0.0015	0.192	0.018	0.0477	0.0043		179	15	186	9	86	215	287	111	a
0.0232	0.0011	0.151	0.048	0.047	0.017	0.746	143	42	148	7	59	870	340	85	a
0.1711	0.0083	1.83	0.12	0.0775	0.0028	0.873	1055	43	1018	46	1133	72	300	105	a
0.1712	0.0093	1.83	0.11	0.0775	0.0021	0.915	1055	41	1018	51	1133	53	135	105	a
0.0305	0.0011	0.204	0.016	0.0484	0.0039	0.828	188	14	194	7	120	190	285	185	a
0.0398	0.0020	0.273	0.018	0.0496	0.0030		245	14	252	12	178	143	298	139	a
0.0318	0.0013	0.213	0.042	0.049	0.011	0.821	196	35	202	8	133	516	150	150	a
0.0421	0.0021	0.292	0.016	0.0503	0.0026		260	12	266	13	207	118	248	105	a
0.0465	0.0023	0.326	0.016	0.0509	0.0022		287	12	293	14	238	102	190	80	a
0.0313	0.0012	0.211	0.013	0.0490	0.0029	0.848	194	11	198	7	146	138	265	100	a
0.0432	0.0022	0.302	0.016	0.0507	0.0025		268	12	272	13	226	112	370	77	a
0.0423	0.0021	0.296	0.013	0.0506	0.0021		263	10	267	13	223	97	239	114	a
0.0497	0.0022	0.354	0.045	0.0516	0.0066	0.896	308	34	313	14	269	295	200	150	a
0.225	0.011	2.55	0.17	0.0822	0.0032		1285	48	1306	59	1250	76	152	74	a
0.0231	0.0010	0.1536	0.0087	0.0483	0.0019	0.843	145	8	147	6	113	94	130	70	a
0.0654	0.0026	0.487	0.035	0.0540	0.0035	0.481	403	24	408	16	373	147	195	95	a
0.0413	0.0017	0.289	0.048	0.0508	0.0094	0.863	258	38	261	10	232	426	220	125	a
0.0467	0.0018	0.332	0.023	0.0516	0.0033	0.899	291	18	294	11	267	146	245	100	a
0.0529	0.0024	0.383	0.045	0.0525	0.0063	0.901	329	33	332	15	306	272	235	135	a
0.0490	0.0024	0.352	0.017	0.0521	0.0023		306	13	308	15	291	100	153	131	a
0.0450	0.0017	0.320	0.018	0.0516	0.0022	0.497	282	14	284	11	266	99	260	125	a
0.0340	0.0013	0.235	0.011	0.0501	0.0015	0.518	214	9	215	8	198	71	170	130	a
0.0536	0.0027	0.390	0.019	0.0528	0.0024	0.000	334	14	336	16	321	102	258	92	a
0.0460	0.0019	0.330	0.016	0.0521	0.0015	0.688	290	12	290	12	288	65	205	85	a
0.0421	0.0021	0.299	0.014	0.0516	0.0023		266	11	266	13	267	103	255	109	a
0.0471	0.0018	0.339	0.015	0.0523	0.0015	0.660	297	12	296	11	298	66	235	80	a
0.0419	0.0021	0.298	0.013	0.0516	0.0020	0.000	265	10	265	13	266	91	207	108	a
0.01699	0.00074	0.113	0.015	0.0483	0.0068	0.672	109	13	109	5	114	333	185	150	a
0.01408	0.00053	0.0931	0.0094	0.0479	0.0052	0.607	90	9	90	3	96	258	185	110	a

$^{206}Pb^*/^{238}U$	± 2σ (abs)	$^{207}Pb^*/^{235}U$	± 2σ (abs)	$^{207}Pb^*/^{206}Pb^*$	± 2σ (abs)	corr. coef.	$^{206}Pb^*/^{238}U$ age (Ma)	± 2σ (Ma)	$^{207}Pb^*/^{235}U$ age (Ma)	± 2σ (Ma)	$^{207}Pb^*/^{206}Pb^*$ age (Ma)	± 2σ (Ma)	Length (μm)	Width (μm)	Accept/ Reject
0.0376	0.0019	0.265	0.017	0.0512	0.0031		239	13	238	12	248	138	167	105	a
0.0725	0.0036	0.564	0.029	0.0564	0.0026		454	19	451	22	467	101	211	126	a
0.1685	0.0098	1.67	0.11	0.0719	0.0020	0.923	997	42	1004	54	983	56	115	95	a
0.0414	0.0021	0.296	0.015	0.0519	0.0025		263	12	262	13	280	109	168	127	a
0.186	0.011	1.92	0.13	0.0748	0.0022	0.920	1088	46	1100	57	1064	60	200	70	a
0.0521	0.0020	0.385	0.019	0.0535	0.0018	0.641	331	14	328	12	352	76	200	90	a
0.0505	0.0019	0.372	0.023	0.0534	0.0028	0.911	321	17	318	12	344	120	205	125	a
0.0471	0.0018	0.344	0.019	0.0529	0.0023	0.506	300	14	297	11	325	98	215	135	a
0.1059	0.0053	0.908	0.045	0.0622	0.0025		656	24	649	31	682	85	194	125	a
0.0626	0.0031	0.477	0.047	0.0553	0.0050		396	32	391	19	424	202	229	59	a
0.0520	0.0023	0.386	0.023	0.0538	0.0022	0.621	331	17	327	14	361	94	195	125	a
0.1150	0.0058	1.015	0.056	0.0640	0.0028		711	28	702	33	740	93	317	87	a
0.1230	0.0062	1.110	0.060	0.0654	0.0027		758	29	748	35	788	88	191	101	a
0.0446	0.0017	0.325	0.017	0.0528	0.0021	0.532	286	13	282	11	320	89	160	100	a
0.0507	0.0019	0.376	0.018	0.0537	0.0018	0.640	324	13	319	12	359	74	200	150	a
0.0440	0.0017	0.320	0.015	0.0527	0.0017	0.596	282	12	278	10	318	74	150	115	a
0.01015	0.00047	0.067	0.020	0.048	0.017	0.412	66	19	65	3	106	818	210	130	a
0.0417	0.0017	0.302	0.015	0.0525	0.0017	0.608	268	11	263	10	308	72	195	120	a
0.0402	0.0015	0.290	0.015	0.0523	0.0020	0.498	258	12	254	9	300	86	210	135	a
0.0614	0.0024	0.471	0.023	0.0555	0.0017	0.726	392	16	384	14	434	67	115	95	a
0.0273	0.0013	0.191	0.022	0.0506	0.0061	0.802	177	19	174	8	223	280	185	85	a
0.0404	0.0020	0.293	0.014	0.0525	0.0023		261	11	255	13	308	100	126	90	a
0.0644	0.0029	0.498	0.039	0.0562	0.0038	0.495	411	26	402	17	459	151	180	100	a
0.0976	0.0040	0.830	0.049	0.0617	0.0027	0.745	614	27	600	23	662	92	220	105	a
0.0386	0.0015	0.279	0.013	0.0524	0.0015	0.610	250	10	244	9	302	63	255	95	a
0.1757	0.0088	1.87	0.11	0.0770	0.0030		1069	41	1044	48	1120	77	133	87	a
0.1136	0.0048	1.013	0.051	0.0647	0.0018	0.857	710	26	694	28	764	58	250	105	a
0.0421	0.0016	0.308	0.021	0.0530	0.0033	0.887	273	16	266	10	329	142	250	120	a
0.1444	0.0072	1.407	0.079	0.0706	0.0029		892	33	870	41	947	84	163	96	a
0.0473	0.0018	0.351	0.017	0.0538	0.0019	0.597	306	13	298	11	364	78	210	110	a
0.1352	0.0068	1.284	0.069	0.0689	0.0028		839	30	818	39	895	82	190	110	a
0.0635	0.0035	0.495	0.036	0.0566	0.0029	0.675	408	25	397	21	474	114	175	85	a
0.0441	0.0017	0.326	0.022	0.0536	0.0033	0.894	287	17	278	10	356	140	205	145	a
0.1760	0.0088	1.89	0.12	0.0778	0.0030		1077	41	1045	48	1142	76	167	120	a
0.0450	0.0018	0.334	0.016	0.0539	0.0017	0.616	293	12	284	11	365	72	235	145	a
0.1712	0.0086	1.83	0.11	0.0775	0.0030		1056	39	1019	47	1133	76	252	77	a
0.0395	0.0020	0.290	0.015	0.0533	0.0025		259	12	250	12	342	106	152	84	a
0.1559	0.0081	1.60	0.10	0.0742	0.0024	0.885	969	40	934	45	1048	66	150	120	a
0.0473	0.0019	0.356	0.022	0.0546	0.0030	0.907	309	17	298	12	397	122	205	125	a
0.00505	0.00025	0.0338	0.0059	0.0486	0.0095		34	6	32	2	127	461	130	110	a
0.0296	0.0015	0.213	0.011	0.0521	0.0025		196	9	188	9	288	111	265	117	a
0.0658	0.0029	0.524	0.031	0.0578	0.0022	0.711	428	20	411	18	521	84	175	90	a
0.1419	0.0064	1.406	0.093	0.0719	0.0033	0.808	891	39	855	36	982	92	180	120	a
0.00277	0.00016	0.0185	0.0044	0.048	0.013		19	4	18	1	117	646	255	110	a
0.02424	0.00089	0.1720	0.0090	0.0515	0.0022	0.827	161	8	154	6	262	98	290	120	a
0.00922	0.00058	0.063	0.034	0.049	0.029	0.388	62	32	59	4	166	1388	285	95	a
0.0582	0.0025	0.456	0.032	0.0568	0.0035	0.924	381	23	365	15	483	136	235	125	a
0.1528	0.0083	1.57	0.16	0.0745	0.0059	0.736	958	65	916	46	1056	160	175	95	a
0.1531	0.0070	1.582	0.096	0.0749	0.0027	0.855	963	38	918	39	1066	73	210	105	a
0.0285	0.0015	0.206	0.029	0.0525	0.0079	0.810	190	25	181	10	308	342	205	100	a
0.1183	0.0059	1.114	0.057	0.0683	0.0027		760	27	721	34	878	83	156	102	a

$^{206}Pb^*/^{238}U$	± 2σ (abs)	$^{207}Pb^*/^{235}U$	± 2σ (abs)	$^{207}Pb^*/^{206}Pb^*$	± 2σ (abs)	corr. coef.	$^{206}Pb^*/^{238}U$ age (Ma)	± 2σ (Ma)	$^{207}Pb^*/^{235}U$ age (Ma)	± 2σ (Ma)	$^{207}Pb^*/^{206}Pb^*$ age (Ma)	± 2σ (Ma)	Length (μm)	Width (μm)	Accept/ Reject
0.1502	0.0070	1.553	0.087	0.0750	0.0021	0.888	952	35	902	39	1068	55	140	105	a
0.0352	0.0013	0.261	0.015	0.0537	0.0027	0.875	236	12	223	8	360	112	250	125	a
0.1517	0.0076	1.579	0.090	0.0755	0.0030		962	36	911	43	1081	81	208	100	a
0.1431	0.0072	1.461	0.085	0.0740	0.0031		914	35	862	40	1042	86	215	96	a
0.0426	0.0016	0.325	0.020	0.0553	0.0029	0.894	286	15	269	10	423	118	150	140	a
0.0332	0.0014	0.246	0.034	0.0539	0.0080	0.831	224	27	210	9	366	336	170	85	a
0.1442	0.0064	1.490	0.079	0.0749	0.0020	0.882	926	32	868	36	1066	54	195	150	a
0.0403	0.0016	0.307	0.038	0.0552	0.0074	0.863	272	30	254	10	421	299	190	140	a
0.0698	0.0035	0.580	0.034	0.0603	0.0031		465	22	435	21	613	112	224	125	a
0.0372	0.0019	0.281	0.063	0.055	0.012		251	50	235	12	405	483	249	210	a
0.1525	0.0076	1.619	0.090	0.0770	0.0030		978	35	915	43	1122	78	114	96	a
0.1551	0.0071	1.661	0.090	0.0777	0.0021	0.890	994	34	929	40	1140	53	230	125	a
0.0418	0.0016	0.321	0.020	0.0557	0.0030	0.893	283	15	264	10	440	118	180	105	a
0.0397	0.0015	0.303	0.016	0.0554	0.0023	0.899	269	13	251	9	428	93	170	145	a
0.0348	0.0014	0.263	0.023	0.0548	0.0048	0.851	237	18	220	9	405	195	295	80	a
0.1550	0.0072	1.690	0.092	0.0791	0.0021	0.889	1005	35	929	40	1175	52	240	100	a
0.1394	0.0071	1.459	0.084	0.0759	0.0020	0.892	913	35	841	40	1092	53	195	115	a
0.1704	0.0085	1.98	0.12	0.0842	0.0032		1108	40	1014	47	1297	75	261	78	a
0.1510	0.0075	1.655	0.090	0.0795	0.0031		991	34	906	42	1184	76	177	113	a
0.00500	0.00018	0.0352	0.0031	0.0511	0.0048		35	3	32	1	246	218	215	110	a
0.0892	0.0042	0.811	0.068	0.0659	0.0045	0.598	603	38	551	25	803	143	220	100	a
0.00392	0.00020	0.0276	0.0058	0.051	0.011		28	6	25	1	248	491	250	70	a
0.1597	0.0080	1.82	0.13	0.0825	0.0038	0.822	1051	47	955	45	1257	91	350	80	a
0.0594	0.0023	0.498	0.029	0.0607	0.0028	0.533	410	20	372	14	630	100	145	120	a
0.0454	0.0019	0.365	0.022	0.0583	0.0029	0.908	316	17	286	11	542	110	220	115	a
0.0428	0.0020	0.342	0.032	0.0579	0.0054	0.884	299	25	270	12	527	203	260	90	a
0.00809	0.00040	0.059	0.010	0.0526	0.0095		58	10	52	3	312	411	278	98	a
0.0435	0.0017	0.356	0.018	0.0594	0.0020	0.547	309	13	274	10	581	71	185	135	a
0.0614	0.0027	0.534	0.054	0.0630	0.0064	0.917	434	36	384	16	708	215	280	100	a
0.1437	0.0070	1.69	0.13	0.0851	0.0045	0.759	1003	49	865	39	1318	103	260	110	a
0.1429	0.0071	1.691	0.091	0.0858	0.0034		1005	34	861	40	1334	76	171	122	a
0.0523	0.0021	0.460	0.038	0.0637	0.0050	0.906	384	26	329	13	732	166	235	100	a
0.0703	0.0030	0.674	0.055	0.0695	0.0050	0.936	523	33	438	18	912	147	230	90	a
0.1260	0.0070	1.47	0.21	0.085	0.011	0.964	918	88	765	40	1305	249	205	115	a
0.0345	0.0016	0.299	0.017	0.0629	0.0020	0.531	266	13	219	10	706	67	150	110	a
0.0433	0.0033	0.406	0.049	0.0680	0.0067	0.903	346	35	273	20	869	205	165	95	a
0.167	0.015	2.48	0.25	0.1075	0.0032	0.921	1265	72	997	83	1757	54	210	150	a
0.0444	0.0018	0.428	0.042	0.0699	0.0069	0.884	362	30	280	11	925	203	230	90	a
0.01375	0.00079	0.119	0.017	0.0627	0.0097	0.597	114	15	88	5	699	330	270	105	a
0.0054	0.0015	0.045	0.016	0.061	0.014	0.378	45	16	35	10	638	510	185	75	a
0.0704	0.0036	0.804	0.097	0.0829	0.0096	0.930	599	55	438	22	1267	227	55	40	r
0.0539	0.0021	0.579	0.032	0.0778	0.0028	0.514	464	20	339	13	1143	71	175	100	r
0.0408	0.0019	0.417	0.042	0.0741	0.0073	0.877	354	30	258	12	1045	198	290	115	r
0.00319	0.00015	0.0283	0.0081	0.064	0.021		28	8	21	1	750	703	215	90	r
0.0534	0.0027	0.60	0.28	0.081	0.034		475	181	335	16	1221	815	247	103	r
0.1248	0.0062	1.89	0.15	0.1097	0.0067		1077	54	758	36	1794	110	141	133	r
0.0436	0.0021	0.471	0.058	0.0782	0.0098	0.880	392	40	275	13	1152	249	205	110	r
0.0344	0.0013	0.366	0.043	0.0771	0.0097	0.842	316	32	218	8	1125	252	205	100	r
0.0451	0.0017	0.502	0.049	0.0807	0.0079	0.886	413	33	284	11	1215	193	170	120	r
0.0295	0.0015	0.325	0.065	0.080	0.015		286	50	187	9	1196	363	185	86	r
0.1169	0.0071	1.95	0.16	0.1207	0.0063	0.675	1097	56	713	41	1967	93	250	90	r

$^{206}Pb^*/^{238}U$	± 2σ (abs)	$^{207}Pb^*/^{235}U$	± 2σ (abs)	$^{207}Pb^*/^{206}Pb^*$	± 2σ (abs)	corr. coef.	$^{206}Pb^*/^{238}U$ age (Ma)	± 2σ (Ma)	$^{207}Pb^*/^{235}U$ age (Ma)	± 2σ (Ma)	$^{207}Pb^*/^{206}Pb^*$ age (Ma)	± 2σ (Ma)	Length (μm)	Width (μm)	Accept/ Reject
0.0301	0.0011	0.354	0.023	0.0853	0.0046	0.855	307	17	191	7	1323	105	265	135	r
0.0657	0.0033	0.953	0.079	0.1052	0.0076		680	41	410	20	1719	133	168	78	r
0.0435	0.0018	0.617	0.056	0.1029	0.0090	0.888	488	35	274	11	1677	161	210	95	r
0.1095	0.0072	2.35	0.21	0.1556	0.0080	0.597	1227	65	670	42	2408	87	155	125	r
0.0687	0.0055	1.17	0.27	0.124	0.028	0.928	788	127	428	33	2011	403	180	90	r
0.0929	0.0048	1.99	0.13	0.1557	0.0047	0.644	1113	43	573	28	2409	51	235	110	r
0.0575	0.0049	1.03	0.28	0.130	0.036	0.912	719	142	361	30	2098	482	105	80	r
0.0531	0.0025	0.964	0.098	0.132	0.013	0.909	685	51	333	15	2120	169	160	130	r
0.0445	0.0025	0.89	0.15	0.145	0.026	0.883	647	82	281	15	2289	303	195	75	r
0.0682	0.0060	1.85	0.34	0.197	0.032	0.935	1063	121	425	36	2797	263	225	110	r
0.087	0.010	4.58	0.66	0.381	0.020	0.978	1745	120	539	60	3836	80	195	100	r
0.000266	0.000013	0.0058	0.0098	0.16	0.34		6	10	2	0	2443	3587	280	113	a
0.00361	0.00028	0.085	0.018	0.172	0.038		83	17	23	2	2575	371	175	85	r
8. Solimões River, Brazil (3.6424˚S, 61.4510˚W)															
0.00618	0.00029	0.011	0.015	0.013	0.037	*	11	15	40	2			300	125	r
0.00703	0.00054	0.020	0.022	0.020	0.025	0.132	20	22	45	3			130	105	a
0.177	0.011	2.88	0.20	0.1180	0.0032	0.893	1376	53	1050	60	1926	49	180	80	r
0.00670	0.00034	0.032	0.010	0.034	0.013	0.104	32	10	43	2			155	110	a
0.269	0.018	6.71	0.46	0.1808	0.0048	0.889	2074	60	1537	89	2660	44	255	90	r
0.171	0.011	2.46	0.18	0.1041	0.0032	0.891	1260	53	1020	60	1699	56	230	130	a
0.0204	0.0010	0.115	0.014	0.0408	0.0034		110	13	130	6			289	112	a
0.01647	0.00082	0.0925	0.0071	0.0407	0.0018		90	7	105	5			163	131	a
0.1810	0.0099	2.38	0.14	0.0954	0.0027	0.888	1237	41	1072	54	1536	52	200	150	a
0.229	0.013	3.67	0.24	0.1160	0.0031	0.912	1564	53	1331	68	1895	48	165	140	a
0.00517	0.00020	0.0289	0.0039	0.0406	0.0063	*	29	4	33	1			145	125	a
0.00393	0.00020	0.0221	0.0047	0.0409	0.0063		22	5	25	1			166	127	a
0.258	0.014	4.60	0.30	0.1291	0.0034	0.914	1749	55	1481	74	2086	46	180	125	a
0.0302	0.0012	0.181	0.018	0.0436	0.0047	0.817	169	16	192	7			205	145	a
0.1933	0.0097	1.71	0.26	0.0643	0.0052		1014	96	1139	52	752	171	251	81	a
0.257	0.014	4.44	0.29	0.1251	0.0033	0.917	1719	55	1476	74	2030	46	175	90	a
0.01102	0.00046	0.0652	0.0063	0.0429	0.0077	*	64	6	71	3			340	140	a
0.1712	0.0087	1.99	0.11	0.0842	0.0022	0.893	1111	36	1019	48	1297	51	175	100	a
0.242	0.015	3.65	0.26	0.1097	0.0031	0.923	1561	57	1395	76	1794	51	70	85	a
0.187	0.016	2.27	0.30	0.0879	0.0067	0.842	1202	92	1105	86	1381	147	70	65	a
0.1755	0.0088	2.02	0.13	0.0833	0.0029	0.875	1121	45	1043	48	1276	69	250	105	a
0.00356	0.00013	0.0213	0.0029	0.0434	0.0068	*	21	3	23	1			205	95	a
0.1724	0.0084	1.94	0.11	0.0818	0.0022	0.901	1096	39	1025	46	1240	52	180	100	a
0.1727	0.0084	1.94	0.11	0.0816	0.0022	0.903	1096	39	1027	46	1237	52	200	110	a
0.1730	0.0088	1.94	0.10	0.0813	0.0022	0.895	1095	36	1029	48	1228	53	250	80	a
0.1799	0.0092	2.03	0.13	0.0819	0.0024	0.902	1126	42	1066	50	1242	58	145	90	a
0.1813	0.0092	2.06	0.14	0.0823	0.0032	0.868	1134	48	1074	50	1252	77	130	115	a
0.1079	0.0047	0.858	0.070	0.0577	0.0040	0.682	629	38	661	27	517	151	195	145	a
0.0323	0.0013	0.212	0.017	0.0476	0.0037	0.844	195	14	205	8	82	184	185	120	a
0.1713	0.0088	1.87	0.10	0.0792	0.0026	0.873	1070	37	1019	48	1176	66	190	95	a
0.1117	0.0056	0.902	0.060	0.0586	0.0019		653	32	683	32	551	72	148	86	a
0.0311	0.0012	0.207	0.012	0.0482	0.0026	0.853	191	10	197	7	110	125	180	145	a
0.1098	0.0055	0.900	0.054	0.0595	0.0016		652	29	671	32	585	58	123	81	a
0.0315	0.0012	0.211	0.014	0.0486	0.0031	0.843	194	12	200	7	128	150	155	105	a
0.1768	0.0092	1.89	0.11	0.0776	0.0021	0.915	1078	40	1049	50	1138	53	155	75	a
0.0950	0.0047	0.755	0.047	0.0577	0.0017		571	27	585	28	518	65	199	121	a
0.0312	0.0016	0.210	0.014	0.0488	0.0017		194	12	198	10	139	84	171	83	a

$^{206}Pb^*/^{238}U$	± 2σ (abs)	$^{207}Pb^*/^{235}U$	± 2σ (abs)	$^{207}Pb^*/^{206}Pb^*$	± 2σ (abs)	corr. coef.	$^{206}Pb^*/^{238}U$ age (Ma)	± 2σ (Ma)	$^{207}Pb^*/^{235}U$ age (Ma)	± 2σ (Ma)	$^{207}Pb^*/^{206}Pb^*$ age (Ma)	± 2σ (Ma)	Length (μm)	Width (μm)	Accept/ Reject
0.218	0.011	2.41	0.17	0.0799	0.0022		1245	51	1273	58	1196	54	171	88	a
0.0201	0.0010	0.132	0.013	0.0476	0.0030		126	12	128	6	81	152	158	120	a
0.0292	0.0011	0.197	0.012	0.0489	0.0026	0.842	182	10	185	7	143	126	145	105	a
0.0373	0.0019	0.257	0.015	0.0500	0.0014		233	12	236	12	197	63	174	138	a
0.0381	0.0019	0.265	0.031	0.0504	0.0039		239	25	241	12	216	181	233	117	a
0.0968	0.0049	0.79	0.15	0.059	0.011	0.947	592	87	596	29	579	421	130	85	a
0.0244	0.0012	0.165	0.013	0.0489	0.0025		155	11	155	8	143	118	323	163	a
0.216	0.011	2.45	0.17	0.0821	0.0021		1256	50	1261	58	1248	51	256	77	a
0.1642	0.0081	1.62	0.12	0.0715	0.0033	0.847	977	46	980	45	971	94	220	95	a
0.0318	0.0016	0.220	0.015	0.0500	0.0019		202	12	202	10	195	91	205	124	a
0.0336	0.0014	0.233	0.014	0.0503	0.0041	0.760	213	11	213	9	210	190	165	105	a
0.1791	0.0090	1.85	0.13	0.0748	0.0023		1062	47	1062	49	1062	61	147	97	a
0.0836	0.0042	0.665	0.040	0.0577	0.0016		518	24	518	25	518	63	196	147	a
0.1822	0.0091	1.90	0.13	0.0757	0.0020		1082	45	1079	50	1087	54	197	108	a
0.0744	0.0037	0.579	0.034	0.0565	0.0015		464	22	463	22	471	60	268	93	a
0.0833	0.0034	0.666	0.032	0.0580	0.0016	0.811	518	20	516	20	529	62	170	100	a
0.0690	0.0034	0.531	0.033	0.0558	0.0017		432	22	430	21	444	68	140	136	a
0.0555	0.0024	0.412	0.020	0.0538	0.0022	0.508	350	14	348	14	364	93	140	100	a
0.0538	0.0023	0.398	0.027	0.0536	0.0030	0.495	340	19	338	14	356	126	200	125	a
0.1740	0.0087	1.79	0.12	0.0746	0.0020		1041	43	1034	48	1057	53	188	107	a
0.0407	0.0020	0.291	0.018	0.0518	0.0016		259	14	257	13	276	72	213	94	a
0.0435	0.0022	0.313	0.018	0.0522	0.0015		277	14	275	13	293	65	183	137	a
0.0439	0.0022	0.317	0.018	0.0524	0.0015		280	14	277	14	301	65	266	89	a
0.252	0.013	3.22	0.25	0.0927	0.0026		1462	60	1448	65	1482	54	181	112	a
0.0400	0.0017	0.286	0.013	0.0518	0.0017	0.449	255	10	253	10	277	76	235	140	a
0.1093	0.0055	0.946	0.064	0.0628	0.0021		676	34	669	32	701	70	139	102	a
0.0427	0.0021	0.308	0.018	0.0523	0.0015		273	14	270	13	298	67	181	87	a
0.0429	0.0017	0.310	0.018	0.0524	0.0026	0.899	274	14	271	11	304	114	245	105	a
0.0453	0.0017	0.330	0.016	0.0528	0.0017	0.607	290	12	286	10	322	73	150	115	a
0.01234	0.00050	0.0821	0.0038	0.0483	0.0022	0.530	80	4	79	3	114	107	185	100	a
0.00803	0.00037	0.0529	0.0096	0.048	0.017	*	52	9	52	2	87	861	200	115	a
0.0525	0.0020	0.391	0.021	0.0540	0.0021	0.592	335	15	330	12	370	89	205	105	a
0.1051	0.0053	0.906	0.068	0.0625	0.0025		655	36	644	31	691	86	137	107	a
0.0221	0.0011	0.1520	0.0083	0.0499	0.0013		144	7	141	7	192	62	217	127	a
0.0792	0.0034	0.639	0.030	0.0585	0.0020	0.728	502	19	491	21	548	76	185	125	a
0.0267	0.0011	0.1867	0.0089	0.0507	0.0024	0.790	174	8	170	7	225	107	250	85	a
0.00363	0.00015	0.0238	0.0016	0.0476	0.0050	*	24	2	23	1	77	252	295	85	a
0.0456	0.0019	0.336	0.015	0.0534	0.0014	0.642	294	11	287	12	346	60	115	135	a
0.0210	0.0011	0.145	0.015	0.0499	0.0034		137	13	134	7	193	157	229	80	a
0.02399	0.00098	0.1669	0.0080	0.0505	0.0025	0.753	157	7	153	6	217	113	180	105	a
0.0446	0.0022	0.330	0.019	0.0537	0.0016		289	15	281	14	357	67	153	103	a
0.0471	0.0019	0.352	0.018	0.0542	0.0020	0.581	306	14	297	12	381	84	155	90	a
0.0873	0.0035	0.732	0.038	0.0607	0.0021	0.762	557	22	540	21	630	76	140	110	a
0.0439	0.0018	0.327	0.015	0.0539	0.0019	0.897	287	11	277	11	368	81	280	70	a
0.0828	0.0036	0.688	0.032	0.0603	0.0016	0.806	532	19	513	22	614	57	160	125	a
0.0862	0.0038	0.724	0.034	0.0609	0.0017	0.805	553	20	533	22	636	59	140	100	a
0.1615	0.0082	1.685	0.100	0.0756	0.0021	0.904	1003	38	965	46	1086	55	225	95	a
0.0686	0.0034	0.550	0.034	0.0581	0.0019		445	22	428	21	534	70	196	96	a
0.0315	0.0012	0.228	0.020	0.0525	0.0049	0.829	208	17	200	7	307	213	190	115	a
0.0560	0.0024	0.436	0.021	0.0565	0.0022	0.540	368	15	351	15	471	85	125	90	a
0.0526	0.0026	0.406	0.038	0.0560	0.0033		346	28	330	16	454	129	179	94	a

$^{206}Pb^*/^{238}U$	± 2σ (abs)	$^{207}Pb^*/^{235}U$	± 2σ (abs)	$^{207}Pb^*/^{206}Pb^*$	± 2σ (abs)	corr. coef.	$^{206}Pb^*/^{238}U$ age (Ma)	± 2σ (Ma)	$^{207}Pb^*/^{235}U$ age (Ma)	± 2σ (Ma)	$^{207}Pb^*/^{206}Pb^*$ age (Ma)	± 2σ (Ma)	Length (μm)	Width (μm)	Accept/ Reject
0.1475	0.0068	1.498	0.086	0.0737	0.0023	0.871	930	35	887	38	1033	63	210	140	a
0.1505	0.0075	1.54	0.10	0.0744	0.0020		948	40	904	42	1052	54	118	110	a
0.0452	0.0017	0.343	0.016	0.0550	0.0015	0.658	299	12	285	11	411	62	205	95	a
0.1600	0.0076	1.689	0.095	0.0766	0.0021	0.897	1004	36	957	42	1110	54	175	100	a
0.0384	0.0016	0.287	0.014	0.0541	0.0025	0.852	256	11	243	10	376	105	115	100	a
0.1526	0.0071	1.587	0.089	0.0754	0.0021	0.885	965	35	916	40	1080	57	260	80	a
0.1565	0.0078	1.65	0.11	0.0764	0.0022		989	43	938	44	1104	57	211	113	a
0.1620	0.0081	1.735	0.092	0.0777	0.0022	0.884	1022	34	968	45	1138	57	210	80	a
0.1026	0.0047	0.925	0.045	0.0654	0.0021	0.801	665	24	630	27	786	68	210	95	a
0.0933	0.0047	0.819	0.048	0.0637	0.0017		608	27	575	28	732	56	140	124	a
0.1535	0.0071	1.611	0.088	0.0761	0.0020	0.891	975	34	921	39	1098	53	205	130	a
0.1440	0.0072	1.476	0.093	0.0743	0.0020		920	38	867	41	1050	53	177	141	a
0.1284	0.0057	1.259	0.070	0.0711	0.0023	0.846	827	31	779	33	960	66	160	95	a
0.1459	0.0066	1.505	0.080	0.0748	0.0020	0.885	933	32	878	37	1064	53	155	135	a
0.1576	0.0079	1.69	0.11	0.0776	0.0021		1003	42	943	44	1137	55	159	122	a
0.1576	0.0079	1.69	0.11	0.0777	0.0021		1004	42	943	44	1139	53	163	106	a
0.0905	0.0045	0.797	0.047	0.0639	0.0017		595	27	558	27	737	57	182	112	a
0.1486	0.0068	1.553	0.084	0.0758	0.0020	0.889	952	33	893	38	1090	53	190	110	a
0.0705	0.0031	0.585	0.028	0.0602	0.0022	0.676	468	18	439	19	613	77	205	105	a
0.1485	0.0068	1.552	0.090	0.0758	0.0025	0.863	951	36	892	38	1090	66	155	150	a
0.1309	0.0062	1.299	0.065	0.0720	0.0020	0.860	845	29	793	35	986	57	175	145	a
0.1336	0.0067	1.34	0.13	0.0727	0.0038		863	54	808	38	1005	106	176	116	a
0.1537	0.0071	1.636	0.088	0.0772	0.0020	0.891	984	34	922	39	1126	52	145	130	a
0.0347	0.0017	0.261	0.018	0.0545	0.0021		235	14	220	11	390	89	273	76	a
0.1531	0.0071	1.632	0.091	0.0773	0.0022	0.884	983	35	918	40	1129	56	245	115	a
0.1437	0.0064	1.489	0.086	0.0752	0.0025	0.852	926	35	865	36	1074	67	180	95	a
0.1391	0.0067	1.427	0.076	0.0744	0.0029	0.812	900	32	840	38	1052	79	175	90	a
0.1390	0.0067	1.426	0.072	0.0744	0.0021	0.868	900	30	839	38	1053	56	225	105	a
0.1430	0.0069	1.486	0.075	0.0754	0.0020	0.873	925	31	862	39	1078	55	170	115	a
0.1289	0.0060	1.286	0.063	0.0724	0.0019	0.863	839	28	781	34	996	54	165	120	a
0.1527	0.0070	1.638	0.089	0.0778	0.0021	0.888	985	34	916	39	1142	53	145	115	a
0.1345	0.0063	1.367	0.068	0.0737	0.0021	0.861	875	29	813	36	1033	57	140	115	a
0.0886	0.0036	0.786	0.049	0.0644	0.0030	0.684	589	28	547	22	754	99	190	95	a
0.1629	0.0081	1.808	0.095	0.0805	0.0022	0.886	1048	34	973	45	1209	53	165	100	a
0.1317	0.0062	1.336	0.066	0.0736	0.0020	0.863	862	29	797	35	1031	55	165	160	a
0.1608	0.0076	1.79	0.10	0.0806	0.0022	0.890	1041	37	961	42	1212	54	135	85	a
0.1464	0.0071	1.561	0.080	0.0773	0.0020	0.878	955	32	881	40	1130	53	140	102	a
0.0497	0.0025	0.397	0.025	0.0579	0.0019		339	18	313	15	525	71	182	103	a
0.0279	0.0014	0.209	0.013	0.0543	0.0018		193	11	178	9	383	74	157	111	a
0.1595	0.0080	1.77	0.12	0.0807	0.0021		1036	43	954	44	1213	52	257	79	a
0.0718	0.0032	0.615	0.032	0.0621	0.0030	0.519	486	20	447	19	676	104	220	110	a
0.0312	0.0012	0.237	0.012	0.0550	0.0020	0.880	216	10	198	7	412	82	180	100	a
0.1586	0.0078	1.770	0.092	0.0809	0.0021	0.884	1034	34	949	44	1219	52	205	100	a
0.1673	0.0082	1.92	0.12	0.0833	0.0027	0.878	1088	41	997	45	1275	62	270	110	a
0.0780	0.0039	0.683	0.040	0.0635	0.0018		529	24	484	23	725	59	207	140	a
0.01595	0.00066	0.1161	0.0054	0.0528	0.0021	0.684	111	5	102	4	319	92	125	70	a
0.1211	0.0061	1.213	0.074	0.0727	0.0019		806	34	737	35	1004	54	217	115	a
0.1572	0.0077	1.761	0.091	0.0813	0.0023	0.872	1031	34	941	43	1228	56	160	135	a
0.0423	0.0018	0.334	0.016	0.0573	0.0022	0.886	293	12	267	11	503	86	165	120	a
0.0353	0.0018	0.273	0.018	0.0561	0.0019		245	14	223	11	458	74	152	124	a
0.1168	0.0058	1.165	0.070	0.0723	0.0019		784	33	712	34	995	53	172	116	a

$^{206}Pb^*/^{238}U$	± 2σ (abs)	$^{207}Pb^*/^{235}U$	± 2σ (abs)	$^{207}Pb^*/^{206}Pb^*$	± 2σ (abs)	corr. coef.	$^{206}Pb^*/^{238}U$ age (Ma)	± 2σ (Ma)	$^{207}Pb^*/^{235}U$ age (Ma)	± 2σ (Ma)	$^{207}Pb^*/^{206}Pb^*$ age (Ma)	± 2σ (Ma)	Length (μm)	Width (μm)	Accept/ Reject
0.1571	0.0076	1.77	0.10	0.0819	0.0023	0.885	1036	38	941	42	1243	55	180	110	a
0.0222	0.0011	0.167	0.013	0.0544	0.0027		157	12	142	7	388	112	192	112	a
0.0375	0.0016	0.296	0.014	0.0571	0.0022	0.875	263	11	238	10	497	85	200	100	a
0.0444	0.0022	0.358	0.034	0.0585	0.0036		311	25	280	14	547	133	178	169	a
0.0262	0.0013	0.200	0.012	0.0555	0.0018		185	10	166	8	434	74	160	117	a
0.1560	0.0078	1.79	0.12	0.0832	0.0022		1042	42	935	44	1274	51	161	111	a
0.1348	0.0067	1.450	0.089	0.0780	0.0020		910	37	815	38	1148	52	146	91	a
0.0450	0.0020	0.370	0.061	0.060	0.010	0.879	320	45	284	12	592	380	195	95	a
0.0248	0.0010	0.192	0.016	0.0561	0.0082	0.581	178	13	158	6	458	323	225	140	a
0.0373	0.0015	0.301	0.038	0.0586	0.0079	0.851	267	29	236	9	552	295	140	100	a
0.1472	0.0070	1.701	0.098	0.0838	0.0025	0.864	1009	37	885	39	1289	59	190	70	a
0.1615	0.0081	2.01	0.13	0.0904	0.0024		1120	45	965	45	1434	51	184	111	a
0.1757	0.0088	2.33	0.15	0.0962	0.0025		1222	47	1044	48	1552	49	163	103	a
0.1860	0.0093	2.57	0.17	0.1002	0.0026		1292	49	1100	51	1627	49	184	101	a
0.0408	0.0015	0.356	0.020	0.0633	0.0028	0.900	309	15	258	10	717	96	220	135	a
0.0496	0.0025	0.446	0.049	0.0652	0.0047		375	35	312	15	781	151	225	106	a
0.351	0.018	9.38	0.84	0.1938	0.0050		2376	82	1939	84	2775	43	180	138	a
0.00397	0.00029	0.0314	0.0092	0.057	0.018	*	31	9	26	2	509	707	190	110	a
0.0367	0.0015	0.335	0.018	0.0662	0.0042	0.814	293	14	232	10	813	134	160	115	a
0.0397	0.0017	0.382	0.023	0.0698	0.0057	0.801	328	17	251	10	921	167	235	100	r
0.1516	0.0081	2.24	0.15	0.1070	0.0065	0.629	1193	46	910	46	1748	112	195	105	r
0.0213	0.0011	0.196	0.058	0.067	0.014		182	49	136	7	824	441	154	93	r
0.00354	0.00015	0.0308	0.0031	0.063	0.012	*	31	3	23	1	708	405	270	95	r
0.01063	0.00059	0.104	0.033	0.071	0.026	0.450	100	30	68	4	957	744	210	75	a
0.1269	0.0063	2.10	0.21	0.1203	0.0066		1150	69	770	36	1960	98	181	131	r
0.00215	0.00011	0.0212	0.0064	0.072	0.016		21	6	14	1	973	450	228	107	r
0.00554	0.00023	0.0566	0.0044	0.0742	0.0098	*	56	4	36	2	1046	267	215	110	r
0.0778	0.0031	1.241	0.067	0.1158	0.0036	0.571	820	30	483	19	1892	56	145	90	r
0.1402	0.0069	3.25	0.17	0.1680	0.0046	0.713	1469	40	846	39	2538	46	200	110	r
0.0444	0.0038	0.71	0.19	0.115	0.031	0.882	542	111	280	24	1883	490	200	120	r
0.0334	0.0015	0.525	0.042	0.114	0.015	0.718	428	28	212	9	1865	240	231	105	r
0.01204	0.00060	0.218	0.044	0.131	0.019		200	37	77	4	2117	252	173	101	r
0.00404	0.00020	0.074	0.012	0.133	0.015		72	11	26	1	2135	202	163	100	r
0.01739	0.00087	0.47	0.11	0.194	0.031		388	73	111	6	2777	266	249	94	r
9. Solimões River, Brazil (3.6136˚S, 61.2547˚W)															
0.183	0.017	2.50	0.29	0.0991	0.0044	0.897	1273	85	1084	95	1607	82	90	75	a
0.180	0.011	2.39	0.17	0.0960	0.0027	0.894	1238	50	1069	58	1547	53	135	80	a
0.290	0.022	6.35	0.54	0.1585	0.0042	0.921	2025	74	1644	108	2440	45	90	60	a
0.202	0.012	2.70	0.19	0.0968	0.0026	0.908	1328	52	1187	64	1563	51	170	70	a
0.259	0.013	2.81	0.32	0.0785	0.0032		1357	85	1485	67	1160	81	97	54	a
0.235	0.015	3.39	0.25	0.1045	0.0029	0.920	1501	58	1360	78	1706	51	90	90	a
0.0453	0.0023	0.301	0.018	0.0481	0.0017		267	14	286	14	105	81	115	85	a
0.177	0.016	2.03	0.25	0.0830	0.0046	0.881	1124	82	1051	89	1269	109	90	40	a
0.205	0.038	2.59	0.94	0.092	0.020	0.773	1299	265	1204	201	1458	421	80	75	a
0.1383	0.0075	1.179	0.077	0.0618	0.0020	0.885	791	36	835	42	668	69	75	50	a
0.1133	0.0053	0.919	0.057	0.0588	0.0023	0.813	662	30	692	30	562	84	121	65	a
0.1102	0.0058	0.889	0.054	0.0585	0.0017	0.875	646	29	674	34	548	62	100	70	a
0.1268	0.0073	1.069	0.087	0.0611	0.0032	0.810	738	43	770	42	644	113	130	45	a
0.0853	0.0037	0.648	0.036	0.0551	0.0019	0.768	507	22	528	22	416	77	160	60	a
0.1418	0.0071	1.260	0.074	0.0645	0.0017	0.895	828	33	855	40	756	57	105	70	a
0.0951	0.0048	0.752	0.045	0.0574	0.0016		570	26	586	28	505	62	142	67	a

$^{206}Pb^*/^{238}U$	± 2σ (abs)	$^{207}Pb^*/^{235}U$	± 2σ (abs)	$^{207}Pb^*/^{206}Pb^*$	± 2σ (abs)	corr. coef.	$^{206}Pb^*/^{238}U$ age (Ma)	± 2σ (Ma)	$^{207}Pb^*/^{235}U$ age (Ma)	± 2σ (Ma)	$^{207}Pb^*/^{206}Pb^*$ age (Ma)	± 2σ (Ma)	Length (μm)	Width (μm)	Accept/ Reject
0.0596	0.0026	0.430	0.023	0.0523	0.0017	0.696	363	16	373	16	298	75	110	65	a
0.176	0.011	1.89	0.14	0.0778	0.0024	0.903	1078	49	1047	58	1142	62	145	65	a
0.0652	0.0033	0.478	0.027	0.0532	0.0014		397	18	407	20	335	61	132	67	a
0.1399	0.0068	1.248	0.073	0.0647	0.0019	0.881	822	33	844	38	764	61	130	70	a
0.172	0.010	1.82	0.13	0.0766	0.0022	0.908	1051	45	1023	55	1112	57	135	70	a
0.257	0.018	3.52	0.29	0.0995	0.0029	0.935	1533	66	1474	93	1615	53	95	60	a
0.188	0.012	2.07	0.16	0.0801	0.0025	0.912	1140	53	1110	64	1199	61	100	70	a
0.290	0.018	4.41	0.33	0.1103	0.0029	0.935	1715	61	1643	91	1804	48	175	70	a
0.180	0.012	1.94	0.38	0.078	0.011	0.609	1096	132	1068	68	1151	268	110	40	a
0.201	0.012	2.31	0.16	0.0833	0.0022	0.921	1216	49	1182	64	1277	52	110	51	a
0.263	0.018	3.65	0.28	0.1007	0.0027	0.937	1561	61	1505	90	1637	49	110	70	a
0.322	0.024	5.27	0.51	0.1186	0.0047	0.920	1865	83	1801	115	1936	70	95	75	a
0.202	0.010	2.16	0.24	0.0775	0.0042		1167	76	1185	54	1134	109	92	76	a
0.1708	0.0093	1.76	0.13	0.0748	0.0029	0.870	1032	48	1017	51	1064	78	165	72	a
0.0438	0.0017	0.308	0.034	0.0511	0.0059	0.861	273	26	276	11	246	266	145	65	a
0.182	0.012	1.94	0.14	0.0769	0.0020	0.925	1094	49	1081	63	1119	53	115	55	a
0.177	0.011	1.83	0.13	0.0753	0.0022	0.915	1058	47	1049	59	1077	57	210	75	a
0.1936	0.0097	2.05	0.15	0.0769	0.0022		1133	49	1141	52	1118	56	111	43	a
0.1223	0.0062	1.07	0.10	0.0636	0.0050	0.626	740	51	744	36	729	166	105	55	a
0.0594	0.0024	0.441	0.022	0.0538	0.0018	0.646	371	16	372	14	363	73	100	80	a
0.0450	0.0017	0.322	0.015	0.0518	0.0016	0.528	283	11	284	10	276	69	125	60	a
0.0928	0.0046	0.755	0.072	0.0590	0.0034		571	41	572	27	568	127	90	47	a
0.0604	0.0025	0.453	0.033	0.0544	0.0034	0.915	380	23	378	15	389	142	110	60	a
0.1070	0.0053	0.912	0.061	0.0619	0.0021		658	32	655	31	670	73	100	51	a
0.171	0.012	1.71	0.17	0.0724	0.0041	0.853	1013	64	1020	64	998	114	85	95	a
0.177	0.013	1.79	0.15	0.0734	0.0022	0.925	1043	54	1052	69	1024	61	120	70	a
0.0725	0.0029	0.565	0.032	0.0565	0.0023	0.629	455	20	451	18	472	89	75	65	a
0.187	0.011	1.93	0.15	0.0749	0.0026	0.905	1092	52	1106	61	1065	69	126	60	a
0.1182	0.0059	1.051	0.076	0.0645	0.0025		730	38	720	34	759	82	165	53	a
0.231	0.014	2.64	0.19	0.0828	0.0023	0.931	1311	53	1340	72	1264	54	95	50	a
0.201	0.012	2.13	0.15	0.0768	0.0020	0.927	1160	47	1183	63	1116	52	70	65	a
0.208	0.013	2.22	0.16	0.0776	0.0021	0.934	1188	52	1216	71	1137	53	120	60	a
0.1022	0.0044	0.875	0.045	0.0621	0.0017	0.827	638	24	627	26	678	60	95	45	a
0.1205	0.0058	1.087	0.064	0.0654	0.0020	0.851	747	31	733	33	788	65	115	60	a
0.0494	0.0019	0.368	0.020	0.0539	0.0022	0.911	318	15	311	12	367	93	140	90	a
0.1642	0.0082	1.69	0.11	0.0746	0.0020		1004	42	980	46	1057	54	147	61	a
0.1695	0.0096	1.62	0.13	0.0694	0.0029	0.873	978	49	1010	53	909	86	100	65	a
0.1038	0.0052	0.91	0.11	0.0634	0.0048		656	59	637	30	722	161	120	66	a
0.229	0.014	2.48	0.22	0.0783	0.0035	0.900	1265	65	1331	75	1155	88	65	45	a
0.0736	0.0031	0.592	0.048	0.0583	0.0041	0.930	472	31	458	19	543	155	105	55	a
0.1633	0.0091	1.70	0.11	0.0754	0.0020	0.908	1008	41	975	50	1080	53	111	75	a
0.221	0.015	2.32	0.20	0.0764	0.0027	0.924	1220	60	1285	80	1106	71	80	60	a
0.1631	0.0086	1.70	0.23	0.0754	0.0078	0.571	1007	87	974	48	1080	207	95	95	a
0.0473	0.0024	0.355	0.020	0.0544	0.0016		309	15	298	15	389	65	159	106	a
0.0556	0.0028	0.434	0.027	0.0567	0.0019		366	19	349	17	480	73	131	64	a
0.205	0.010	2.50	0.19	0.0884	0.0027		1273	54	1204	55	1392	60	123	68	a
0.0894	0.0039	0.779	0.045	0.0632	0.0024	0.734	585	26	552	23	714	79	145	85	a
0.1179	0.0055	1.130	0.076	0.0695	0.0031	0.753	768	36	718	32	914	92	75	60	a
0.166	0.010	1.85	0.14	0.0808	0.0025	0.900	1063	48	991	57	1216	60	130	80	a
0.1914	0.0096	2.30	0.16	0.0873	0.0024		1213	49	1129	52	1366	52	152	53	a
0.1907	0.0095	2.30	0.16	0.0875	0.0024		1213	48	1125	52	1372	52	76	59	a

$^{206}Pb^*/^{238}U$	± 2σ (abs)	$^{207}Pb^*/^{235}U$	± 2σ (abs)	$^{207}Pb^*/^{206}Pb^*$	± 2σ (abs)	corr. coef.	$^{206}Pb^*/^{238}U$ age (Ma)	± 2σ (Ma)	$^{207}Pb^*/^{235}U$ age (Ma)	± 2σ (Ma)	$^{207}Pb^*/^{206}Pb^*$ age (Ma)	± 2σ (Ma)	Length (μm)	Width (μm)	Accept/ Reject
0.0481	0.0024	0.384	0.025	0.0578	0.0021		330	18	303	15	524	80	136	54	a
0.1615	0.0098	1.82	0.16	0.0818	0.0041	0.826	1053	57	965	54	1242	97	120	70	a
0.0817	0.0041	0.724	0.092	0.0643	0.0055		553	54	506	24	752	182	100	61	a
0.0906	0.0045	0.83	0.33	0.067	0.018		615	183	559	27	827	576	116	62	a
0.0453	0.0023	0.367	0.021	0.0588	0.0016		318	15	285	14	560	61	155	65	a
0.1353	0.0068	1.46	0.11	0.0781	0.0029		913	44	818	39	1148	74	145	61	a
0.1380	0.0069	1.52	0.13	0.0797	0.0038		937	52	833	39	1190	94	114	64	a
0.1643	0.0088	2.01	0.17	0.0888	0.0047	0.772	1119	58	981	49	1399	102	130	70	a
0.0622	0.0026	0.561	0.061	0.0654	0.0070	0.907	452	40	389	16	787	226	165	70	a
0.00477	0.00024	0.0370	0.0050	0.0563	0.0056		37	5	31	2	465	221	121	55	a
0.0350	0.0014	0.301	0.032	0.0624	0.0069	0.829	268	25	222	9	688	236	130	70	a
0.0739	0.0031	0.749	0.098	0.0735	0.0096	0.921	567	57	459	19	1027	265	135	55	a
0.0723	0.0036	0.749	0.071	0.0751	0.0037		568	41	450	22	1072	100	101	49	a
0.155	0.012	2.48	0.32	0.1162	0.0092	0.662	1267	95	928	68	1899	143	65	65	r
0.257	0.013	6.49	0.49	0.1831	0.0049		2044	66	1474	66	2682	44	110	55	r
0.1789	0.0089	3.82	0.27	0.1547	0.0045		1596	58	1061	49	2398	49	127	69	r
0.00	0.00	0.0206	0.0027	0.0806	0.0080		21	3	12	1	1212	195	108	63	r
0.01156	0.00054	0.144	0.018	0.090	0.012	0.455	137	16	74	3	1434	246	115	60	r
0.230	0.011	11.3	5.3	0.357	0.096		2549	437	1334	61	3736	410	116	97	r
0.00617	0.00040	0.122	0.033	0.143	0.043	*	117	30	40	3	2265	516	115	70	r
10. Solimões River, Brazil (3.2979°S, 60.3071°W)															
0.1739	0.0098	4.13	0.27	0.1723	0.0076	0.655	1661	52	1034	54	2581	73	150	75	r
0.00494	0.00025	0.008	0.021	0.012	0.019		8	20	32	2			135	90	r
0.274	0.019	11.90	0.93	0.315	0.014	0.665	2597	73	1561	95	3546	70	115	70	r
0.00174	0.00015	0.0056	0.0054	0.023	0.018	*	6	5	11	1			160	70	r
0.00328	0.00016	0.0110	0.0044	0.0242	0.0055		11	4	21	1			154	87	r
0.196	0.021	3.927	1.045	0.145	0.022	0.983	1619	215	1154	115	2291	263	155	70	r
0.00488	0.00024	0.0220	0.0071	0.0327	0.0061		22	6	31	2			121	52	a
0.179	0.010	2.33	0.14	0.0943	0.0025	0.895	1221	42	1062	55	1514	50	120	90	a
0.1101	0.0075	0.781	0.069	0.0514	0.0022	0.872	586	39	674	43	259	98	115	65	a
0.174	0.017	2.16	0.23	0.0901	0.0026	0.936	1170	73	1036	92	1427	54	105	100	a
0.00873	0.00044	0.0497	0.0054	0.0413	0.0023		49	5	56	3			137	57	a
0.0457	0.0023	0.283	0.035	0.0449	0.0032		253	25	288	14			102	65	a
0.00623	0.00055	0.035	0.013	0.041	0.011	0.212	35	12	40	4			165	65	a
0.0367	0.0018	0.229	0.021	0.0452	0.0020		209	17	232	11			178	66	a
0.0367	0.0018	0.229	0.022	0.0452	0.0020		209	17	232	11			151	52	a
0.00229	0.00011	0.0132	0.0033	0.0419	0.0062		13	3	15	1			159	63	a
0.0662	0.0029	0.453	0.025	0.0496	0.0033	0.896	379	18	413	17	176	153	135	90	a
0.218	0.011	2.16	0.15	0.0720	0.0023		1169	45	1271	58	986	63	129	58	a
0.261	0.016	4.26	0.31	0.1184	0.0032	0.920	1685	60	1494	83	1932	48	150	70	a
0.1785	0.0099	2.09	0.12	0.0848	0.0025	0.893	1144	40	1059	54	1311	57	205	65	a
0.239	0.012	2.54	0.16	0.0769	0.0020		1282	43	1382	63	1119	50	158	67	a
0.0284	0.0020	0.180	0.033	0.0459	0.0060	0.854	168	28	180	13			110	70	a
0.0253	0.0014	0.159	0.012	0.0457	0.0018	0.881	150	10	161	9			145	85	a
0.00671	0.00050	0.0406	0.0076	0.0439	0.0056	0.356	40	7	43	3			130	80	a
0.228	0.011	2.44	0.16	0.0774	0.0022		1254	44	1327	60	1131	53	142	75	a
0.1013	0.0077	0.785	0.068	0.0562	0.0018	0.899	588	39	622	45	462	70	180	65	a
0.217	0.013	2.81	0.17	0.0938	0.0026	0.914	1358	46	1267	67	1504	52	115	756	a
0.214	0.012	2.74	0.16	0.0925	0.0025	0.913	1339	43	1253	63	1479	50	135	105	a
0.257	0.016	3.81	0.28	0.1076	0.0029	0.927	1595	60	1473	84	1759	49	110	75	a
0.276	0.017	4.36	0.32	0.1148	0.0030	0.929	1705	61	1570	88	1876	48	140	80	a

$^{206}Pb^*/^{238}U$	± 2σ (abs)	$^{207}Pb^*/^{235}U$	± 2σ (abs)	$^{207}Pb^*/^{206}Pb^*$	± 2σ (abs)	corr. coef.	$^{206}Pb^*/^{238}U$ age (Ma)	± 2σ (Ma)	$^{207}Pb^*/^{235}U$ age (Ma)	± 2σ (Ma)	$^{207}Pb^*/^{206}Pb^*$ age (Ma)	± 2σ (Ma)	Length (μm)	Width (μm)	Accept/ Reject
0.0311	0.0014	0.204	0.012	0.0475	0.0041	0.736	188	11	198	8	75	206	135	85	a
0.204	0.010	2.08	0.13	0.0739	0.0020		1142	40	1198	55	1038	51	172	69	a
0.106	0.013	0.84	0.11	0.0575	0.0017	0.941	618	60	647	75	510	66	85	80	a
0.222	0.014	2.88	0.20	0.0939	0.0025	0.924	1376	53	1294	72	1506	50	115	65	a
0.217	0.011	2.30	0.14	0.0769	0.0021		1212	41	1265	58	1118	51	116	81	a
0.0371	0.0019	0.248	0.019	0.0485	0.0018		225	15	235	12	124	83	176	62	a
0.260	0.017	3.79	0.26	0.1057	0.0029	0.931	1590	56	1490	89	1726	50	160	70	a
0.250	0.017	3.49	0.27	0.1011	0.0026	0.936	1524	62	1439	89	1644	49	115	60	a
0.0612	0.0038	0.438	0.049	0.0519	0.0033	0.572	369	34	383	23	283	147	150	60	a
0.1574	0.0079	1.452	0.087	0.0669	0.0019		911	34	943	44	834	55	126	47	a
0.1860	0.0093	1.85	0.13	0.0720	0.0028		1063	44	1100	51	987	72	85	74	a
0.0445	0.0025	0.306	0.027	0.0499	0.0026	0.923	271	21	280	15	191	121	140	65	a
0.0717	0.0034	0.531	0.026	0.0537	0.0014	0.815	433	18	446	21	360	59	150	65	a
0.0549	0.0024	0.390	0.018	0.0515	0.0014	0.741	334	13	344	15	264	60	125	90	a
0.1873	0.0094	1.88	0.12	0.0729	0.0021		1075	38	1107	51	1010	53	129	58	a
0.0741	0.0038	0.555	0.030	0.0543	0.0021	0.752	448	20	461	23	382	85	125	90	a
0.0559	0.0028	0.402	0.037	0.0522	0.0025		343	23	351	17	292	95	132	72	a
0.0577	0.0031	0.417	0.028	0.0524	0.0015	0.783	354	20	362	19	304	66	150	60	a
0.1329	0.0066	1.17	0.11	0.0639	0.0036		788	50	805	38	740	114	141	67	a
0.1457	0.0083	1.33	0.13	0.0663	0.0042	0.782	859	58	877	47	815	133	145	65	a
0.0410	0.0025	0.284	0.020	0.0503	0.0014	0.752	254	16	259	15	207	63	135	100	a
0.0591	0.0040	0.431	0.033	0.0528	0.0014	0.841	364	24	370	25	320	62	155	60	a
0.1853	0.0093	1.89	0.13	0.0738	0.0024		1076	41	1096	51	1037	61	111	62	a
0.1800	0.0094	1.92	0.11	0.0773	0.0021	0.906	1088	37	1067	51	1129	53	145	70	a
0.0626	0.0031	0.463	0.030	0.0536	0.0016		386	20	392	19	353	62	113	64	a
0.0499	0.0029	0.357	0.028	0.0518	0.0021	0.648	310	21	314	18	277	94	150	90	a
0.0572	0.0025	0.417	0.019	0.0529	0.0016	0.699	354	14	358	15	326	68	85	60	a
0.0516	0.0026	0.372	0.024	0.0522	0.0015		321	17	325	16	294	62	87	90	a
0.180	0.010	1.91	0.11	0.0766	0.0020	0.914	1083	39	1069	55	1111	52	115	75	a
0.176	0.011	1.83	0.13	0.0754	0.0021	0.918	1055	46	1044	59	1078	55	145	75	a
0.186	0.016	1.99	0.19	0.0776	0.0023	0.939	1113	64	1102	88	1135	60	140	80	a
0.0715	0.0036	0.544	0.037	0.0552	0.0016		441	22	445	22	422	62	185	57	a
0.0422	0.0021	0.298	0.024	0.0511	0.0020		265	18	267	13	245	86	98	68	a
0.0888	0.0044	0.711	0.054	0.0581	0.0021		545	26	549	26	532	64	154	60	a
0.0671	0.0029	0.507	0.025	0.0548	0.0023	0.625	417	17	419	18	405	93	180	70	a
0.0519	0.0026	0.377	0.036	0.0527	0.0026		325	25	326	16	316	109	138	85	a
0.0576	0.0029	0.426	0.031	0.0535	0.0019		360	20	361	18	352	71	157	55	a
0.168	0.010	1.66	0.12	0.0721	0.0020	0.917	995	45	998	56	988	56	155	60	a
0.0502	0.0022	0.364	0.017	0.0526	0.0019	0.561	315	13	316	13	311	81	115	85	a
0.00592	0.00030	0.0383	0.0099	0.0469	0.0071		38	9	38	2	43	334	221	51	a
0.0406	0.0023	0.288	0.020	0.0516	0.0017	0.662	257	16	256	14	266	74	115	90	a
0.1482	0.0091	1.41	0.10	0.0691	0.0021	0.902	894	44	891	51	903	62	120	65	a
0.1727	0.0086	1.76	0.11	0.0741	0.0023		1033	39	1027	48	1045	59	159	63	a
0.182	0.011	1.87	0.13	0.0744	0.0020	0.924	1070	47	1078	61	1053	54	150	60	a
0.0760	0.0038	0.598	0.042	0.0570	0.0019		476	24	472	23	493	66	151	76	a
0.1783	0.0089	1.86	0.12	0.0755	0.0023		1065	37	1058	49	1081	51	109	54	a
0.199	0.011	2.13	0.13	0.0776	0.0020	0.923	1159	41	1172	60	1136	52	125	60	a
0.1574	0.0078	1.550	0.082	0.0714	0.0022	0.876	950	33	942	43	970	64	110	85	a
0.0692	0.0032	0.538	0.027	0.0564	0.0020	0.711	437	18	431	19	466	78	105	75	a
0.0739	0.0039	0.583	0.037	0.0572	0.0016	0.821	467	24	460	23	501	61	125	80	a
0.0646	0.0032	0.499	0.035	0.0561	0.0018		411	21	404	20	454	61	151	55	a

$^{206}Pb^*/^{238}U$	± 2σ (abs)	$^{207}Pb^*/^{235}U$	± 2σ (abs)	$^{207}Pb^*/^{206}Pb^*$	± 2σ (abs)	corr. coef.	$^{206}Pb^*/^{238}U$ age (Ma)	± 2σ (Ma)	$^{207}Pb^*/^{235}U$ age (Ma)	± 2σ (Ma)	$^{207}Pb^*/^{206}Pb^*$ age (Ma)	± 2σ (Ma)	Length (μm)	Width (μm)	Accept/ Reject
0.0901	0.0041	0.748	0.038	0.0602	0.0026	0.708	567	22	556	24	611	93	140	80	a
0.1086	0.0063	0.949	0.073	0.0634	0.0020	0.862	678	38	665	37	722	69	90	50	a
0.0798	0.0040	0.645	0.042	0.0586	0.0018		506	24	495	24	553	61	158	63	a
0.0290	0.0014	0.203	0.015	0.0510	0.0017		188	12	184	9	239	73	127	85	a
0.1660	0.0083	1.71	0.10	0.0746	0.0020		1011	36	990	46	1059	51	136	68	a
0.1675	0.0088	1.736	0.096	0.0751	0.0021	0.899	1022	36	999	49	1072	56	160	60	a
0.1908	0.0095	2.12	0.13	0.0805	0.0024		1155	41	1126	52	1210	56	166	50	a
0.1304	0.0071	1.222	0.081	0.0679	0.0020	0.877	810	37	790	40	867	62	115	100	a
0.0550	0.0028	0.418	0.028	0.0551	0.0018		355	19	345	17	416	68	122	85	a
0.1457	0.0076	1.428	0.079	0.0711	0.0021	0.884	901	33	877	43	960	59	125	75	a
0.202	0.012	2.07	0.18	0.0744	0.0031	0.896	1138	58	1185	67	1051	84	110	90	a
0.0304	0.0015	0.217	0.014	0.0517	0.0015		199	11	193	10	274	62	150	83	a
0.0588	0.0025	0.458	0.023	0.0566	0.0026	0.466	383	16	368	15	474	100	130	55	a
0.0728	0.0036	0.591	0.039	0.0589	0.0018		472	23	453	22	564	63	155	75	a
0.01997	0.00100	0.140	0.017	0.0508	0.0035		133	14	127	6	230	151	144	70	a
0.1574	0.0079	1.631	0.097	0.0752	0.0021		982	36	942	44	1073	52	122	41	a
0.1195	0.0060	1.113	0.067	0.0676	0.0018		760	30	728	34	855	53	118	65	a
0.1611	0.0081	1.69	0.10	0.0761	0.0020		1005	35	963	45	1099	50	127	73	a
0.0219	0.0011	0.155	0.012	0.0512	0.0017		146	9	140	7	248	68	134	75	a
0.0661	0.0036	0.530	0.043	0.0581	0.0025	0.685	432	29	413	22	535	94	170	75	a
0.01503	0.00075	0.104	0.015	0.0503	0.0042		101	13	96	5	210	183	196	55	a
0.0753	0.0061	0.62	0.24	0.060	0.018	0.941	493	153	468	36	607	636	130	55	a
0.0550	0.0024	0.432	0.022	0.0569	0.0028	0.898	365	16	345	15	489	108	145	65	a
0.1714	0.0086	1.89	0.13	0.0800	0.0029		1078	44	1020	47	1196	68	122	71	a
0.1229	0.0058	1.179	0.064	0.0696	0.0032	0.756	791	30	747	33	917	95	185	75	a
0.1623	0.0081	1.75	0.11	0.0782	0.0022		1027	36	970	45	1151	51	139	89	a
0.1592	0.0080	1.70	0.10	0.0775	0.0022		1009	37	953	44	1134	55	152	66	a
0.0676	0.0034	0.554	0.034	0.0594	0.0041	0.904	448	22	422	20	582	148	125	70	a
0.232	0.024	2.28	0.29	0.0714	0.0030	0.948	1207	89	1344	127	968	85	150	60	a
0.1393	0.0070	1.413	0.084	0.0736	0.0020		894	33	841	40	1029	52	172	47	a
0.224	0.011	2.94	0.18	0.0952	0.0025		1393	45	1304	59	1532	48	101	71	a
0.0877	0.0047	0.768	0.049	0.0636	0.0017	0.840	579	28	542	28	727	58	130	90	a
0.0966	0.0054	0.876	0.094	0.0657	0.0048	0.574	639	51	595	32	798	153	110	80	a
0.1532	0.0076	1.646	0.086	0.0779	0.0021	0.880	988	33	919	42	1145	54	140	70	a
0.1557	0.0080	1.687	0.091	0.0786	0.0022	0.885	1004	35	933	45	1161	55	115	75	a
0.0916	0.0046	0.819	0.065	0.0649	0.0028		607	33	565	27	770	83	137	60	a
0.1846	0.0092	2.20	0.15	0.0864	0.0029		1181	44	1092	50	1348	58	130	92	a
0.0593	0.0030	0.488	0.035	0.0597	0.0021		404	22	372	18	592	70	127	85	a
0.1316	0.0066	1.361	0.080	0.0750	0.0020		872	33	797	38	1069	52	131	61	a
0.0404	0.0020	0.319	0.022	0.0572	0.0053	0.806	281	17	256	12	500	203	125	60	a
0.1378	0.0069	1.467	0.087	0.0772	0.0021		917	34	832	39	1126	51	111	70	a
0.1564	0.0078	1.77	0.10	0.0820	0.0022		1033	36	937	44	1245	50	124	66	a
0.211	0.011	2.83	0.19	0.0973	0.0030		1364	48	1234	56	1573	55	110	64	a
0.0289	0.0013	0.221	0.011	0.0556	0.0022	0.842	203	9	183	8	437	89	165	70	a
0.00489	0.00026	0.0349	0.0062	0.052	0.018	*	35	6	31	2	279	800	140	85	a
0.0548	0.0036	0.456	0.060	0.0604	0.0050	0.932	382	42	344	22	619	180	150	60	a
0.1658	0.0083	1.96	0.11	0.0858	0.0023		1102	37	989	46	1333	49	134	76	a
0.0452	0.0020	0.368	0.017	0.0590	0.0017	0.591	318	13	285	12	568	61	125	55	a
0.0531	0.0040	0.444	0.072	0.0607	0.0065	0.926	373	50	334	24	627	232	140	60	a
0.0452	0.0062	0.373	0.074	0.0599	0.0057	0.547	322	55	285	38	601	205	120	65	a
0.0328	0.0016	0.262	0.022	0.0578	0.0025		236	16	208	10	522	85	174	95	a

$^{206}Pb^*/^{238}U$	± 2σ (abs)	$^{207}Pb^*/^{235}U$	± 2σ (abs)	$^{207}Pb^*/^{206}Pb^*$	± 2σ (abs)	corr. coef.	$^{206}Pb^*/^{238}U$ age (Ma)	± 2σ (Ma)	$^{207}Pb^*/^{235}U$ age (Ma)	± 2σ (Ma)	$^{207}Pb^*/^{206}Pb^*$ age (Ma)	± 2σ (Ma)	Length (μm)	Width (μm)	Accept/ Reject
0.1055	0.0060	1.058	0.070	0.0728	0.0019	0.863	733	34	646	35	1008	54	175	80	a
0.1199	0.0060	1.267	0.075	0.0766	0.0021		831	32	730	35	1112	51	152	60	a
0.0291	0.0013	0.233	0.016	0.0581	0.0063	0.694	213	14	185	8	534	237	170	75	a
0.212	0.011	3.07	0.34	0.1053	0.0066		1426	80	1237	57	1720	110	116	50	a
0.0765	0.0035	0.757	0.042	0.0717	0.0042	0.921	572	24	475	21	979	119	120	75	a
0.1553	0.0099	2.05	0.15	0.0957	0.0026	0.892	1132	50	931	55	1542	51	140	85	a
0.1334	0.0067	1.65	0.11	0.0898	0.0028		990	39	807	38	1422	55	219	97	a
0.00945	0.00041	0.0765	0.0051	0.0587	0.0059	*	75	5	61	3	555	221	120	55	a
0.0821	0.0041	0.862	0.055	0.0762	0.0021		631	27	508	24	1099	51	201	70	a
0.122	0.012	1.48	0.17	0.0883	0.0025	0.916	922	68	740	71	1389	53	110	70	a
0.0383	0.0016	0.361	0.021	0.0683	0.0053	0.801	313	16	242	10	879	161	125	70	a
0.00449	0.00022	0.038	0.010	0.0606	0.0098		37	9	29	1	626	313	102	71	a
0.0545	0.0024	0.554	0.029	0.0737	0.0038	0.896	448	19	342	15	1033	105	125	110	r
0.0823	0.0045	0.937	0.075	0.0825	0.0091	0.903	671	40	510	27	1258	216	135	55	r
0.0251	0.0030	0.231	0.089	0.067	0.019	0.827	211	74	160	19	838	605	145	75	a
0.103	0.017	1.29	0.25	0.0913	0.0031	0.924	841	109	629	100	1452	65	60	35	r
0.151	0.050	2.36	0.83	0.1130	0.0035	0.971	1229	250	908	279	1848	55	190	90	r
0.0379	0.0024	0.379	0.026	0.0725	0.0027	0.916	326	19	240	15	1001	76	115	60	r
0.1410	0.0071	2.15	0.13	0.1104	0.0030		1164	39	850	40	1806	47	116	71	r
0.0374	0.0016	0.380	0.018	0.0736	0.0022	0.903	327	13	237	10	1032	60	82	60	r
0.0704	0.0031	0.82	0.19	0.085	0.038	0.843	610	106	439	19	1311	862	125	70	r
0.00418	0.00042	0.0381	0.0077	0.0661	0.0073	0.099	38	8	27	3	810	233	100	90	r
0.00346	0.00017	0.033	0.019	0.068	0.024		33	17	22	1	874	674	141	78	r
0.1121	0.0056	1.68	0.15	0.1086	0.0046		1000	53	685	33	1776	73	148	66	r
0.1713	0.0086	3.64	0.49	0.154	0.013		1559	102	1019	47	2394	139	105	85	r
0.0870	0.0068	1.32	0.14	0.1100	0.0041	0.740	854	62	538	41	1799	69	145	80	r
0.102	0.023	1.71	0.43	0.1221	0.0037	0.935	1013	162	624	136	1987	54	120	65	r
0.00794	0.00034	0.0863	0.0089	0.079	0.015	*	84	8	51	2	1168	386	110	70	r
0.00	0.00	0.0035	0.0019	0.081	0.026		4	2	2	0	1218	591	184	88	r
0.0231	0.0012	0.296	0.029	0.0929	0.0040		263	21	147	7	1486	76	184	55	r
0.0547	0.0027	0.85	0.57	0.113	0.039		626	299	343	17	1851	596	131	55	r
0.00476	0.00022	0.0569	0.0057	0.087	0.016	*	56	5	31	1	1353	354	220	80	r
0.095	0.010	1.97	0.23	0.150	0.012	0.960	1105	80	586	61	2349	132	130	80	r
0.0784	0.0050	1.47	0.16	0.1362	0.0068	0.965	919	66	487	30	2180	87	260	80	r
0.01218	0.00064	0.157	0.025	0.094	0.028	*	148	22	78	4	1500	559	115	60	r
0.0261	0.0013	0.375	0.030	0.1043	0.0039		323	20	166	8	1701	61	150	63	r
0.0735	0.0088	1.64	0.81	0.162	0.059	0.942	986	313	457	53	2474	614	175	75	r
0.00296	0.00014	0.0598	0.0048	0.146	0.017	*	59	5	19	1	2305	202	150	70	r
11. Amazon River, Brazil (3.0708°S, 59.7117°W)															
0.00222	0.00012	0.0085	0.0042	0.028	0.026	*	9	4	14	1			265	150	r
0.00581	0.00027	0.0240	0.0052	0.030	0.012	*	24	5	37	2			190	150	r
0.263	0.018	7.04	0.63	0.194	0.011	0.736	2116	80	1505	91	2777	95	200	110	r
0.00564	0.00025	0.0256	0.0023	0.0330	0.0044	*	26	2	36	2			205	95	a
0.00186	0.00010	0.0090	0.0033	0.035	0.024	*	9	3	12	1			145	125	a
0.00883	0.00048	0.0453	0.0071	0.0372	0.0082	*	45	7	57	3			175	135	a
0.00383	0.00018	0.0195	0.0037	0.037	0.013	*	20	4	25	1			150	110	a
0.302	0.019	6.86	0.46	0.1647	0.0048	0.900	2094	60	1702	96	2504	49	150	110	a
0.0379	0.0018	0.235	0.019	0.0451	0.0054	0.778	215	16	240	11	-53	292	330	110	a
0.0393	0.0019	0.251	0.015	0.0462	0.0024	0.869	227	12	249	12	7	127	245	100	a
0.00561	0.00026	0.0330	0.0054	0.043	0.012	*	33	5	36	2			200	105	a
0.1712	0.0094	1.94	0.12	0.0823	0.0026	0.882	1096	42	1019	60	1252	63	185	135	a

$^{206}Pb^*/^{238}U$	± 2σ (abs)	$^{207}Pb^*/^{235}U$	± 2σ (abs)	$^{207}Pb^*/^{206}Pb^*$	± 2σ (abs)	corr. coef.	$^{206}Pb^*/^{238}U$ age (Ma)	± 2σ (Ma)	$^{207}Pb^*/^{235}U$ age (Ma)	± 2σ (Ma)	$^{207}Pb^*/^{206}Pb^*$ age (Ma)	± 2σ (Ma)	Length (μm)	Width (μm)	Accept/ Reject
0.299	0.018	5.41	0.34	0.1314	0.0034	0.921	1887	54	1684	89	2117	46	165	130	a
0.1757	0.0091	1.98	0.11	0.0819	0.0022	0.899	1110	37	1043	50	1244	52	130	140	a
0.231	0.013	3.14	0.19	0.0983	0.0026	0.917	1442	46	1342	83	1593	49	170	105	a
0.235	0.013	3.20	0.20	0.0986	0.0027	0.917	1457	47	1363	85	1597	50	190	140	a
0.1774	0.0092	1.97	0.11	0.0805	0.0022	0.900	1105	37	1053	50	1209	53	230	115	a
0.205	0.012	2.48	0.15	0.0880	0.0025	0.914	1267	45	1200	64	1382	54	145	110	a
0.184	0.010	2.07	0.12	0.0818	0.0022	0.909	1140	39	1087	55	1242	52	220	125	a
0.1197	0.0059	0.992	0.053	0.0601	0.0017	0.876	700	27	729	38	607	61	160	75	a
0.0973	0.0047	0.761	0.040	0.0567	0.0018	0.833	575	23	598	28	482	69	125	100	a
0.0620	0.0029	0.444	0.027	0.0519	0.0034	0.898	373	19	388	17	282	151	145	115	a
0.1806	0.0097	2.00	0.12	0.0804	0.0029	0.873	1116	41	1070	62	1206	72	170	125	a
0.1708	0.0088	1.83	0.11	0.0777	0.0038	0.815	1056	40	1016	48	1138	97	200	110	a
0.1663	0.0085	1.565	0.097	0.0683	0.0037	0.814	957	39	992	47	877	111	170	115	a
0.1723	0.0093	1.84	0.11	0.0776	0.0034	0.844	1061	40	1025	51	1137	87	115	140	a
0.186	0.010	2.08	0.12	0.0809	0.0021	0.910	1141	39	1099	64	1220	52	160	125	a
0.180	0.010	1.97	0.13	0.0794	0.0036	0.847	1105	46	1066	55	1181	91	155	100	a
0.195	0.011	2.23	0.13	0.0830	0.0026	0.896	1191	41	1149	57	1268	61	160	130	a
0.1099	0.0053	0.904	0.050	0.0597	0.0026	0.781	654	27	672	31	591	95	165	115	a
0.193	0.010	2.18	0.13	0.0819	0.0024	0.905	1175	40	1138	57	1242	56	180	95	a
0.0608	0.0028	0.441	0.023	0.0526	0.0021	0.650	371	16	380	17	313	89	150	105	a
0.0966	0.0051	0.772	0.049	0.0579	0.0028	0.755	581	28	594	33	527	106	230	85	a
0.195	0.011	2.19	0.13	0.0818	0.0022	0.910	1179	40	1146	67	1240	54	150	100	a
0.1256	0.0064	1.083	0.060	0.0625	0.0021	0.859	745	29	763	37	693	71	145	100	a
0.1089	0.0059	0.899	0.053	0.0599	0.0017	0.872	651	28	666	38	599	62	160	145	a
0.0734	0.0036	0.552	0.030	0.0545	0.0020	0.748	446	20	456	22	393	82	153	105	a
0.1805	0.0098	1.94	0.11	0.0780	0.0021	0.909	1095	38	1070	53	1147	53	180	110	a
0.195	0.011	2.19	0.13	0.0814	0.0022	0.913	1179	40	1151	67	1231	53	135	90	a
0.216	0.012	2.59	0.15	0.0867	0.0024	0.914	1297	43	1263	64	1354	54	160	110	a
0.199	0.011	2.26	0.13	0.0822	0.0022	0.915	1199	40	1170	58	1250	51	180	125	a
0.206	0.011	2.38	0.15	0.0837	0.0031	0.885	1235	45	1207	73	1285	73	160	95	a
0.0660	0.0036	0.491	0.030	0.0540	0.0016	0.801	406	21	412	23	371	67	130	80	a
0.253	0.014	3.33	0.20	0.0955	0.0027	0.923	1487	48	1452	92	1538	53	205	130	a
0.0687	0.0033	0.516	0.027	0.0545	0.0016	0.776	423	18	428	21	393	68	180	100	a
0.249	0.014	3.22	0.20	0.0939	0.0028	0.918	1462	48	1433	91	1506	56	255	90	a
0.1722	0.0089	1.779	0.097	0.0749	0.0021	0.901	1038	36	1024	49	1067	56	155	125	a
0.0542	0.0026	0.394	0.021	0.0527	0.0019	0.646	337	15	340	16	314	81	170	110	a
0.1616	0.0083	1.567	0.087	0.0704	0.0023	0.882	957	34	965	46	939	66	180	95	a
0.0473	0.0021	0.338	0.016	0.0518	0.0015	0.672	296	12	298	13	279	65	180	80	a
0.1776	0.0092	1.85	0.10	0.0754	0.0020	0.909	1062	36	1054	50	1078	52	220	90	a
0.225	0.013	2.66	0.19	0.0856	0.0040	0.870	1316	53	1309	83	1329	91	125	90	a
0.491	0.048	12.19	1.25	0.1799	0.0051	0.957	2619	96	2577	209	2652	47	105	120	a
0.198	0.011	2.15	0.12	0.0790	0.0021	0.918	1166	40	1162	69	1173	52	155	100	a
0.0862	0.0040	0.689	0.034	0.0580	0.0016	0.830	532	20	533	24	529	59	135	145	a
0.1786	0.0093	1.84	0.10	0.0747	0.0020	0.908	1060	36	1060	51	1062	54	180	110	a
0.1078	0.0052	0.915	0.047	0.0616	0.0017	0.862	660	25	660	30	659	58	126	125	a
0.234	0.014	2.80	0.18	0.0868	0.0024	0.929	1357	48	1356	90	1357	53	200	90	a
0.0819	0.0039	0.649	0.034	0.0574	0.0017	0.811	508	21	508	25	508	64	220	120	a
0.234	0.013	2.80	0.17	0.0867	0.0024	0.922	1355	45	1355	69	1354	54	175	110	a
0.001325	0.000084	0.0085	0.0026	0.046	0.021	*	9	3	9	1	16	1103	135	90	a
0.1673	0.0087	1.682	0.097	0.0729	0.0024	0.881	1002	37	997	48	1011	67	275	115	a
0.1818	0.0099	1.87	0.11	0.0745	0.0025	0.894	1069	39	1077	54	1054	67	150	100	a

$^{206}Pb^*/^{238}U$	± 2σ (abs)	$^{207}Pb^*/^{235}U$	± 2σ (abs)	$^{207}Pb^*/^{206}Pb^*$	± 2σ (abs)	corr. coef.	$^{206}Pb^*/^{238}U$ age (Ma)	± 2σ (Ma)	$^{207}Pb^*/^{235}U$ age (Ma)	± 2σ (Ma)	$^{207}Pb^*/^{206}Pb^*$ age (Ma)	± 2σ (Ma)	Length (μm)	Width (μm)	Accept/ Reject
0.188	0.010	1.96	0.11	0.0756	0.0020	0.919	1102	39	1111	56	1084	53	190	145	a
0.0728	0.0040	0.568	0.032	0.0565	0.0015	0.831	456	21	453	24	473	59	165	115	a
0.191	0.010	1.99	0.11	0.0759	0.0020	0.917	1113	39	1125	56	1091	53	200	90	a
0.0483	0.0023	0.353	0.018	0.0530	0.0016	0.663	307	14	304	14	328	71	195	130	a
0.193	0.010	2.02	0.11	0.0760	0.0020	0.918	1124	38	1139	56	1096	53	170	120	a
0.0509	0.0024	0.375	0.022	0.0535	0.0027	0.903	323	16	320	16	349	114	140	100	a
0.1667	0.0097	1.69	0.10	0.0736	0.0020	0.911	1005	39	994	54	1029	56	155	115	a
0.0549	0.0025	0.410	0.020	0.0541	0.0016	0.712	349	15	345	15	376	65	175	95	a
0.1740	0.0091	1.730	0.098	0.0721	0.0023	0.891	1020	37	1034	58	990	65	270	85	a
0.379	0.026	6.14	0.45	0.1175	0.0036	0.943	1996	64	2071	123	1919	55	155	100	a
0.226	0.013	2.56	0.16	0.0819	0.0023	0.926	1288	46	1315	85	1244	56	150	120	a
0.1006	0.0047	0.855	0.043	0.0617	0.0019	0.825	627	24	618	28	662	66	155	115	a
0.0576	0.0027	0.436	0.022	0.0548	0.0016	0.731	367	16	361	17	404	65	110	115	a
0.216	0.012	2.36	0.14	0.0792	0.0021	0.924	1229	42	1260	63	1177	53	175	135	a
0.0984	0.0047	0.834	0.044	0.0615	0.0019	0.819	616	24	605	27	656	67	180	110	a
0.0455	0.0022	0.333	0.019	0.0531	0.0027	0.888	292	15	287	14	334	114	175	90	a
0.203	0.011	2.14	0.12	0.0764	0.0021	0.921	1162	40	1193	71	1106	54	225	90	a
0.217	0.013	2.36	0.15	0.0789	0.0024	0.920	1231	45	1266	80	1170	60	165	110	a
0.206	0.012	2.17	0.13	0.0765	0.0022	0.920	1172	42	1208	62	1107	57	135	80	a
0.248	0.015	2.87	0.18	0.0838	0.0026	0.924	1374	48	1430	75	1289	61	95	95	a
0.204	0.011	2.13	0.13	0.0757	0.0031	0.882	1157	43	1195	60	1087	82	245	95	a
0.1549	0.0078	1.548	0.082	0.0725	0.0019	0.896	950	33	928	44	1000	53	190	120	a
0.0423	0.0020	0.310	0.015	0.0531	0.0018	0.534	274	12	267	12	334	76	245	135	a
0.274	0.016	3.28	0.20	0.0867	0.0023	0.940	1476	48	1563	102	1355	51	220	115	a
0.192	0.011	1.91	0.12	0.0721	0.0022	0.910	1084	41	1132	68	989	63	110	85	a
0.0267	0.0012	0.189	0.013	0.0513	0.0049	0.705	175	11	170	8	254	218	160	150	a
0.256	0.015	2.87	0.18	0.0814	0.0022	0.937	1374	47	1467	95	1232	54	250	130	a
0.1591	0.0081	1.641	0.088	0.0748	0.0020	0.897	986	34	952	52	1063	53	170	130	a
0.245	0.016	2.68	0.19	0.0794	0.0026	0.929	1324	51	1412	82	1183	65	165	80	a
0.211	0.012	2.16	0.13	0.0743	0.0020	0.926	1168	41	1233	62	1049	55	140	105	a
0.205	0.012	2.07	0.13	0.0734	0.0024	0.911	1140	42	1202	63	1025	67	106	90	a
0.1507	0.0076	1.522	0.081	0.0732	0.0019	0.892	939	33	905	43	1020	53	130	85	a
0.231	0.014	2.46	0.15	0.0771	0.0020	0.936	1260	45	1342	72	1123	53	120	105	a
0.1597	0.0081	1.657	0.090	0.0752	0.0022	0.885	992	34	955	45	1074	58	210	125	a
0.256	0.015	2.84	0.18	0.0803	0.0023	0.936	1366	47	1472	95	1205	55	125	100	a
0.1505	0.0076	1.527	0.082	0.0736	0.0022	0.875	941	33	904	42	1029	61	180	160	a
0.190	0.011	1.85	0.12	0.0705	0.0036	0.857	1064	44	1124	58	944	104	155	125	a
0.0622	0.0030	0.490	0.034	0.0572	0.0045	0.896	405	23	389	19	499	172	270	120	a
0.304	0.019	3.53	0.23	0.0843	0.0025	0.943	1534	52	1710	93	1300	58	105	60	a
0.226	0.013	2.33	0.15	0.0747	0.0022	0.930	1222	45	1316	84	1061	59	155	100	a
0.0788	0.0037	0.660	0.035	0.0608	0.0022	0.734	515	21	489	22	632	77	130	135	a
0.273	0.016	2.90	0.19	0.0770	0.0026	0.932	1382	50	1557	82	1121	68	160	120	a
0.362	0.024	4.04	0.30	0.0808	0.0026	0.954	1641	60	1992	153	1218	64	120	70	a
0.1603	0.0084	1.716	0.094	0.0776	0.0021	0.895	1014	35	959	46	1137	53	170	160	a
0.309	0.021	3.31	0.24	0.0778	0.0022	0.955	1484	57	1735	105	1142	57	105	145	a
0.1634	0.0083	1.770	0.095	0.0786	0.0021	0.894	1034	35	976	46	1161	53	210	135	a
0.1603	0.0081	1.721	0.092	0.0779	0.0022	0.885	1017	34	958	45	1144	56	175	140	a
0.1178	0.0061	1.122	0.063	0.0691	0.0019	0.863	764	30	718	39	902	57	150	100	a
0.195	0.011	1.80	0.17	0.0673	0.0079	0.665	1047	63	1146	58	846	245	180	100	a
0.1805	0.0099	1.621	0.094	0.0651	0.0018	0.921	978	36	1069	54	779	59	115	80	a
0.1489	0.0075	1.574	0.087	0.0767	0.0029	0.836	960	34	895	42	1112	75	175	125	a

$^{206}Pb^*/^{238}U$	± 2σ (abs)	$^{207}Pb^*/^{235}U$	± 2σ (abs)	$^{207}Pb^*/^{206}Pb^*$	± 2σ (abs)	corr. coef.	$^{206}Pb^*/^{238}U$ age (Ma)	± 2σ (Ma)	$^{207}Pb^*/^{235}U$ age (Ma)	± 2σ (Ma)	$^{207}Pb^*/^{206}Pb^*$ age (Ma)	± 2σ (Ma)	Length (μm)	Width (μm)	Accept/ Reject
0.151	0.010	1.61	0.11	0.0772	0.0022	0.909	974	44	908	57	1127	56	180	90	a
0.00408	0.00019	0.0282	0.0017	0.0501	0.0035	*	28	2	26	1	200	161	210	125	a
0.0730	0.0036	0.619	0.038	0.0615	0.0033	0.557	489	24	454	23	658	113	110	105	a
0.0462	0.0021	0.368	0.022	0.0578	0.0031	0.885	318	16	291	13	523	118	195	150	a
0.0269	0.0012	0.206	0.016	0.0556	0.0062	0.691	190	14	171	8	437	250	180	135	a
0.01411	0.00082	0.104	0.012	0.054	0.010	0.267	101	11	90	5	355	425	205	160	a
0.187	0.010	1.508	0.090	0.0586	0.0017	0.930	933	36	1104	66	551	62	100	95	a
0.0479	0.0023	0.402	0.030	0.0609	0.0049	0.866	343	21	301	15	636	174	125	90	a
0.0641	0.0033	0.570	0.053	0.0645	0.0078	0.882	458	34	400	21	759	255	280	140	a
0.0392	0.0018	0.341	0.023	0.0631	0.0051	0.822	298	17	248	11	713	172	200	140	a
0.0391	0.0018	0.341	0.035	0.063	0.010	0.772	298	26	247	11	717	336	190	105	a
0.0388	0.0018	0.347	0.026	0.0649	0.0065	0.804	302	20	245	11	770	210	160	95	a
0.00790	0.00043	0.064	0.014	0.059	0.023	*	63	14	51	3	553	842	175	100	a
0.1632	0.0087	2.40	0.24	0.107	0.015	0.950	1242	72	974	48	1743	258	190	115	a
0.0783	0.0045	0.843	0.090	0.078	0.011	0.900	621	49	486	27	1148	286	115	100	a
0.1168	0.0059	1.493	0.082	0.0928	0.0025	0.820	928	33	712	38	1483	51	160	95	r
0.01296	0.00061	0.116	0.011	0.0652	0.0087	0.289	112	10	83	4	781	282	220	120	r
0.0430	0.0023	0.502	0.065	0.085	0.017	0.792	413	44	271	14	1306	391	152	140	r
0.00928	0.00045	0.0937	0.0095	0.073	0.011	*	91	9	60	3	1020	304	210	85	r
0.0380	0.0018	0.485	0.034	0.0926	0.0079	0.816	401	23	240	11	1479	162	180	115	r
0.00302	0.00016	0.0350	0.0070	0.084	0.031	*	35	7	19	1	1296	715	245	120	r
0.00209	0.00029	0.025	0.023	0.09	0.14	*	25	23	13	2	1334	3115	205	100	r
0.00213	0.00013	0.0265	0.0060	0.090	0.037	*	27	6	14	1	1428	784	165	115	r
0.01495	0.00085	0.210	0.033	0.102	0.026	0.296	194	27	96	5	1659	477	165	110	r
0.132	0.010	6.18	0.59	0.339	0.019	0.973	2002	83	800	57	3659	88	80	85	r
0.0934	0.0061	3.48	0.30	0.271	0.018	0.950	1523	68	575	36	3309	107	170	75	r
0.00	0.00	0.015	0.020	0.28	0.43	*	15	20	2	1	3364	2387	175	110	r
0.0084	0.0019	0.46	0.30	0.39	0.42	*	383	211	54	12	3890	1598	70	60	r
12. Amazon River, Brazil (3.2162°S, 59.2255°W)															
0.00966	0.00048	0.0389	0.0077	0.0292	0.0036		39	8	62	3			113	92	r
0.230	0.012	5.39	0.34	0.1703	0.0046	0.847	1883	54	1332	64	2561	45	130	80	r
0.1766	0.0093	2.79	0.17	0.1144	0.0033	0.855	1352	46	1049	51	1870	52	175	75	a
0.175	0.017	2.60	0.39	0.108	0.010	0.747	1301	110	1039	93	1762	170	135	45	a
0.236	0.012	4.55	0.29	0.1401	0.0040	0.870	1741	52	1365	65	2228	49	110	75	a
0.203	0.010	3.02	0.25	0.1079	0.0061	0.749	1413	63	1191	55	1765	103	140	95	a
0.233	0.012	3.81	0.23	0.1186	0.0032	0.889	1595	48	1350	62	1935	49	125	95	a
0.248	0.013	4.34	0.26	0.1268	0.0033	0.893	1701	49	1430	65	2054	46	100	85	a
0.223	0.011	3.33	0.20	0.1081	0.0033	0.875	1487	48	1298	57	1768	56	130	100	a
0.201	0.014	2.73	0.21	0.0983	0.0027	0.919	1335	57	1181	74	1592	51	110	95	a
0.216	0.011	3.09	0.19	0.1039	0.0031	0.882	1429	48	1258	58	1695	55	115	70	a
0.1681	0.0099	1.97	0.14	0.0850	0.0030	0.875	1105	48	1002	55	1314	68	80	85	a
0.0438	0.0023	0.278	0.031	0.0461	0.0042	0.890	249	24	276	14	0	218	90	95	a
0.200	0.011	2.64	0.17	0.0956	0.0027	0.900	1311	47	1176	60	1540	53	180	70	a
0.362	0.020	9.50	0.63	0.1902	0.0050	0.900	2387	61	1993	96	2744	44	220	85	a
0.254	0.013	4.13	0.25	0.1178	0.0031	0.902	1660	49	1461	66	1922	47	145	115	a
0.215	0.011	2.92	0.22	0.0988	0.0042	0.849	1388	56	1253	61	1601	79	145	65	a
0.1112	0.0057	0.864	0.053	0.0564	0.0018	0.866	632	29	679	33	468	69	115	75	a
0.260	0.013	4.09	0.24	0.1142	0.0030	0.906	1652	48	1488	67	1867	47	120	70	a
0.1703	0.0085	1.55	0.25	0.0659	0.0080		950	101	1014	47	804	254	150	63	a
0.273	0.014	4.43	0.27	0.1176	0.0031	0.909	1718	50	1557	71	1920	48	120	85	a
0.234	0.012	2.52	0.22	0.0779	0.0049		1277	64	1358	62	1144	125	123	53	a

$^{206}Pb^*/^{238}U$	± 2σ (abs)	$^{207}Pb^*/^{235}U$	± 2σ (abs)	$^{207}Pb^*/^{206}Pb^*$	± 2σ (abs)	corr. coef.	$^{206}Pb^*/^{238}U$ age (Ma)	± 2σ (Ma)	$^{207}Pb^*/^{235}U$ age (Ma)	± 2σ (Ma)	$^{207}Pb^*/^{206}Pb^*$ age (Ma)	± 2σ (Ma)	Length (μm)	Width (μm)	Accept/ Reject
0.224	0.011	3.01	0.22	0.0974	0.0044	0.839	1409	55	1303	59	1574	84	145	110	a
0.1781	0.0083	2.02	0.11	0.0824	0.0022	0.890	1123	37	1057	46	1254	52	125	90	a
0.1287	0.0080	1.071	0.081	0.0603	0.0022	0.880	739	40	780	46	616	80	100	75	a
0.200	0.010	2.43	0.15	0.0882	0.0026	0.896	1253	45	1176	56	1387	57	115	65	a
0.231	0.011	3.12	0.18	0.0980	0.0027	0.903	1437	45	1338	60	1587	51	160	75	a
0.0936	0.0047	0.719	0.049	0.0557	0.0026		550	29	577	28	440	105	129	76	a
0.227	0.011	2.99	0.18	0.0953	0.0026	0.907	1404	45	1320	60	1535	51	120	90	a
0.233	0.013	3.13	0.20	0.0973	0.0027	0.914	1441	49	1353	68	1573	52	130	65	a
0.201	0.012	2.41	0.16	0.0869	0.0024	0.916	1245	48	1181	63	1358	52	95	90	a
0.1853	0.0088	2.10	0.12	0.0823	0.0023	0.892	1150	39	1096	48	1252	54	115	90	a
0.1715	0.0097	1.83	0.12	0.0772	0.0021	0.909	1055	42	1020	53	1127	54	125	110	a
0.1993	0.0100	2.06	0.13	0.0749	0.0034		1135	43	1171	54	1067	91	170	99	a
0.259	0.014	3.65	0.23	0.1021	0.0028	0.915	1561	50	1486	70	1663	51	100	90	a
0.1040	0.0050	0.841	0.071	0.0586	0.0037	0.657	620	39	638	29	554	139	150	90	a
0.1909	0.0094	2.14	0.12	0.0814	0.0022	0.901	1162	40	1126	51	1230	54	160	100	a
0.302	0.019	4.81	0.34	0.1154	0.0031	0.931	1787	59	1703	92	1886	49	90	80	a
0.0407	0.0019	0.280	0.024	0.0500	0.0033	0.890	251	19	257	12	194	151	155	80	a
0.1777	0.0096	1.90	0.16	0.0776	0.0044	0.806	1082	55	1054	53	1137	113	90	90	a
0.1758	0.0086	1.86	0.11	0.0768	0.0020	0.899	1067	38	1044	47	1115	53	130	80	a
0.1058	0.0049	0.872	0.049	0.0598	0.0017	0.845	637	26	648	28	596	63	120	70	a
0.1886	0.0090	2.06	0.12	0.0794	0.0021	0.901	1137	39	1114	49	1181	53	140	65	a
0.1726	0.0086	1.79	0.11	0.0754	0.0026	0.873	1043	41	1026	47	1079	69	110	75	a
0.1874	0.0094	1.93	0.12	0.0749	0.0033		1093	41	1107	51	1066	88	108	98	a
0.1942	0.0094	2.12	0.12	0.0793	0.0021	0.904	1157	39	1144	51	1180	54	110	85	a
0.1774	0.0085	1.85	0.11	0.0754	0.0024	0.880	1062	40	1053	46	1080	64	110	80	a
0.1395	0.0070	1.28	0.19	0.0666	0.0072		837	83	842	40	824	225	144	82	a
0.209	0.010	2.31	0.13	0.0802	0.0033		1214	41	1221	56	1202	80	109	78	a
0.0912	0.0046	0.735	0.045	0.0585	0.0024		560	26	562	27	549	91	100	64	a
0.336	0.020	5.36	0.38	0.1158	0.0033	0.931	1878	60	1865	95	1892	52	125	70	a
0.0355	0.0017	0.248	0.015	0.0506	0.0018	0.902	225	12	225	10	225	83	160	85	a
0.0411	0.0020	0.292	0.035	0.0515	0.0051	0.882	260	27	260	12	265	227	190	75	a
0.0917	0.0042	0.748	0.047	0.0591	0.0022	0.773	567	27	566	25	572	80	180	75	a
0.1312	0.0063	1.192	0.079	0.0659	0.0027	0.819	797	37	795	36	803	85	140	90	a
0.1631	0.0082	1.618	0.094	0.0719	0.0030		977	36	974	45	984	85	164	71	a
0.1520	0.0076	1.467	0.086	0.0700	0.0029		917	35	912	43	927	86	103	57	a
0.0495	0.0023	0.361	0.028	0.0529	0.0031	0.910	313	21	312	14	324	134	280	64	a
0.0862	0.0046	0.695	0.046	0.0585	0.0021	0.803	536	27	533	27	549	77	170	70	a
0.188	0.016	1.96	0.20	0.0757	0.0035	0.908	1101	67	1109	87	1086	92	140	70	a
0.0584	0.0026	0.438	0.029	0.0544	0.0025	0.524	369	21	366	16	387	102	120	90	a
0.193	0.010	2.02	0.13	0.0762	0.0024	0.902	1123	44	1135	56	1099	63	100	80	a
0.1810	0.0090	1.90	0.14	0.0763	0.0041		1082	48	1072	50	1102	108	187	84	a
0.1191	0.0065	1.057	0.099	0.0643	0.0044	0.697	732	49	725	38	753	145	115	65	a
0.0511	0.0026	0.377	0.024	0.0535	0.0022		325	18	321	16	351	93	134	80	a
0.0548	0.0027	0.409	0.037	0.0541	0.0033		348	27	344	17	374	139	165	62	a
0.0464	0.0022	0.338	0.024	0.0529	0.0027	0.911	296	18	293	13	323	115	120	65	a
0.1658	0.0079	1.679	0.097	0.0735	0.0022	0.885	1001	37	989	44	1027	59	130	105	a
0.0479	0.0023	0.352	0.019	0.0532	0.0014	0.713	306	15	302	14	338	60	105	75	a
0.235	0.012	2.91	0.18	0.0897	0.0037		1383	46	1361	62	1419	79	152	78	a
0.0562	0.0027	0.425	0.025	0.0548	0.0017	0.711	359	18	353	16	403	68	140	70	a
0.0525	0.0026	0.393	0.028	0.0543	0.0026		336	20	330	16	383	107	139	67	a
0.1631	0.0082	1.669	0.094	0.0742	0.0030		997	36	974	45	1048	81	163	72	a

$^{206}Pb^*/^{238}U$	± 2σ (abs)	$^{207}Pb^*/^{235}U$	± 2σ (abs)	$^{207}Pb^*/^{206}Pb^*$	± 2σ (abs)	corr. coef.	$^{206}Pb^*/^{238}U$ age (Ma)	± 2σ (Ma)	$^{207}Pb^*/^{235}U$ age (Ma)	± 2σ (Ma)	$^{207}Pb^*/^{206}Pb^*$ age (Ma)	± 2σ (Ma)	Length (μm)	Width (μm)	Accept/ Reject
0.1846	0.0092	2.01	0.20	0.0789	0.0059		1118	68	1092	50	1170	149	107	70	a
0.0429	0.0020	0.314	0.021	0.0531	0.0024	0.908	277	16	271	12	334	104	140	85	a
0.208	0.011	2.19	0.15	0.0762	0.0026	0.904	1178	48	1221	60	1101	68	90	80	a
0.0372	0.0016	0.269	0.016	0.0524	0.0019	0.903	242	13	236	10	303	83	80	45	a
0.0679	0.0030	0.535	0.029	0.0572	0.0016	0.761	435	19	423	18	500	62	125	110	a
0.232	0.012	2.91	0.17	0.0909	0.0036		1385	44	1346	61	1446	76	153	61	a
0.1569	0.0073	1.592	0.090	0.0736	0.0022	0.874	967	35	940	40	1030	60	110	105	a
0.0845	0.0042	0.699	0.044	0.0600	0.0026		538	26	523	25	605	93	179	85	a
0.1603	0.0076	1.644	0.094	0.0744	0.0021	0.884	987	36	958	42	1052	57	110	95	a
0.0361	0.0016	0.262	0.014	0.0526	0.0015	0.522	236	11	229	10	309	65	105	100	a
0.253	0.013	3.39	0.22	0.0971	0.0041		1502	50	1455	65	1568	80	81	50	a
0.1780	0.0089	1.93	0.11	0.0785	0.0032		1090	37	1056	49	1159	80	90	82	a
0.248	0.012	3.28	0.20	0.0958	0.0038		1475	46	1429	64	1543	75	110	81	a
0.1105	0.0055	0.988	0.058	0.0649	0.0026		698	29	676	32	770	86	91	76	a
0.1423	0.0065	1.394	0.078	0.0711	0.0021	0.860	887	33	858	37	959	61	110	85	a
0.0387	0.0017	0.283	0.015	0.0530	0.0015	0.546	253	12	244	11	330	66	125	110	a
0.0394	0.0020	0.289	0.018	0.0532	0.0021		258	14	249	12	337	91	113	93	a
0.0386	0.0019	0.283	0.021	0.0532	0.0027	0.896	253	17	244	12	337	116	130	85	a
0.0376	0.0019	0.275	0.019	0.0531	0.0024		247	15	238	12	331	104	142	91	a
0.0622	0.0029	0.488	0.032	0.0569	0.0024	0.583	403	22	389	17	487	95	110	70	a
0.1731	0.0087	1.86	0.11	0.0781	0.0034		1069	40	1029	48	1150	88	106	66	a
0.0398	0.0018	0.294	0.016	0.0536	0.0016	0.570	262	13	252	11	354	66	155	75	a
0.0763	0.0034	0.626	0.043	0.0595	0.0028	0.611	494	27	474	21	584	103	135	90	a
0.1842	0.0092	2.06	0.12	0.0810	0.0034		1134	39	1090	50	1221	81	98	103	a
0.1391	0.0063	1.367	0.074	0.0713	0.0019	0.871	875	32	839	36	966	55	100	90	a
0.0327	0.0016	0.238	0.028	0.0528	0.0042		217	23	208	10	320	179	105	85	a
0.1805	0.0090	2.01	0.12	0.0807	0.0035		1118	41	1070	49	1213	86	193	76	a
0.1625	0.0076	1.717	0.099	0.0766	0.0024	0.868	1015	37	971	42	1112	62	120	95	a
0.1561	0.0074	1.621	0.090	0.0753	0.0020	0.885	978	35	935	41	1077	53	115	95	a
0.1567	0.0074	1.639	0.091	0.0758	0.0020	0.885	985	35	938	41	1091	53	155	95	a
0.1506	0.0069	1.550	0.084	0.0746	0.0020	0.879	950	33	904	39	1059	53	135	100	a
0.1073	0.0054	0.974	0.066	0.0659	0.0031		691	34	657	31	802	99	155	64	a
0.0294	0.0013	0.213	0.012	0.0527	0.0016	0.893	196	10	187	8	316	69	175	800	a
0.1472	0.0071	1.506	0.085	0.0742	0.0020	0.880	933	35	885	40	1047	55	105	75	a
0.1450	0.0066	1.489	0.082	0.0745	0.0021	0.864	926	34	873	37	1055	57	130	100	a
0.1436	0.0066	1.470	0.080	0.0743	0.0020	0.875	918	33	865	37	1049	53	135	80	a
0.1264	0.0063	1.231	0.083	0.0706	0.0034		815	38	767	36	947	99	153	70	a
0.1552	0.0078	1.65	0.17	0.0772	0.0060		990	67	930	43	1126	155	106	78	a
0.1192	0.0055	1.142	0.064	0.0695	0.0020	0.844	773	30	726	32	913	59	175	65	a
0.1670	0.0079	1.84	0.10	0.0801	0.0022	0.883	1061	37	995	44	1199	54	125	70	a
0.1434	0.0072	1.480	0.086	0.0749	0.0020	0.882	922	35	864	41	1065	54	130	70	a
0.216	0.011	2.78	0.17	0.0931	0.0041		1349	47	1263	58	1489	83	103	86	a
0.0793	0.0038	0.681	0.045	0.0622	0.0026	0.686	527	27	492	23	682	89	105	90	a
0.0288	0.0013	0.213	0.014	0.0537	0.0024	0.866	196	12	183	8	359	101	110	85	a
0.1203	0.0064	1.169	0.074	0.0705	0.0022	0.855	786	35	732	37	942	63	215	55	a
0.1457	0.0073	1.528	0.094	0.0761	0.0033		942	38	877	41	1098	88	123	80	a
0.1828	0.0091	2.15	0.12	0.0851	0.0034		1164	39	1082	50	1319	78	136	94	a
0.0817	0.0037	0.709	0.041	0.0630	0.0021	0.747	544	24	506	22	708	70	100	105	a
0.1396	0.0063	1.447	0.077	0.0752	0.0020	0.868	909	32	842	36	1074	53	130	95	a
0.1557	0.0078	1.71	0.10	0.0797	0.0034		1013	38	933	44	1190	85	104	67	a
0.0869	0.0042	0.779	0.054	0.0650	0.0029	0.685	585	31	537	25	774	95	110	55	a

$^{206}Pb^*/^{238}U$	± 2σ (abs)	$^{207}Pb^*/^{235}U$	± 2σ (abs)	$^{207}Pb^*/^{206}Pb^*$	± 2σ (abs)	corr. coef.	$^{206}Pb^*/^{238}U$ age (Ma)	± 2σ (Ma)	$^{207}Pb^*/^{235}U$ age (Ma)	± 2σ (Ma)	$^{207}Pb^*/^{206}Pb^*$ age (Ma)	± 2σ (Ma)	Length (μm)	Width (μm)	Accept/ Reject
0.1455	0.0073	1.565	0.089	0.0780	0.0032		956	35	876	41	1147	81	187	73	a
0.275	0.014	4.39	0.27	0.1158	0.0047		1711	51	1567	70	1893	72	131	76	a
0.0378	0.0017	0.293	0.022	0.0563	0.0031	0.889	261	18	239	11	465	122	100	80	a
0.1290	0.0064	1.32	0.14	0.0743	0.0056		855	59	782	37	1049	152	120	56	a
0.305	0.015	5.35	2.13	0.127	0.036		1876	340	1714	76	2062	493	102	43	a
0.204	0.010	2.64	0.17	0.0938	0.0042		1311	46	1197	55	1503	84	126	74	a
0.0201	0.0010	0.149	0.014	0.0536	0.0032		141	12	129	6	353	134	135	95	a
0.0373	0.0017	0.290	0.017	0.0564	0.0018	0.914	258	13	236	11	469	72	125	85	a
0.01492	0.00071	0.1086	0.0078	0.0528	0.0026	0.738	105	7	95	5	320	111	150	70	a
0.1396	0.0064	1.488	0.084	0.0773	0.0023	0.845	926	34	843	36	1129	60	180	95	a
0.1650	0.0083	1.90	0.14	0.0836	0.0044		1082	48	985	46	1283	102	101	74	a
0.332	0.017	6.41	0.99	0.140	0.014		2034	136	1848	81	2228	172	86	59	a
0.1311	0.0063	1.387	0.081	0.0767	0.0024	0.839	883	34	794	36	1114	62	140	95	a
0.0315	0.0016	0.246	0.019	0.0567	0.0029		224	16	200	10	480	112	188	75	a
0.1359	0.0069	1.471	0.090	0.0785	0.0025	0.848	919	37	821	39	1161	62	125	65	a
0.0749	0.0036	0.673	0.059	0.0651	0.0045	0.939	522	36	466	21	778	146	90	65	a
0.0900	0.0045	0.849	0.090	0.0684	0.0057	0.948	624	49	556	27	882	173	160	70	a
0.00367	0.00019	0.0265	0.0058	0.052	0.010	*	27	6	24	1	301	454	110	85	a
0.0243	0.0013	0.188	0.021	0.0561	0.0051	0.810	175	18	155	8	458	200	110	95	a
0.0394	0.0019	0.324	0.024	0.0596	0.0030	0.900	285	18	249	12	590	109	130	30	a
0.01118	0.00056	0.084	0.013	0.0546	0.0055		82	13	72	4	396	227	132	76	a
0.02009	0.00093	0.157	0.011	0.0567	0.0025	0.812	148	9	128	6	480	98	150	80	a
0.1679	0.0084	2.23	0.22	0.0963	0.0071		1190	70	1001	47	1553	139	160	75	a
0.0230	0.0011	0.189	0.016	0.0597	0.0038	0.810	176	13	146	7	592	137	150	70	a
0.0810	0.0041	0.825	0.054	0.0739	0.0033		611	30	502	24	1039	91	100	77	a
0.1385	0.0069	1.74	0.15	0.0911	0.0058		1023	56	836	39	1448	121	94	73	a
0.00337	0.00017	0.0267	0.0053	0.0576	0.0073		27	5	22	1	513	277	70	136	a
0.1341	0.0095	1.69	0.13	0.0914	0.0026	0.887	1005	49	811	54	1456	53	160	60	a
0.0223	0.0014	0.194	0.022	0.0631	0.0053	0.812	180	19	142	9	711	178	155	80	a
0.1443	0.0072	1.97	0.16	0.0990	0.0059		1105	56	869	41	1605	111	110	99	a
0.00403	0.00020	0.033	0.011	0.059	0.013		33	11	26	1	584	457	146	77	a
0.1403	0.0084	1.89	0.19	0.0979	0.0069	0.626	1079	66	846	48	1584	131	100	70	a
0.00849	0.00042	0.072	0.016	0.0616	0.0087		71	15	54	3	661	301	136	53	a
0.01262	0.00060	0.113	0.012	0.0649	0.0055	0.633	109	11	81	4	772	178	125	55	r
0.0340	0.0017	0.338	0.092	0.072	0.013		295	70	215	11	989	377	134	66	r
0.00675	0.00045	0.063	0.030	0.068	0.030	0.021	62	29	43	3	865	921	100	90	a
0.0740	0.0039	0.928	0.057	0.0910	0.0026	0.702	666	30	460	23	1446	54	120	75	r
0.01301	0.00065	0.127	0.027	0.0709	0.0096		122	24	83	4	954	276	143	82	r
0.0808	0.0040	1.06	0.18	0.095	0.011		734	87	501	24	1532	220	104	87	r
0.00584	0.00029	0.0561	0.0089	0.0697	0.0096	*	55	9	38	2	918	285	115	60	r
0.00673	0.00034	0.067	0.024	0.072	0.016		66	22	43	2	997	457	128	65	r
0.0353	0.0016	0.445	0.054	0.0914	0.0094	0.861	374	38	224	10	1454	197	90	95	r
0.00868	0.00066	0.097	0.015	0.0807	0.0093	0.470	94	13	56	4	1214	226	90	75	r
0.00244	0.00031	0.032	0.018	0.096	0.045	*	32	17	16	2	1543	881	160	100	r
0.00143	0.00032	0.019	0.028	0.10	0.12	*	19	28	9	2	1547	2426	175	85	r
0.00171	0.00013	0.0266	0.0073	0.113	0.028	*	27	7	11	1	1841	442	95	85	r
0.00481	0.00033	0.077	0.013	0.117	0.015	*	76	12	31	2	1906	233	125	110	r
0.0630	0.0031	1.99	0.42	0.230	0.034		1113	142	394	19	3049	239	96	83	r
0.0547	0.0096	1.63	0.56	0.217	0.055	0.921	983	214	343	59	2956	407	155	85	r
0.0599	0.0046	2.01	0.51	0.243	0.053	0.917	1118	173	375	28	3141	345	155	75	r
0.00041	0.00048	0.012	0.036	0.20	0.35	*	12	36	3	3	2862	2781	144	94	r

$^{206}Pb^*/^{238}U$	± 2σ (abs)	$^{207}Pb^*/^{235}U$	± 2σ (abs)	$^{207}Pb^*/^{206}Pb^*$	± 2σ (abs)	corr. coef.	$^{206}Pb^*/^{238}U$ age (Ma)	± 2σ (Ma)	$^{207}Pb^*/^{235}U$ age (Ma)	± 2σ (Ma)	$^{207}Pb^*/^{206}Pb^*$ age (Ma)	± 2σ (Ma)	Length (μm)	Width (μm)	Accept/ Reject
13. Rio Amazons, Brazil (3.3743°S, 58.7234°W)															
0.344	0.017	4.46	0.49	0.0940	0.0037		1723	90	1906	83	1507	74	121	83	a
0.1299	0.0065	1.02	0.14	0.0572	0.0047		716	71	787	37	500	179	103	67	a
0.340	0.017	4.57	0.40	0.0974	0.0025		1744	73	1888	82	1575	49	83	51	a
0.1361	0.0068	1.126	0.073	0.0600	0.0017		766	35	823	39	604	62	115	74	a
0.1767	0.0088	1.63	0.11	0.0667	0.0018		980	43	1049	49	829	56	94	60	a
0.254	0.013	2.86	0.21	0.0815	0.0022		1371	56	1461	66	1233	53	94	82	a
0.251	0.013	2.81	0.30	0.0812	0.0033		1359	81	1446	65	1225	80	111	60	a
0.1287	0.0064	1.064	0.071	0.0600	0.0019		736	35	780	37	603	67	138	59	a
0.0581	0.0029	0.407	0.028	0.0508	0.0018		347	20	364	18	232	84	115	82	a
0.378	0.019	5.97	0.61	0.1144	0.0031		1971	89	2068	89	1871	49	97	67	a
0.211	0.011	2.22	0.16	0.0762	0.0021		1188	50	1237	57	1100	55	123	54	a
0.1990	0.0099	2.04	0.17	0.0744	0.0025		1130	56	1170	54	1053	68	79	55	a
0.0546	0.0027	0.386	0.022	0.0513	0.0014		332	16	343	17	255	61	122	98	a
0.234	0.012	2.67	0.19	0.0827	0.0022		1319	53	1355	61	1262	51	114	69	a
0.0559	0.0028	0.401	0.024	0.0521	0.0016		342	18	351	17	288	70	167	85	a
0.259	0.013	3.19	0.26	0.0894	0.0026		1454	62	1483	67	1412	55	14	49	a
0.1716	0.0086	1.68	0.13	0.0711	0.0023		1001	48	1021	47	959	67	135	65	a
0.249	0.012	3.04	0.22	0.0887	0.0023		1419	56	1433	65	1397	50	106	71	a
0.1147	0.0057	0.983	0.060	0.0621	0.0017		695	31	700	33	678	58	125	69	a
0.1127	0.0056	0.961	0.063	0.0619	0.0019		684	33	688	33	669	67	116	71	a
0.0330	0.0017	0.228	0.020	0.0500	0.0028		208	17	209	10	193	129	161	102	a
0.0817	0.0041	0.651	0.039	0.0578	0.0016		509	24	506	24	522	62	139	65	a
0.0820	0.0041	0.667	0.039	0.0590	0.0016		519	24	508	24	567	58	114	108	a
0.0849	0.0042	0.697	0.049	0.0596	0.0022		537	30	525	25	588	80	143	79	a
0.0714	0.0036	0.57	0.11	0.0574	0.0072		455	70	445	22	508	276	109	53	a
0.1786	0.0089	1.91	0.14	0.0777	0.0024		1085	49	1059	49	1138	62	95	63	a
0.0897	0.0045	0.751	0.046	0.0607	0.0018		569	27	554	27	628	64	109	93	a
0.0539	0.0027	0.409	0.026	0.0551	0.0018		348	18	338	17	416	71	131	56	a
0.244	0.012	3.20	0.23	0.0950	0.0025		1456	56	1408	64	1528	50	150	71	a
0.0971	0.0049	0.840	0.051	0.0627	0.0017		619	28	597	29	699	58	116	86	a
0.1583	0.0079	1.64	0.11	0.0752	0.0020		986	41	948	44	1073	52	124	95	a
0.1531	0.0077	1.57	0.11	0.0743	0.0023		958	44	918	43	1051	62	121	63	a
0.305	0.015	4.83	0.44	0.1150	0.0034		1791	76	1716	76	1879	53	76	69	a
0.1626	0.0081	1.72	0.12	0.0768	0.0024		1017	46	971	45	1116	61	97	69	a
0.1350	0.0067	1.34	0.11	0.0720	0.0033		863	50	816	38	985	94	139	98	a
0.0752	0.0038	0.628	0.038	0.0606	0.0017		495	23	468	23	625	61	160	90	a
0.1789	0.0089	2.04	0.14	0.0825	0.0023		1127	47	1061	49	1257	54	75	69	a
0.311	0.016	5.25	0.43	0.1223	0.0032		1861	70	1748	77	1990	46	77	58	a
0.282	0.014	4.40	0.46	0.1130	0.0043		1712	86	1603	71	1849	68	128	66	a
0.296	0.015	4.79	0.45	0.1176	0.0037		1784	79	1670	74	1920	56	93	80	a
0.1061	0.0053	0.984	0.068	0.0673	0.0022		696	35	650	31	847	69	140	53	a
0.1734	0.0087	1.97	0.13	0.0825	0.0022		1106	46	1031	48	1258	53	98	67	a
0.01225	0.00061	0.0867	0.0081	0.0513	0.0031		84	8	79	4	255	140	129	60	a
0.1516	0.0076	1.63	0.12	0.0780	0.0025		982	46	910	43	1147	65	103	57	a
0.0418	0.0021	0.324	0.024	0.0563	0.0024		285	19	264	13	462	96	133	65	a
0.0279	0.0014	0.209	0.023	0.0545	0.0040		193	19	177	9	390	164	122	70	a
0.0796	0.0040	0.703	0.048	0.0640	0.0023		541	29	494	24	743	76	89	68	a
0.1053	0.0053	1.008	0.067	0.0694	0.0023		708	34	645	31	911	67	177	83	a
0.1907	0.0095	2.45	0.17	0.0933	0.0025		1258	50	1125	52	1493	51	150	75	a
0.219	0.011	3.14	0.37	0.1043	0.0061		1443	90	1274	58	1702	107	115	75	a

$^{206}Pb^*/^{238}U$	± 2σ (abs)	$^{207}Pb^*/^{235}U$	± 2σ (abs)	$^{207}Pb^*/^{206}Pb^*$	± 2σ (abs)	corr. coef.	$^{206}Pb^*/^{238}U$ age (Ma)	± 2σ (Ma)	$^{207}Pb^*/^{235}U$ age (Ma)	± 2σ (Ma)	$^{207}Pb^*/^{206}Pb^*$ age (Ma)	± 2σ (Ma)	Length (μm)	Width (μm)	Accept/ Reject
0.356	0.018	8.21	0.76	0.1674	0.0045		2254	84	1962	85	2531	45	132	66	a
0.0568	0.0028	0.516	0.034	0.0658	0.0023		422	23	356	17	800	73	82	66	a
0.0840	0.0042	0.838	0.063	0.0723	0.0027		618	35	520	25	996	75	116	68	a
0.1235	0.0062	1.47	0.11	0.0866	0.0027		920	43	750	36	1353	61	128	78	a
0.1479	0.0074	2.02	0.19	0.0991	0.0049		1122	63	889	42	1607	92	131	48	a
0.1306	0.0065	1.75	0.13	0.0974	0.0036		1028	48	791	37	1575	69	100	57	r
0.1256	0.0063	1.67	0.97	0.097	0.036		998	369	763	36	1558	701	99	75	r
0.0939	0.0047	1.11	0.18	0.0860	0.0086		760	85	579	28	1338	193	78	48	r
0.1134	0.0057	1.70	0.34	0.108	0.014		1007	129	692	33	1774	234	136	61	r
0.0699	0.0035	1.065	0.067	0.1104	0.0033		736	33	436	21	1807	54	100	67	r
0.0588	0.0029	1.04	0.28	0.128	0.023		724	139	368	18	2075	318	112	50	r
0.1956	0.0098	9.27	1.71	0.344	0.029		2365	169	1152	53	3679	129	130	84	r
14. Amazon River, Brazil (2.2836˚S, 56.3744˚W)															
0.00729	0.00031	0.0167	0.0071	0.0166	0.0090	*	17	7	47	2			113	68	r
0.0481	0.0021	0.143	0.065	0.022	0.014	0.822	136	58	303	13			238	102	r
0.1345	0.0083	0.45	0.29	0.024	0.028	0.918	378	200	813	47			120	78	r
0.0525	0.0028	0.18	0.17	0.024	0.035	0.835	165	149	330	17			138	86	r
0.02398	0.00097	0.118	0.011	0.0358	0.0041	0.707	113	10	153	6			152	91	a
0.0735	0.0022	0.371	0.064	0.0366	0.0097	0.877	320	47	457	13			123	90	a
0.1442	0.0056	0.825	0.062	0.0415	0.0040	0.665	611	34	869	31			181	71	a
0.02567	0.00083	0.1513	0.0100	0.0427	0.0033	0.738	143	9	163	5			166	91	a
0.01157	0.00044	0.0684	0.0043	0.0429	0.0028	0.454	67	4	74	3			143	62	a
0.0258	0.0011	0.171	0.065	0.048	0.023	0.717	160	56	164	7	95	1139	110	78	a
0.01884	0.00058	0.1248	0.0045	0.0480	0.0012	0.782	119	4	120	4	99	62	125	97	a
0.0340	0.0012	0.231	0.030	0.0491	0.0083	0.780	211	25	216	8	153	354	73	64	a
0.03113	0.00097	0.213	0.013	0.0496	0.0036	0.784	196	11	198	6	175	161	167	101	a
0.0657	0.0019	0.450	0.023	0.0497	0.0029	0.898	377	16	410	12	181	128	151	93	a
0.0415	0.0022	0.287	0.019	0.0502	0.0029	0.880	256	15	262	13	204	127	101	52	a
0.01882	0.00070	0.1308	0.0072	0.0504	0.0027	0.700	125	6	120	4	213	121	141	67	a
0.1175	0.0037	0.838	0.072	0.0517	0.0061	0.931	618	40	716	21	272	251	153	105	a
0.0155	0.0032	0.11	0.11	0.053	0.061	0.556	108	103	99	20	311	2656	110	72	a
0.0560	0.0022	0.407	0.036	0.0527	0.0062	0.863	346	26	351	13	315	266	135	67	a
0.1622	0.0056	1.18	0.21	0.053	0.017	0.932	791	96	969	31	318	743	170	130	a
0.0808	0.0025	0.594	0.028	0.0533	0.0027	0.922	473	18	501	15	340	114	155	90	a
0.0341	0.0011	0.251	0.010	0.0533	0.0020	0.846	227	8	216	7	340	86	146	76	a
0.01979	0.00080	0.1490	0.0069	0.0546	0.0016	0.817	141	6	126	5	396	63	120	81	a
0.0322	0.0011	0.243	0.012	0.0547	0.0027	0.825	221	10	204	7	400	109	137	60	a
0.0780	0.0023	0.593	0.022	0.0551	0.0018	0.632	473	14	484	14	416	72	109	41	a
0.0566	0.0043	0.43	0.27	0.055	0.049	0.858	365	194	355	26	428	1269	89	74	a
0.0521	0.0016	0.398	0.017	0.0555	0.0022	0.896	340	12	327	10	432	83	100	95	a
0.00492	0.00022	0.0382	0.0028	0.0563	0.0042	*	38	3	32	1	463	165	106	78	a
0.0383	0.0014	0.299	0.012	0.0566	0.0016	0.894	266	10	242	8	475	64	117	76	a
0.0742	0.0021	0.586	0.021	0.0572	0.0017	0.613	468	13	462	13	499	65	120	82	a
0.0697	0.0024	0.555	0.022	0.0578	0.0015	0.712	449	14	434	15	523	58	110	75	a
0.0325	0.0011	0.260	0.018	0.0580	0.0046	0.795	234	14	206	7	531	174	182	96	a
0.083	0.010	0.67	0.29	0.058	0.039	0.892	519	176	514	62	539	1465	168	66	a
0.0693	0.0020	0.561	0.033	0.0588	0.0046	0.887	452	21	432	12	558	172	170	67	a
0.0737	0.0026	0.601	0.025	0.0591	0.0017	0.695	478	16	459	16	571	64	125	56	a
0.0435	0.0017	0.357	0.020	0.0595	0.0031	0.875	310	15	275	11	585	107	87	68	a
0.0702	0.0030	0.577	0.027	0.0596	0.0016	0.766	462	17	437	18	589	54	112	66	a
0.1824	0.0090	1.50	0.15	0.060	0.011	0.944	931	63	1080	49	591	388	208	100	a

$^{206}Pb^*/^{238}U$	± 2σ (abs)	$^{207}Pb^*/^{235}U$	± 2σ (abs)	$^{207}Pb^*/^{206}Pb^*$	± 2σ (abs)	corr. coef.	$^{206}Pb^*/^{238}U$ age (Ma)	± 2σ (Ma)	$^{207}Pb^*/^{235}U$ age (Ma)	± 2σ (Ma)	$^{207}Pb^*/^{206}Pb^*$ age (Ma)	± 2σ (Ma)	Length (μm)	Width (μm)	Accept/ Reject
0.0351	0.0015	0.289	0.016	0.0597	0.0029	0.855	258	13	223	9	593	105	110	95	a
0.0877	0.0027	0.729	0.026	0.0603	0.0015	0.747	556	15	542	16	614	53	94	59	a
0.1367	0.0040	1.16	0.18	0.061	0.018	0.923	780	87	826	23	650	618	127	100	a
0.1091	0.0053	0.926	0.092	0.0616	0.0079	0.931	665	49	667	31	660	251	83	63	a
0.0957	0.0038	0.813	0.036	0.0616	0.0018	0.796	604	20	589	23	661	62	110	60	a
0.0795	0.0024	0.676	0.032	0.0617	0.0031	0.920	524	19	493	14	662	109	151	101	a
0.0442	0.0018	0.376	0.025	0.0617	0.0044	0.858	324	18	279	11	664	154	95	65	a
0.0432	0.0024	0.369	0.030	0.0619	0.0050	0.867	319	22	273	15	672	174	95	97	a
0.0580	0.0041	0.505	0.080	0.063	0.013	0.875	415	54	364	25	712	423	101	92	a
0.0601	0.0027	0.525	0.029	0.0633	0.0030	0.917	428	20	377	16	718	97	103	91	a
0.0388	0.0013	0.341	0.022	0.0637	0.0046	0.830	298	16	246	8	732	154	175	80	a
0.1097	0.0031	0.979	0.032	0.0647	0.0016	0.769	693	16	671	18	765	52	110	96	a
0.0322	0.0011	0.288	0.019	0.0650	0.0049	0.796	257	15	204	7	775	159	132	83	a
0.0393	0.0012	0.354	0.019	0.0653	0.0040	0.836	308	14	248	8	786	123	167	120	a
0.0698	0.0022	0.629	0.028	0.0654	0.0028	0.918	496	17	435	14	787	87	155	99	a
0.0330	0.0013	0.301	0.021	0.0662	0.0050	0.809	267	16	209	8	814	157	171	76	a
0.1310	0.0037	1.201	0.042	0.0665	0.0020	0.760	801	19	793	21	822	62	97	64	a
0.1328	0.0039	1.235	0.065	0.0674	0.0054	0.933	816	30	804	22	851	167	108	58	a
0.1338	0.0032	1.248	0.072	0.0676	0.0064	0.928	822	32	809	18	858	198	207	117	a
0.1301	0.0036	1.214	0.040	0.0677	0.0019	0.775	807	18	788	21	859	54	141	132	a
0.1407	0.0042	1.328	0.050	0.0685	0.0024	0.754	858	22	848	24	882	70	120	98	a
0.1028	0.0030	0.971	0.034	0.0685	0.0019	0.719	689	17	631	18	884	57	144	84	a
0.0451	0.0017	0.429	0.029	0.0691	0.0052	0.855	363	20	284	11	900	149	252	57	a
0.1101	0.0054	1.049	0.063	0.0691	0.0035	0.705	728	31	673	32	901	106	85	55	a
0.1250	0.0036	1.191	0.043	0.0691	0.0023	0.709	796	20	759	20	902	67	150	78	a
0.1096	0.0039	1.058	0.043	0.0700	0.0021	0.764	733	21	671	23	928	61	127	109	a
0.0563	0.0017	0.545	0.024	0.0703	0.0030	0.898	442	16	353	11	936	88	100	60	a
0.1462	0.0040	1.418	0.047	0.0703	0.0020	0.779	896	20	879	22	937	59	152	75	a
0.1081	0.0031	1.051	0.036	0.0706	0.0020	0.716	730	18	662	18	945	57	86	80	a
0.1381	0.0087	1.359	0.089	0.0713	0.0025	0.878	871	39	834	49	967	71	130	68	a
0.1285	0.0035	1.264	0.041	0.0713	0.0018	0.775	830	18	779	20	967	51	161	108	a
0.1537	0.0036	1.515	0.068	0.0715	0.0051	0.939	937	27	922	20	972	146	133	100	a
0.1107	0.0031	1.099	0.036	0.0720	0.0018	0.741	753	17	677	18	987	51	125	110	a
0.0724	0.0023	0.727	0.029	0.0728	0.0025	0.931	555	17	451	14	1009	70	65	65	a
0.1450	0.0040	1.461	0.047	0.0730	0.0019	0.791	914	20	873	22	1014	53	78	60	a
0.1711	0.0059	1.734	0.069	0.0735	0.0022	0.838	1021	26	1018	32	1028	61	130	75	a
0.1207	0.0045	1.226	0.051	0.0737	0.0019	0.814	813	23	735	26	1033	53	87	83	a
0.0466	0.0018	0.474	0.037	0.0738	0.0069	0.851	394	25	294	11	1035	178			r
0.1489	0.0047	1.521	0.058	0.0741	0.0024	0.772	939	23	895	26	1044	65	127	87	a
0.1598	0.0044	1.636	0.053	0.0742	0.0019	0.818	984	20	956	25	1047	51	102	92	a
0.1409	0.0051	1.444	0.058	0.0743	0.0019	0.842	907	24	850	29	1050	52	121	74	a
0.0638	0.0059	0.658	0.077	0.0748	0.0075	0.922	513	47	399	36	1063	189	138	68	a
0.0506	0.0043	0.529	0.056	0.0757	0.0067	0.905	431	37	318	27	1088	176	113	63	r
0.1511	0.0036	1.58	0.11	0.0758	0.0093	0.932	962	43	907	20	1089	245	172	73	a
0.1687	0.0053	1.769	0.064	0.0760	0.0020	0.835	1034	23	1005	29	1096	54	135	85	a
0.1659	0.0077	1.741	0.089	0.0761	0.0025	0.860	1024	33	989	42	1098	66	127	62	a
0.1425	0.0055	1.511	0.064	0.0769	0.0019	0.850	935	26	859	31	1119	50	133	100	a
0.1144	0.0077	1.215	0.091	0.0770	0.0037	0.792	808	42	698	44	1121	93	92	62	a
0.1775	0.0088	1.886	0.100	0.0771	0.0021	0.898	1076	35	1053	48	1124	53	138	101	a
0.1329	0.0067	1.412	0.077	0.0771	0.0024	0.847	894	32	804	38	1123	62	110	76	a
0.1747	0.0051	1.861	0.063	0.0773	0.0020	0.829	1067	22	1038	28	1128	53	155	100	a

$^{206}Pb^*/^{238}U$	± 2σ (abs)	$^{207}Pb^*/^{235}U$	± 2σ (abs)	$^{207}Pb^*/^{206}Pb^*$	± 2σ (abs)	corr. coef.	$^{206}Pb^*/^{238}U$ age (Ma)	± 2σ (Ma)	$^{207}Pb^*/^{235}U$ age (Ma)	± 2σ (Ma)	$^{207}Pb^*/^{206}Pb^*$ age (Ma)	± 2σ (Ma)	Length (μm)	Width (μm)	Accept/ Reject
0.1493	0.0040	1.591	0.050	0.0773	0.0019	0.792	967	20	897	23	1129	50	141	80	a
0.1465	0.0040	1.564	0.050	0.0774	0.0020	0.785	956	20	881	22	1132	51	155	112	a
0.0261	0.0029	0.28	0.34	0.08	0.12	0.721	251	269	166	18	1146	3043	180	110	a
0.1334	0.0056	1.446	0.070	0.0786	0.0027	0.791	908	29	807	32	1162	69	97	90	a
0.1359	0.0039	1.474	0.053	0.0787	0.0025	0.713	920	22	821	22	1164	64	97	91	a
0.1219	0.0056	1.334	0.083	0.0794	0.0049	0.582	861	36	741	32	1182	118	180	103	a
0.1342	0.0039	1.473	0.050	0.0796	0.0020	0.780	919	20	812	22	1188	49	164	116	a
0.1740	0.0050	1.912	0.064	0.0797	0.0021	0.823	1085	22	1034	27	1189	51	135	54	a
0.1354	0.0072	1.500	0.084	0.0803	0.0022	0.867	930	34	819	41	1204	55	80	65	a
0.1432	0.0041	1.591	0.062	0.0806	0.0032	0.646	967	24	863	23	1211	75	99	68	a
0.1338	0.0056	1.51	0.10	0.0818	0.0065	0.948	934	41	810	32	1241	148	124	75	a
0.1680	0.0050	1.902	0.065	0.0821	0.0021	0.818	1082	23	1001	28	1248	51	83	78	a
0.1953	0.0063	2.212	0.087	0.0822	0.0028	0.809	1185	28	1150	34	1249	68	100	60	a
0.0313	0.0010	0.357	0.032	0.0827	0.0095	0.769	310	24	199	6	1262	209	188	105	r
0.1526	0.0064	1.742	0.083	0.0828	0.0027	0.819	1024	31	916	36	1265	64	136	68	a
0.00370	0.00036	0.0423	0.0073	0.083	0.015	*	42	7	24	2	1270	357	122	98	r
0.1413	0.0039	1.617	0.053	0.0830	0.0022	0.749	977	20	852	22	1269	52	130	65	a
0.1669	0.0046	1.919	0.063	0.0834	0.0023	0.786	1088	22	995	25	1279	53	80	75	a
0.1328	0.0038	1.546	0.053	0.0844	0.0024	0.724	949	21	804	21	1302	53	124	90	a
0.287	0.012	3.35	0.15	0.0845	0.0022	0.919	1492	35	1628	58	1304	52	80	65	a
0.1790	0.0048	2.097	0.066	0.0849	0.0021	0.810	1148	22	1062	26	1314	49	120	82	a
0.155	0.011	1.82	0.17	0.0856	0.0089	0.637	1054	60	926	63	1330	200	137	91	a
0.0267	0.0024	0.320	0.037	0.0868	0.0085	0.820	282	29	170	15	1356	189	130	107	r
0.1675	0.0047	2.006	0.075	0.0868	0.0032	0.693	1118	25	998	26	1357	72	102	62	a
0.1460	0.0052	1.750	0.084	0.0869	0.0042	0.620	1027	31	879	29	1359	93	124	71	a
0.2095	0.0061	2.524	0.088	0.0874	0.0025	0.824	1279	25	1226	32	1369	54	114	60	a
0.2258	0.0045	2.722	0.073	0.0874	0.0033	0.661	1334	20	1312	23	1370	73	113	90	a
0.1178	0.0043	1.423	0.070	0.0876	0.0042	0.522	898	29	718	25	1374	89	97	73	a
0.1757	0.0047	2.138	0.068	0.0883	0.0022	0.800	1161	22	1043	26	1389	47	214	57	a
0.1845	0.0056	2.254	0.080	0.0886	0.0025	0.812	1198	25	1091	30	1396	53	140	88	a
0.337	0.013	4.18	0.21	0.0898	0.0064	0.797	1669	42	1875	65	1420	137	125	98	a
0.1626	0.0049	2.039	0.080	0.0909	0.0044	0.566	1128	27	971	27	1445	93	122	80	a
0.1718	0.0047	2.154	0.100	0.0909	0.0051	0.958	1166	32	1022	26	1445	104	98	78	a
0.1564	0.0040	1.975	0.057	0.0916	0.0024	0.738	1107	19	937	22	1459	49	112	97	a
0.2091	0.0089	2.64	0.15	0.0917	0.0074	0.609	1313	43	1224	47	1461	154	167	67	a
0.2157	0.0066	2.753	0.098	0.0926	0.0024	0.846	1343	26	1259	35	1480	48	165	84	a
0.2567	0.0099	3.31	0.14	0.0934	0.0024	0.900	1482	33	1473	51	1496	47	150	50	a
0.331	0.015	4.28	0.28	0.0939	0.0095	0.732	1690	53	1843	75	1506	191	122	68	a
0.2207	0.0061	2.86	0.29	0.094	0.019	0.947	1371	76	1285	32	1508	379	128	68	a
0.1854	0.0054	2.418	0.083	0.0946	0.0025	0.803	1248	25	1097	30	1520	50	106	70	a
0.00788	0.00038	0.105	0.015	0.096	0.017	*	101	14	51	2	1556	291	100	76	r
0.0531	0.0023	0.713	0.077	0.097	0.013	0.862	547	46	333	14	1576	258	136	81	r
0.00375	0.00027	0.0512	0.0080	0.099	0.017	*	51	8	24	2	1603	329	107	83	r
0.1188	0.0045	1.64	0.24	0.100	0.025	0.916	986	94	724	26	1626	472	114	68	r
0.2871	0.0066	4.00	0.16	0.1011	0.0074	0.963	1634	33	1627	33	1644	135	164	70	a
0.1688	0.0064	2.40	0.37	0.103	0.030	0.935	1242	110	1005	36	1679	530	88	88	a
0.0190	0.0029	0.271	0.042	0.1037	0.0052	0.901	244	34	121	18	1691	91	103	63	r
0.2262	0.0065	3.25	0.11	0.1043	0.0026	0.832	1470	26	1315	34	1702	45	140	57	a
0.2226	0.0097	3.27	0.16	0.1065	0.0031	0.866	1473	37	1295	51	1740	53	135	66	a
0.2191	0.0065	3.23	0.11	0.1070	0.0028	0.823	1465	27	1277	35	1749	47	91	81	a
0.2382	0.0071	3.53	0.12	0.1073	0.0029	0.831	1533	28	1378	37	1754	48	144	88	a

$^{206}Pb^*/^{238}U$	± 2σ (abs)	$^{207}Pb^*/^{235}U$	± 2σ (abs)	$^{207}Pb^*/^{206}Pb^*$	± 2σ (abs)	corr. coef.	$^{206}Pb^*/^{238}U$ age (Ma)	± 2σ (Ma)	$^{207}Pb^*/^{235}U$ age (Ma)	± 2σ (Ma)	$^{207}Pb^*/^{206}Pb^*$ age (Ma)	± 2σ (Ma)	Length (μm)	Width (μm)	Accept/ Reject
0.327	0.013	4.96	0.25	0.1100	0.0079	0.742	1812	43	1823	64	1799	131	124	80	a
0.1999	0.0057	3.03	0.10	0.1100	0.0029	0.787	1416	25	1175	30	1799	47	106	73	a
0.2664	0.0085	4.17	0.15	0.1136	0.0029	0.858	1668	30	1522	43	1857	46	83	58	a
0.2728	0.0097	4.28	0.17	0.1138	0.0029	0.878	1690	33	1555	49	1861	45	140	70	a
0.0607	0.0027	0.95	0.16	0.114	0.028	0.862	680	85	380	16	1864	450	180	67	r
0.2505	0.0072	3.97	0.14	0.1151	0.0030	0.826	1629	28	1441	37	1881	48	118	106	a
0.2416	0.0071	3.84	0.15	0.1152	0.0044	0.731	1601	32	1395	37	1884	69	110	77	a
0.2072	0.0062	3.29	0.11	0.1153	0.0030	0.795	1479	27	1214	33	1884	47	93	68	a
0.1476	0.0064	2.38	0.42	0.117	0.037	0.929	1236	125	888	36	1909	568	124	72	r
0.2435	0.0069	4.00	0.18	0.1190	0.0088	0.960	1634	36	1405	36	1942	132	107	76	a
0.3384	0.0070	5.71	0.15	0.1224	0.0044	0.729	1933	23	1879	34	1991	64	93	87	a
0.0813	0.0050	1.381	0.091	0.1233	0.0042	0.604	881	39	504	30	2005	59	130	78	r
0.207	0.018	3.56	0.31	0.1247	0.0033	0.924	1541	70	1215	95	2024	47	113	94	a
0.0512	0.0066	0.91	0.13	0.128	0.013	0.921	655	72	322	40	2075	172	106	98	r
0.2638	0.0084	4.75	0.17	0.1306	0.0033	0.839	1776	30	1509	43	2106	44	74	67	a
0.2351	0.0073	4.58	0.17	0.1413	0.0040	0.770	1746	31	1361	38	2243	48	169	124	a
0.3043	0.0059	6.05	0.15	0.1442	0.0054	0.567	1983	22	1713	29	2279	64	151	88	a
0.0406	0.0014	0.886	0.041	0.1583	0.0065	0.874	644	22	256	9	2438	69	125	102	r
0.1437	0.0063	3.39	0.41	0.171	0.036	0.930	1502	94	865	36	2567	347	120	94	r
0.2068	0.0064	4.91	0.18	0.1722	0.0046	0.689	1804	30	1212	34	2579	44	120	89	r
0.0146	0.0022	0.348	0.067	0.173	0.028	0.668	303	51	93	14	2589	247	139	80	r
0.341	0.011	8.50	0.31	0.1810	0.0045	0.828	2286	33	1890	51	2662	41	99	76	a
0.0588	0.0043	1.52	0.12	0.1882	0.0075	0.950	940	48	368	26	2726	66	167	98	r
0.1090	0.0042	2.88	0.34	0.192	0.031	0.926	1377	89	667	25	2757	246	199	122	r
0.4183	0.0088	11.08	0.27	0.1920	0.0053	0.749	2530	23	2253	40	2760	45	103	87	a
0.324	0.013	9.65	0.43	0.2164	0.0055	0.828	2402	41	1807	63	2954	40	99	57	r
0.135	0.015	4.69	0.70	0.252	0.039	0.955	1765	126	817	83	3195	227	163	84	r
0.0498	0.0016	1.76	0.23	0.257	0.044	0.846	1032	83	313	10	3229	247	131	82	r
0.0946	0.0095	4.17	0.60	0.320	0.047	0.936	1669	117	583	56	3569	211	143	121	r
0.149	0.026	7.31	1.68	0.355	0.079	0.962	2150	205	896	147	3730	304	125	92	r
0.213	0.017	10.69	1.43	0.364	0.057	0.968	2497	124	1244	92	3768	238	122	110	r
15. Amazon River, Brazil (2.4326˚S, 54.3715˚W)															
0.04683	0.00093	0.2254	0.0086	0.0349	0.0024	0.778	206	7	295	6			85	78	r
0.01526	0.00050	0.0937	0.0093	0.0446	0.0092	0.042	91	9	98	3			133	54	a
0.0314	0.0012	0.049	0.010	0.0113	0.0048	0.538	48	10	200	7			99	46	r
0.0536	0.0013	0.333	0.012	0.0450	0.0018	0.887	292	9	336	8			102	56	a
0.03777	0.00080	0.211	0.015	0.0405	0.0052	0.728	194	13	239	5			144	81	a
0.0937	0.0021	0.679	0.019	0.0526	0.0017	0.618	526	12	578	12	310	72			a
0.0927	0.0021	0.681	0.021	0.0533	0.0020	0.504	527	13	572	12	340	85	136	87	a
0.0109	0.0011	0.199	0.022	0.1332	0.0063	0.769	185	18	70	7	2140	83	75	60	r
0.0879	0.0019	0.610	0.022	0.0503	0.0021	0.923	483	14	543	12	210	97	145	67	a
0.0961	0.0022	0.573	0.023	0.0432	0.0025	0.913	460	15	592	13			137	90	a
0.0980	0.0024	0.703	0.025	0.0520	0.0022	0.510	541	15	603	14	287	99	124	97	a
0.0708	0.0018	0.479	0.026	0.0490	0.0036	0.887	397	18	441	11	149	172	125	113	a
0.0980	0.0031	0.760	0.028	0.0563	0.0018	0.740	574	16	603	18	463	70	117	52	a
0.0796	0.0032	0.610	0.028	0.0556	0.0018	0.751	483	17	493	19	436	71	129	53	a
0.0937	0.0021	0.736	0.028	0.0569	0.0031	0.909	560	16	577	12	489	122	111	52	a
0.0938	0.0025	0.731	0.030	0.0565	0.0028	0.924	557	17	578	15	473	109	120	72	a
0.0940	0.0025	0.738	0.037	0.0570	0.0041	0.911	561	22	579	15	491	160	96	87	a
0.1046	0.0040	0.876	0.039	0.0607	0.0025	0.719	639	21	642	23	630	88	96	80	a
0.0771	0.0037	0.511	0.040	0.0481	0.0046	0.906	419	27	479	22	103	227	45	35	a

$^{206}Pb^*/^{238}U$	± 2σ (abs)	$^{207}Pb^*/^{235}U$	± 2σ (abs)	$^{207}Pb^*/^{206}Pb^*$	± 2σ (abs)	corr. coef.	$^{206}Pb^*/^{238}U$ age (Ma)	± 2σ (Ma)	$^{207}Pb^*/^{235}U$ age (Ma)	± 2σ (Ma)	$^{207}Pb^*/^{206}Pb^*$ age (Ma)	± 2σ (Ma)	Length (μm)	Width (μm)	Accept/ Reject
0.1123	0.0035	1.103	0.041	0.071	0.0024	0.686	755	20	686	20	964	69	138	50	a
0.0273	0.0021	0.147	0.041	0.039	0.013	0.737	140	36	174	13			95	61	a
0.1280	0.0033	1.229	0.042	0.0696	0.0021	0.718	814	19	776	19	917	61	107	50	a
0.1317	0.0037	1.302	0.043	0.0717	0.0019	0.778	847	19	797	21	977	54	117	115	a
0.1410	0.0038	1.276	0.045	0.0657	0.0022	0.743	835	20	850	21	796	69	135	107	r
0.1171	0.0035	0.988	0.045	0.0612	0.0035	0.485	698	23	714	20	646	124	149	65	a
0.1364	0.0033	1.417	0.046	0.0754	0.0031	0.529	896	20	824	19	1078	82	161	60	a
0.1397	0.0038	1.380	0.047	0.0716	0.0020	0.773	880	20	843	21	975	56	144	87	a
0.1387	0.0037	1.195	0.047	0.0625	0.0028	0.645	798	22	838	21	690	96	118	63	a
0.0446	0.0044	0.419	0.048	0.068	0.0057	0.904	355	34	282	27	870	175	132	41	a
0.1461	0.0041	1.409	0.048	0.0699	0.0020	0.786	893	20	879	23	926	59	95	56	a
0.1375	0.0041	1.311	0.048	0.0692	0.0022	0.765	851	21	831	23	904	66	95	92	a
0.1457	0.0041	1.429	0.050	0.0711	0.0019	0.797	901	21	877	23	960	56	91	48	a
0.1462	0.0040	1.483	0.051	0.0736	0.0022	0.760	923	21	880	23	1030	60	105	60	a
0.1259	0.0061	1.060	0.056	0.0610	0.0017	0.883	734	27	765	35	641	58	95	40	a
0.0576	0.0025	0.281	0.057	0.035	0.010	0.853	252	45	361	15			135	61	r
0.1497	0.0042	1.466	0.058	0.0710	0.0023	0.764	917	24	899	24	959	66	114	55	a
0.1074	0.0041	0.797	0.059	0.0538	0.0052	0.929	595	33	657	24	364	217	140	51	a
0.1567	0.0049	1.587	0.062	0.0735	0.0024	0.784	965	24	938	27	1027	67	144	74	a
0.1355	0.0047	1.359	0.062	0.0727	0.0034	0.666	871	27	819	26	1006	95	89	66	a
0.1439	0.0049	1.550	0.064	0.0781	0.0026	0.764	950	26	866	28	1150	67	90	60	a
0.0788	0.0022	0.528	0.064	0.0485	0.0092	0.885	430	43	489	13	126	445	96	69	a
0.1248	0.0056	1.353	0.067	0.079	0.0024	0.818	869	29	758	32	1164	60	100	92	a
0.0486	0.0040	0.370	0.068	0.055	0.015	0.821	320	50	306	25	422	617	140	124	a
0.2297	0.0047	2.064	0.068	0.0652	0.0035	0.655	1137	23	1333	25	780	114	136	62	a
0.1604	0.0053	1.788	0.068	0.0809	0.0021	0.827	1041	25	959	29	1218	52	142	97	a
0.1376	0.0043	1.194	0.069	0.0629	0.0048	0.944	798	32	831	24	705	161	148	100	a
0.0434	0.0025	0.035	0.069	0.006	0.016	0.708	35	68	274	15			82	54	r
0.0911	0.0070	0.528	0.070	0.0420	0.0071	0.466	430	46	562	42			98	49	a
0.0616	0.0028	0.694	0.071	0.082	0.011	0.874	535	42	385	17	1238	269	146	61	r
0.0652	0.0020	0.266	0.073	0.030	0.012	0.862	240	58	407	12			93	50	r
0.0633	0.0024	0.315	0.074	0.036	0.013	0.861	278	57	396	14			125	81	a
0.0271	0.0015	0.120	0.074	0.032	0.025	0.723	115	67	172	9			70	58	a
0.1603	0.0049	1.809	0.075	0.0818	0.0028	0.754	1049	27	959	27	1242	66	75	54	a
0.1286	0.0070	1.347	0.078	0.076	0.0022	0.868	866	34	780	40	1094	57	156	91	a
0.1596	0.0057	1.551	0.079	0.0705	0.0025	0.812	951	31	954	32	942	74	104	85	a
0.1166	0.0046	1.662	0.079	0.1034	0.0037	0.631	994	30	711	26	1686	65	88	58	r
0.1789	0.0061	1.855	0.083	0.0752	0.0026	0.818	1065	29	1061	33	1074	70	78	41	a
0.1470	0.0077	1.439	0.083	0.0710	0.0022	0.878	905	35	884	43	957	64	93	42	a
0.1679	0.0055	2.090	0.084	0.090	0.0026	0.802	1145	28	1001	30	1431	54	181	118	a
0.1472	0.0045	1.624	0.084	0.080	0.0049	0.953	979	33	885	26	1198	120	92	55	a
0.1642	0.0064	1.679	0.086	0.0742	0.0024	0.843	1001	32	980	35	1046	64	101	53	a
0.1288	0.0060	1.110	0.089	0.0625	0.0067	0.939	758	43	781	35	692	228	88	59	a
0.1364	0.0048	2.275	0.092	0.1210	0.0035	0.671	1205	29	824	27	1971	52	126	88	r
0.1658	0.0063	1.968	0.096	0.086	0.0028	0.814	1105	33	989	35	1340	62	139	88	a
0.1711	0.0061	2.168	0.096	0.092	0.0026	0.825	1171	31	1018	34	1466	53	116	80	a
0.0988	0.0049	1.131	0.098	0.083	0.0093	0.924	768	47	607	28	1270	219	77	64	a
0.1734	0.0069	2.068	0.099	0.086	0.0028	0.829	1138	33	1031	38	1349	63	125	60	a
0.1751	0.0063	2.223	0.099	0.092	0.0025	0.832	1188	31	1040	35	1469	52	107	79	a
0.1660	0.0070	1.99	0.10	0.087	0.0025	0.852	1110	35	990	39	1355	55	90	55	a
0.1499	0.0041	1.75	0.11	0.085	0.0085	0.935	1027	39	900	23	1308	194	141	80	a

$^{206}Pb^*/^{238}U$	± 2σ (abs)	$^{207}Pb^*/^{235}U$	± 2σ (abs)	$^{207}Pb^*/^{206}Pb^*$	± 2σ (abs)	corr. coef.	$^{206}Pb^*/^{238}U$ age (Ma)	± 2σ (Ma)	$^{207}Pb^*/^{235}U$ age (Ma)	± 2σ (Ma)	$^{207}Pb^*/^{206}Pb^*$ age (Ma)	± 2σ (Ma)	Length (μm)	Width (μm)	Accept/ Reject
0.1476	0.0063	1.70	0.11	0.084	0.0054	0.591	1008	40	888	35	1281	126	156	75	a
0.1863	0.0064	2.68	0.11	0.10	0.0028	0.819	1322	31	1101	35	1701	49	153	60	a
0.1472	0.0047	1.07	0.11	0.0525	0.0079	0.944	737	56	885	27	309	341	113	54	a
0.1592	0.0081	2.02	0.12	0.092	0.0025	0.873	1124	39	952	45	1472	51	100	71	a
0.1625	0.0082	2.07	0.12	0.092	0.0024	0.877	1138	38	970	45	1472	50	122	62	a
0.1641	0.0070	1.70	0.12	0.0749	0.0035	0.786	1007	44	980	39	1066	94	115	90	a
0.1758	0.0072	1.47	0.12	0.0606	0.0035	0.791	918	49	1044	39	625	126	94	66	a
0.0897	0.0056	1.13	0.12	0.091	0.013	0.914	768	57	554	33	1454	269	73	60	r
0.3032	0.0059	4.60	0.12	0.1101	0.0044	0.664	1750	22	1707	29	1801	73	158	60	a
0.2053	0.0071	3.01	0.12	0.11	0.0027	0.839	1410	31	1204	38	1737	47	97	84	a
0.1251	0.0060	1.15	0.13	0.0664	0.0091	0.941	775	59	760	34	820	288	109	97	a
0.1623	0.0066	2.69	0.13	0.12	0.0032	0.798	1326	35	970	36	1960	47	94	73	r
0.1698	0.0059	2.05	0.13	0.087	0.0050	0.602	1132	43	1011	32	1371	110			a
0.2009	0.0072	2.85	0.13	0.10	0.0029	0.832	1370	34	1180	39	1680	52	120	60	a
0.1548	0.0049	3.28	0.13	0.1538	0.0042	0.600	1477	31	928	27	2389	47	118	78	r
0.1903	0.0068	2.01	0.13	0.0764	0.0086	0.948	1118	45	1123	37	1107	224	85	59	a
0.3104	0.0068	4.94	0.14	0.1154	0.0045	0.711	1809	23	1743	33	1886	70	95	62	a
0.2482	0.0054	2.51	0.14	0.0735	0.0079	0.954	1276	40	1429	28	1027	217	146	84	a
0.2104	0.0075	3.39	0.14	0.12	0.0029	0.837	1503	32	1231	40	1910	45	126	99	a
0.1621	0.0080	2.02	0.14	0.090	0.0054	0.698	1122	47	968	44	1432	115	160	125	a
0.1892	0.0090	2.69	0.14	0.10	0.0026	0.880	1326	39	1117	49	1683	47	70	60	a
0.1636	0.0053	2.20	0.14	0.097	0.0069	0.961	1180	45	977	29	1574	132	123	75	a
0.1899	0.0090	2.68	0.14	0.10	0.0049	0.766	1323	39	1121	49	1668	89	146	64	a
0.112	0.010	1.47	0.14	0.095	0.0055	0.770	917	59	685	60	1526	109	136	35	r
0.2896	0.0064	2.98	0.15	0.0747	0.0073	0.960	1403	38	1639	32	1061	197	164	63	a
0.2038	0.0075	3.24	0.15	0.12	0.0032	0.825	1467	35	1196	40	1886	50	78	61	a
0.2185	0.0075	3.88	0.16	0.13	0.0032	0.820	1609	33	1274	40	2080	44	129	77	a
0.313	0.010	3.92	0.16	0.0908	0.0047	0.811	1618	33	1756	52	1442	98	127	90	a
0.2719	0.0058	4.25	0.16	0.1134	0.0080	0.961	1684	32	1551	29	1855	127	125	40	a
0.1897	0.0067	2.89	0.16	0.11	0.0059	0.584	1380	43	1120	36	1810	98	118	79	a
0.2349	0.0085	3.99	0.17	0.12	0.0053	0.730	1632	34	1360	45	2002	77	84	62	a
0.0265	0.0052	0.33	0.17	0.090	0.014	0.935	289	128	169	33	1427	288	124	85	a
0.0919	0.0042	0.33	0.17	0.026	0.022	0.892	292	131	567	25			125	89	r
0.193	0.011	2.77	0.17	0.10	0.0028	0.893	1348	47	1135	59	1704	50	197	136	a
0.2324	0.0098	3.52	0.18	0.11	0.0033	0.860	1531	40	1347	51	1795	55			a
0.210	0.010	2.85	0.18	0.098	0.0041	0.834	1370	46	1231	54	1594	77	121	60	a
0.1856	0.0066	2.45	0.18	0.096	0.012	0.945	1258	53	1098	36	1544	238	130	60	a
0.3251	0.0080	5.71	0.18	0.1273	0.0058	0.681	1933	28	1815	39	2061	80	196	78	a
0.2267	0.0075	2.61	0.19	0.083	0.011	0.952	1303	52	1317	39	1280	256	122	51	a
0.242	0.011	2.99	0.19	0.0898	0.0030	0.892	1405	47	1395	59	1420	63	80	58	a
0.2084	0.0100	3.21	0.19	0.11	0.0034	0.861	1460	45	1220	53	1828	55	170	100	a
0.1564	0.0097	1.79	0.19	0.083	0.0100	0.481	1040	70	937	54	1264	235	78	65	a
0.258	0.010	4.39	0.20	0.12	0.0031	0.877	1710	37	1479	52	2005	44	105	54	a
0.0810	0.0066	0.46	0.20	0.041	0.024	0.901	382	138	502	39			95	57	a
0.2718	0.0058	4.39	0.20	0.12	0.010	0.958	1710	38	1550	29	1913	158	163	64	a
0.2402	0.0085	3.44	0.20	0.1039	0.0053	0.733	1514	47	1388	44	1696	94	240	57	a
0.0190	0.0027	0.24	0.20	0.092	0.093	0.635	220	167	121	17	1475	1919	130	90	a
0.234	0.011	4.30	0.21	0.13	0.0043	0.839	1693	40	1355	57	2142	56	75	45	a
0.359	0.011	5.83	0.21	0.1177	0.0046	0.832	1951	31	1980	54	1921	70	69	54	a
0.218	0.011	3.58	0.22	0.12	0.0042	0.844	1544	48	1269	59	1944	64			a
0.414	0.012	6.24	0.22	0.1092	0.0047	0.834	2010	30	2235	54	1786	78	75	65	a

$^{206}Pb^*/^{238}U$	± 2σ (abs)	$^{207}Pb^*/^{235}U$	± 2σ (abs)	$^{207}Pb^*/^{206}Pb^*$	± 2σ (abs)	corr. coef.	$^{206}Pb^*/^{238}U$ age (Ma)	± 2σ (Ma)	$^{207}Pb^*/^{235}U$ age (Ma)	± 2σ (Ma)	$^{207}Pb^*/^{206}Pb^*$ age (Ma)	± 2σ (Ma)	Length (μm)	Width (μm)	Accept/ Reject
0.0283	0.0029	0.37	0.22	0.094	0.072	0.742	317	164	180	18	1509	1444	127	75	a
0.1717	0.0073	2.33	0.22	0.098	0.0093	0.966	1221	68	1021	40	1593	177	196	50	a
0.159	0.016	2.28	0.24	0.10	0.0034	0.910	1208	73	950	88	1703	61	112	70	a
0.349	0.010	7.37	0.24	0.15	0.0053	0.776	2157	29	1929	48	2382	59	106	48	a
0.088	0.011	1.24	0.24	0.1025	0.0081	0.680	819	110	542	67	1669	146	95	72	r
0.301	0.012	3.50	0.25	0.084	0.011	0.589	1527	56	1697	62	1299	251	122	103	a
0.1054	0.0047	2.47	0.25	0.170	0.027	0.915	1262	75	646	27	2555	268	72	66	r
0.146	0.011	2.44	0.26	0.1213	0.0090	0.616	1254	76	878	61	1975	133	99	97	r
0.216	0.014	3.62	0.26	0.12	0.0035	0.897	1555	58	1261	74	1981	51	81	75	a
0.3585	0.0079	3.92	0.27	0.079	0.012	0.966	1618	56	1975	37	1179	288	70	62	a
0.0280	0.0069	0.34	0.28	0.088	0.032	0.908	298	212	178	43	1385	698	132	121	a
0.2767	0.0074	2.28	0.30	0.060	0.017	0.954	1205	92	1575	38	591	606	98	60	a
0.1486	0.0061	2.05	0.32	0.10	0.021	0.946	1132	106	893	34	1624	392	110	74	a
0.201	0.020	3.02	0.33	0.11	0.0041	0.916	1411	83	1180	107	1780	68	126	75	a
0.314	0.017	5.76	0.34	0.13	0.0034	0.916	1941	51	1762	81	2137	45	125	92	a
0.0728	0.0092	1.16	0.35	0.116	0.059	0.864	783	162	453	55	1891	918	86	53	r
0.223	0.023	3.40	0.39	0.11	0.012	0.785	1504	91	1300	123	1804	195	100	30	a
0.1118	0.0081	1.51	0.41	0.098	0.041	0.920	936	167	683	47	1591	781	97	76	r
0.2303	0.0093	3.70	0.50	0.12	0.031	0.949	1571	107	1336	49	1903	482	104	65	a
0.2231	0.0098	2.36	0.55	0.077	0.036	0.946	1230	166	1298	52	1113	948	107	77	a
0.1001	0.0094	3.61	0.62	0.261	0.041	0.947	1551	136	615	55	3254	246	83	77	r
0.168	0.019	3.18	0.67	0.137	0.025	0.970	1453	162	1002	106	2192	311	183	60	r
0.138	0.022	2.77	0.73	0.145	0.017	0.643	1348	196	836	124	2290	206	82	63	r
0.183	0.020	4.11	0.76	0.163	0.027	0.971	1657	151	1083	107	2488	281	89	64	r
0.081	0.017	2.51	0.88	0.224	0.087	0.921	1274	256	502	100	3012	622	80	44	r
0.130	0.020	3.721	1.024	0.207	0.047	0.963	1576	220	790	114	2882	365	173	71	r
0.083	0.021	3.235	1.039	0.284	0.086	0.933	1466	249	511	126	3387	472	69	54	r
0.067	0.026	1.57	1.60	0.17	0.25	0.877	959	633	418	154	2557	2435	75	65	a
0.115	0.033	2.66	2.20	0.168	0.027	0.634	1319	609	704	191	2533	272	109	55	a
0.138	0.025	7.54	2.34	0.397	0.067	0.977	2178	279	832	143	3899	256	78	70	r
0.325	0.021	0.5	2.8	0.01	0.14	0.952	420	1879	1816	104			102	50	r
0.172	0.050	7.61	3.36	0.321	0.070	0.983	2186	397	1022	276	3575	333	103	86	r
0.168	0.058	3.63	3.56	0.16	0.28	0.937	1557	781	1002	322	2419	3014	115	64	a
0.439	0.097	16.31	4.68	0.27	0.10	0.982	2895	275	2347	437	3302	601	143	104	r
0.101	0.071	5.20	5.17	0.372	0.073	0.989	1853	846	623	413	3799	297	77	42	r
0.11	0.14	3.28	9.43	0.216	0.039	0.892	1475	2240	672	818	2953	288	77	65	r
0.13	0.14	6.87	11.52	0.388	0.045	0.875	2094	1487	779	804	3862	174	146	90	r
0.12	0.23	6.26	16.36	0.388	0.039	0.932	2012	2288	714	1304	3862	153	61	56	r
0.29	0.25	16.72	20.74	0.414	0.034	0.946	2919	1188	1656	1237	3961	124	151	55	r
0.38	0.19	17.94	23.78	0.34	0.91	0.969	2987	1275	2084	895	3668	4080	192	140	r
17. Purus River, Brazil (4.0261˚S, 61.5141˚W)															
0.243	0.012	2.46	0.18	0.0735	0.0019		1261	53	1403	63	1028	54	158	54	a
0.236	0.012	2.36	0.17	0.0726	0.0019		1231	51	1366	62	1003	53	98	95	a
0.362	0.018	4.90	0.62	0.0983	0.0040		1803	107	1991	86	1592	76	126	60	a
0.265	0.013	2.91	0.25	0.0797	0.0026		1383	65	1513	68	1188	65	121	58	a
0.0972	0.0049	0.726	0.045	0.0542	0.0016		554	27	598	29	379	67	66	58	a
0.365	0.018	5.57	0.55	0.1106	0.0031		1912	85	2008	87	1809	50	186	83	a
0.351	0.018	5.25	0.48	0.1083	0.0029		1860	78	1941	84	1771	49	166	62	a
0.276	0.014	3.43	0.26	0.0901	0.0024		1511	60	1571	70	1427	50	105	78	a
0.220	0.011	2.38	0.23	0.0784	0.0037		1237	69	1284	58	1157	94	95	72	a
0.0581	0.0029	0.41	0.00	0.05	0.00		352	0	364	18	277	0	117	88	a

$^{206}Pb^*/^{238}U$	± 2σ (abs)	$^{207}Pb^*/^{235}U$	± 2σ (abs)	$^{207}Pb^*/^{206}Pb^*$	± 2σ (abs)	corr. coef.	$^{206}Pb^*/^{238}U$ age (Ma)	± 2σ (Ma)	$^{207}Pb^*/^{235}U$ age (Ma)	± 2σ (Ma)	$^{207}Pb^*/^{206}Pb^*$ age (Ma)	± 2σ (Ma)	Length (μm)	Width (μm)	Accept/ Reject
0.1490	0.0074	1.353	0.089	0.0659	0.0019		869	38	895	42	803	60	198	64	a
0.212	0.011	2.28	0.16	0.0780	0.0021		1205	51	1239	57	1146	54	99	73	a
0.252	0.013	3.02	0.28	0.0868	0.0037		1411	72	1448	65	1357	81	263	85	a
0.284	0.014	3.74	0.30	0.0955	0.0026		1580	65	1612	72	1538	52	173	67	a
0.1125	0.0056	0.948	0.063	0.0612	0.0018		677	33	687	33	645	64	114	70	a
0.219	0.011	2.45	0.17	0.0814	0.0022		1259	51	1274	58	1232	52	129	70	a
0.220	0.011	2.50	0.18	0.0822	0.0022		1271	51	1283	58	1251	53	133	101	a
0.0538	0.0027	0.393	0.022	0.0530	0.0015		336	16	338	16	327	66	161	102	a
0.0790	0.0039	0.620	0.036	0.0569	0.0015		490	23	490	24	488	59	195	107	a
0.1415	0.0071	1.32	0.12	0.0675	0.0032		853	51	853	40	853	100	87	72	a
0.1430	0.0071	1.37	0.14	0.0697	0.0038		878	59	861	40	920	111	128	92	a
0.1894	0.0095	2.10	0.15	0.0804	0.0022		1149	48	1118	52	1207	55	118	70	a
0.1163	0.0058	1.053	0.064	0.0657	0.0018		730	31	709	34	797	57	112	66	a
0.0411	0.0021	0.302	0.020	0.0532	0.0020		268	15	260	13	339	86	94	61	a
0.1900	0.0095	2.12	0.14	0.0811	0.0022		1157	47	1121	52	1224	53	122	74	a
0.0620	0.0031	0.483	0.033	0.0565	0.0020		400	23	388	19	474	76	97	68	a
0.1298	0.0065	1.234	0.090	0.0689	0.0024		816	41	787	37	897	72	153	64	a
0.0280	0.0014	0.200	0.035	0.0519	0.0067		185	30	178	9	281	296	114	78	a
0.1523	0.0076	1.56	0.10	0.0743	0.0020		955	41	914	43	1050	55	129	74	a
0.0400	0.0020	0.298	0.018	0.0540	0.0017		265	14	253	12	372	70	141	100	a
0.1905	0.0095	2.21	0.21	0.0841	0.0041		1184	68	1124	52	1295	94	119	102	a
0.236	0.012	3.14	0.23	0.0967	0.0028		1443	57	1364	62	1562	53	123	85	a
0.1542	0.0077	1.64	0.19	0.0770	0.0053		984	75	924	43	1120	137	147	70	a
0.0549	0.0027	0.436	0.028	0.0576	0.0021		368	20	345	17	516	81	75	62	a
0.0525	0.0026	0.415	0.028	0.0573	0.0021		352	20	330	16	502	80	78	66	a
0.266	0.013	3.95	0.30	0.1077	0.0028		1624	61	1520	68	1761	48	97	62	a
0.279	0.014	4.38	0.34	0.1137	0.0030		1709	63	1588	71	1859	47	132	55	a
0.1507	0.0075	1.62	0.29	0.0779	0.0072		977	113	905	42	1143	184	88	59	a
0.0944	0.0047	0.863	0.056	0.0663	0.0022		632	31	581	28	816	69	143	56	a
0.0940	0.0047	0.868	0.095	0.0670	0.0045		635	51	579	28	838	141	103	72	a
0.1870	0.0093	2.31	0.16	0.0898	0.0024		1217	48	1105	51	1421	51	426	171	a
0.0834	0.0042	0.754	0.045	0.0656	0.0019		570	26	516	25	793	60	70	58	a
0.1167	0.0058	1.232	0.075	0.0765	0.0021		815	34	712	34	1109	54	87	57	a
0.0401	0.0020	0.336	0.046	0.0608	0.0060		294	35	253	12	631	212	94	57	a
0.0582	0.0029	0.52	0.10	0.0652	0.0091		427	70	364	18	781	293	156	93	a
0.253	0.013	4.35	0.32	0.1249	0.0033		1703	61	1452	65	2027	46	118	75	a
0.0988	0.0049	1.02	0.46	0.075	0.023		715	231	607	29	1069	626	105	73	a
0.01799	0.00090	0.145	0.026	0.0583	0.0078		137	23	115	6	540	291	139	81	a
0.1900	0.0095	2.74	1.26	0.105	0.029		1340	341	1121	52	1710	501	117	88	a
0.0203	0.0010	0.169	0.011	0.0601	0.0023		158	9	130	6	607	83	144	86	a
0.0754	0.0038	0.770	0.095	0.0740	0.0060		580	55	469	23	1043	163	152	73	a
0.1492	0.0075	2.01	0.16	0.0980	0.0036		1120	53	896	42	1586	68	180	78	a
0.1198	0.0060	1.55	0.12	0.0940	0.0039		951	48	730	35	1507	78	102	91	r
0.1198	0.0060	1.55	0.12	0.0940	0.0039		951	48	730	35	1507	78	122	75	r
0.0656	0.0033	0.694	0.050	0.0767	0.0032		535	30	409	20	1114	83			r
0.286	0.014	7.05	0.57	0.1791	0.0051		2118	71	1619	72	2645	47	138	60	r
0.0213	0.0011	0.217	0.076	0.074	0.020		199	63	136	7	1037	534	93	59	r
0.1007	0.0050	1.46	0.11	0.1053	0.0047		915	47	619	30	1719	82	110	72	r
0.0696	0.0035	0.95	0.45	0.099	0.033		676	233	434	21	1598	633	95	40	r
0.0597	0.0030	1.93	0.17	0.234	0.014		1091	60	374	18	3081	95	110	49	r

18. Negro River, Brazil (2.4352˚S, 60.0622˚W)

$^{206}Pb^*/^{238}U$	± 2σ (abs)	$^{207}Pb^*/^{235}U$	± 2σ (abs)	$^{207}Pb^*/^{206}Pb^*$	± 2σ (abs)	corr. coef.	$^{206}Pb^*/^{238}U$ age (Ma)	± 2σ (Ma)	$^{207}Pb^*/^{235}U$ age (Ma)	± 2σ (Ma)	$^{207}Pb^*/^{206}Pb^*$ age (Ma)	± 2σ (Ma)	Length (μm)	Width (μm)	Accept/ Reject
0.1476	0.0052	1.390	0.060	0.0683	0.0022	0.819	884	26	888	29	877	67			a
0.0379	0.0027	0.266	0.028	0.0509	0.0031	0.911	239	22	240	17	237	138			a
0.0449	0.0024	0.294	0.037	0.0475	0.0082	0.824	262	29	283	15	74	408			a
0.1526	0.0050	1.394	0.053	0.0663	0.0017	0.855	887	23	916	28	815	53			a
0.0953	0.0029	0.596	0.023	0.0453	0.0016	0.749	475	15	587	17					a
0.0749	0.0024	0.367	0.030	0.0355	0.0039	0.895	318	22	466	14					r
0.03695	0.00099	0.1904	0.0070	0.0374	0.0015	0.834	177	6	234	6					a
0.289	0.021	4.00	0.45	0.1003	0.0036	0.931	1634	92	1638	107	1630	67	107	67	a
0.1468	0.0047	1.341	0.053	0.0662	0.0020	0.817	864	23	883	26	814	63	180	65	a
0.2249	0.0077	2.62	0.11	0.0846	0.0022	0.877	1307	31	1308	40	1306	52	118	108	a
0.0862	0.0025	0.506	0.022	0.0426	0.0019	0.626	416	15	533	15			74	55	a
0.0358	0.0010	0.1512	0.0073	0.0306	0.0018	0.798	143	6	227	6			117	62	r
0.03625	0.00097	0.2312	0.0078	0.0462	0.0015	0.850	211	6	230	6	11	76	115	96	a
0.1261	0.0043	0.968	0.038	0.0557	0.0015	0.849	688	20	766	24	441	59	155	85	a
0.1312	0.0053	1.043	0.058	0.0577	0.0029	0.757	726	29	795	30	517	111	123	66	a
0.1057	0.0071	0.89	0.25	0.061	0.013	0.958	648	135	647	41	650	452	96	80	a
0.1251	0.0038	0.746	0.033	0.0433	0.0019	0.779	566	19	760	22			107	73	a
0.1341	0.0042	1.078	0.039	0.0583	0.0015	0.846	743	19	811	24	542	55	135	93	a
0.1379	0.0043	1.026	0.040	0.0539	0.0016	0.838	717	20	833	24	369	67	123	74	a
0.1271	0.0038	0.985	0.035	0.0562	0.0014	0.839	696	18	771	22	460	55	107	76	a
0.0513	0.0039	0.236	0.019	0.0333	0.0013	0.841	215	16	323	24	-850	111	162	142	r
0.280	0.011	3.71	0.25	0.0962	0.0035	0.870	1573	53	1589	55	1551	68	139	77	a
0.0552	0.0019	0.120	0.020	0.0157	0.0039	0.833	115	19	347	12	-3862	1494	103	93	r
0.1251	0.0039	0.828	0.031	0.0480	0.0013	0.851	613	17	760	22	99	64	78	72	a
0.0857	0.0031	0.536	0.023	0.0454	0.0016	0.765	436	16	530	18			127	69	a
0.1291	0.0049	1.057	0.082	0.0594	0.0053	0.947	732	40	783	28	581	195	108	99	a
0.1934	0.0071	1.986	0.087	0.0745	0.0019	0.886	1111	29	1140	39	1054	52	96	73	a
0.0636	0.0021	0.479	0.020	0.0546	0.0020	0.507	397	14	397	13	397	84	85	56	a
0.1915	0.0098	1.600	0.091	0.0606	0.0017	0.927	970	35	1130	53	625	59	99	76	a
0.1883	0.0085	1.73	0.10	0.0666	0.0028	0.860	1020	37	1112	46	826	88	152	60	a
0.178	0.010	1.498	0.096	0.0609	0.0020	0.914	930	39	1058	56	637	72	87	82	a
0.250	0.052	3.15	2.78	0.091	0.016	0.875	1444	681	1440	268	1450	340	120	72	a
0.01878	0.00056	0.0982	0.0053	0.0379	0.0027	0.589	95	5	120	4			104	86	a
0.1252	0.0066	0.969	0.061	0.0561	0.0025	0.834	688	31	761	38	457	100	108	78	a
0.273	0.011	3.42	0.16	0.0910	0.0023	0.913	1510	36	1555	55	1447	47	117	109	a
0.1405	0.0098	1.267	0.099	0.0654	0.0029	0.874	831	44	847	56	787	93	100	42	a
0.1402	0.0046	1.113	0.043	0.0576	0.0015	0.861	760	21	846	26	514	56	164	100	a
0.1721	0.0068	1.75	0.11	0.0735	0.0035	0.784	1025	42	1024	37	1029	95	133	60	a
0.0496	0.0014	0.2273	0.0095	0.0333	0.0015	0.869	208	8	312	9			155	92	r
0.1410	0.0045	1.179	0.044	0.0607	0.0015	0.855	791	20	850	26	627	54	144	68	a
0.0984	0.0033	0.611	0.027	0.0450	0.0018	0.751	484	17	605	19			130	88	a
0.0891	0.0032	0.551	0.023	0.0449	0.0014	0.798	446	15	550	19			120	87	a
0.273	0.010	3.61	0.17	0.0960	0.0025	0.899	1552	37	1555	52	1547	50	99	95	a
0.1690	0.0057	1.404	0.055	0.0603	0.0015	0.886	890	23	1006	32	613	54	177	91	a
0.1340	0.0062	0.949	0.058	0.0514	0.0028	0.804	678	30	811	35	258	123	181	77	a
0.1574	0.0060	1.254	0.054	0.0578	0.0014	0.895	825	24	942	33	521	55	127	85	a
0.1611	0.0064	1.144	0.057	0.0515	0.0019	0.871	774	27	963	36	263	84	112	93	a
0.0447	0.0013	0.2170	0.0077	0.0352	0.0011	0.580	199	6	282	8			221	93	a
0.316	0.015	3.54	0.19	0.0812	0.0021	0.941	1536	43	1772	74	1226	51	97	58	a
0.0880	0.0026	0.541	0.019	0.0446	0.0012	0.798	439	13	544	16			160	118	a
0.2194	0.0099	1.676	0.084	0.0554	0.0014	0.936	1000	32	1279	52	429	58	121	66	a

$^{206}Pb^*/^{238}U$	± 2σ (abs)	$^{207}Pb^*/^{235}U$	± 2σ (abs)	$^{207}Pb^*/^{206}Pb^*$	± 2σ (abs)	corr. coef.	$^{206}Pb^*/^{238}U$ age (Ma)	± 2σ (Ma)	$^{207}Pb^*/^{235}U$ age (Ma)	± 2σ (Ma)	$^{207}Pb^*/^{206}Pb^*$ age (Ma)	± 2σ (Ma)	Length (μm)	Width (μm)	Accept/ Reject
0.0529	0.0016	0.2610	0.0093	0.0358	0.0011	0.662	235	8	333	10			140	83	a
0.315	0.019	4.38	0.29	0.1008	0.0025	0.946	1709	54	1767	95	1640	46	94	65	a
0.252	0.012	2.40	0.14	0.0691	0.0027	0.903	1242	41	1448	60	902	80	96	56	a
0.1090	0.0060	0.927	0.075	0.0616	0.0025	0.823	666	40	667	35	662	86	164	66	a
0.345	0.015	4.37	0.27	0.0919	0.0038	0.898	1707	50	1910	74	1465	79	120	50	a
0.157	0.012	1.52	0.47	0.0700	0.0091	0.649	937	188	941	64	928	266	116	76	a
0.286	0.011	2.85	0.13	0.0723	0.0019	0.925	1368	34	1619	55	995	54	70	45	a
0.31	0.72	4.671	33.085	0.110	0.019	0.989	1762	5924	1732	3535	1798	310	110	76	r
0.2159	0.0077	2.50	0.12	0.0840	0.0024	0.867	1272	34	1260	41	1292	57	100	60	a
0.228	0.031	2.856	2.023	0.091	0.012	0.844	1370	533	1325	161	1442	253	121	31	a
0.1600	0.0094	1.57	0.16	0.0710	0.0041	0.815	957	65	957	52	958	119	110	92	a
0.228	0.024	2.75	0.64	0.0877	0.0066	0.889	1343	173	1322	126	1377	144	121	70	a
0.115	0.012	1.00	0.13	0.0631	0.0021	0.926	702	64	699	71	711	70	93	66	a
0.1765	0.0062	1.800	0.082	0.0740	0.0024	0.834	1046	30	1048	34	1041	66	140	62	a
0.186	0.014	1.93	0.18	0.0752	0.0024	0.929	1092	63	1101	79	1074	65	113	62	a
0.2279	0.0098	2.75	0.16	0.0875	0.0026	0.890	1342	42	1324	52	1371	57	104	87	a
0.2181	0.0081	2.52	0.12	0.0838	0.0023	0.881	1278	35	1272	43	1289	54	125	78	a
0.1506	0.0052	1.443	0.084	0.0695	0.0037	0.683	907	35	904	29	914	109	94	69	a
0.2059	0.0084	2.29	0.20	0.0808	0.0044	0.779	1210	63	1207	45	1216	108	111	45	a
0.0453	0.0016	0.319	0.014	0.0510	0.0019	0.888	281	11	286	10	241	88	163	67	a
0.1590	0.0077	1.55	0.10	0.0706	0.0022	0.878	950	41	951	43	946	65	95	63	a
0.099	0.010	0.82	0.11	0.0599	0.0020	0.916	606	61	608	59	601	71	126	100	a
0.176	0.033	1.80	0.49	0.0741	0.0037	0.953	1044	179	1045	183	1044	101	136	76	a
0.162	0.015	1.59	0.25	0.0714	0.0059	0.836	966	97	966	83	968	168	124	72	a
0.1582	0.0056	1.547	0.085	0.0709	0.0029	0.780	949	34	947	31	956	83	135	78	a
0.1211	0.0039	1.047	0.040	0.0627	0.0017	0.806	727	20	737	22	698	58	91	70	a
0.2296	0.0099	2.71	0.17	0.0855	0.0037	0.845	1330	47	1332	52	1327	84	127	58	a
0.230	0.036	2.76	1.90	0.087	0.049	0.979	1345	512	1336	187	1360	1093	79	76	a
0.124	0.028	1.11	1.32	0.065	0.055	0.966	756	636	752	163	769	1787	116	70	a
0.306	0.019	4.43	0.29	0.1048	0.0028	0.938	1717	54	1722	92	1711	49	103	67	a
0.1780	0.0065	1.822	0.082	0.0742	0.0020	0.867	1053	29	1056	35	1048	55	136	90	a
0.0319	0.0015	0.220	0.028	0.0501	0.0077	0.784	202	24	203	10	199	357	122	58	a
0.1134	0.0036	0.973	0.047	0.0622	0.0030	0.614	690	24	693	21	681	102	84	60	a
0.177	0.012	1.83	0.16	0.0747	0.0023	0.921	1055	56	1052	66	1061	61	110	95	a
0.1763	0.0061	1.785	0.081	0.0734	0.0022	0.849	1040	29	1047	33	1025	60	100	68	a
0.2110	0.0072	2.39	0.11	0.0821	0.0023	0.865	1239	33	1234	39	1247	56	108	60	a
0.0367	0.0017	0.234	0.013	0.0462	0.0021	0.866	214	11	233	10	9	112	97	87	a
0.179	0.015	1.84	0.19	0.0749	0.0023	0.933	1061	68	1059	80	1064	63	152	77	a
0.209	0.017	2.32	0.23	0.0806	0.0025	0.940	1220	72	1224	93	1212	60	115	87	a
0.1910	0.0074	2.03	0.10	0.0771	0.0022	0.873	1126	35	1127	40	1123	58	173	76	a
0.0813	0.0046	0.648	0.048	0.0578	0.0019	0.820	508	30	504	27	524	72	132	52	a
0.1328	0.0053	1.210	0.055	0.0661	0.0019	0.842	805	25	804	30	809	61	114	48	a
0.1802	0.0076	1.84	0.11	0.0740	0.0023	0.870	1059	40	1068	41	1042	64	89	62	a
0.1687	0.0079	1.70	0.12	0.0732	0.0043	0.766	1010	47	1005	44	1020	119	79	67	a
0.2142	0.0077	2.45	0.11	0.0828	0.0023	0.877	1256	32	1251	41	1266	53	76	76	a
0.138	0.013	1.30	0.69	0.068	0.028	0.967	847	304	835	74	880	838	100	68	a
0.184	0.014	1.91	0.22	0.0749	0.0036	0.889	1083	76	1091	74	1067	98	125	54	a
0.1498	0.0093	1.43	0.10	0.0691	0.0021	0.906	901	43	900	52	903	61	88	58	a
0.219	0.016	2.49	0.31	0.0827	0.0077	0.797	1270	89	1274	85	1263	183	106	75	a
0.153	0.017	1.48	0.21	0.0701	0.0023	0.944	924	88	921	96	931	66	84	45	a
0.1847	0.0076	1.92	0.11	0.0754	0.0023	0.872	1089	37	1093	41	1080	62	125	56	a

$^{206}Pb^*/^{238}U$	± 2σ (abs)	$^{207}Pb^*/^{235}U$	± 2σ (abs)	$^{207}Pb^*/^{206}Pb^*$	± 2σ (abs)	corr. coef.	$^{206}Pb^*/^{238}U$ age (Ma)	± 2σ (Ma)	$^{207}Pb^*/^{235}U$ age (Ma)	± 2σ (Ma)	$^{207}Pb^*/^{206}Pb^*$ age (Ma)	± 2σ (Ma)	Length (μm)	Width (μm)	Accept/ Reject
0.211	0.014	3.24	0.23	0.1112	0.0029	0.916	1467	56	1237	75	1819	47	165	76	a
0.197	0.010	2.95	0.17	0.1088	0.0029	0.879	1396	44	1158	54	1780	49	136	66	a
0.230	0.012	4.08	0.23	0.1288	0.0033	0.883	1651	47	1334	60	2082	45	103	62	a
0.2032	0.0093	3.24	0.17	0.1156	0.0029	0.871	1466	41	1192	50	1889	45	129	66	a
0.1713	0.0072	2.23	0.11	0.0946	0.0024	0.862	1192	34	1019	39	1521	47	125	56	a
0.2038	0.0094	3.67	0.20	0.1306	0.0034	0.852	1565	43	1196	50	2107	45	115	56	r
0.1587	0.0065	2.039	0.098	0.0932	0.0024	0.849	1129	33	950	36	1491	48	165	76	a
0.205	0.010	3.39	0.19	0.1198	0.0030	0.877	1501	43	1202	54	1953	45	128	83	a
0.0577	0.0021	0.602	0.068	0.076	0.011	0.870	478	43	361	13	1087	295	116	68	r
0.201	0.015	3.35	0.28	0.1209	0.0035	0.906	1492	64	1179	83	1969	52	84	62	a
0.1792	0.0089	2.22	0.13	0.0897	0.0025	0.885	1186	40	1062	49	1420	52	140	62	a
0.224	0.011	3.72	0.21	0.1205	0.0030	0.890	1576	45	1303	59	1964	44	118	73	a
0.1312	0.0068	2.14	0.12	0.1182	0.0031	0.810	1161	40	794	39	1929	47	89	75	r
0.2007	0.0096	3.35	0.18	0.1211	0.0030	0.870	1493	43	1179	52	1972	45	126	76	a
0.1206	0.0052	1.225	0.060	0.0737	0.0019	0.843	812	27	734	30	1033	52	106	84	a
0.223	0.012	3.47	0.21	0.1127	0.0028	0.901	1520	47	1298	62	1844	45	156	68	a
0.1686	0.0068	1.929	0.096	0.0830	0.0024	0.856	1091	33	1004	38	1269	55	78	52	a
0.256	0.033	3.70	0.50	0.1047	0.0031	0.961	1571	107	1471	170	1709	54	93	61	a
0.211	0.014	3.31	0.24	0.1136	0.0028	0.917	1483	56	1235	75	1858	45	154	72	a
0.1527	0.0068	1.723	0.089	0.0819	0.0022	0.865	1017	33	916	38	1243	52	122	61	a
0.328	0.022	5.57	0.42	0.1230	0.0031	0.940	1912	65	1831	104	2001	45	118	48	a
0.1303	0.0063	2.29	0.35	0.128	0.020	0.954	1210	108	790	36	2065	274	113	75	r
0.156	0.016	2.12	0.24	0.0985	0.0044	0.886	1155	77	934	89	1596	83	138	54	a
0.118	0.029	1.82	0.45	0.1121	0.0029	0.958	1054	162	719	167	1834	47	158	78	r
0.257	0.014	4.32	0.27	0.1219	0.0030	0.914	1696	52	1473	74	1984	44	131	76	a
0.209	0.025	2.37	0.29	0.0822	0.0027	0.954	1235	88	1225	131	1251	64	128	61	a
0.252	0.060	3.94	0.95	0.1135	0.0030	0.979	1622	195	1447	310	1856	47	95	54	a
0.0381	0.0021	0.428	0.052	0.081	0.013	0.807	361	37	241	13	1232	306	109	72	r
0.1744	0.0086	2.73	0.16	0.1136	0.0035	0.832	1337	43	1036	47	1857	56	104	48	a
0.339	0.030	8.69	0.86	0.1861	0.0047	0.937	2306	90	1880	144	2708	41	88	66	a
0.313	0.020	3.68	0.30	0.0854	0.0033	0.931	1568	66	1754	99	1324	76	151	50	a
0.1953	0.0094	2.34	0.13	0.0870	0.0023	0.898	1225	39	1150	50	1360	50	136	66	a
0.214	0.016	1.98	0.16	0.0671	0.0019	0.949	1107	53	1248	83	840	58	101	51	a
0.116	0.011	0.56	0.11	0.0353	0.0070	0.717	454	73	706	66			98	65	r
0.1700	0.0075	1.712	0.088	0.0730	0.0019	0.891	1013	33	1012	41	1015	53	116	78	a
0.111	0.015	1.07	0.15	0.0702	0.0019	0.945	739	74	676	88	935	56	97	72	a
0.253	0.015	3.20	0.22	0.0917	0.0025	0.932	1456	53	1453	79	1461	51	97	72	a
0.209	0.010	2.11	0.12	0.0733	0.0021	0.915	1151	39	1221	55	1022	57	91	38	a
0.221	0.018	3.34	0.29	0.1098	0.0028	0.938	1491	69	1286	97	1795	46	122	70	a
0.275	0.026	4.64	0.47	0.1226	0.0031	0.952	1757	84	1564	134	1994	45	131	61	a
0.216	0.075	3.55	1.24	0.1193	0.0045	0.975	1538	278	1260	398	1945	67	129	61	a
0.236	0.012	3.94	0.22	0.1211	0.0030	0.893	1622	45	1365	60	1973	44	140	85	a
0.285	0.020	4.68	0.36	0.1191	0.0030	0.938	1763	64	1616	101	1942	45	75	55	a
0.1216	0.0056	1.165	0.060	0.0695	0.0018	0.861	784	28	740	32	914	53	140	81	a
0.308	0.058	5.1923	1.0028	0.1221	0.0033	0.976	1851	164	1733	288	1987	48	120	48	a
0.192	0.019	3.30	0.34	0.1247	0.0032	0.931	1482	80	1133	103	2024	45	114	61	r
0.175	0.019	2.69	0.30	0.1116	0.0039	0.915	1327	83	1040	103	1826	63	104	94	a
0.211	0.013	3.66	0.25	0.1259	0.0033	0.895	1563	54	1234	69	2042	47	112	63	a
0.136	0.029	1.67	0.43	0.089	0.013	0.811	997	164	823	166	1404	282	113	65	a
0.1251	0.0061	1.632	0.089	0.0946	0.0025	0.825	983	34	760	35	1521	50	104	42	a
0.207	0.014	3.23	0.23	0.1129	0.0030	0.911	1463	56	1214	74	1847	48	85	82	a

$^{206}Pb^*/^{238}U$	± 2σ (abs)	$^{207}Pb^*/^{235}U$	± 2σ (abs)	$^{207}Pb^*/^{206}Pb^*$	± 2σ (abs)	corr. coef.	$^{206}Pb^*/^{238}U$ age (Ma)	± 2σ (Ma)	$^{207}Pb^*/^{235}U$ age (Ma)	± 2σ (Ma)	$^{207}Pb^*/^{206}Pb^*$ age (Ma)	± 2σ (Ma)	Length (μm)	Width (μm)	Accept/ Reject
0.170	0.015	2.21	0.21	0.0939	0.0025	0.931	1183	66	1015	85	1506	51	95	50	a
0.185	0.022	3.37	0.41	0.1323	0.0037	0.929	1498	94	1093	117	2129	49	127	105	r
0.147	0.030	3.69	1.75	0.182	0.080	0.963	1570	379	883	168	2675	730	102	59	r
0.157	0.017	2.38	0.28	0.1103	0.0032	0.923	1238	83	939	97	1804	53	129	52	r
0.317	0.041	5.35	0.71	0.1223	0.0032	0.968	1877	114	1776	199	1991	46	91	60	a
0.258	0.027	4.43	0.50	0.1244	0.0050	0.922	1717	94	1480	136	2020	72	89	61	a
0.262	0.075	4.81	2.71	0.133	0.056	0.668	1787	474	1498	383	2143	739	70	42	a
0.1469	0.0096	1.23	0.11	0.0609	0.0041	0.815	816	52	884	54	636	146	119	81	a
0.228	0.026	3.46	0.41	0.1098	0.0028	0.956	1517	94	1325	138	1796	46	91	68	a
0.182	0.034	2.87	0.64	0.114	0.014	0.832	1374	169	1080	186	1866	219	78	70	a
0.145	0.013	1.46	0.14	0.0728	0.0021	0.931	913	57	874	73	1007	59	94	56	a
0.309	0.028	5.08	0.49	0.1190	0.0030	0.956	1832	83	1737	139	1941	46	78	48	a
0.309	0.028	5.08	0.49	0.1190	0.0030	0.956	1832	83	1737	139	1941	46	123	86	a
0.242	0.038	3.23	0.72	0.097	0.014	0.852	1464	173	1399	199	1559	267	76	72	a
0.179	0.015	2.36	0.21	0.0954	0.0025	0.933	1230	64	1063	84	1535	48	130	89	a
0.1442	0.0075	1.18	0.14	0.0593	0.0067	0.578	791	66	868	42	578	244	101	90	a
0.203	0.033	3.49	0.57	0.1248	0.0033	0.958	1524	129	1189	175	2027	47	124	57	a
0.0694	0.0037	0.533	0.032	0.0557	0.0021	0.747	434	21	433	22	439	82	160	70	a
0.0738	0.0043	0.537	0.034	0.0527	0.0017	0.822	436	22	459	26	318	74	73	50	a
0.202	0.026	3.02	0.49	0.108	0.010	0.840	1413	125	1188	142	1772	172	101	90	a
0.1391	0.0060	1.410	0.072	0.0735	0.0021	0.855	893	30	839	34	1029	57	124	57	a
0.200	0.011	2.33	0.15	0.0843	0.0024	0.909	1220	44	1176	59	1298	55	160	70	a
0.1329	0.0073	1.68	0.11	0.0915	0.0030	0.829	1000	40	804	42	1458	62	101	59	a
0.229	0.015	3.41	0.24	0.1080	0.0030	0.916	1506	56	1328	77	1767	50	98	67	a
0.232	0.022	4.00	0.40	0.1248	0.0032	0.942	1634	82	1347	117	2026	45	106	56	a
0.1717	0.0087	1.74	0.10	0.0733	0.0021	0.897	1022	38	1022	48	1022	59	117	56	a
0.196	0.021	3.34	0.37	0.1234	0.0031	0.940	1491	86	1156	113	2006	44	125	54	a
0.258	0.048	3.40	0.69	0.0956	0.0065	0.943	1505	159	1480	246	1540	129	89	57	a
19. Negro River, Brazil (3.1807°S, 60.0054°W)															
0.1533	0.0077	1.420	0.082	0.0672	0.0028		897	33	919	43	843	86	123	61	a
0.1512	0.0076	2.21	0.13	0.1062	0.0044		1186	39	908	42	1736	75	294	102	r
0.820	0.041	13.19	0.45	0.1167	0.0045		2693	30	3861	147	1906	70	161	52	r
0.291	0.015	4.49	0.22	0.1119	0.0043		1730	40	1647	73	1831	69	215	98	a
0.1683	0.0084	1.78	0.11	0.0769	0.0030		1039	37	1003	47	1117	78	170	71	a
0.1622	0.0081	1.620	0.092	0.0724	0.0028		978	34	969	45	998	78	85	60	a
0.200	0.010	2.38	0.21	0.0863	0.0051		1238	60	1178	54	1344	113	142	65	a
0.306	0.015	4.76	0.23	0.1129	0.0044		1778	40	1720	76	1846	70	287	112	a
0.384	0.019	6.29	0.30	0.1186	0.0049		2017	39	2097	90	1936	74	159	112	a
0.0834	0.0042	1.064	0.062	0.0925	0.0045		736	27	517	25	1478	93	156	69	r
0.1865	0.0093	2.23	0.14	0.0869	0.0033		1192	40	1103	51	1358	74	181	134	a
0.1592	0.0080	1.669	0.094	0.0760	0.0029		997	34	952	44	1096	77	92	113	a
0.391	0.020	4.55	0.20	0.0845	0.0032		1741	35	2127	91	1304	74	102	45	a
0.581	0.029	8.85	0.34	0.1104	0.0043		2323	33	2955	120	1807	70	152	75	a
0.1792	0.0090	2.20	0.14	0.0891	0.0034		1181	41	1062	49	1406	73	178	97	a
0.0301	0.0015	0.209	0.024	0.0503	0.0058		193	19	191	9	210	267	251	128	a
0.1783	0.0089	1.93	0.12	0.0786	0.0030		1092	39	1057	49	1163	77	205	83	a
0.253	0.013	3.35	0.18	0.0961	0.0037		1492	39	1451	65	1550	72	110	105	a
0.00603	0.00030	0.0385	0.0032	0.0463	0.0039		38	3	39	2	15	203	152	94	a
0.1653	0.0083	1.743	0.099	0.0765	0.0029		1024	35	986	46	1108	76	187	76	a
0.0458	0.0023	0.331	0.017	0.0524	0.0025		290	12	289	14	303	108	215	65	a
0.0325	0.0016	0.220	0.014	0.0492	0.0030		202	10	206	10	158	143	297	149	a

$^{206}Pb^*/^{238}U$	± 2σ (abs)	$^{207}Pb^*/^{235}U$	± 2σ (abs)	$^{207}Pb^*/^{206}Pb^*$	± 2σ (abs)	corr. coef.	$^{206}Pb^*/^{238}U$ age (Ma)	± 2σ (Ma)	$^{207}Pb^*/^{235}U$ age (Ma)	± 2σ (Ma)	$^{207}Pb^*/^{206}Pb^*$ age (Ma)	± 2σ (Ma)	Length (μm)	Width (μm)	Accept/ Reject
0.1322	0.0066	2.42	0.26	0.133	0.011		1250	68	800	38	2138	143	242	103	r
0.1235	0.0062	2.40	0.24	0.141	0.011		1243	63	751	36	2240	135	108	44	r
0.215	0.011	3.51	0.27	0.1180	0.0062		1529	57	1258	57	1927	94	183	89	a
0.1140	0.0057	1.349	0.069	0.0859	0.0035		867	29	696	33	1335	79	160	105	a
0.339	0.017	6.11	0.34	0.1308	0.0061		1992	46	1881	82	2109	81	238	117	a
0.258	0.013	5.04	0.38	0.1415	0.0078		1826	55	1482	67	2245	95	311	113	a
0.1090	0.0054	0.911	0.051	0.0606	0.0028		657	26	667	32	625	100	123	73	a
0.00	0.00	0.0046	0.0022	0.079	0.046		5	2	3	0	1166	1149	226	98	r
0.1989	0.0099	2.62	0.16	0.0957	0.0038		1308	42	1170	54	1542	75	95	91	a
0.1739	0.0087	3.24	0.27	0.1352	0.0071		1467	62	1033	48	2166	91	270	111	r
0.1807	0.0090	2.30	0.15	0.0925	0.0037		1213	44	1071	50	1477	77	263	113	a
0.0370	0.0019	0.280	0.016	0.0549	0.0029		251	12	234	12	409	118	130	82	a
0.1785	0.0089	2.41	0.15	0.0978	0.0039		1244	44	1059	49	1582	75	148	74	a
0.237	0.012	3.53	0.20	0.1083	0.0042		1535	42	1369	62	1771	71	203	139	a
0.0327	0.0016	0.254	0.020	0.0562	0.0045		230	16	208	10	461	176	216	114	a
0.305	0.015	4.56	0.24	0.1085	0.0044		1741	40	1714	76	1774	74	121	64	a
0.1425	0.0071	1.521	0.080	0.0774	0.0030		939	31	859	40	1131	76	152	96	a
0.253	0.013	4.02	0.21	0.1152	0.0044		1638	41	1455	65	1883	69	219	119	a
0.202	0.010	2.65	0.16	0.0953	0.0036		1314	41	1184	54	1533	72	126	92	a
0.1551	0.0078	1.755	0.096	0.0821	0.0031		1029	34	929	43	1248	75	151	82	a
0.1387	0.0069	1.656	0.087	0.0866	0.0034		992	31	837	39	1352	75	108	52	a
0.0312	0.0016	0.2178	0.0096	0.0506	0.0021		200	8	198	10	221	97	173	85	a
0.367	0.018	6.11	0.31	0.1206	0.0052		1992	41	2017	87	1966	77	193	76	a
0.250	0.012	3.76	0.20	0.1090	0.0042		1583	41	1438	65	1783	70	277	88	a
0.1735	0.0087	2.21	0.13	0.0922	0.0035		1183	40	1032	48	1472	73	170	86	a
0.1462	0.0073	1.579	0.084	0.0783	0.0030		962	31	879	41	1156	76	205	140	a
0.0289	0.0014	0.207	0.011	0.0519	0.0028		191	9	184	9	281	122	226	143	a
0.1656	0.0083	2.02	0.12	0.0884	0.0034		1122	37	988	46	1392	74	191	182	a
0.0502	0.0025	0.397	0.018	0.0573	0.0025		340	13	316	15	505	94	254	92	a
0.0943	0.0047	0.836	0.056	0.0642	0.0036		617	21	581	28	750	118	111	96	a
0.0464	0.0023	0.343	0.033	0.0535	0.0050		299	24	293	14	351	211	252	69	a
0.0375	0.0019	1.04	0.15	0.201	0.027		725	71	238	12	2838	218	199	153	r
0.0300	0.0015	0.182	0.041	0.044	0.010		170	33	190	9			233	94	a
0.0279	0.0014	0.188	0.013	0.0489	0.0032		175	10	178	9	143	155	356	131	a
0.0241	0.0012	0.1754	0.0072	0.0528	0.0022		164	11	154	8	320	94	163	130	a
0.0297	0.0015	0.183	0.014	0.0448	0.0033		171	11	188	9			210	98	a
0.0296	0.0015	0.186	0.031	0.0457	0.0076		173	25	188	9	-20	403	218	112	a
0.1223	0.0061	1.846	0.099	0.1095	0.0046		1062	34	744	35	1791	76	194	117	r
Zircon Standard: Remora 2															
0.0678	0.0020	0.526	0.021	0.0563	0.0019		423	12	429	14	465	74			
0.0644	0.0019	0.492	0.024	0.0554	0.0028		403	11	406	17	427	114			
0.0629	0.0018	0.469	0.022	0.0541	0.0027		393	11	391	16	377	111			
0.0646	0.0019	0.493	0.021	0.0554	0.0022		403	11	407	15	427	90			
0.0655	0.0027	0.489	0.026	0.0542	0.0026		409	16	405	18	379	108			
0.0669	0.0027	0.471	0.026	0.0511	0.0026		417	17	392	18	245	117			
0.0639	0.0026	0.485	0.021	0.0550	0.0021		399	16	401	14	413	85			
0.1132	0.0051	0.933	0.061	0.0597	0.0032		692	30	669	32	594	117			
0.0685	0.0028	0.525	0.027	0.0556	0.0026		427	17	429	18	437	104			
0.0693	0.0029	0.566	0.027	0.0592	0.0025		432	17	455	18	576	93			
0.0652	0.0027	0.475	0.024	0.0528	0.0024		407	16	395	17	320	103			
0.0622	0.0025	0.476	0.020	0.0555	0.0021		389	15	396	14	433	85			

$^{206}Pb^*/^{238}U$	± 2σ (abs)	$^{207}Pb^*/^{235}U$	± 2σ (abs)	$^{207}Pb^*/^{206}Pb^*$	± 2σ (abs)	corr. coef.	$^{206}Pb^*/^{238}U$ age (Ma)	± 2σ (Ma)	$^{207}Pb^*/^{235}U$ age (Ma)	± 2σ (Ma)	$^{207}Pb^*/^{206}Pb^*$ age (Ma)	± 2σ (Ma)	Length (μm)	Width (μm)	Accept/ Reject
0.0631	0.0026	0.483	0.025	0.0554	0.0027		395	16	400	17	430	107			
0.0623	0.0025	0.532	0.026	0.0619	0.0028		390	15	433	17	672	96			
0.0764	0.0041	0.596	0.033	0.0565	0.0021		475	25	475	21	473	83			
0.0687	0.0037	0.535	0.031	0.0565	0.0022		429	22	435	21	472	87			
0.0633	0.0035	0.497	0.027	0.0569	0.0021		396	21	410	18	488	81			
0.0601	0.0033	0.458	0.031	0.0553	0.0025		376	20	383	21	425	102			
0.0569	0.0031	0.439	0.025	0.0560	0.0021		357	19	370	17	451	82			
0.0629	0.0034	0.506	0.032	0.0583	0.0025		393	21	416	21	542	92			
0.0533	0.0029	0.406	0.025	0.0552	0.0023		335	18	346	18	421	93			
0.0960	0.0051	0.748	0.043	0.0565	0.0022		591	30	567	25	472	88			
0.0558	0.0031	0.433	0.042	0.0562	0.0038		350	19	365	30	461	149			
0.0701	0.0038	0.532	0.033	0.0551	0.0024		437	23	433	22	417	96			
0.0689	0.0037	0.546	0.031	0.0574	0.0022		429	22	442	20	509	83			
0.0561	0.0031	0.472	0.051	0.0611	0.0046		352	19	393	35	642	161			
0.0639	0.0036	0.436	0.040	0.0496	0.0030		399	22	368	28	175	140			
0.0803	0.0047	0.96	0.17	0.087	0.010		498	28	686	90	1363	225			
0.0626	0.0036	0.500	0.040	0.0580	0.0031		391	22	412	27	529	115			
0.0802	0.0046	0.632	0.038	0.0571	0.0022		498	28	497	24	495	84			
0.0640	0.0037	0.585	0.075	0.0663	0.0056		400	22	468	48	816	176			
0.0587	0.0034	0.408	0.032	0.0504	0.0026		368	20	348	23	215	119			
0.1037	0.0062	0.928	0.077	0.0650	0.0034		636	36	667	41	773	109			
0.0699	0.0040	0.507	0.048	0.0525	0.0032		436	24	416	32	309	141			
0.0714	0.0041	0.534	0.040	0.0542	0.0022		444	25	434	27	381	92			
0.0641	0.0037	0.489	0.032	0.0553	0.0017		401	22	404	22	424	69			
0.0552	0.0032	0.409	0.025	0.0537	0.0015		346	20	348	18	359	64			
0.0726	0.0041	0.565	0.033	0.0564	0.0015		452	25	455	22	468	59			
0.0603	0.0035	0.462	0.028	0.0556	0.0015		377	21	386	19	436	61			
0.0543	0.0029	0.397	0.023	0.0530	0.0015		341	18	339	17	327	65			
0.0637	0.0034	0.486	0.026	0.0554	0.0014		398	21	402	18	428	56			
0.0413	0.0022	0.331	0.022	0.0582	0.0022		261	13	290	16	537	81			
0.0630	0.0034	0.483	0.035	0.0556	0.0023		394	21	400	24	437	92			
0.0516	0.0027	0.396	0.022	0.0556	0.0015		324	17	339	16	437	60			
0.0677	0.0036	0.528	0.031	0.0565	0.0017		422	22	430	21	472	67			
0.0757	0.0041	0.584	0.036	0.0559	0.0018		470	25	467	23	448	71			
0.0691	0.0037	0.528	0.030	0.0555	0.0015		431	22	431	20	431	61			
0.0726	0.0039	0.550	0.031	0.0549	0.0014		452	24	445	20	410	58			
0.0628	0.0034	0.460	0.028	0.0531	0.0017		392	20	384	20	335	72			
0.0719	0.0042	0.554	0.042	0.0559	0.0031	0.641	448	25	447	27	447	125			
0.0682	0.0025	0.438	0.018	0.0466	0.0012	0.783	425	15	369	13	27	61			
0.0741	0.0030	0.58	0.12	0.056	0.012	0.917	461	18	462	76	464	478			
0.0641	0.0019	0.484	0.022	0.0547	0.0027	0.901	400	11	400	15	401	112			
0.1241	0.0052	1.09	0.18	0.0639	0.0086	0.962	754	30	750	89	739	284			
0.0667	0.0020	0.267	0.042	0.0290	0.0067	0.871	416	12	240	34	-1261	722			
0.0566	0.0017	0.220	0.013	0.0282	0.0022	0.864	355	10	202	11	-1351	246			
0.0549	0.0017	0.169	0.011	0.0224	0.0019	0.856	344	10	159	10	-2169	332			
0.0558	0.0019	0.214	0.027	0.0279	0.0050	0.847	350	12	197	22	-1392	579			
0.0547	0.0018	0.186	0.019	0.0246	0.0035	0.846	343	11	173	16	-1818	510			
0.0848	0.0039	0.570	0.039	0.0488	0.0031	0.614	525	23	458	25	136	150			
0.0755	0.0035	0.571	0.031	0.0549	0.0020	0.737	469	21	459	20	408	82			
0.0671	0.0026	0.462	0.024	0.0499	0.0024	0.532	419	16	385	17	189	110			
0.0620	0.0026	0.438	0.024	0.0513	0.0024	0.523	388	16	369	17	254	109			

$^{206}Pb^*/^{238}U$	± 2σ (abs)	$^{207}Pb^*/^{235}U$	± 2σ (abs)	$^{207}Pb^*/^{206}Pb^*$	± 2σ (abs)	corr. coef.	$^{206}Pb^*/^{238}U$ age (Ma)	± 2σ (Ma)	$^{207}Pb^*/^{235}U$ age (Ma)	± 2σ (Ma)	$^{207}Pb^*/^{206}Pb^*$ age (Ma)	± 2σ (Ma)	Length (μm)	Width (μm)	Accept/ Reject
0.0712	0.0043	0.497	0.036	0.0506	0.0025	0.734	443	26	410	24	224	115			
0.0805	0.0029	0.653	0.033	0.0589	0.0026	0.546	499	17	510	20	562	98			
0.0885	0.0087	0.755	0.077	0.0619	0.0022	0.888	547	51	571	45	670	77			
0.0606	0.0020	0.484	0.027	0.0580	0.0036	0.895	379	12	401	19	529	134			
0.0580	0.0019	0.456	0.027	0.0571	0.0040	0.885	364	12	382	19	494	153			
0.0706	0.0030	0.553	0.032	0.0568	0.0029	0.502	440	18	447	21	485	113			
0.0637	0.0017	0.274	0.023	0.0313	0.0046	0.841	398	10	246	19	-1034	436			
0.0629	0.0015	0.256	0.026	0.0296	0.0053	0.836	393	9	232	21	-1205	553			
0.0687	0.0071	0.433	0.043	0.0457	0.0017	0.888	429	43	366	30	-16	91			
0.0693	0.0024	0.1576	0.0041	0.01649	0.00041	0.884	432	14	149	4	-3589	139			
0.0645	0.0015	0.284	0.016	0.0319	0.0029	0.850	403	9	254	13	-973	271			
0.0638	0.0015	0.465	0.018	0.0529	0.0029	0.867	398	9	388	12	323	126			
0.0707	0.0017	0.596	0.020	0.0611	0.0025	0.898	440	10	475	13	643	88			
0.054	0.019	3.031	1.076	0.406	0.069	0.949	340	118	1416	271	3932	253			
0.0603	0.0044	0.768	0.065	0.0923	0.0083	0.898	378	27	578	37	1473	171			
0.0874	0.0045	0.659	0.039	0.0547	0.0021	0.787	540	27	514	24	398	88			
0.0686	0.0015	0.490	0.017	0.0518	0.0027	0.875	428	9	405	12	275	118			
0.0687	0.0015	0.503	0.018	0.0530	0.0027	0.877	428	9	413	12	331	115			
0.0672	0.0014	0.495	0.020	0.0534	0.0035	0.861	419	8	408	14	347	146			
0.0540	0.0064	0.13	0.17	0.017	0.032	0.832	339	39	123	149	-3334	9852			
0.0679	0.0036	0.74	0.24	0.079	0.038	0.871	424	21	562	137	1171	957			
0.0712	0.0038	0.54	0.19	0.055	0.029	0.874	444	23	436	123	399	1200			
0.0680	0.0021	0.496	0.030	0.0529	0.0043	0.885	424	12	409	21	326	186			
0.0595	0.0020	0.455	0.021	0.0555	0.0025	0.905	372	12	381	15	431	100			
0.0811	0.0027	0.694	0.040	0.0620	0.0043	0.915	503	16	535	24	675	147			
0.0837	0.0024	0.713	0.036	0.0618	0.0036	0.919	518	15	547	21	666	125			
0.0850	0.0028	0.723	0.028	0.0617	0.0019	0.696	526	17	553	17	664	64			
0.0639	0.0022	0.535	0.030	0.0607	0.0038	0.898	400	13	435	20	627	136			
0.0847	0.0028	0.759	0.037	0.0650	0.0034	0.927	524	17	574	21	774	109			
0.0821	0.0027	0.635	0.030	0.0561	0.0027	0.473	509	16	499	19	455	108			
0.0673	0.0027	0.545	0.029	0.0587	0.0028	0.921	420	16	442	19	555	104			
0.0644	0.0023	0.516	0.026	0.0581	0.0030	0.908	402	14	422	18	534	113			
0.0669	0.0015	0.482	0.017	0.0523	0.0029	0.868	417	9	400	12	299	125			
0.0723	0.0017	0.629	0.024	0.0631	0.0037	0.879	450	10	495	15	711	124			
0.0657	0.0014	0.499	0.017	0.0551	0.0030	0.864	410	8	411	12	416	120			
0.0792	0.0024	0.660	0.038	0.0605	0.0056	0.882	491	14	515	23	620	201			
0.0652	0.0014	0.497	0.018	0.0553	0.0032	0.860	407	9	410	12	425	130			
0.0623	0.0059	0.465	0.048	0.0541	0.0017	0.889	390	36	388	34	375	69			
0.0725	0.0073	0.552	0.062	0.0552	0.0018	0.905	451	44	446	40	422	71			
0.0630	0.0060	0.484	0.054	0.0557	0.0020	0.872	394	37	401	37	440	79			
0.0737	0.0075	0.573	0.063	0.0564	0.0017	0.910	458	45	460	41	466	67			
0.0741	0.0077	0.539	0.068	0.0528	0.0026	0.866	461	46	438	45	322	113			
0.0628	0.0059	0.471	0.051	0.0544	0.0019	0.874	393	36	392	35	389	79			
0.0755	0.0073	0.571	0.064	0.0548	0.0023	0.878	469	44	459	42	405	92			
0.0725	0.0070	0.546	0.061	0.0546	0.0021	0.882	451	42	442	40	396	86			
0.0659	0.0064	0.472	0.053	0.0520	0.0021	0.871	411	38	393	36	283	91			
0.0652	0.0062	0.521	0.070	0.0579	0.0043	0.733	407	38	426	47	526	164			
0.0710	0.0070	0.74	0.15	0.075	0.011	0.949	442	42	561	86	1079	285			
0.0663	0.0061	0.478	0.052	0.0523	0.0025	0.836	414	37	396	36	296	110			
0.0650	0.0059	0.482	0.049	0.0538	0.0019	0.871	406	36	400	33	362	81			
0.0624	0.0057	0.453	0.050	0.0527	0.0028	0.809	390	35	380	35	316	119			

$^{206}Pb^*/^{238}U$	± 2σ (abs)	$^{207}Pb^*/^{235}U$	± 2σ (abs)	$^{207}Pb^*/^{206}Pb^*$	± 2σ (abs)	corr. coef.	$^{206}Pb^*/^{238}U$ age (Ma)	± 2σ (Ma)	$^{207}Pb^*/^{235}U$ age (Ma)	± 2σ (Ma)	$^{207}Pb^*/^{206}Pb^*$ age (Ma)	± 2σ (Ma)	Length (μm)	Width (μm)	Accept/ Reject
0.0615	0.0056	0.451	0.048	0.0532	0.0023	0.836	385	34	378	33	337	99			
0.0643	0.0059	0.475	0.049	0.0535	0.0021	0.858	402	36	394	34	351	90			
0.0899	0.0085	0.695	0.070	0.0561	0.0016	0.925	555	50	536	42	456	63			
0.0904	0.0090	0.794	0.099	0.0637	0.0040	0.830	558	53	594	56	733	132			
0.0668	0.0062	0.519	0.055	0.0564	0.0026	0.837	417	37	424	37	468	101			
0.0671	0.0062	0.497	0.051	0.0537	0.0020	0.875	419	38	409	35	357	83			
0.0641	0.0059	0.469	0.050	0.0531	0.0024	0.835	400	35	391	35	333	104			
0.0695	0.0054	0.520	0.047	0.0542	0.0025	0.819	433	32	425	31	380	102			
0.0708	0.0055	0.587	0.064	0.0602	0.0047	0.675	441	33	469	41	610	167			
0.0674	0.0052	0.465	0.049	0.0500	0.0036	0.727	421	31	388	34	196	169			
0.0684	0.0052	0.506	0.043	0.0536	0.0020	0.845	427	32	416	29	356	86			
0.0729	0.0057	0.551	0.048	0.0548	0.0019	0.871	454	35	446	31	405	77			
0.0667	0.0051	0.502	0.042	0.0546	0.0018	0.862	416	31	413	28	396	73			
0.0693	0.0054	0.528	0.047	0.0553	0.0022	0.838	432	32	431	31	424	90			
0.0675	0.0052	0.505	0.042	0.0543	0.0018	0.864	421	32	415	29	382	74			
0.0682	0.0052	0.521	0.045	0.0554	0.0022	0.834	426	32	426	30	429	89			
0.0654	0.0050	0.509	0.043	0.0565	0.0020	0.840	408	30	418	29	470	79			
0.0670	0.0051	0.515	0.048	0.0557	0.0030	0.771	418	31	422	32	442	120			
0.0875	0.0069	0.716	0.062	0.0594	0.0019	0.895	540	41	548	37	580	68			
0.0896	0.0077	0.687	0.065	0.0556	0.0019	0.902	553	46	531	39	436	77			
0.0845	0.0068	0.644	0.062	0.0553	0.0026	0.854	523	41	505	38	425	103			
0.0770	0.0063	0.601	0.053	0.0566	0.0018	0.889	478	38	478	34	477	69			
0.0756	0.0059	0.597	0.049	0.0572	0.0017	0.885	470	35	475	31	499	66			
0.0681	0.0052	0.521	0.045	0.0555	0.0021	0.842	425	32	426	30	431	84			
0.0745	0.0058	0.591	0.068	0.0575	0.0051	0.664	463	35	471	44	511	196			
0.0691	0.0053	0.537	0.044	0.0564	0.0017	0.874	431	32	437	29	467	66			
0.0706	0.0055	0.524	0.045	0.0538	0.0022	0.844	440	33	428	30	364	90			
0.0701	0.0062	0.536	0.056	0.0554	0.0028	0.800	437	38	436	37	428	113			
0.0682	0.0060	0.511	0.053	0.0543	0.0027	0.800	425	36	419	35	384	112			
0.0775	0.0069	0.626	0.067	0.0586	0.0031	0.801	481	41	494	42	552	117			
0.0637	0.0055	0.441	0.052	0.0502	0.0038	0.674	398	33	371	37	206	175			
0.0636	0.0054	0.480	0.044	0.0547	0.0017	0.858	398	33	398	30	399	71			
0.0604	0.0052	0.444	0.042	0.0534	0.0019	0.836	378	31	373	29	345	80			
0.0600	0.0052	0.437	0.048	0.0529	0.0035	0.689	376	32	368	34	324	149			
0.0654	0.0056	0.506	0.046	0.0561	0.0016	0.875	408	34	416	31	458	63			
0.0607	0.0052	0.486	0.045	0.0580	0.0020	0.831	380	31	402	31	530	75			
0.0638	0.0055	0.520	0.050	0.0592	0.0025	0.801	399	33	425	33	574	90			
0.0655	0.0056	0.529	0.057	0.0586	0.0035	0.714	409	34	431	38	552	132			
0.0709	0.0065	0.593	0.064	0.0607	0.0033	0.778	442	39	473	41	627	116			
0.0635	0.0054	0.465	0.052	0.0531	0.0038	0.676	397	33	388	36	333	161			
0.0658	0.0058	0.506	0.047	0.0558	0.0015	0.888	411	35	416	32	443	59			
0.0603	0.0052	0.466	0.044	0.0561	0.0020	0.829	377	32	389	31	456	80			
0.0828	0.0076	0.728	0.077	0.0638	0.0031	0.823	513	45	556	45	736	102			
0.0720	0.0064	0.576	0.055	0.0581	0.0020	0.862	448	38	462	36	532	76			
0.0647	0.0056	0.500	0.045	0.0560	0.0015	0.882	404	34	411	31	452	59			
0.0631	0.0054	0.488	0.046	0.0561	0.0021	0.831	394	33	404	31	458	82			
0.0748	0.0066	0.565	0.053	0.0548	0.0017	0.884	465	39	455	35	405	71			
0.0676	0.0058	0.505	0.046	0.0542	0.0015	0.886	422	35	415	31	377	62			
0.0651	0.0056	0.461	0.050	0.0514	0.0031	0.750	407	34	385	35	257	138			
0.111	0.010	0.954	0.099	0.0622	0.0024	0.899	681	60	680	52	680	84			
0.0659	0.0057	0.534	0.053	0.0588	0.0028	0.778	411	34	434	35	558	105			

$^{206}Pb^*/^{238}U$	± 2σ (abs)	$^{207}Pb^*/^{235}U$	± 2σ (abs)	$^{207}Pb^*/^{206}Pb^*$	± 2σ (abs)	corr. coef.	$^{206}Pb^*/^{238}U$ age (Ma)	± 2σ (Ma)	$^{207}Pb^*/^{235}U$ age (Ma)	± 2σ (Ma)	$^{207}Pb^*/^{206}Pb^*$ age (Ma)	± 2σ (Ma)	Length (μm)	Width (μm)	Accept/ Reject
0.0743	0.0065	0.590	0.056	0.0576	0.0019	0.875	462	39	471	35	514	71			
0.0698	0.0060	0.560	0.060	0.0582	0.0035	0.742	435	36	452	39	538	130			
0.0765	0.0068	0.596	0.064	0.0565	0.0032	0.788	475	41	475	41	472	127			
0.0688	0.0052	0.537	0.058	0.0566	0.0032	0.725	429	31	436	38	476	123			
0.0639	0.0034	0.497	0.044	0.0564	0.0031	0.557	400	21	410	30	468	120			
0.0669	0.0042	0.503	0.043	0.0546	0.0022	0.767	417	26	414	29	395	91			
0.0559	0.0029	0.395	0.031	0.0512	0.0022	0.637	351	18	338	23	252	100			
0.0538	0.0028	0.454	0.045	0.0612	0.0037	0.933	338	17	380	31	647	130			
0.0645	0.0035	0.493	0.040	0.0555	0.0026	0.660	403	21	407	27	433	103			
0.0669	0.0053	0.516	0.064	0.0560	0.0039	0.657	417	32	423	43	452	156			
0.0952	0.0060	0.786	0.094	0.0599	0.0044	0.668	586	35	589	54	600	158			
0.0590	0.0034	0.444	0.031	0.0545	0.0017	0.778	370	20	373	22	392	69			
0.0628	0.0053	0.528	0.071	0.0609	0.0047	0.567	393	32	430	47	636	166			
0.0913	0.0048	0.746	0.050	0.0593	0.0023	0.794	563	28	566	29	578	83			
0.0791	0.0036	0.733	0.059	0.0672	0.0042	0.943	491	22	558	35	844	129			
0.0664	0.0030	0.528	0.039	0.0577	0.0032	0.933	415	18	430	26	517	122			
0.0691	0.0031	0.561	0.038	0.0589	0.0028	0.566	430	19	452	25	563	103			
0.0773	0.0037	0.601	0.037	0.0563	0.0019	0.765	480	22	478	23	466	76			
0.0614	0.0028	0.458	0.032	0.0541	0.0027	0.508	384	17	383	22	376	111			
0.0786	0.0040	0.600	0.036	0.0554	0.0017	0.820	488	24	477	23	426	67			
0.0880	0.0062	0.757	0.067	0.0624	0.0029	0.793	544	37	572	39	687	100			
0.0636	0.0030	0.464	0.029	0.0529	0.0020	0.701	397	18	387	20	326	84			
0.0657	0.0057	0.473	0.046	0.0522	0.0020	0.848	410	35	393	32	296	86			
0.0630	0.0024	0.488	0.026	0.0562	0.0021	0.585	394	15	404	17	460	82			
0.0631	0.0024	0.480	0.023	0.0552	0.0018	0.658	394	15	398	16	420	71			
0.0670	0.0026	0.492	0.027	0.0533	0.0022	0.579	418	16	407	18	341	95			
0.0648	0.0025	0.455	0.037	0.0510	0.0040	0.914	405	15	381	26	240	179			
0.0640	0.0025	0.470	0.032	0.0533	0.0033	0.919	400	15	391	22	340	138			
0.071	0.013	1.14	0.12	0.1159	0.0080	0.715	443	77	771	58	1894	124			
0.065	0.010	0.703	0.075	0.0786	0.0047	0.787	405	61	541	45	1162	119			
0.0634	0.0085	0.666	0.071	0.0763	0.0032	0.833	396	52	519	43	1102	85			
0.070	0.010	0.632	0.068	0.0660	0.0032	0.860	433	61	498	42	805	100			
0.0713	0.0094	0.618	0.067	0.0629	0.0023	0.889	444	56	489	42	706	78			
0.0644	0.0087	1.46	0.16	0.165	0.018	0.910	402	53	915	65	2505	183			
0.077	0.012	1.42	0.16	0.135	0.013	0.934	476	71	899	66	2160	168			
0.082	0.015	2.23	0.25	0.196	0.013	0.591	509	90	1190	80	2797	109			
0.069	0.013	1.10	0.12	0.1154	0.0091	0.678	430	79	752	59	1886	142			
0.105	0.024	4.70	0.57	0.326	0.029	0.958	642	139	1768	101	3598	139			
0.086	0.012	2.00	0.22	0.1677	0.0065	0.759	535	68	1116	76	2535	65			
0.0659	0.0096	0.698	0.074	0.0767	0.0033	0.845	412	58	537	44	1114	87			
0.081	0.029	1.59	0.19	0.143	0.012	0.808	500	174	965	73	2261	148			

(1) Blank entries indicate that no data was collected. For absent correlation coefficients, data was collected prior to introduction of calculation algorithm.
(2) Correlation coefficients market '*', no significant correlation was found.
† Indicates which analyses were included in age spectra and statistical tests. a- accepted analysis, b- rejected analysis

APPENDIX C

AGE BIN SENSITIVITY ANALYSIS

Sensitivity of the binning technique used to the estimate relative contribution of major source regions in northern South America (Figure 1.3) was tested using bootstrap analysis. For each sample size (n) presented, 1,000 synthetic distributions were randomly sampled from an artificial distribution composed of all mainstem zircon analyses gathered between Leticia, Colombia and Santarém, Brazil. This approach was selected to simulate the complexity of the actual distribution of Amazon River zircon age distributions. Synthetic age distributions were then split into age bins that corresponded to regional geochronologic age provinces and bin proportions were calculated. Bin proportion sensitivity was estimated by calculating the standard deviation of all synthetic bin proportion estimates. Figure C.1 shows the estimated precision for the least and greatest sample sizes presented.

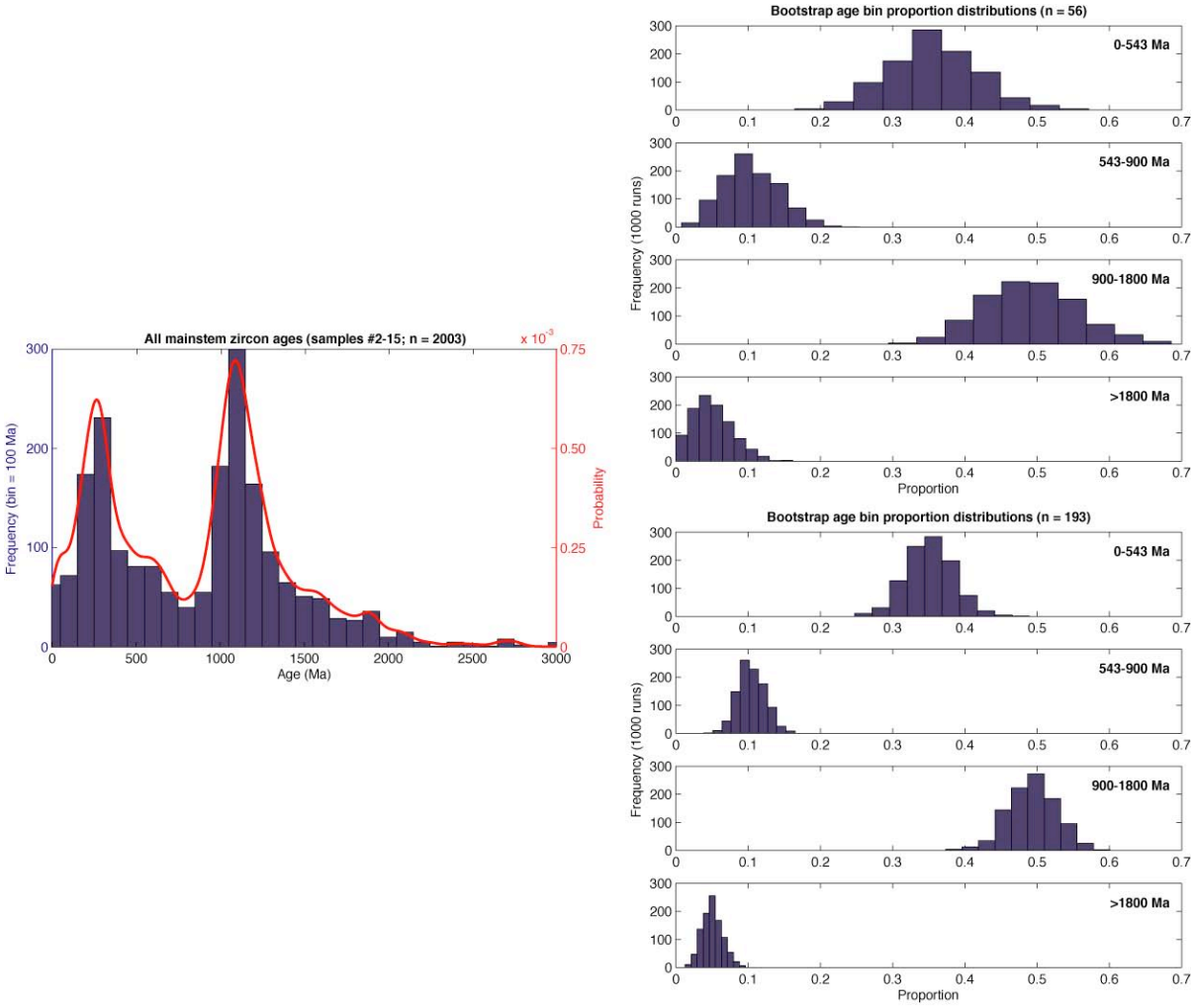

Figure C.1- Results of bootstrap sensitivity analysis for source region age bin precision. Standard deviations for bootstrap distributions were used to approximate precision of age bins presented in Figure 3 (Chapter 2). Sample sizes shown represent the largest and smallest sample sizes presented for modern sand samples.

APPENDIX D

LA-ICP-MS U/PB AND PB/PB AGES FOR DETRITAL ZIRCONS FROM SILICICLASTIC DEPOSITS OF THE AMAZON BASIN

$^{206}Pb/^{238}U$	± 2σ	$^{207}Pb/^{235}U$	± 2σ	$^{207}Pb/^{206}Pb$	± 2σ	Corr. Coef.[‡]	$^{206}Pb/^{238}U$ Age (Ma)	± 2σ	$^{207}Pb/^{206}Pb$ Age (Ma)[§]	± 2σ
a. Solimões Formation near Tefé (3.4004˚S, 64.6156˚W)[†]										
0.0290	0.0047	0.093	0.010	0.0234	0.0044	0.361	184	30		
0.149	0.033	0.83	0.12	0.0402	0.0046	0.928	895	183		
0.0222	0.0054	0.11	0.01	0.036	0.010	0.219	142	34		
0.0294	0.0055	0.160	0.017	0.0394	0.0066	0.680	187	34		
0.0268	0.0036	0.159	0.016	0.0430	0.0046	0.770	171	22		
0.095	0.014	0.672	0.077	0.0515	0.0026	0.914	584	84	261	117
0.0438	0.0061	0.287	0.030	0.0476	0.0015	0.886	276	38	81	73
0.020	0.013	0.126	0.018	0.046	0.055		127	84		
0.0547	0.0076	0.381	0.040	0.0505	0.0016	0.899	343	46	217	75
0.0463	0.0064	0.322	0.033	0.0505	0.0014	0.894	292	40	216	66
0.149	0.028	1.42	0.20	0.0693	0.0022	0.965	896	158	907	65
0.0291	0.0039	0.201	0.020	0.0501	0.0020	0.749	185	24	199	93
0.082	0.013	0.670	0.075	0.0594	0.0030	0.889	507	75	583	111
0.095	0.014	0.822	0.094	0.0627	0.0042	0.863	585	82	699	143
0.0198	0.0039	0.142	0.015	0.0518	0.0014	0.820	127	25	275	62
0.151	0.023	1.59	0.22	0.0761	0.0020	0.961	907	127	1097	53
0.143	0.025	1.46	0.20	0.0745	0.0021	0.964	859	144	1055	56
0.141	0.027	1.45	0.19	0.0747	0.0032	0.946	851	153	1060	87
0.0273	0.0038	0.202	0.020	0.0537	0.0019	0.767	174	24	357	79
0.147	0.026	1.56	0.22	0.0767	0.0042	0.929	885	146	1112	110
0.059	0.010	0.484	0.051	0.0591	0.0027	0.874	372	62	570	101
0.0300	0.0036	0.224	0.022	0.0542	0.0023	0.689	190	22	380	95
0.151	0.031	1.61	0.26	0.0777	0.0048	0.934	904	176	1140	122
0.082	0.013	0.723	0.080	0.0637	0.0021	0.925	510	77	731	71
0.133	0.027	1.37	0.18	0.0748	0.0021	0.966	802	156	1063	55
0.0164	0.0029	0.120	0.012	0.0529	0.0024	0.549	105	18	324	102
0.153	0.030	1.69	0.24	0.0802	0.0021	0.969	918	168	1201	52
0.143	0.024	1.54	0.21	0.0783	0.0023	0.958	859	136	1155	58
0.145	0.024	1.59	0.22	0.0795	0.0025	0.954	872	136	1186	63
0.143	0.025	1.58	0.21	0.0798	0.0035	0.937	864	139	1193	88
0.146	0.021	1.63	0.22	0.0807	0.0025	0.950	879	120	1214	61
0.126	0.020	1.32	0.17	0.0759	0.0021	0.953	766	114	1093	56
0.138	0.020	1.50	0.20	0.0788	0.0021	0.956	831	115	1168	52
0.096	0.016	0.91	0.10	0.0691	0.0021	0.941	589	94	903	61
0.131	0.031	1.40	0.18	0.0775	0.0021	0.969	796	175	1133	53
0.129	0.024	1.37	0.17	0.0771	0.0024	0.954	780	136	1124	63
0.142	0.023	1.58	0.21	0.0806	0.0021	0.960	858	130	1211	52
0.142	0.034	1.58	0.21	0.0809	0.0027	0.964	857	193	1218	65

0.0165	0.0022	0.12	0.01	0.0546	0.0036	0.762	105	14	394	148
0.138	0.023	1.53	0.20	0.0804	0.0025	0.953	833	132	1206	61
0.125	0.019	1.33	0.17	0.0772	0.0022	0.948	758	107	1127	57
0.095	0.015	0.92	0.11	0.0705	0.0024	0.927	586	89	943	71
0.0299	0.0043	0.237	0.024	0.0575	0.0070	0.766	190	27	509	268
0.153	0.034	1.81	0.26	0.0855	0.0029	0.962	920	189	1327	65
0.157	0.032	1.90	0.31	0.0877	0.0038	0.949	942	179	1376	84
0.153	0.031	1.83	0.26	0.0866	0.0034	0.951	917	171	1352	76
0.086	0.012	0.828	0.092	0.0697	0.0024	0.907	532	69	921	72
0.127	0.054	1.39	0.19	0.0796	0.0024	0.977	769	308	1187	60
0.105	0.024	1.08	0.13	0.0747	0.0024	0.953	642	139	1059	65
0.133	0.032	1.51	0.20	0.0823	0.0022	0.968	805	181	1253	53
0.149	0.033	1.80	0.28	0.0875	0.0024	0.969	896	187	1371	52
0.045	0.006	0.384	0.039	0.0621	0.0031	0.778	283	40	678	106
0.052	0.017	0.456	0.050	0.064	0.019	0.692	325	105	737	639
0.139	0.021	1.64	0.22	0.0856	0.0043	0.913	841	119	1328	97
0.153	0.034	1.89	0.30	0.0895	0.0024	0.969	918	189	1416	51
0.133	0.022	1.55	0.20	0.0842	0.0067	0.868	808	125	1297	154
0.097	0.015	1.03	0.12	0.0767	0.0027	0.921	597	90	1114	71
0.036	0.005	0.307	0.031	0.0626	0.0017	0.834	225	29	694	57
0.147	0.028	1.86	0.29	0.0919	0.0027	0.959	882	159	1465	55
0.138	0.023	1.71	0.22	0.0896	0.0028	0.946	834	128	1416	60
0.081	0.010	0.835	0.093	0.0747	0.0020	0.912	503	60	1059	55
0.143	0.022	1.87	0.26	0.0943	0.0031	0.940	864	125	1515	63
0.136	0.026	1.72	0.22	0.0919	0.0076	0.872	820	147	1464	158
0.0488	0.0081	0.454	0.048	0.0675	0.0039	0.773	307	50	854	121
0.0331	0.0057	0.292	0.029	0.0640	0.0022	0.821	210	36	742	72
0.0265	0.0043	0.232	0.023	0.0636	0.0063	0.784	169	27	730	210
0.122	0.022	1.51	0.19	0.0899	0.0041	0.918	740	126	1423	88
0.159	0.039	2.26	0.37	0.1031	0.0034	0.962	951	215	1681	60
0.168	0.047	2.51	0.44	0.1084	0.0049	0.955	999	260	1772	82
0.0279	0.0042	0.250	0.025	0.0651	0.0038	0.526	177	26	776	121
0.0312	0.0043	0.283	0.028	0.0660	0.0048	0.866	198	27	806	151
0.078	0.015	0.854	0.094	0.0789	0.0042	0.870	487	88	1170	106
0.055	0.010	0.558	0.059	0.0732	0.0079	0.607	347	62	1020	220
0.166	0.035	2.58	0.44	0.113	0.011	0.871	989	195	1841	173
0.0373	0.0054	0.358	0.036	0.0697	0.0053	0.464	236	33	918	157
0.0384	0.0053	0.371	0.038	0.0701	0.0071	0.849	243	33	932	208
0.156	0.035	2.39	0.39	0.1114	0.0032	0.961	932	194	1823	52
0.0119	0.0040	0.106	0.011	0.065	0.020		76	26	765	649
0.086	0.016	1.04	0.12	0.0879	0.0029	0.918	533	92	1380	63
0.0090	0.0009	0.0815	0.0078	0.0659	0.0067	0.225	58	6	804	212
0.147	0.052	2.37	0.38	0.1166	0.0075	0.936	886	291	1905	115
0.148	0.038	2.39	0.33	0.1174	0.0054	0.938	887	214	1917	82
0.0239	0.0051	0.235	0.024	0.071	0.012	0.575	152	32	967	354
0.233	0.045	5.61	0.96	0.1743	0.0049	0.955	1352	236	2600	47
0.0322	0.0049	0.339	0.034	0.0764	0.0064	0.850	204	30	1105	168
0.0286	0.0036	0.301	0.030	0.0762	0.0054	0.857	182	22	1100	141
0.144	0.022	2.51	0.34	0.1265	0.0071	0.866	866	124	2050	99
0.29	0.10	10.7	2.0	0.2636	0.0073	0.971	1664	514	3268	43
0.0334	0.0053	0.380	0.038	0.083	0.012	0.742	212	33	1258	294
0.0444	0.0087	0.535	0.055	0.0873	0.0057	0.684	280	54	1367	126
0.125	0.029	2.22	0.28	0.129	0.013	0.809	761	169	2079	176

0.0644	0.0085	0.861	0.092	0.0970	0.0094	0.918	402	52	1566	181
0.00719	0.00093	0.076	0.007	0.0765	0.0036	0.604	46	6	1107	93
0.0236	0.0052	0.275	0.028	0.084	0.011	0.687	151	33	1302	252
0.095	0.014	1.57	0.18	0.1204	0.0043	0.869	583	81	1963	64
0.0554	0.0083	0.787	0.082	0.1030	0.0063	0.638	348	51	1678	114
0.266	0.066	12.9	2.3	0.353	0.014	0.917	1519	337	3720	59
0.0043	0.0052	0.0495	0.0070	0.08	0.12		28	33	1287	2698
0.169	0.039	5.50	0.96	0.236	0.021	0.768	1006	213	3093	144
0.0572	0.0078	0.96	0.10	0.1216	0.0075	0.516	359	47	1980	110
0.055	0.012	0.99	0.10	0.130	0.015	0.883	347	72	2092	207
0.0278	0.0041	0.452	0.045	0.118	0.015	0.743	177	25	1926	221
0.0276	0.0068	0.511	0.051	0.134	0.026	0.588	176	43	2155	338
0.041	0.011	0.912	0.093	0.163	0.043	0.629	257	71	2485	446
c. Novo Remanso near Manacapuru (3.3076˚S, 60.5331˚W)[†]										
0.330	0.079	4.64	0.98	0.1021	0.0068	0.963	1838	382	1663	124
0.361	0.047	6.00	0.79	0.1204	0.0032	0.972	1988	220	1963	47
0.273	0.061	4.01	0.73	0.1063	0.0029	0.980	1558	308	1738	50
0.297	0.012	4.68	0.21	0.1143	0.0028	0.903	1676	60	1870	45
0.299	0.022	4.80	0.39	0.1164	0.0043	0.921	1686	111	1902	66
0.301	0.016	4.86	0.28	0.1172	0.0030	0.925	1696	81	1914	45
0.272	0.062	4.05	0.74	0.1080	0.0028	0.980	1553	315	1765	48
0.296	0.084	4.73	0.91	0.1160	0.0030	0.984	1671	417	1896	47
0.296	0.084	4.73	0.91	0.1160	0.0030	0.984	1671	417	1896	47
0.308	0.085	5.13	1.03	0.1208	0.0033	0.984	1730	419	1969	48
0.283	0.075	4.52	0.84	0.1157	0.0030	0.983	1607	379	1891	47
0.271	0.011	4.19	0.19	0.1120	0.0028	0.893	1548	55	1832	45
0.2445	0.0085	3.54	0.14	0.1050	0.0026	0.872	1410	44	1713	46
0.204	0.011	2.66	0.16	0.0944	0.0028	0.893	1199	59	1516	57
0.202	0.016	2.60	0.21	0.0937	0.0026	0.929	1184	84	1501	53
0.229	0.047	3.25	0.55	0.1029	0.0027	0.976	1329	248	1677	48
0.264	0.034	4.23	0.55	0.1163	0.0032	0.961	1511	173	1900	49
0.220	0.011	3.08	0.16	0.1014	0.0025	0.900	1282	56	1651	46
0.219	0.040	3.06	0.51	0.1012	0.0027	0.972	1277	212	1647	49
0.267	0.019	4.36	0.33	0.1186	0.0032	0.932	1525	98	1935	48
0.329	0.073	6.6	1.4	0.1464	0.0044	0.975	1835	353	2304	52
0.253	0.071	4.05	0.71	0.1160	0.0031	0.981	1455	367	1896	48
0.318	0.036	6.27	0.84	0.143	0.012	0.863	1778	176	2266	146
0.2421	0.0091	3.79	0.16	0.1135	0.0029	0.871	1397	47	1856	45
0.1752	0.0069	2.22	0.10	0.0919	0.0025	0.849	1041	38	1465	51
0.237	0.051	3.66	0.63	0.1121	0.0030	0.975	1369	264	1833	48
0.244	0.011	3.88	0.18	0.1151	0.0029	0.886	1410	54	1882	46
0.2573	0.0087	4.29	0.17	0.1208	0.0032	0.850	1476	45	1969	47
0.254	0.016	4.19	0.33	0.1198	0.0073	0.814	1458	83	1953	108
0.264	0.060	4.50	0.81	0.1238	0.0033	0.977	1509	305	2012	47
0.250	0.057	4.10	0.71	0.1190	0.0031	0.977	1437	293	1941	47
0.241	0.014	3.88	0.23	0.1168	0.0029	0.911	1390	70	1908	45
0.242	0.045	3.92	0.68	0.1176	0.0031	0.971	1395	236	1921	48
0.219	0.044	3.32	0.55	0.1101	0.0029	0.972	1274	232	1801	48
0.2192	0.0091	3.34	0.15	0.1106	0.0029	0.867	1278	48	1809	48
0.249	0.026	4.21	0.45	0.1226	0.0036	0.943	1433	134	1994	52
0.2020	0.0069	2.92	0.12	0.1049	0.0030	0.815	1186	37	1712	53
0.231	0.023	3.68	0.38	0.1159	0.0051	0.908	1337	119	1894	79
0.245	0.048	4.11	0.71	0.1216	0.0033	0.971	1412	246	1980	48
0.242	0.013	4.02	0.22	0.1205	0.0031	0.899	1396	65	1964	46

0.2309	0.0080	3.72	0.15	0.1169	0.0031	0.841	1339	42	1909	47
0.2088	0.0090	3.13	0.15	0.1086	0.0028	0.871	1223	48	1776	47
0.237	0.057	3.91	0.67	0.1195	0.0032	0.976	1372	297	1949	47
0.2170	0.0076	3.34	0.13	0.1117	0.0028	0.848	1266	40	1827	46
0.2331	0.0080	3.80	0.15	0.1183	0.0031	0.842	1351	42	1930	46
0.230	0.010	3.73	0.18	0.1172	0.0030	0.880	1337	54	1914	46
0.2276	0.0071	3.68	0.14	0.1173	0.0029	0.830	1322	37	1915	45
0.236	0.013	3.94	0.23	0.1214	0.0031	0.901	1364	67	1976	46
0.223	0.043	3.57	0.60	0.1163	0.0031	0.970	1297	227	1900	48
0.221	0.052	3.51	0.60	0.1155	0.0032	0.974	1286	276	1888	50
0.223	0.017	3.57	0.27	0.1163	0.0029	0.927	1296	87	1900	45
0.223	0.068	3.59	0.60	0.1169	0.0032	0.979	1297	358	1909	50
0.2200	0.0071	3.53	0.13	0.1162	0.0029	0.830	1282	37	1899	45
0.219	0.039	3.55	0.59	0.1176	0.0031	0.967	1276	207	1920	47
0.2366	0.0082	4.09	0.16	0.1253	0.0032	0.839	1369	43	2033	45
0.180	0.040	2.55	0.51	0.1030	0.0027	0.972	1066	220	1679	48
0.152	0.025	1.97	0.28	0.0939	0.0025	0.957	913	137	1507	49
0.2131	0.0071	3.42	0.13	0.1163	0.0029	0.830	1245	38	1900	45
0.230	0.013	3.91	0.24	0.1234	0.0032	0.901	1333	70	2006	46
0.177	0.010	2.50	0.15	0.1025	0.0029	0.883	1049	57	1669	52
0.349	0.044	9.10	1.43	0.189	0.020	0.816	1932	211	2731	174
0.206	0.013	3.23	0.21	0.1141	0.0029	0.907	1205	69	1865	46
0.1682	0.0064	2.33	0.10	0.1007	0.0025	0.836	1002	36	1637	47
0.2080	0.0075	3.36	0.14	0.1172	0.0029	0.840	1218	40	1914	45
0.2174	0.0071	3.64	0.14	0.1216	0.0033	0.808	1268	37	1979	48
0.195	0.011	3.04	0.19	0.1132	0.0029	0.896	1148	61	1852	46
0.198	0.014	3.17	0.23	0.1158	0.0029	0.912	1166	75	1893	46
0.1742	0.0069	2.57	0.11	0.1068	0.0030	0.817	1035	38	1746	52
0.2013	0.0080	3.27	0.15	0.1180	0.0037	0.804	1182	43	1926	57
0.1686	0.0061	2.50	0.11	0.1076	0.0038	0.732	1005	34	1759	64
0.160	0.033	2.34	0.38	0.1065	0.0028	0.964	954	183	1741	48
0.1785	0.0070	2.83	0.12	0.1149	0.0029	0.831	1059	38	1879	45
0.174	0.040	2.72	0.49	0.1135	0.0030	0.968	1032	217	1857	48
0.208	0.029	3.76	0.53	0.1310	0.0061	0.913	1220	152	2111	81
0.165	0.032	2.57	0.44	0.1125	0.0030	0.962	987	179	1841	48
0.174	0.047	2.83	0.52	0.1179	0.0033	0.970	1035	256	1924	50
0.210	0.012	3.92	0.25	0.1358	0.0052	0.812	1226	62	2174	67
0.234	0.024	4.90	0.59	0.152	0.013	0.764	1353	123	2369	148
0.128	0.021	1.83	0.24	0.1040	0.0028	0.944	774	122	1696	50
0.168	0.050	2.88	0.51	0.1245	0.0033	0.972	1000	276	2022	47
0.147	0.016	2.35	0.25	0.1164	0.0029	0.922	882	88	1902	45
0.1595	0.0078	2.74	0.14	0.1248	0.0031	0.833	954	43	2025	45
0.164	0.010	2.92	0.19	0.1288	0.0037	0.847	981	56	2081	51
0.173	0.007	3.19	0.15	0.1337	0.0035	0.800	1028	40	2147	46
0.149	0.031	2.62	0.41	0.1274	0.0035	0.953	897	174	2063	48
0.1422	0.0062	2.64	0.13	0.1344	0.0049	0.637	857	35	2156	64
0.1200	0.0093	2.05	0.16	0.1241	0.0033	0.854	731	54	2016	47
0.1242	0.0040	2.53	0.10	0.1476	0.0051	0.957	755	23	2319	60
0.1535	0.0040	3.68	0.12	0.1738	0.0048	0.967	920	23	2595	46
0.0838	0.0027	1.387	0.048	0.1200	0.0030	0.949	519	16	1957	45
0.0589	0.0019	0.896	0.032	0.1104	0.0030	0.925	369	12	1806	49
c. Iranduba Formation near Manacapuru (3.3076˚S, 60.5331˚W)[†]										
0.291	0.020	4.91	0.36	0.1222	0.0036	0.925	1647	100	1989	53
0.243	0.020	3.57	0.31	0.1062	0.0030	0.938	1405	104	1736	52

0.245	0.052	3.62	0.63	0.1072	0.0028	0.977	1414	271	1753	49
0.257	0.070	4.00	0.71	0.1130	0.0030	0.981	1474	358	1848	48
0.281	0.018	4.82	0.33	0.1243	0.0032	0.928	1596	92	2019	46
0.301	0.019	5.49	0.45	0.1323	0.0081	0.829	1694	96	2129	107
0.262	0.077	4.29	0.77	0.1188	0.0032	0.982	1500	392	1938	48
0.272	0.018	4.69	0.34	0.1254	0.0040	0.911	1548	94	2034	57
0.241	0.051	3.78	0.65	0.1138	0.0031	0.974	1390	266	1861	50
0.245	0.010	3.91	0.18	0.1158	0.0029	0.878	1411	51	1893	46
0.236	0.050	3.69	0.63	0.1133	0.0032	0.973	1368	262	1853	51
0.242	0.048	3.86	0.67	0.1157	0.0031	0.973	1396	251	1891	48
0.241	0.048	3.83	0.66	0.1155	0.0030	0.973	1390	250	1888	47
0.244	0.049	3.95	0.68	0.1175	0.0031	0.973	1408	251	1919	47
0.1985	0.0076	2.79	0.12	0.1017	0.0028	0.848	1167	41	1656	50
0.247	0.010	4.09	0.19	0.1198	0.0031	0.873	1426	53	1953	47
0.238	0.012	3.83	0.21	0.1169	0.0029	0.899	1374	62	1909	45
0.247	0.017	4.12	0.29	0.1208	0.0033	0.920	1425	86	1968	48
0.236	0.062	3.84	0.66	0.1181	0.0034	0.976	1367	326	1927	52
0.2330	0.0077	3.76	0.14	0.1169	0.0029	0.843	1350	40	1910	45
0.143	0.031	1.72	0.23	0.0870	0.0029	0.959	862	177	1360	63
0.150	0.045	1.85	0.29	0.0895	0.0047	0.953	901	253	1414	100
0.233	0.062	3.85	0.66	0.1198	0.0034	0.976	1352	322	1954	51
0.2235	0.0070	3.58	0.13	0.1163	0.0029	0.828	1300	37	1900	45
0.2253	0.0080	3.64	0.15	0.1171	0.0029	0.848	1310	42	1913	45
0.249	0.020	4.38	0.35	0.1275	0.0033	0.931	1434	101	2064	45
0.245	0.010	4.27	0.20	0.1263	0.0034	0.864	1415	53	2047	47
0.216	0.052	3.40	0.57	0.1141	0.0030	0.975	1260	278	1866	48
0.227	0.061	3.71	0.63	0.1188	0.0034	0.976	1318	320	1938	51
0.236	0.013	4.00	0.23	0.1229	0.0033	0.895	1367	67	1999	48
0.224	0.073	3.63	0.61	0.1177	0.0032	0.980	1300	383	1921	49
0.168	0.036	2.25	0.39	0.0973	0.0026	0.969	1001	198	1572	50
0.2172	0.0069	3.45	0.13	0.1152	0.0029	0.826	1267	37	1883	45
0.238	0.011	4.08	0.21	0.1242	0.0033	0.879	1377	58	2018	47
0.2106	0.0073	3.29	0.14	0.1132	0.0038	0.782	1232	39	1852	61
0.2207	0.0085	3.57	0.15	0.1174	0.0030	0.855	1286	45	1917	46
0.225	0.063	3.70	0.62	0.1193	0.0035	0.976	1308	331	1946	52
0.2215	0.0081	3.60	0.15	0.1179	0.0029	0.850	1290	43	1925	45
0.230	0.018	3.84	0.31	0.1214	0.0031	0.927	1333	93	1977	46
0.2149	0.0083	3.42	0.15	0.1154	0.0029	0.857	1255	44	1886	45
0.2180	0.0069	3.52	0.13	0.1172	0.0029	0.823	1271	36	1913	45
0.2341	0.0084	4.01	0.17	0.1242	0.0035	0.828	1356	44	2018	50
0.2192	0.0089	3.58	0.16	0.1184	0.0029	0.863	1278	47	1932	45
0.228	0.069	3.84	0.65	0.1222	0.0039	0.975	1324	362	1988	57
0.237	0.010	4.13	0.19	0.1266	0.0035	0.850	1370	50	2051	49
0.142	0.021	1.79	0.24	0.0911	0.0025	0.951	857	120	1449	51
0.178	0.052	2.54	0.49	0.1036	0.0033	0.972	1055	284	1690	60
0.212	0.011	3.43	0.20	0.1173	0.0040	0.846	1239	58	1915	62
0.2093	0.0066	3.36	0.13	0.1165	0.0032	0.797	1225	35	1903	49
0.2242	0.0073	3.82	0.15	0.1234	0.0034	0.809	1304	39	2006	48
0.199	0.013	3.10	0.22	0.1132	0.0033	0.899	1168	72	1852	52
0.2024	0.0064	3.21	0.12	0.1149	0.0029	0.812	1188	34	1878	45
0.2048	0.0069	3.28	0.13	0.1163	0.0029	0.825	1201	37	1900	45
0.2156	0.0070	3.61	0.14	0.1213	0.0031	0.817	1259	37	1976	45
0.230	0.012	4.10	0.24	0.1296	0.0045	0.846	1332	62	2092	60
0.1793	0.0057	2.69	0.10	0.1088	0.0029	0.789	1063	31	1779	48

0.1978	0.0071	3.21	0.13	0.1175	0.0029	0.828	1164	38	1919	45
0.174	0.019	2.60	0.29	0.1079	0.0029	0.937	1037	106	1765	49
0.198	0.007	3.21	0.12	0.1177	0.0030	0.811	1163	35	1922	45
0.205	0.010	3.41	0.17	0.1208	0.0032	0.861	1199	51	1968	47
0.1552	0.0086	2.20	0.13	0.1029	0.0026	0.873	930	48	1677	47
0.154	0.046	2.18	0.35	0.1028	0.0031	0.971	923	259	1675	55
0.180	0.045	2.87	0.57	0.1160	0.0031	0.971	1064	247	1895	48
0.177	0.039	2.82	0.54	0.1152	0.0031	0.966	1053	211	1883	49
0.153	0.005	2.215	0.082	0.1052	0.0027	0.773	917	28	1717	47
0.178	0.054	2.85	0.55	0.1160	0.0032	0.975	1058	297	1895	49
0.212	0.017	3.88	0.32	0.1325	0.0046	0.887	1242	89	2132	61
0.175	0.044	2.77	0.51	0.1150	0.0031	0.971	1039	244	1880	48
0.175	0.048	2.79	0.52	0.1154	0.0034	0.970	1041	264	1886	53
0.1556	0.0090	2.30	0.14	0.1071	0.0027	0.873	932	50	1751	47
0.1840	0.0094	3.03	0.16	0.1196	0.0030	0.867	1089	51	1950	45
0.179	0.065	2.89	0.56	0.1173	0.0032	0.978	1061	354	1915	49
0.180	0.064	2.91	0.58	0.1176	0.0031	0.978	1065	347	1920	48
0.178	0.062	2.87	0.55	0.1170	0.0033	0.977	1056	340	1911	50
0.179	0.062	2.89	0.56	0.1174	0.0031	0.978	1060	340	1917	48
0.175	0.045	2.80	0.52	0.1161	0.0031	0.971	1040	249	1897	48
0.146	0.005	2.091	0.075	0.1040	0.0029	0.728	878	26	1696	51
0.178	0.048	2.90	0.56	0.1181	0.0032	0.972	1057	264	1928	49
0.0947	0.0029	1.128	0.038	0.0864	0.0022	0.649	583	17	1346	49
0.174	0.034	2.81	0.51	0.1175	0.0031	0.962	1032	187	1918	47
0.172	0.034	2.78	0.50	0.1172	0.0031	0.962	1025	185	1913	47
0.148	0.035	2.18	0.30	0.1067	0.0055	0.932	890	196	1744	94
0.156	0.017	2.37	0.26	0.1101	0.0048	0.881	934	93	1801	79
0.134	0.026	1.87	0.24	0.1016	0.0027	0.955	809	147	1654	49
0.177	0.057	2.95	0.56	0.1209	0.0034	0.974	1051	311	1969	50
0.174	0.051	2.86	0.52	0.1196	0.0032	0.973	1032	282	1951	48
0.161	0.039	2.55	0.42	0.1145	0.0031	0.967	964	219	1871	48
0.147	0.028	2.21	0.35	0.1087	0.0031	0.953	886	155	1777	52
0.153	0.035	2.37	0.34	0.1123	0.0030	0.963	917	195	1837	48
0.17	0.10	2.79	0.51	0.1199	0.0039	0.982	1004	554	1955	58
0.1130	0.0034	1.498	0.050	0.0961	0.0025	0.674	690	20	1550	48
0.163	0.022	2.65	0.36	0.1180	0.0030	0.944	974	122	1927	45
0.168	0.039	2.80	0.49	0.1207	0.0035	0.962	1004	213	1967	51
0.1344	0.0077	1.95	0.12	0.1054	0.0027	0.853	813	44	1722	47
0.177	0.061	3.08	0.58	0.1260	0.0051	0.964	1052	332	2042	71
0.175	0.038	3.02	0.56	0.1250	0.0039	0.956	1041	206	2029	56
0.107	0.018	1.40	0.17	0.0950	0.0028	0.933	656	106	1529	56
0.170	0.019	2.89	0.33	0.1231	0.0056	0.880	1014	105	2002	80
0.153	0.030	2.42	0.39	0.1147	0.0030	0.958	916	170	1875	48
0.163	0.029	2.69	0.45	0.1196	0.0032	0.955	974	162	1951	47
0.180	0.015	3.18	0.27	0.1284	0.0035	0.904	1065	82	2076	48
0.175	0.014	3.10	0.25	0.1282	0.0041	0.877	1041	76	2074	57
0.137	0.031	2.09	0.28	0.1108	0.0030	0.958	828	173	1812	48
0.178	0.044	3.23	0.62	0.1318	0.0051	0.951	1054	239	2122	68
0.107	0.026	1.46	0.17	0.0990	0.0027	0.953	655	152	1606	51
0.128	0.030	1.93	0.24	0.1091	0.0029	0.957	778	169	1784	49
0.114	0.022	1.62	0.20	0.1032	0.0028	0.945	695	126	1682	50
0.145	0.015	2.43	0.26	0.1214	0.0033	0.913	874	86	1977	48
0.175	0.012	3.36	0.24	0.1392	0.0042	0.859	1039	67	2217	52
0.146	0.036	2.50	0.39	0.1238	0.0033	0.961	881	203	2011	47

0.153	0.068	2.72	0.45	0.1286	0.0036	0.976	919	382	2079	49
0.1328	0.0071	2.38	0.15	0.1300	0.0079	0.959	804	40	2098	107
0.0919	0.0045	1.566	0.088	0.1235	0.0062	0.943	567	27	2008	89
0.090	0.003	1.578	0.059	0.1271	0.0034	0.953	556	18	2059	47
0.154	0.013	4.23	0.44	0.200	0.019	0.965	921	72	2825	158
e. Alter do Chão Formation at Serra do Óbidos (1.9292˚S, 55.5091˚W)[†]										
0.36	0.12	6.3	1.6	0.1274	0.0034	0.988	1967	570	2062	47
0.352	0.015	6.16	0.30	0.1268	0.0034	0.908	1945	72	2054	47
0.342	0.015	5.87	0.28	0.1244	0.0031	0.912	1898	70	2020	45
0.348	0.019	6.12	0.36	0.1274	0.0033	0.928	1926	90	2062	46
0.335	0.086	5.9	1.3	0.1279	0.0034	0.983	1862	413	2069	47
0.353	0.034	6.56	0.66	0.1348	0.0049	0.941	1948	161	2162	63
0.325	0.078	5.7	1.2	0.1275	0.0033	0.982	1812	378	2064	46
0.314	0.091	5.4	1.1	0.1237	0.0033	0.985	1762	448	2011	47
0.331	0.014	5.93	0.29	0.1301	0.0036	0.900	1841	70	2100	48
0.336	0.098	6.2	1.3	0.1330	0.0037	0.984	1868	472	2138	48
0.319	0.076	5.7	1.2	0.1301	0.0034	0.981	1785	370	2099	46
0.297	0.013	4.99	0.24	0.1219	0.0034	0.889	1677	63	1984	50
0.302	0.023	5.17	0.41	0.1241	0.0032	0.942	1701	114	2016	46
0.303	0.011	5.30	0.23	0.1269	0.0034	0.876	1706	55	2056	47
0.299	0.032	5.20	0.57	0.1259	0.0039	0.949	1689	158	2041	55
0.324	0.013	6.09	0.30	0.1361	0.0040	0.881	1811	66	2178	51
0.295	0.065	5.09	0.97	0.1253	0.0035	0.978	1666	325	2033	49
0.305	0.023	5.44	0.46	0.1295	0.0058	0.899	1714	115	2091	78
0.323	0.015	6.14	0.33	0.1378	0.0045	0.876	1806	72	2200	56
0.2190	0.0089	3.07	0.14	0.1016	0.0028	0.867	1277	47	1654	52
0.273	0.012	4.54	0.21	0.1207	0.0031	0.892	1556	59	1967	45
0.289	0.064	5.08	0.96	0.1273	0.0033	0.978	1639	318	2062	46
0.294	0.013	5.23	0.27	0.1292	0.0040	0.875	1659	66	2087	55
0.294	0.078	5.3	1.0	0.1297	0.0035	0.981	1659	388	2094	48
0.327	0.026	6.51	0.59	0.1443	0.0072	0.888	1825	126	2280	86
0.298	0.075	5.4	1.0	0.1318	0.0035	0.980	1682	372	2123	46
0.306	0.072	5.7	1.1	0.1362	0.0036	0.979	1719	356	2179	46
0.276	0.013	4.74	0.24	0.1245	0.0031	0.901	1571	65	2021	45
0.291	0.072	5.3	1.0	0.1318	0.0035	0.979	1646	358	2122	46
0.278	0.011	4.90	0.22	0.1278	0.0034	0.875	1581	56	2068	47
0.266	0.010	4.54	0.19	0.1238	0.0031	0.872	1520	51	2012	45
0.286	0.072	5.21	0.97	0.1323	0.0035	0.979	1619	359	2129	46
0.277	0.063	4.92	0.90	0.1288	0.0035	0.977	1575	320	2082	47
0.270	0.068	4.70	0.85	0.1264	0.0035	0.978	1539	348	2049	49
0.307	0.070	6.0	1.2	0.1427	0.0040	0.976	1725	347	2261	49
0.2599	0.0093	4.41	0.18	0.1230	0.0031	0.865	1489	48	2000	44
0.284	0.082	5.22	0.97	0.1334	0.0036	0.981	1611	410	2143	47
0.261	0.076	4.48	0.81	0.1243	0.0033	0.981	1497	388	2019	47
0.286	0.022	5.34	0.42	0.1353	0.0034	0.936	1622	108	2168	43
0.255	0.052	4.34	0.76	0.1231	0.0032	0.974	1467	267	2002	47
0.259	0.010	4.45	0.20	0.1248	0.0031	0.877	1484	53	2026	44
0.271	0.066	4.89	0.89	0.1309	0.0036	0.977	1545	333	2111	48
0.254	0.012	4.35	0.22	0.1241	0.0031	0.891	1459	60	2016	44
0.286	0.088	5.5	1.0	0.1385	0.0037	0.982	1621	444	2209	46
0.291	0.025	5.68	0.54	0.1417	0.0076	0.874	1644	123	2248	93
0.253	0.022	4.45	0.39	0.1275	0.0033	0.937	1455	111	2063	46
0.263	0.071	4.79	0.86	0.1320	0.0036	0.979	1507	361	2125	47
0.278	0.014	5.34	0.31	0.1392	0.0044	0.876	1583	72	2217	55

0.257	0.052	4.59	0.81	0.1297	0.0034	0.973	1472	267	2094	46
0.28	0.10	5.6	1.0	0.1432	0.0043	0.982	1610	519	2267	51
0.255	0.064	4.57	0.81	0.1301	0.0035	0.977	1465	328	2099	47
0.163	0.034	2.13	0.36	0.0949	0.0030	0.963	972	191	1527	59
0.268	0.013	5.04	0.28	0.1364	0.0040	0.877	1531	68	2182	52
0.2278	0.0079	3.75	0.15	0.1194	0.0035	0.817	1323	41	1947	52
0.2333	0.0081	3.93	0.16	0.1221	0.0030	0.847	1352	43	1987	44
0.1790	0.0061	2.50	0.11	0.1013	0.0042	0.694	1062	33	1648	77
0.231	0.049	3.87	0.66	0.1215	0.0033	0.972	1339	255	1979	48
0.234	0.053	3.98	0.68	0.1231	0.0032	0.974	1357	274	2001	47
0.264	0.014	4.97	0.29	0.1365	0.0040	0.885	1512	73	2184	52
0.246	0.052	4.37	0.76	0.1289	0.0036	0.971	1416	271	2083	50
0.264	0.078	5.01	0.99	0.1376	0.0042	0.977	1511	398	2197	53
0.227	0.008	3.84	0.16	0.1223	0.0031	0.847	1321	44	1991	45
0.278	0.092	5.6	1.0	0.1459	0.0050	0.977	1579	465	2299	59
0.248	0.076	4.54	0.83	0.1326	0.0039	0.978	1431	391	2133	52
0.259	0.016	4.92	0.34	0.1379	0.0055	0.859	1484	82	2201	70
0.239	0.057	4.30	0.74	0.1302	0.0035	0.974	1384	298	2100	47
0.255	0.074	4.84	0.85	0.1378	0.0044	0.974	1462	378	2200	56
0.35	0.10	9.2	2.3	0.1923	0.0081	0.967	1914	481	2762	69
0.244	0.062	4.51	0.78	0.1340	0.0037	0.975	1408	322	2151	48
0.216	0.051	3.67	0.61	0.1233	0.0032	0.973	1259	272	2004	47
0.24	0.12	4.31	0.76	0.1328	0.0038	0.985	1363	607	2135	50
0.252	0.027	4.89	0.55	0.1409	0.0055	0.919	1448	141	2238	67
0.201	0.017	3.31	0.30	0.1195	0.0033	0.922	1180	94	1949	49
0.401	0.030	13.8	1.7	0.249	0.025	0.636	2173	139	3179	157
0.229	0.027	4.21	0.51	0.1334	0.0039	0.941	1330	143	2143	51
0.283	0.068	6.49	1.20	0.1665	0.0083	0.950	1605	341	2522	84
0.263	0.012	5.66	0.41	0.156	0.011	0.527	1507	59	2410	123
0.26	0.12	5.7	1.0	0.1568	0.0080	0.971	1513	628	2422	87
0.214	0.026	3.93	0.48	0.1333	0.0037	0.941	1249	137	2142	48
0.220	0.011	4.23	0.24	0.1391	0.0046	0.833	1284	61	2216	58
0.177	0.043	2.91	0.55	0.1189	0.0031	0.969	1052	233	1939	47
0.1841	0.0065	3.19	0.13	0.1257	0.0031	0.799	1089	36	2039	44
0.180	0.048	3.06	0.60	0.1238	0.0033	0.971	1065	262	2011	47
0.179	0.041	3.08	0.60	0.1250	0.0033	0.966	1062	223	2028	47
0.179	0.047	3.13	0.61	0.1271	0.0033	0.970	1059	255	2059	46
0.190	0.011	3.52	0.21	0.1344	0.0038	0.854	1120	58	2157	49
0.180	0.050	3.21	0.63	0.1294	0.0034	0.971	1066	272	2089	47
0.176	0.038	3.14	0.59	0.1297	0.0035	0.962	1043	206	2094	47
0.186	0.021	3.60	0.43	0.1402	0.0059	0.888	1101	116	2229	72
0.297	0.137	9.6	1.8	0.2341	0.0205	0.937	1678	680	3080	140
0.1578	0.0074	2.82	0.14	0.1295	0.0033	0.815	945	41	2091	45
0.155	0.012	2.76	0.21	0.1289	0.0033	0.886	930	66	2082	45
0.1390	0.0094	2.33	0.16	0.1215	0.0031	0.862	839	53	1979	46
0.145	0.026	2.52	0.46	0.1259	0.0047	0.927	872	148	2042	65
0.152	0.010	2.73	0.19	0.1303	0.0033	0.865	910	56	2103	44
0.1597	0.0083	3.03	0.17	0.1374	0.0036	0.822	955	46	2195	45
0.31	0.14	12.6	2.5	0.292	0.041	0.876	1758	665	3427	218
0.148	0.030	2.76	0.38	0.1359	0.0036	0.949	887	166	2175	46
0.153	0.011	2.97	0.22	0.1407	0.0038	0.858	919	62	2236	47
0.1599	0.0070	3.23	0.17	0.1464	0.0059	0.607	956	39	2304	69
0.174	0.049	3.76	0.69	0.1568	0.0093	0.920	1034	268	2421	101
0.141	0.025	2.70	0.36	0.1394	0.0037	0.937	849	140	2220	47

0.151	0.034	3.21	0.51	0.1543	0.0045	0.945	906	190	2394	49
0.1271	0.0050	2.47	0.10	0.1407	0.0036	0.685	772	29	2236	44
0.121	0.016	2.28	0.31	0.1365	0.0045	0.887	737	93	2184	57
0.192	0.027	5.31	0.90	0.201	0.026	0.548	1131	146	2831	208
0.123	0.029	2.90	0.36	0.1711	0.0053	0.922	747	165	2568	52
0.114	0.049	2.57	0.35	0.1628	0.0056	0.949	697	286	2485	58
0.094	0.006	1.88	0.11	0.1451	0.0038	0.693	578	32	2289	46
0.110	0.030	2.44	0.29	0.1611	0.0045	0.936	673	176	2468	47
0.159	0.011	4.98	0.55	0.227	0.029	0.957	951	61	3033	207
0.076	0.010	1.60	0.17	0.1524	0.0041	0.837	474	62	2373	45
0.146	0.032	4.9	1.1	0.245	0.031	0.523	876	177	3151	201
0.083	0.014	1.87	0.21	0.1643	0.0044	0.869	512	83	2501	45

† Letters associated with sample names are as in Figures 1-3

‡ Blank value indicates no significant correlation coefficient could be calculated, "-" indicates analysis was run prior to introduction of correlation coefficient calculation algorithm

§ $^{207}Pb/^{206}Pb$ age omitted for very young, slightly reversely discordant analyses where calculated age is negative